eCAM
Evidence-Based Complementary and Alternative Medicine

Primo Vascular System: Past, Present, and Future

Guest Editors: Byung-Cheon Lee, Walter J. Akers, XiangHong Jing, M. Isabel Miguel Perez, and Yeonhee Ryu

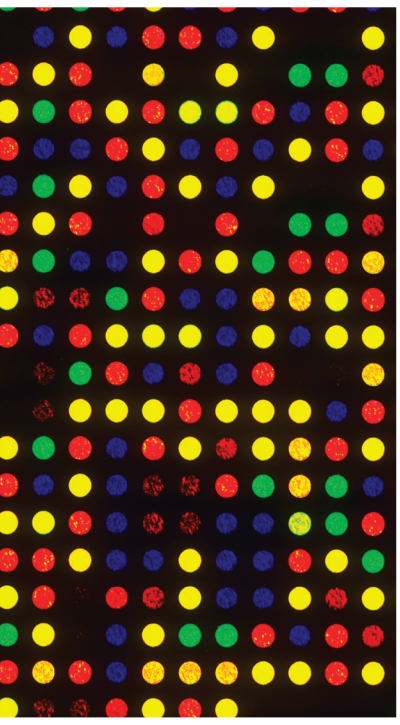

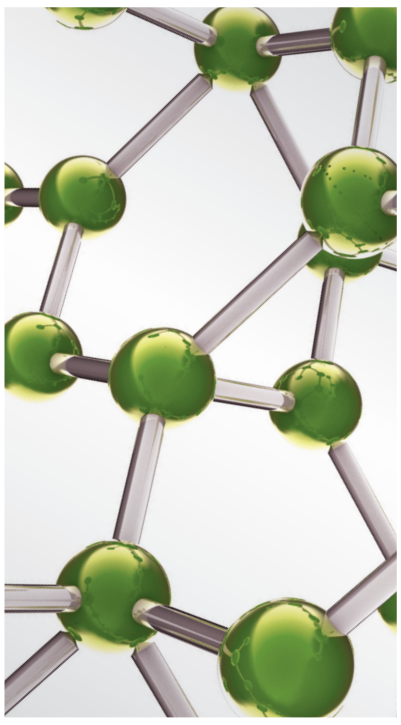


Primo Vascular System: Past, Present, and Future

Evidence-Based Complementary and Alternative Medicine

Primo Vascular System: Past, Present, and Future

Guest Editors: Byung-Cheon Lee, Walter J. Akers, Xianghong Jing, M. Isabel Miguel Perez, and Yeonhee Ryu

Editorial Board

Contents

Hindawi Publishing Corporation
Evidence-Based Complementary and Alternative Medicine
Volume 2013, Article ID 240168, 2 pages
http://dx.doi.org/10.1155/2013/240168

Editorial

Primo Vascular System: Past, Present, and Future

Byung-Cheon Lee,[1] Walter J. Akers,[2] Xianghong Jing,[3] M. Isabel Miguel Perez,[4] and Yeonhee Ryu[5]

[1] *Ki Primo Research Laboratory, Division of Electrical Engineering, KAIST Institute for Information Technology Convergence, Korea Advanced Institute of Science and Technology (KAIST), Daejeon 305-701, Republic of Korea*
[2] *Department of Radiology, Washington University School of Medicine, St. Louis, MO 63110, USA*
[3] *Institute of Acupuncture and Moxibustion, China Academy of Chinese Medical Sciences, Beijing 100700, China*
[4] *Unit of Human Anatomy and Embryology, University of Barcelona, Casanova, 143 08036 Barcelona, Spain*
[5] *Acupuncture, Moxibustion & Meridian Research Group, Medical Research Division, Korea Institute of Oriental Medicine, Daejeon 305-811, Republic of Korea*

Correspondence should be addressed to Byung-Cheon Lee; donboscolee@gmail.com

Received 4 August 2013; Accepted 4 August 2013

What is Primo Vascular System (PVS)? Let us take a journey through oriental medicine in a time machine. Over the past 2000 years, acupuncture and moxibustion in Chinese medicine have been developed based on the concept of the meridian system; however, the anatomical reality of the meridian system has been controversial in various aspects. Even today, the meridian system is still being investigated with well-known anatomical structures. Among them, connective tissues called the fascia system are representative ones for which the putative function of the meridian system has been established and is understood [1].

A fundamental insight into the acupuncture meridian system and its novel anatomical structures was conceived by Kim in the 1960s [2]. According to his idea, the meridian system has the role of circulating DNA microparticles, named "Signals," with several hormones independently from the cardiovascular and the lymph systems. In the 1970s, Fujiwara tried to duplicate and verify Kim's findings; however, his works have also been neglected [3]. Since 2002, Soh's group at Seoul National University, Republic of Korea, has tried to verify the findings of Bonghan Kim's work, and they found much evidence suggesting that Bonghan Kim's ideas on the acupuncture meridian system are reasonable [4].

At present, what do we study about the PVS? to answer this question and for insight into current works on this novel system, we have a new special issue, Primo Vascular System, in which we have published several research papers and a few review articles. The research papers can be classified as those directly related to the function of PVS and those focusing on the discovery of this new PVS. Representative articles in the former category are the C. H. Leem group's stem cell work *"Expression of stem cell markers in primo vessel of rat,"* and K.-S. Soh group's endothelial cell work *"Discovery of endothelium and mesenchymal properties of primo vessels in the mesentery."* In the latter category are the works of Y. H. Ryu laboratory *"Primo vascular system accompanying a blood vessel from tumor tissue and a method to distinguish it from the blood or the lymph system"* S. Z. Yoon's medical team *"Composition of the extracellular matrix of lymphatic novel threadlike structures: is it keratin?"* and B.-C. Lee's laboratory *"Evidence for the primo vascular system above the epicardia of rat hearts."* Also, a Chinese team led by X. Jing has published a very meaningful idea that the PVS could represent artifacts from pathological conditions *"Preliminary research of relationship between acute peritonitis and celiac primo vessels,"* but another Chinese team led by W.-B. Zhang has suggested via heparin treatment that the PVS might have real anatomical structures *"Study on the formation of novel threadlike structure through intravenous injection of heparin in rats and refined observation in minipigs."* Based on these data, admittedly, at present, for the PVS to be established absolutely, an international exchange is needed.

On the other hand among controversial research articles, we published a few review papers in which we should pay

more attention to two teams, K.-S. Soh's and B. Zhu's ("*50 years of Bong-Han theory and 10 years of primo vascular system*" and "*Historical review about research on "Bonghan system" in China*"). Through their review articles, even beginner in PVS could figure out the overall feature of PVS. Especially for the research history of PVS we recommend a review article by Kim [5] in related journal to ECAM, Journal of Acupuncture and Meridian Studies. We also suggest researchers to pay some attention to two review articles: one is J. Jeon's approach on the relationship between the history of acupuncture meridian system and PVS "*The meanings and prospects of primo vascular system from the viewpoint of historical context.*" The other is novel insight into the function of PVS as DNA particles circulation system suggested by S. Z. Yoon "*Toward a theory of the primo vascular system: a hypothetical circulatory system at the subcellular level.*"

In the future, what will we study about the PVS? Based on our long research careers, we editors suggest the following areas of study to establish an international unified consensus for the novel system that is called the Primo Vascular System:

(1) the establishment of the Primo Vascular System in terms of a novel circulation system,

(2) the concept of "Sanal" and the relationship between stem cells and Sanals,

(3) the involvement of Sanals in cancer metastasis,

(4) The potential of the PVS in the brain for diagnosing and treating degenerative brain diseases.

Now let us think of "time" by leaving the time machine. Time really flows in only one direction, toward the future! Thus, our research minds should be directed beyond the past and the present and toward the future. With free, dedicated efforts toward human-oriented holistic medicine, we should be able to build a real evidence-based alternative medicine. Given the present circumstances, a new circulation concept, the Primo Vascular System, is waiting for us to establish fully its potential for benefitting all mankind in ways not previously known.

Byung-Cheon Lee
Walter J. Akers
Xianghong Jing
M. Isabel Miguel Perez
Yeonhee Ryu

References

[1] H. M. Langevin and J. A. Yandow, "Relationship of acupuncture points and meridians to connective tissue planes," *Anatomical Record*, vol. 269, no. 6, pp. 257–265, 2002.

[2] B. H. Kim, "The Kyungrak system," *Journal of Jo Sun Medicine*, vol. 108, pp. 1–38, 1965 (Korean).

[3] S. Fujiwara and S. B. Yu, "'Bonghan theory' morphological studies," *Igaku No Ayumi*, vol. 60, pp. 567–577, 1967 (Japanese).

[4] K.-S. Soh, "Bonghan circulatory system as an extension of acupuncture meridians," *Journal of Acupuncture and Meridian Studies*, vol. 2, no. 2, pp. 93–106, 2009.

[5] H. G. Kim, "Formative research on the primo vascular system and acceptance by the Korean scientific community: the gap between creative basic science and practical convergence technology," *Journal of Acupuncture and Meridian Studies*, 2013.

Hindawi Publishing Corporation
Evidence-Based Complementary and Alternative Medicine
Volume 2013, Article ID 569161, 8 pages
http://dx.doi.org/10.1155/2013/569161

Research Article

Preliminary Research of Relationship between Acute Peritonitis and Celiac Primo Vessels

Xiaoyu Wang,[1] Hong Shi,[1] Jingjing Cui,[1] Wanzhu Bai,[1] Wei He,[1] Hongyan Shang,[1] Yangshuai Su,[1] Juanjuan Xin,[1,2] Xianghong Jing,[1] and Bing Zhu[1]

[1] *Institute of Acupuncture and Moxibustion, China Academy of Chinese Medical Sciences, Beijing 100700, China*
[2] *Shandong University of Traditional Chinese Medicine, Jinan 250355, China*

Correspondence should be addressed to Xianghong Jing; xianghongjing@hotmail.com and Bing Zhu; zhubing@mail.cintcm.ac.cn

Received 8 February 2013; Accepted 11 March 2013

Academic Editor: Byung-Cheon Lee

Previous studies demonstrated that primo vessels (PVs) were distributed in different parts of the body in mammals, and PVs were also involved in some processes of pathology such as cancer. Whether PVs are intrinsic structures in mammals or not is still ignored. In this study, a peritonitis model rat was induced by i.p. administration of *E. coli* in rats. PVs were observed in all infected rats, but it appeared less in untreated rats, taking 10.53% (4/38). In addition, we examined cell types in celiac PVs by fluorescent staining with 4′,6-diamidino-2-phenylindole (DAPI) and Alexa Fluor 488 phalloidin, as well as immunofluorescent staining with CD11b and intercellular adhesion molecule-1(ICAM-1), and found the following. (1) The rod-shaped nuclei aligned longitudinally along PVs. (2) DAPI-, phalloidin-, CD11b-, and ICAM-1-positive labeling coexisted in PVs, suggesting that fibroblasts and leucocytes might be two kinds of cell types in PVs for both infected and control rats. (3) The difference was that numerous cells in PVs of the infected rats contained DAPI-labeled multilobal nucleus and were expressed with CD11b- and ICAM-1-positive labeling on the cytoplasm and membrane, showing the typical characteristics of neutrophil. (4) The cells in PVs from the untreated rats are those of loose connective tissue. Therefore, it is reasonably considered that PVs from infected rats might be the pathological products which might be involved in inflammation.

1. Introduction

Bong-han Kim reported for the first time in 1962 that the Bonham system, which was considered as the anatomical basis of classical acupuncture meridians, included several subsystems such as Bonghan corpuscles and Bonghan ducts [1, 2]. The structure was also found by Fujiwara's follow-up [3]. Unfortunately, Bonghan theory was not clearly confirmed by most investigators [4] because the method employed by Kim was not disclosed and the experiments were hard to reproduce.

Recently, a series of reports Professor Soh KS's group showed that the primo vessels (PVs), which were referred to Bonghan ducts (BHDs) and identified as a part of a circulatory system by Kim [1, 2] in the early 1960s, could be found in different parts of the body such as on the surface of the internal organs of rats, rabbits, and swine [5–7], inside the blood and lymphatic vessels [8, 9], in the epineurium, running along the sciatic nerve [10], and below the skin [11]. However, whether PVs are intrinsic structures in mammals or not still remains elusive.

In order to confirm the structure of PVs, a lot of labs in Korea, China, and USA tried to repeat the labeling methods of PVs provided by Soh. According to the method reported by Lee et al. [12], PVs in enterocoelia were identified and stained by dropping 0.2% diluted Trypan blue solution. But PVs can not be found in all the subjects by the staining method. During experiments of searching PVs we found that the percentage of celiac PVs emergence was related to a lot of factors such as age and method of anesthesia. This indicated that the PVs may be related to a pathological process. Recent studies showed that PVs played an important role in cancer, especially in tumor metastasis, and regeneration [13, 14]. Here a question was raised: is PV an intrinsic structure of mammals

or pathological products? In this study, we tried to address the relationship between peritonitis and celiac PVs by establishing an acute peritonitis model. We first summed up the data during the search of PVs in juvenile rats and adult rats, compared the different emergence of PVs due to different methods of anesthesia. Moreover, whether acute peritonitis correlated with the occurrence of celiac PVs was investigated by fluorescent staining with 4′,6-diamidino-2-phenylindole (DAPI) and Alexa Fluor 488 phalloidin, as well as immunofluorescent staining with CD11b and intercellular adhesion molecule-1(ICAM-1). The results will be helpful to understand the cell types and chemical characteristics in PVs.

2. Materials and Methods

2.1. Animal Preparation. Male and female Sprague-Dawley (SD) rats weighing 150–350 g were purchased from Institute of Animal, Academy of Chinese Medical Sciences. The animals were housed under a 12 h light/dark with free access to food and water. All animals were treated according to the Guide for Use and Care of Medical Laboratory Animals from Ministry of Public Health of People's Republic of China.

2.2. Animal Model of Acute Peritonitis and Cytometry of Blood and Reroperitoneum. Fifity-nine male and female SD rats, weighing 250–350 g were conducted in the experiments. 39 rats were subjected to acute peritonitis and 20 rats as control. Acute peritonitis model (PM) was made through intraperitoneal (i.p.) injection of sterile phosphate-buffered saline (PBS, 10 mL/kg) containing 3.3×10^8 colony forming units of *E. coli* (ATCC 25922, Beijing Century Ocote Biotechnology Co. Ltd.) [15]. Control animals just received the same volume PBS.

24 h after i.p. injection of *E. coli*, the rats were anesthetized by intramuscular injection (i.m.) of 10% urethane (1.5 g/kg). The reroperitoneum of the rats was collected for leukocyte counting. The venous blood was collected for blood analysis. Cell counting was performed by automated blood cell analyzer (Nihon Kohden, 5108K).

2.3. Methods for Identifying PVs. To identify PVs inside the abdominal cavity, surgery was performed in rats. All surgical procedures were performed under anesthesia with urethane ($1.5\ g/kg^{-1}$) i.p. or i.m. For acute peritonitis and control, the operation was done 24 h after i.p. injection of *E. coli* and PBS. The middle of the rats' abdomen was incised and the intra-abdominal organs were exposed carefully. Then a 0.2% trypan blue solution 1-2 mL was dropped on the exposed organs as in the previous report [12]. After rinsing away the dye with warm saline, primo nodes and primo vessels were identified through a surgical microscope (SZX12, Olympus, Japan). Finally, the images were captured with a CCD camera (Nikon SMZ750) *in situ* and *in vivo*.

2.4. Fluorescent Staining of PVs with Alexa Fluor 488 Phalloidin and DAPI. After intraoperative imaging of the PVs, *in vitro* examination was performed with histological staining of the samples. PVs were fixed with 4% paraformaldehyde in 0.1 M phosphate-buffered solution (PB, pH 7.4) for 2 hours at 4°C, then moved to 25% sucrose in 0.1 M PB (pH 7.4). Alexa Fluor 488 phalloidin (specific to F-actin) and DAPI were employed to identify the morphology of cell nuclei and F-actin, and the cells shape and arrangements of PVs were clearly detected. The PVs were incubated for 2 h by Alexa Fluor 488 Phalloidin, which was dissolved in methanol (1 : 50; Molecular Probes, Eugene, OR, USA) in the dark at room temperature (RT) and then washed with 0.1 M PB. DAPI (0.1 mg/mL, Molecular Probes, Eugene, OR, USA) was added and incubated for 30 min.

2.5. Fluorescent/Immunofluorescent Staining with DAPI, Alexa Fluor 488 Phalloidin, CD11b and CD54/ICAM-1. Fluorescent staining with DAPI and Alexa Fluor 488 Phalloidin were used for identifying the morphology of cell nuclei and F-actin, while immunofluorescent staining with CD11b and CD54/ICAM-1 was used for determining the immune cells and intercellular adhesion molecule that was mainly expressed in the membrane of neutrophils. The staining included DAPI/Phalloidin, DAPI/CD11b, and DAPI/ICAM-1.

Before staining, the PVs mounted on the microslide were incubated in a blocking solution containing 3% normal goat serum and 0.5% Triton X-100 in 0.1 M phosphate-buffered solution (PB, pH 7.4) for 30 min. For phalloidin staining, the sample was further stained with Alexa Fluor 488 phalloidin dissolution (1 : 50; Molecular Probes, Eugene, OR, USA) for 2 h and then washed with 0.1 M PB. After that, the tissue was counterstaining with DAPI (Molecular Probes, Eugene, OR, USA). For CD11b staining, the sample was further transferred to mouse anti-CD11b monoclonal antibody (1 : 1000; Abcam, Hong Kong) at a dilution of 0.1 M PB containing 0.5% Triton X-100 overnight at 4°C. On the following day, after washing three times with 0.1 M PB, PVs were exposed to Alexa Fluor 594 goat antimouse IgG secondary antibody (1 : 500; Molecular Probes, Eugene, OR, USA) for 2 h and then washed with 0.1 M PB. After that, the tissue was counterstaining with DAPI. The procedure for ICAM-1 staining was the same as for CD11b staining. The difference is that rabbit anti-ICAM-1 antibody was used as primary antibody (1 : 100; Bioss, China) and Alexa Fluor 488 goat antirabbit IgG as secondary antibody.

2.6. Observation and Statistical Analysis. All Quantitative data are expressed as mean ± SE. The tissue samples were observed and recorded with confocal imaging system (FV1000, Olympus, Japan) and analyzed by the Olympus Image Processing Software. Comparisons between two groups were analyzed by independent t test. $P < 0.05$ was considered as a statistical significance.

3. Results

3.1. Intraoperative Visualization of PVs and the Related Factors of Emergence Rate of Celiac PVs. The PVs and the corpuscles were observed on surfaces of different internal organs such as the stomach, liver, large and small intestines, and bladder. Figure 1 showed a representative stereomicroscopic image of

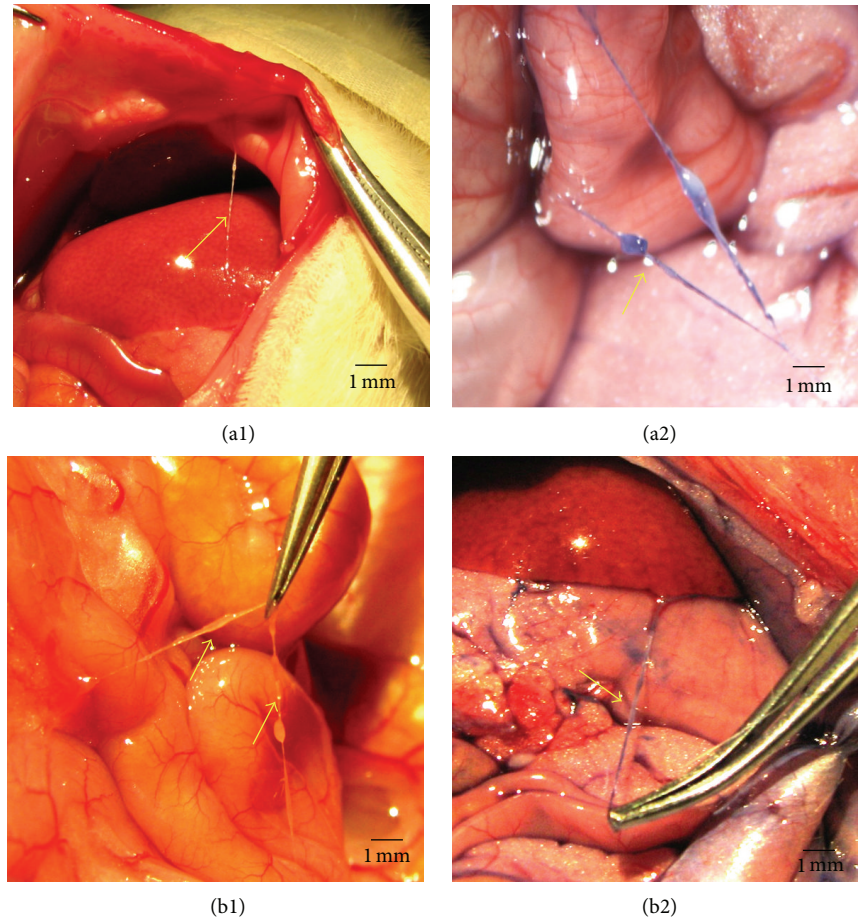

Figure 1: *In situ* and *in vivo* stereomicroscopic image of a typical Primo-vessel (arrow) and a corpuscle (arrow). (a1) and (a2) showed the primo vessel on the surface of intestine in the control rats. (a1) displayed that the PV was unstained and it was connected to the abnormal wall. (a2) displayed that the PV was stained with Trypan blue. (b1) and (b2) showed the primo vessel on the surface of intestine (unstained, (b1)) and stomach (stained with Trypan blue, (b2)) in PM rats. The primo vessels are semitransparent, freely movable strands irregularly fixed on the peritonea.

a PV and its corpuscles (arrow) on the surface of the intestine. The PVs are thin, semitransparent, and freely movable strands on the peritonea, and some of them were connected to the wall of peritoneal cavity, the same as described by Lee et al. [12].

In the present study, the emergence rate of celiac PVs could be affected by urethane injection methods, age, and infection. The rate was 81.84% (22/27) with i.p. and significantly higher than that (4/38, 10.53%) in i.m. (Figure 2(a)). The rate was increased with age: 0% in 5-week old ($n = 15$) group, 10.53% (4/38) in 10-week group, and 35% (7/20) in 15-week group (Figure 2(b)). For the infection, the rate is 100% in the infected rats ($n = 20$), but only 10.53% (4/38) in the control rats (Figure 2(c)).

3.2. Changes of Cytometry in Blood and Ascites of Peritonitis Model. After 24 h of *E. coli* injection, the rats appeared less active, less eating, and less drinking. The count of total leukocytes and lymphocytes in peripheral blood decreased significantly ($P < 0.05$). The percentage of neutrophil increased remarkably in blood ($P < 0.05$) of PM compared with that of the control (Figures 3(a) and 3(b)). The count of total leukocytes and neutrophils in the ascites was significantly higher than that in the blood ($P < 0.01$). The percentage of neutrophil increased significantly in the ascites ($P < 0.01$) than that in the blood (Figures 3(c) and 3(d)).

3.3. Cell Types and Chemical Characteristics of PVs Examined with DAPI, Alexa Fluor 488 Phalloidin, CD11b, and ICAM-1. The cell types and chemical characteristics of celiac PVs were examined by fluorescent staining with DAPI and Alexa Fluor 488 phalloidin, as well as immunofluorescent staining with CD11b and intercellular adhesion molecule-1(ICAM-1). We found that DAPI-, phalloidin-, CD11b-, and ICAM-1-positive labeling coexisted in PVs (Figures 4 and 5). In the PVs from control rats, the cells labeled with DAPI/phalloidin had elongated nuclei and flattened processes (Figures 4(a)–4(a3)), suggesting that fibroblasts might be an important cellular component of PVs. Using DAPI/CD11b, many CD11b-positive cells showed different shapes, and some of them closely were connected together (Figures 4(b)–4(b3)). Figures 4(c)–4(c3) showed that some of ICAM-1-positive cells

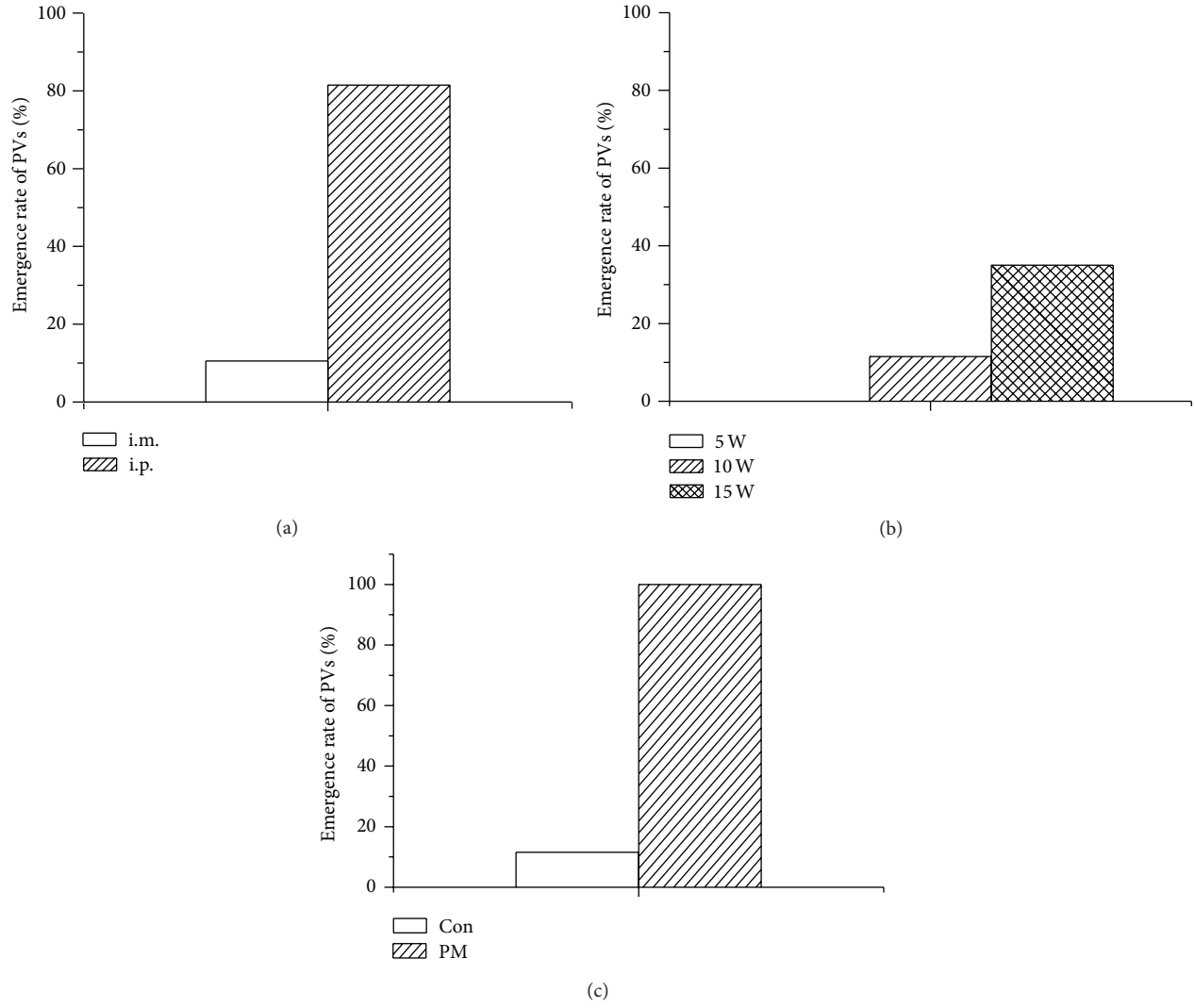

Figure 2: Affecting factors such as anesthesia methods, age of rats, and peritonitis on emergence rate of celiac PVs. (a) For anesthesia methods, the rate was 81.84% (22/27) with i.p. anesthetized cases which was significantly higher than 10.53% (4/38) that with i.m. (b) For the age, the rate was increased following the growth of rats in which took up 0% in 5-week old ($n = 15$) group, 10.53% (4/38) in 10-week group, and 35% (7/20) in 15-week group. (c) For the infection, the rate was 100% in the infected rats ($n = 20$), whereas the rate in the control rats was only 10.53% (4/38).

are sparely distributed in PVs. In contrast, more numerous phalloidin- and CD11b-positive cells were observed in the PVs from infected rat than that from control rat (Figures 5(a)–5(a3); Figures 5(b)–5(b3). It should be noted that many CD11b-positive cells contained multilobal nucleus, showing the characteristics of neutrophil (Figures 5(b1)–5(b3)). Furthermore, there were more ICAM-1-positive cells in the infected cases than those of control cases (Figures 4(c)–4(c3); Figures 5(c)–5(c3)).

4. Discussion

In this study, we found that PVs can be induced more by i.p. injection of urethane than i.m. The emergence rate of celiac PVs increased with the age. The cells of PVs in control rats included rod-shaped nuclei that aligned longitudinally along the PVs, and also CD11b and ICAM-1 were coexpressed. This indicated that some exfoliative cells or degenerative cells might contribute to the structure of celiac PVs in control and they might form a chronic inflammation. Further study showed that PVs were observed in all infected rats. DAPI-, phalloidin-, CD11b-, and ICAM-1-positive labeling also coexisted in PVs of infected rats. This indicated that high percentage of PVs emergence is due to acute peritonitis.

In order to determine cell types and chemical characteristics in PVs, the distribution of CD11b, which is an adhesion molecule of leukocyte integrin in neutrophils surface, and ICAM-1 in celiac PVs cells were investigated. The CD11b positive cells were mainly monocytes and polymorphonuclear neutrophils and could be found in PVs. Neutrophils are the most immediate response in inflammation. CD11b directly or indirectly mediates phagocytosis and anti-infection of the

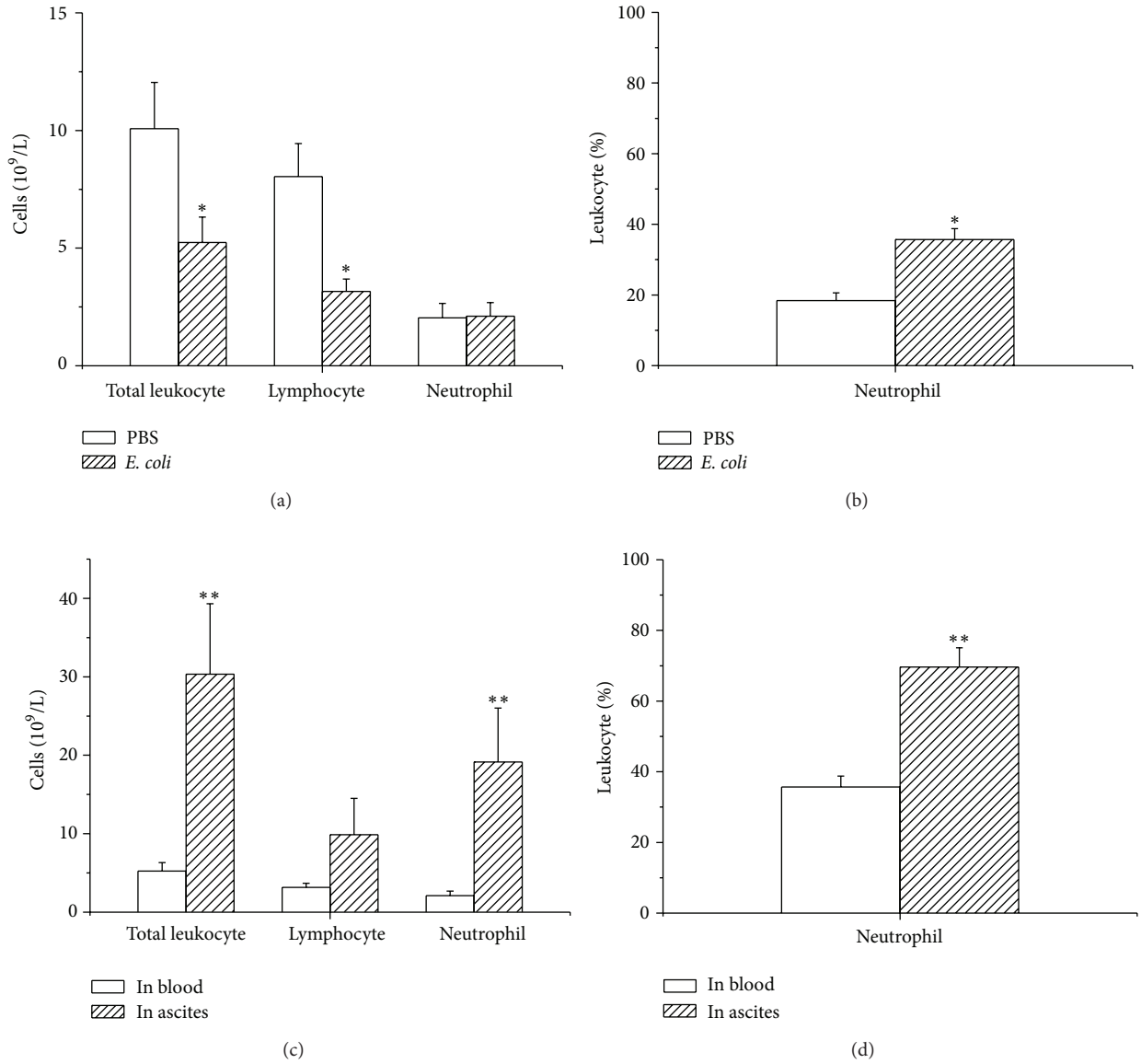

Figure 3: (a) and (b) showed changes of cell count in the blood 24 h after i.p. administration of *E. coli*. (a) The count of total leukocytes and lymphocytes in the blood of the PM decreased significantly ($^{*}P < 0.05$) compared with the control. (b) The neutrophil increased markedly in the blood ($^{*}P < 0.05$) of PM compared with that of the control. (c) and (d) showed changes of cell count in blood and ascites 24 h after i.p. administration of *E. coli*. (c) The count of total leukocyte and neutrophils in the ascites was significantly higher than that in the blood ($^{**}P < 0.01$). (d) The percentage neutrophil increased significantly in the blood than that in the ascites ($^{**}P < 0.01$).

neutrophils, and its increasing is also identified as the symbol during the neutrophils activation [16]. In this work, the cells of PVs in PM and controls expressed CD11b in the membrane were like neutrophils (Figures 4(b) and 5(b)). This indicated that PVs may be involved in peritonitis.

ICAM-1, as the immunoglobulin superfamily of adhesion molecules [17], could promote intercellular contact/adhesion and induce transendothelial migration of leukocytes. As a costimulatory molecule and signal transducer, it can also trigger intracellular signals and ultimately leads to the activation of lymphocytes, secretion of cytokines, and induction of proinflammatory cascades [18, 19], suggesting that ICAM-1 could be involved at the beginning of inflammation.

Based on the present findings, fibroblasts and leukocytes might be two kinds of cell types in PVs for both of infected and untreated rats. Both CD11b and ICAM-1 were expressed in fibroblasts and leukocytes of celiac PVs. Growing evidence revealed that fibroblasts and leukocytes play an important role in early stage of inflammation. The presumed monocyte origin of fibrocytes is reflected by expression of CD11b, CD11c, and CD11d [20]. The highly expressed CD11b in the fibroblasts of PVs indicated that the activated fibroblasts might be originated from monocyte. The coexpressed CD11b

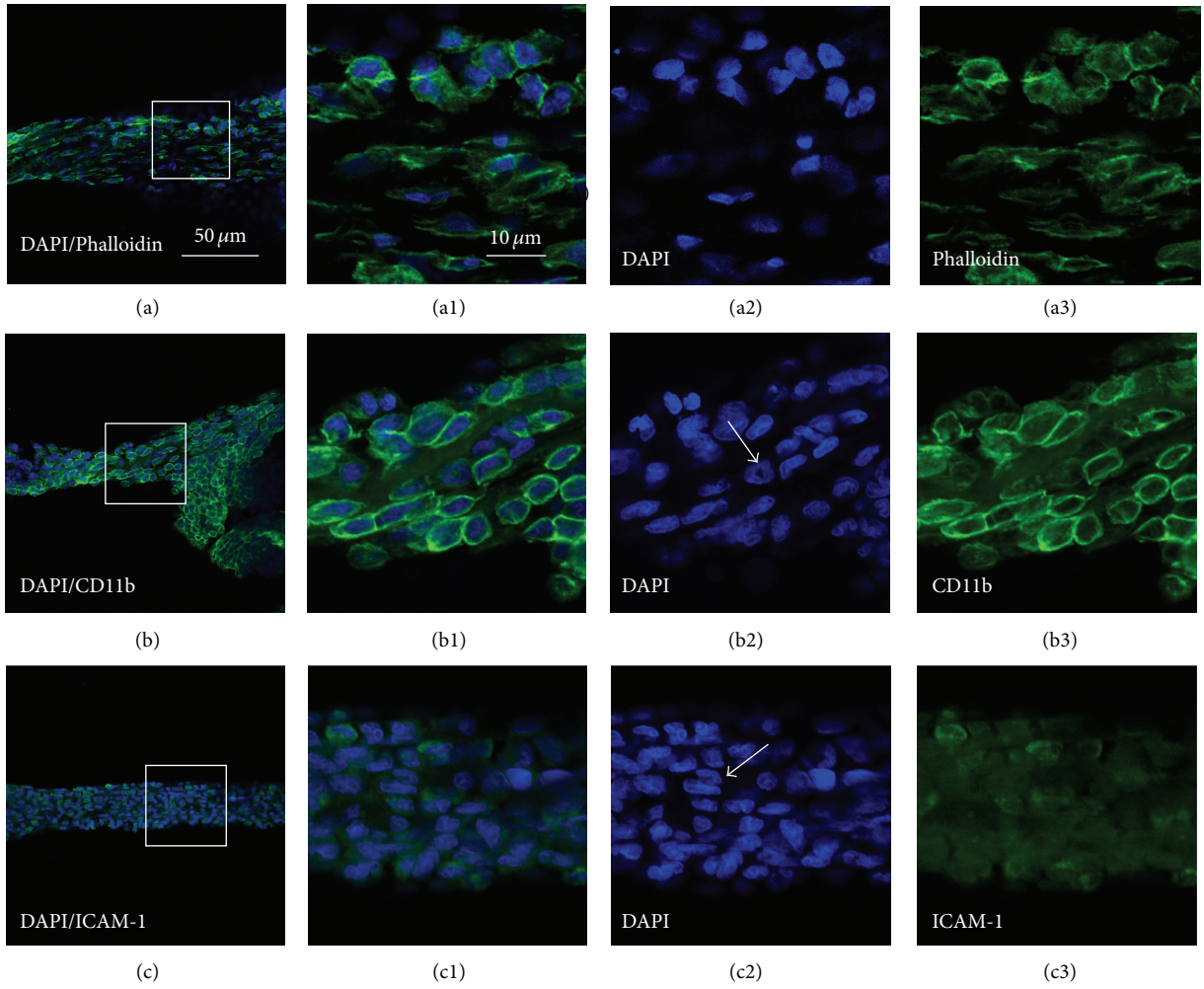

Figure 4: Cell types of primo vessels (PVs) in the control rats determined with DAPI/Phalloidin (a)–(a3), DAPI/CD11b (b)–(b3) and DAPI/ICAM-1 (c)–(c3) by fluorescent and immunofluorescent staining, respectively. (a)–(a3), DAPI/phalloidin-positive cells (a) and its higher resolutions (a1) emerged from images of DAPI (a2) and phalloidin (a3); (b)–(b3). DAPI/CD11b-positive cells (b) and its higher resolutions (b1) emerged from images of DAPI (b2) and CD11b (b3), typical multilobal nuclei showed in (b2) (white arrow); (c)–(c3): DAPI/ICAM-1-positive cells (c) and its higher resolutions (c1) emerged from images of DAPI (c2) and ICAM-1 (c3). Scale bar, the same for (a)–(c) (showed in (a)) and the same for the others (showed in (a1)).

and ICAM-1 of cells in PVs in peritonitis and control rats indicated that the PVs may be involved in inflammation.

Recently studies have shown that there is a putative primo vessel inside the lymph vessel, which is proposed to participate in the cancer metastasis [21, 22]. But inflammatory process is often associated with angiogenesis and lymphangiogenesis. Studies also showed that lymphangiogenesis plays an important role in the spread of inflammation and tumor metastasis. There are considerable inflammatory cells and lymphangiogenesis existing in tumor microenvironment [23]. Thus, although Yoo et al. [13] reported that a novel function of the primo vascular system, which was different from that of lymphatics, was in conjunction with cancer events, it is easy to speculate that PVs are involved in the inflammation of tumor metastasis.

So far, the specific function of PVs in biological processes remains unclear. As reported, the structure of the PVs is distinct from the well-known tissues such as nerves and blood vessels and may be related to acupuncture meridian [1–3]. However, our previous study demonstrated that the PVs on the surface of internal organs are involved in neither the inhibition of the gastric motility induced by acupuncturing at CV12 nor the facilitation of gastric motility induced by acupuncturing at ST36 [24]. Here our data showed that PVs were related to the process of inflammation. Further study on the role of PVs in inflammation and effect of acupuncture is encouraged in the future.

In conclusion, the emergence of PVs could be affected by age and urethane injection methods. PVs may not be an

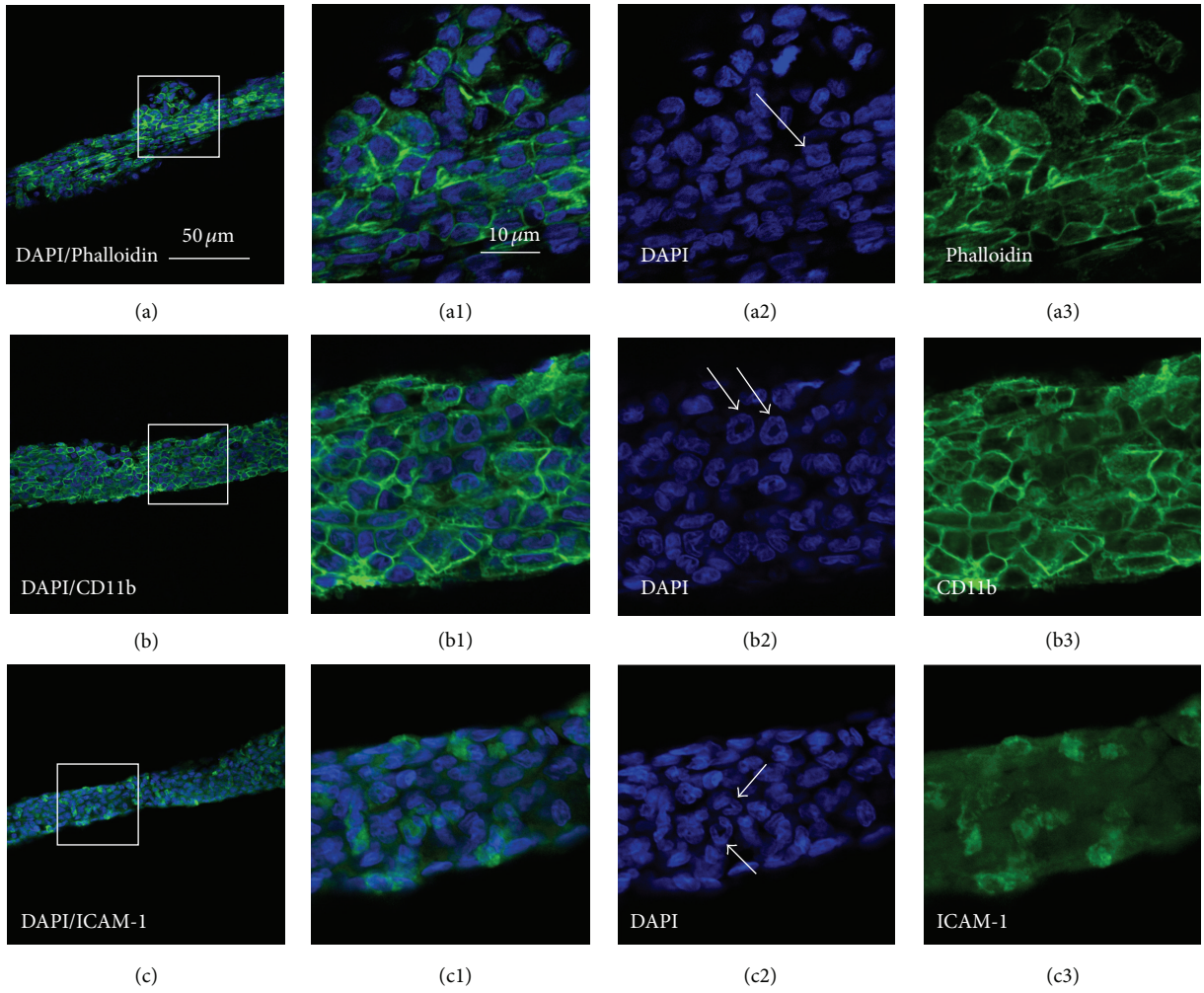

Figure 5: Cell types of primo vessels (PVs) in the infected rats determined with DAPI/phalloidin (a)–(a3), DAPI/CD11b (b)–(b3) and DAPI/ICAM-1 (c)–(c3) by fluorescent and immunofluorescent staining, respectively. (a)–(a3). DAPI/phalloidin-positive cells (a) and its higher resolutions (a1) emerged from images of DAPI (a2) and phalloidin (a3); (b)–(b3). DAPI/CD11b-positive cells (b) and its higher resolutions (b1) emerged from images of DAPI (b2) and CD11b (b3), typical multilobal nuclei showed in (b2) (white arrows); (c)–(c3): DAPI/ICAM-1-positive cells (c) and its higher resolutions (c1) emerged from images of DAPI (c2) and ICAM-1 (c3). Scale bar, the same for (a)–(c) (showed in (a)) and the same for the others (showed in (a1)).

intrinsic structure of the body and may be a pathological product which is related to the process of inflammation.

Conflict of Interests

The authors declare that there is no conflict of interests.

Authors' Contribution

Xiaoyu Wang and Hong Shi contributed equally to this work.

Acknowledgments

This work was supported by the National Key Basic Research Program 973 (no. 2010CB530507) and National Natural Science Foundation of China (no. 81173205). They thank Dr. Haifa Qiao for word polishing.

References

[1] B. H. Kim, "On the Kyungrak system," *Journal of Academy of Medical Sciences*, vol. 90, pp. 1–41, 1963.

[2] B. H. Kim, "Sanal theory," *Journal of Academy of Medical Sciences*, vol. 168, pp. 5–38, 1965.

[3] S. Fujiwara and S. B. Yu, "'Bonghan theory' morphological studies," *Igaku No Ayumi*, vol. 60, pp. 567–577, 1967.

[4] X. Liu, "Verification and confirmation about "Bonhan ducts" as meridian," *Zhen Ci Yan Jiu*, vol. 34, pp. 353–354, 2009.

[5] S. J. Cho, B. S. Kim, and Y. S. Park, "Threadlike structures in the aorta and coronary artery of swine," *Journal of International Society of Life Information Science*, vol. 22, no. 2, pp. 609–611, 2004.

[6] K. J. Lee, S. Kim, T. E. Jung, D. Jin, D. H. Kim, and H. W. Kim, "Unique duct system and the corpuscle-like structures found on the surface of the liver," *Journal of International Society of Life Information Science*, vol. 22, no. 2, pp. 460–462, 2004.

[7] H. S. Shin, H. M. Johng, B. C. Lee et al., "Feulgen reaction study of novel threadlike structures (Bonghan ducts) on the surfaces of mammalian organs," *Anatomical Record B*, vol. 284, no. 1, pp. 35–40, 2005.

[8] B. C. Lee, K. Y. Baik, H. M. Johng et al., "Acridine orange staining method to reveal the characteristic features of an intravascular threadlike structure," *Anatomical Record B*, vol. 278, no. 1, pp. 27–30, 2004.

[9] B. C. Lee, J. S. Yoo, K. Y. Baik, K. W. Kim, and K. S. Soh, "Novel threadlike structures (Bonghan ducts) inside lymphatic vessels of rabbits visualized with a Janus Green B staining method," *Anatomical Record B*, vol. 286, no. 1, pp. 1–7, 2005.

[10] Z. F. Jia, B. C. Lee, K. H. Eom et al., "Fluorescent nanoparticles for observing primo vascular system along sciatic nerve," *Journal of Acupuncture and Meridian Studies*, vol. 3, no. 3, pp. 150–155, 2010.

[11] J. P. Jones and Y. K. Bae, "Ultrasonic visualization and stimulation of classical oriental acupuncture points," *Acupuncture in Medicine*, vol. 15, no. 2, pp. 24–26, 2004.

[12] B. C. Lee, K. W. Kim, and K. S. Soh, "Visualizing the network of bonghan ducts in the omentum and peritoneum by using trypan blue," *Journal of Acupuncture and Meridian Studies*, vol. 2, no. 1, pp. 66–70, 2009.

[13] J. S. Yoo, M. Hossein Ayati, H. B. Kim, W. B. Zhang, and K. S. Soh, "Characterization of the primo-vascular system in the abdominal cavity of lung cancer mouse model and its differences from the lymphatic system," *PLoS ONE*, vol. 5, no. 4, Article ID e9940, 2010.

[14] J. S. Yoo, H. B. Kim, N. Won et al., "Evidence for an additional metastatic route: in vivo imaging of cancer cells in the primo-vascular system around tumors and organs," *Molecular Imaging and Biology*, vol. 13, no. 3, pp. 471–480, 2011.

[15] X. Wang, J. Nie, Z. Jia et al., "Impaired TGF-β signalling enhances peritoneal inflammation induced by *E. Coli* in rats," *Nephrology Dialysis Transplantation*, vol. 25, no. 2, pp. 399–412, 2010.

[16] E.-M. Lilius and J. Nuutila, "Bacterial infections, DNA virus infections, and RNA virus infections manifest differently in neutrophil receptor expression," *The Scientific World Journal*, vol. 2012, Article ID 527347, 2012.

[17] D. E. Staunton, S. D. Marlin, C. Stratowa, M. L. Dustin, and T. A. Springer, "Primary structure of ICAM-1 demonstrates interaction between members of the immunoglobulin and integrin supergene families," *Cell*, vol. 52, no. 6, pp. 925–933, 1988.

[18] B. Salomon and J. A. Bluestone, "LFA-1 interaction with ICAM-1 and ICAM-2 regulates Th2 cytokine production," *Journal of Immunology*, vol. 161, no. 10, pp. 5138–5142, 1998.

[19] C. Lawson and S. Wolf, "ICAM-1 signaling in endothelial cells," *Pharmacological Reports*, vol. 61, no. 1, pp. 22–32, 2009.

[20] D. Pilling, T. Fan, D. Huang, B. Kaul, and R. H. Gomer, "Identification of markers that distinguish monocyte-derived fibrocytes from monocytes, macrophages, and fibroblasts," *PLoS ONE*, vol. 4, no. 10, Article ID e7475, 2009.

[21] S. Lee, Y. Ryu, J.-K. Lee, K.-S. Soh, S. Kim, and J. Lim, "Primo vessel inside a lymph vessel emerging from a cancer tissue," *Journal of Acupuncture and Meridian Studies*, vol. 5, no. 5, pp. 206–209, 2012.

[22] Y.-I. Noh, S. J. Jung, and S.-S. Lee, "Isolation and morphological features of primo vessels in rabbit lymph vessels," *Journal of Acupuncture and Meridian Studies*, vol. 5, no. 5, pp. 201–205, 2012.

[23] K. Alitalo, T. Tammela, and T. V. Petrova, "Lymphangiogenesis in development and human disease," *Nature*, vol. 438, no. 7070, pp. 946–953, 2005.

[24] X. Wang, H. Shi, H. Shang et al., "Are primo vessels (PVs) on the surface of gastrointestine involved in regulation of gastric motility induced by stimulating acupoints ST36 or CV12?" *Evidence-Based Complementary and Alternative Medicine*, vol. 2012, Article ID 787683, 8 pages, 2012.

Hindawi Publishing Corporation
Evidence-Based Complementary and Alternative Medicine
Volume 2013, Article ID 510461, 8 pages
http://dx.doi.org/10.1155/2013/510461

Research Article

Evidence for the Primo Vascular System above the Epicardia of Rat Hearts

Ho-Sung Lee,[1,2] Jeong Yim Lee,[1] Dae-In Kang,[2] Se Hoon Kim,[3] Inhyung Lee,[4] Sang Hyun Park,[1] Seung Zhoo Yoon,[5] Yeon Hee Ryu,[6] and Byung-Cheon Lee[1,2]

[1] *Ki Primo Research Laboratory, Division of Electrical Engineering, KAIST Institute for Information Technology Convergence, Korea Advanced Institute of Science and Technology (KAIST), Daejeon 305-701, Republic of Korea*
[2] *Pharmacopuncture Medical Research Center, Korean Pharmacopuncture Institute, Seoul 157-200, Republic of Korea*
[3] *Department of Pathology, Yonsei University College of Medicine, Seoul 120-752, Republic of Korea*
[4] *Department of Veterinary, Seoul National University, Seoul 151-742, Republic of Korea*
[5] *Department of Anesthesiology and Pain Medicine, College of Medicine, Korea University, Seoul 136-713, Republic of Korea*
[6] *Acupuncture, Moxibustion & Meridian Research Group, Medical Research Division, Korea Institute of Oriental Medicine, Daejeon 305-811, Republic of Korea*

Correspondence should be addressed to Yeon Hee Ryu; yhryu@kiom.re.kr and Byung-Cheon Lee; donboscolee@gmail.com

Received 23 February 2013; Revised 25 June 2013; Accepted 27 June 2013

Academic Editor: M. Isabel Miguel Perez

We for the first time reported evidence for the existence of a novel network, a PVS, abovethe epicardium of the rat heart. (1) We were consecutively able to visualize the PVs and the PNs above the epicardial spaces of five rats' hearts by using Cr-Hx spraying or injection. (2) Hematoxylin and eosin (H&E) and toluidine blue staining of the PVs and the PNs showed that they consisted of a basophilic matrix; specifically the PNs contained several mast cells, some of which were degranulating into pericardial space. Also, 4′, 6-diamidino-2 phenylindole (DAPI) images of the PVs and the PNs showed that they contained various kinds of cells. (3) Transmission electron microscopic (TEM) longitudinal image of the PVs showed that the sinuses contained many granules with high-electron-density cores in parallel with putative endothelial cells. (4) TEM images of the PNs demonstrated that they consisted of lumen-containing cells surrounded by fibers and that they had mast cells that were degranulating toward the epicardium of the rat heart. The above data suggest that mast-cells-containing novel network exists above the epicardium of the rat heart.

1. Introduction

Mast cells have been considered as mediators for allergy reactions because they release histamine [1]. These big-sized cells were first reported as Ehrlich [2]. Histological works have shown these cells to be distributed in various tissues such as skin [3–6], and interestingly there has been an insistence that these mast cells are found at acupuncture points [7–9]. Moreover, oriental medical doctors have suggested that acupuncture effects may be mediated via these mast cells [10].

The concept of the acupuncture meridian system has had a long history that supports Chinese medicine and the clinical effects of acupuncture. However, even in modern medicine, the concept of the acupuncture meridian includes ambiguous ideas, such as nerve system mediation [11–13] or connective tissues [14–16]. A novel concept for the acupuncture meridian system was proposed by Bonghan Kim who demonstrated anatomical realities, Bonghan corpuscles (primo nodes (PNs)), and Bonghan ducts (primo vessels (PVs)), corresponding to the acupuncture meridian system [17].

In previous works on primo nodes and primo vessels, we first reported the existence of mast cells in primo nodes by using transmission electron microscopy [18]; our observations were confirmed by Kwon et al. with more detailed evidence [19]. Interestingly, some research showed that mast cells resided in the connective tissues of hearts [20]. Moreover, the mast cells inside the heart were thought to have specific functions as they contained renin and stem-cell-related factors [21, 22].

Table 1: Data on primo nodes and primo vessels visualized above epicardium of rat heart. The numbers are rat numbers sacrificed for these experiments which were all successfully visualized. *L* means the longest and shortest length of oval shaped primo nodes. *D* and *d* indicate the thickest and thinnest diameter of primo vessels visualized in each rat. The methods applied were spray or injection method.

Primo nodes and primo vessels above epicardium of heart of rat				
Number	L (mm × mm)	D (μm)	d (μm)	Method
1	0.15 × 0.07	29	10	Spray
	0.09 × 0.07	22	8	Spray
2	0.23 × 0.16	28	10	Spray
	0.14 × 0.07	19	12	Spray
	0.16 × 0.09	27	15	Spray
	0.09 × 0.06	27	17	Spray
3	0.13 × 0.13	17	5	Injection
	0.56 × 0.19	22	14	Injection
	0.20 × 0.42	22	14	Injection
	0.25 × 0.18	22	14	Injection
4	0.20 × 0.41	33	24	Injection
	0.24 × 0.11	38	26	Injection
	0.33 × 0.11	20	11	Injection
5	0.08 × 0.04	13	4	Injection
	0.06 × 0.04	27	9	Injection
	0.07 × 0.02	9	6	Injection
	0.17 × 0.13	17	4	Injection
	0.07 × 0.05	11	7	Injection
	0.12 × 0.03	14	4	Injection
	0.07 × 0.03	6	4	Injection
Average ± SD	0.17 ± 0.12 × 0.12 ± 0.11	21.15 ± 8.20	10.90 ± 6.33	

Here, we for the first time report our findings on a novel network system above the rat heart by using chromium-hematoxylin staining. We also use light and electron microscope images to demonstrate that this system of primo vessels and primo nodes contains mast cells. In the discussion, we shall share recent findings on mast cells in the heart and in the acupuncture meridian system.

2. Material and Method

2.1. Laboratory Animal Preparation. Male Wistar rats aged 5~6 weeks ($n = 7$; Samtako Bio Korea, Bio Korea, Gyunggi-Do, Korea) were housed in a room that was temperature controlled at 24~25°C and light controlled with a 12/12-hour light/dark cycle and were provided water and commercial rat chow ad libitum. The rats were acclimatized for 1 week before the experiment. These experiments were carried out in accordance with the guidelines (KAIST approval number: KA2011-13) of the Laboratory Animal Care Advisory Committee of the Korea Advanced Institute of Science and Technology (KAIST). The rats were anesthetized by using an intramuscular injection of a combination of ketamine (45 mg/kg) and lompun (5 mg/kg) into the right hind femoral limb.

2.2. Preparation of Chromium-Hematoxylin Solution (Cr-Hx). Fifty ml of hematoxylin (1%) and 50 ml of chromium potassium sulfate (3%) were mixed to make 100 ml of a Cr-Hx solution to which 0.1 g of potassium iodate had been added. The solution was boiled until it became a deep blue. The deep-blue solution was filtered with a 0.45 μm pore size membrane filter before use. For the visualizing experiment, we diluted Cr-Hx by a factor of 10 with phosphate buffered saline (PBS, pH 7.4).

2.3. Surgical and Observation Procedures. In order to visualize the network of the primo vascular system (PVS) that consists of primo nodes (PNs) and primo vessels (PVs), we used different staining methods. One method was to spray 10% Cr-Hx solution in phosphate-buffered saline at pH 7.4 (PBS) onto the surfaces of the epicardia of the rat hearts after the chests had been opened under deep anesthesia. In the other method, which was better for visualizing the primo vascular system above the epicardium of the rat heart, we opened the abdominal cavity to find the diaphragm and injected about 0.5 ml of 10% Cr-Hx solution in PBS into the pericardial cavity from the opposite side of diaphragm for 30 minutes to 2 hours. However, because the Cr-Hx solution is injected manually, the injection point may differ slightly from injection to injection. In order to overcome this shortcoming, we confirmed where the Cr-Hx solution had been injected by dissecting the chest under a stereomicroscope (SZ61, Olympus, Japan). After the chest had been opened, we exposed the transparent pericardium and visualized the PVS in the pericardial cavity; then, we cut the pericardium and washed it with PBS to clean out the Cr-Hx solution remaining in the epicardium of the heart. The washing step was performed under a stereomicroscope during the dissection of the rat heart.

2.4. Microscopic Examination. The isolated whole specimens were first stained with 4′,6′-diamidino-2-phenylindole (DAPI) and examined using light microscopy. For the

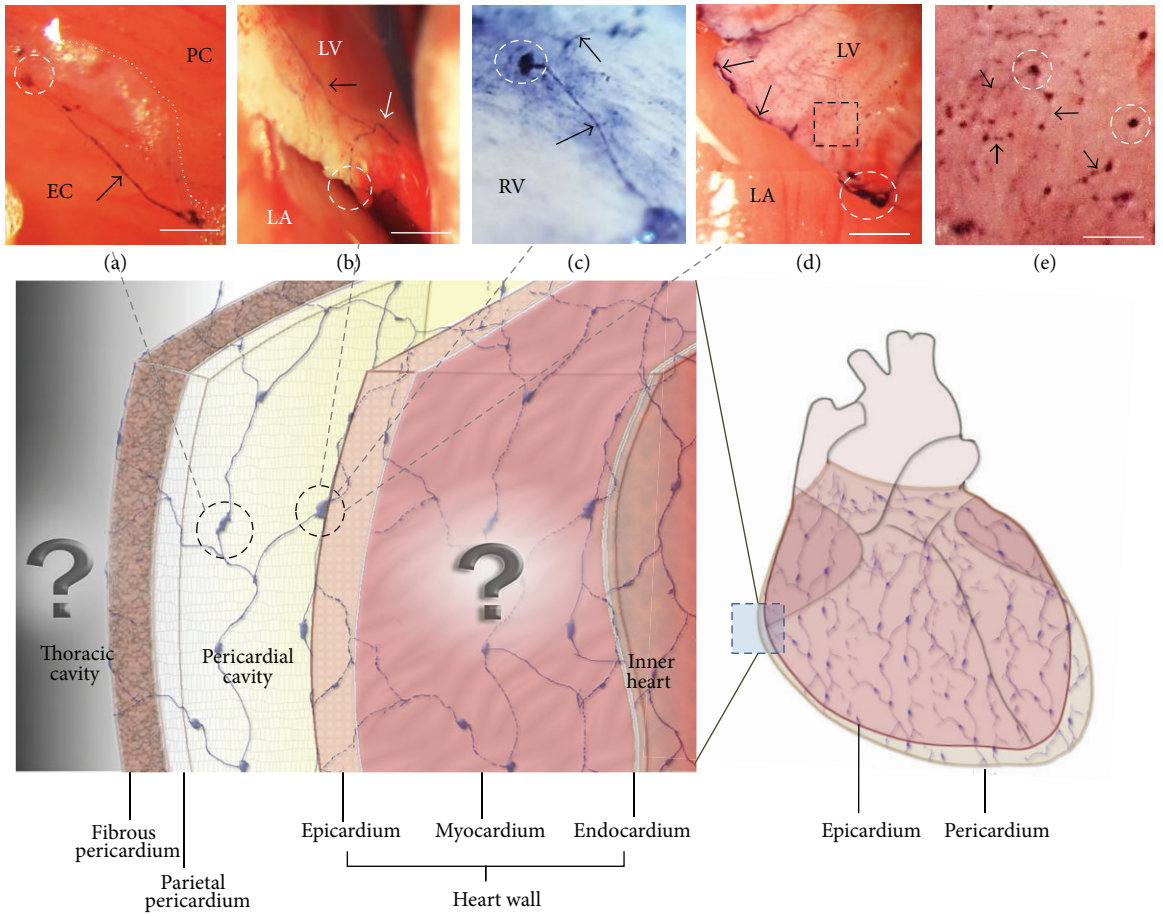

Figure 1: Illustration of the PVS above the epicardium of the rat heart with real stereoscopic images of the PVS stained with Cr-Hx. The illustration suggests the network system of the PVS; the two question marks remain to be studied. The real stereomicroscopic images in (a), (b), (c), and (d) show PNs (dotted circles) and PVs (arrows). The stereoscopic image in (e) is a magnified image of the area in the dotted rectangle of image (d). Tiny node-like structures are visualized in image (e). The scale bars of (a), (b), (c), (d), and (e) are 507 μm, 1106 μm, 207 μm, 430 μm, and 56 μm, respectively.

light microscope and the transmission electron microscope examinations of the PV cross sections, the specimens were fixed in 2.5% paraformaldehyde and 2.5% glutaraldehyde in a neutral 0.1 M phosphate buffer for 1 hour. The specimens were postfixed for 1 hour in 1% (w/v) osmic acid dissolved in PBS, dehydrated in graded ethanol, and embedded in Epon812 (EMS, Fort Washington, PA, USA). Semithin sections of 1 μm in thickness stained with 1% toluidine blue were observed and photographed under a light microscope (BX 53, Olympus) with a CCD camera (eXcope X3, DIX, Korea). Ultrathin sections were cut and mounted on nickel grids and were double stained with uranyl acetate, followed by staining with lead citrate. The sections were examined with a Technai G2 Spirit transmission electron microscope (FEI, USA).

3. Results

As recorded in Table 1, we consistently were able to visualize the PVs and the PNs above the epicardia of five rats' hearts. The PNs were oval shaped, and the PVs looked threadlike with diameters of about 15 μm. Some stereomicroscopic images of PVs and PNs visualized by using Cr-Hx staining, along with an illustration of the heart, are shown in Figure 1. Figure 1 shows distinctive images of PNs and PVs; specifically, a fine network view of a PV is demonstrated under high magnification in image (e). A representative magnified image is also shown in Figure 2, which shows PNs and PVs stained with DAPI and demonstrates the distinctive network of the PV. We took one PN with a PV to reveal the pattern of nuclei.

In order to investigate cross-sectional images of PNs and PVs, we sectioned and stained them with hematoxylin and eosin (H&E). Figure 3 presents representative hematoxylin-and-eosin-stained images of PNs and PVs above the epicardium of the rat heart. The PNs and the PVs are basophilic; however, the epicardium-containing heart tissues are eosinophilic. For more information on the relative positions of the epicardium and the PVS, as shown in Figure 4, we used two images. One image was H&E-stained PVs and PNs positioned apart from the epicardium. The other involved toluidine-blue-stained PNs almost embedded in the epicardium of the rat heart. Noticeably, the PN contained mast cells, among which a mast cell was observed to be degranulating into the pericardium of the rat heart.

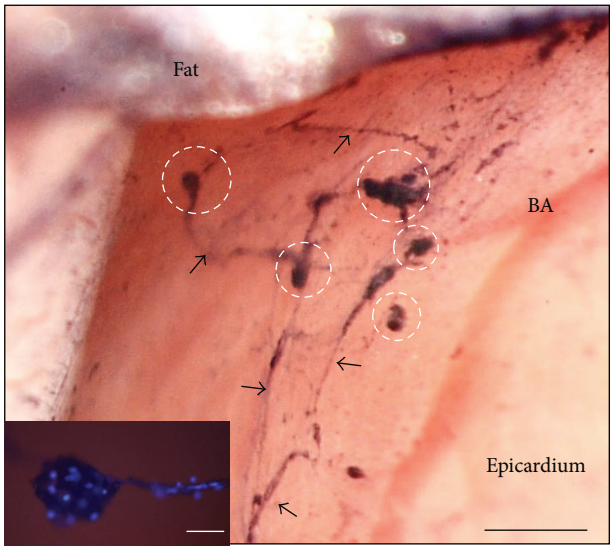

Figure 2: Representative stereoscopic image of the PVS, stained with Cr-Hx, above the epicardium of the rat heart. Dotted circles indicate primo PNs, and arrows mean PVs. BA means branch of artery, which is not stained with Cr-Hx. The inset fluorescence image of PNs and PVs stained with (DAPI) demonstrates that they have several kinds of cells. The scale bars of the main figure and the inset are 270 μm and 40 μm, respectively.

For more detailed information on the PNs and the PVs, we conducted transmission electron microscopy (TEM). Figures 5 and 6 demonstrate that PNs consist of two kinds of fibers: one is collagen fibers, and the other is very fine fibers. Also, TEM images of PNs clearly show mast cells' degranulating. As shown in Figure 7, we also found that longitudinal images of PNs showed the presence of high-electron-density microgranules in the lumen of the PV.

4. Discussion

The data in this research suggest three characteristics for the newly found network, the primo vascular system, and we observed the following. (1) Hematoxylin-and-eosin (H&E) and toluidine-blue staining of the PVs and the PNs showed that they consisted of a basophilic matrix; specifically, a PN was observed to contain several mast cells, one of which was degranulating into the pericardial space. The DAPI-stained PVs and PNs showed that they contained some cells. (2) Transmission-electron-microscope (TEM) longitudinal image of the PVs showed that the lumen contained many granules with high-electron-density cores in parallel with putative endothelial cells. (3) A TEM image of a PN demonstrated that it consisted of lumen-containing cells surrounded by fibers and that it had mast cells degranulating toward the epicardium of the rat heart. Given all the experimental data, we draw a tentative conclusion that a novel system exists under the pericardial space of the rat heart.

Kim was the first to discover a network floating freely above internal organs such as the heart [17]. He suggested the following peculiar characteristic of the network system (the primo vascular system): it contained some flowing DNA that was different from nuclei DNA and extracellular DNA (eDNA). Thus, the strong basophilic matrix that we observed could be interpreted as supporting his eDNA concept. In a previous work, we were able to demonstrate the existence of eDNA in the PVS above the pia mater of the rat brain [23], and recently, we were able to detect DNA signals in primo vessels floating in the lymphatic vessels of rabbits [24]. Therefore, one of authors, Lee BC, presented a hypothesis for an overall feature of the PVS; that is, the PVS is an eDNA circulation system for the acupuncture meridian system [25, 26].

Another interestingly finding is the existence of mast cells in PNs. Recently, the importance of mast cells emerged after reports that mast cells contained renin and stem-cell-related factors [1, 20, 27, 28]. This research shows the importance of mast cells in terms of renin-containing cells because renin has been considered to be a key blood-pressure-modulating hormone and because the newly found network is located under the pericardial space of the rat heart [22, 29]. Recently, cardiologists have paid attention to the existence of mast cells in connective tissues inside the heart as renin is mainly found only in the kidney as a renin-angiotensin system [21]. However, the PNs in the newly found network contained several mast cells, some of which were observed to be degranulating into not only the pericardial space but also the epicardium of the rat heart. Thus, our data on mast cells suggest that the primo network above the epicardium of the rat heart may have a role in modulating blood pressure directly.

On the other hand, acupuncture points have been reported to consist of more mast cells than nonacupuncture points. This finding encouraged oriental medical doctors to connect mast cells to the function of acupuncture. Many clinical and research data reported that the stimulation of acupuncture points modulated blood pressure [30]. All of the above data and ideas imply that newly found PVS above the heart plays a role in transmitting certain signals to modulate blood pressure.

During examination of TEM images, we noticed that the PN had sinus-containing cells; moreover, the PN connected with the PV clearly showed high-electron-density microvesicles aligned in the lumen structure along adjacent cells. Noticeably, these microvesicles in the PN and the PV share characteristics similar to those of general endothelial cells in terms of the TEM image. Based on our analysis of the TEM images, we temporarily conjecture that the PVS found above the heart may be endothelial cells with fluid channels. Precisely, we examined the microvesicles found in the PV and found them to be very similar to neuroendocrine microvesicles in terms of high electron density, size, and overall morphology [31]. This conjecture comes from Bonghan theory [17], our previous hormone analysis [32], and the characteristics of Cr-Hx staining, which was used to visualize the PVS [33].

Thus, given these TEM data, we paid attention to Bonghan theory that the PVS functions as a hormone-transporting channel. The data presented here and in previous works provide evidence that supports Bonghan Kim's first insistence that the PVS plays a role in transporting hormones independently from the blood stream. As Bonghan Kim considered

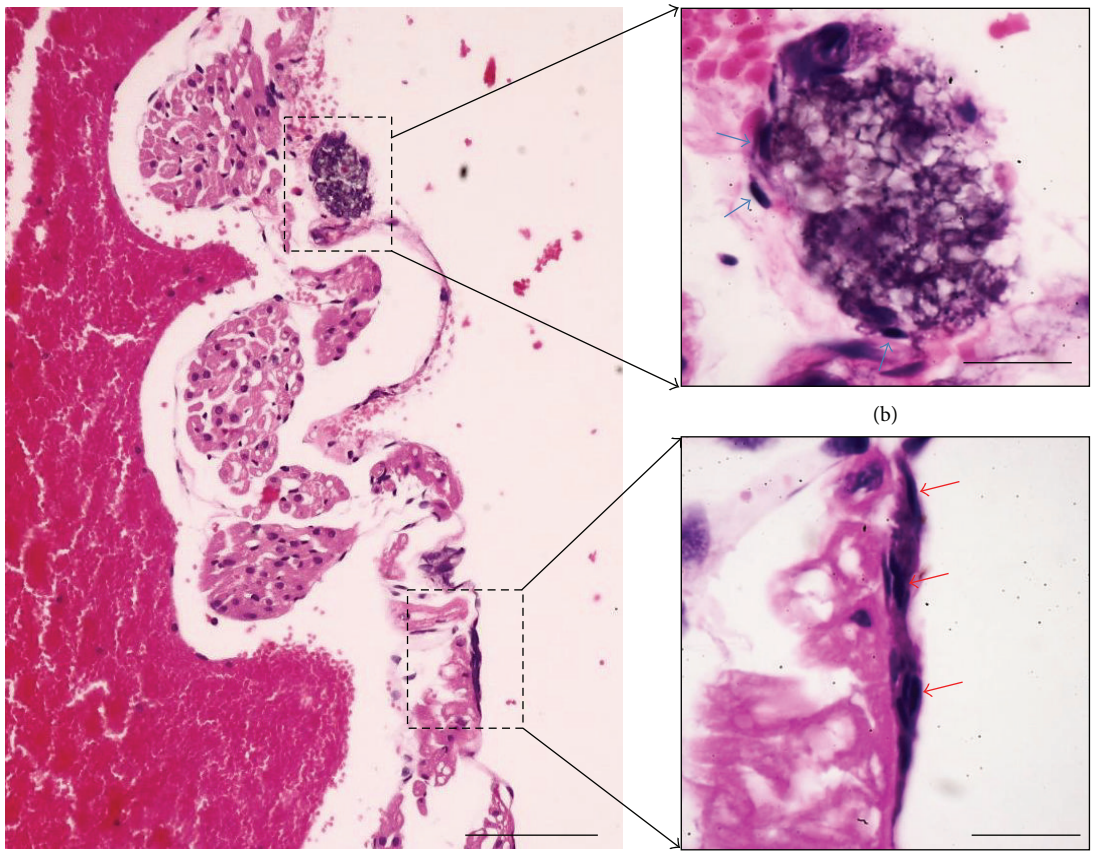

Figure 3: (a) Low-magnification image showing two basophilic structures located above the eosinophilic epicardium of the rat heart. The two structures are magnified into (b) and (c), respectively. (b) Sectioned PN enveloped by heavily hematoxylin-and-eosin-stained cells (arrows). (c) Longitudinal-sectioned PV also consisting of strongly hematoxylin-and-eosin-stained cells (arrows). The scale bars of (a), (b), and (c) are 85 μm, 15 μm, and 18 μm, respectively.

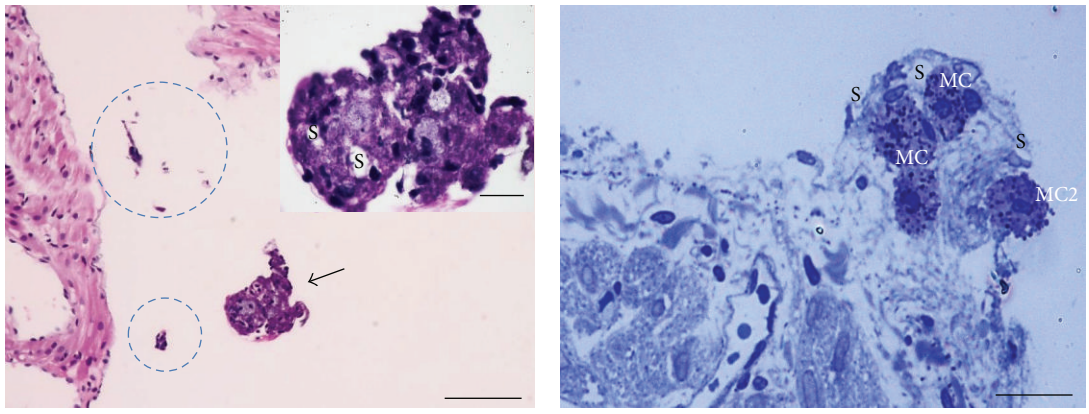

Figure 4: Comparative positions of a PN and a PV stained with (a) hematoxylin and eosin (H&E) and with (b) toluidine blue (TB). Image (a) shows a randomly cut PV (dotted circles) and a cross-sectioned PN (arrow) above the epicardium (EC). H&E staining of the PV and the PN suggest they are basophilic; however, the epicardium is eosinophilic. The inset image is a magnified view of a PN with sinuses (S). Image (b) shows a toluidine-blue-stained PN in which four mast cells (MC) are found. Among the MCs, one MC is just releasing from the PN. The scale bars of (a), (a)'s inset, and (b) are 30 μm, 12 μm, and 25 μm, respectively.

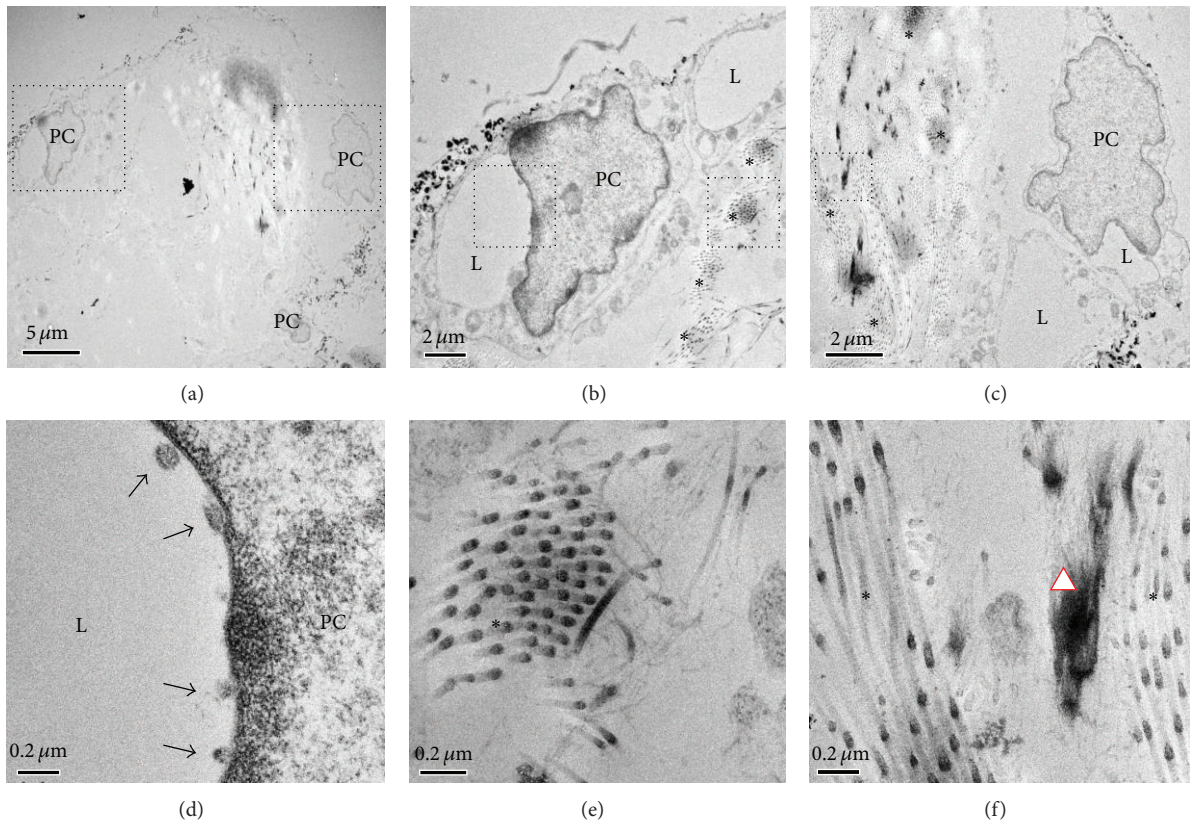

Figure 5: Transmission electron microscopy images of cross-sectioned PNs. (a) Low-magnification view of a PN in which the outermost area consists of two cells (PC: putative endothelial cells). (b) Magnified view of the left rectangle in image (a), showing distinctive lumens (L) in the PC. (c) Magnified view of the right rectangle in image (a), also showing a lumen-containing PC. (d) High-magnification view of the lumen (L) indicated by the rectangle in (b); in (d) some microgranules are seen (arrows). Asterisks in images (b) and (c) are magnified into images (e) and (f), respectively, and demonstrate bundles of collagen fibers. The triangle in image (f) means cluster of fine fibers.

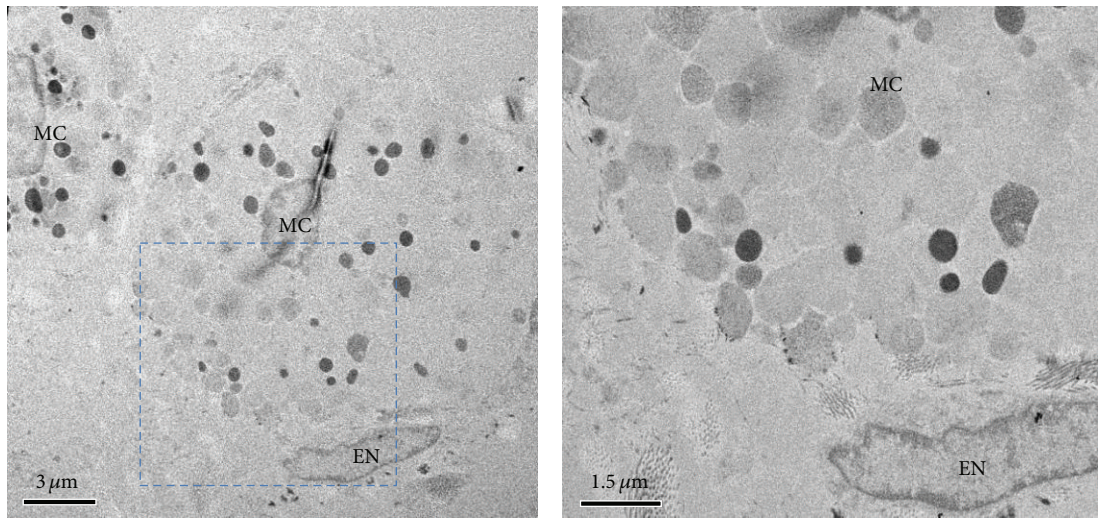

Figure 6: Transmission electron microscopy images of mast cells in cross-sectioned PNs. (a) Low-magnification view of two mast cells just above the EN of the heart. (b) Magnified view of the rectangle in image (a) shows more distinctive granules just above the EN.

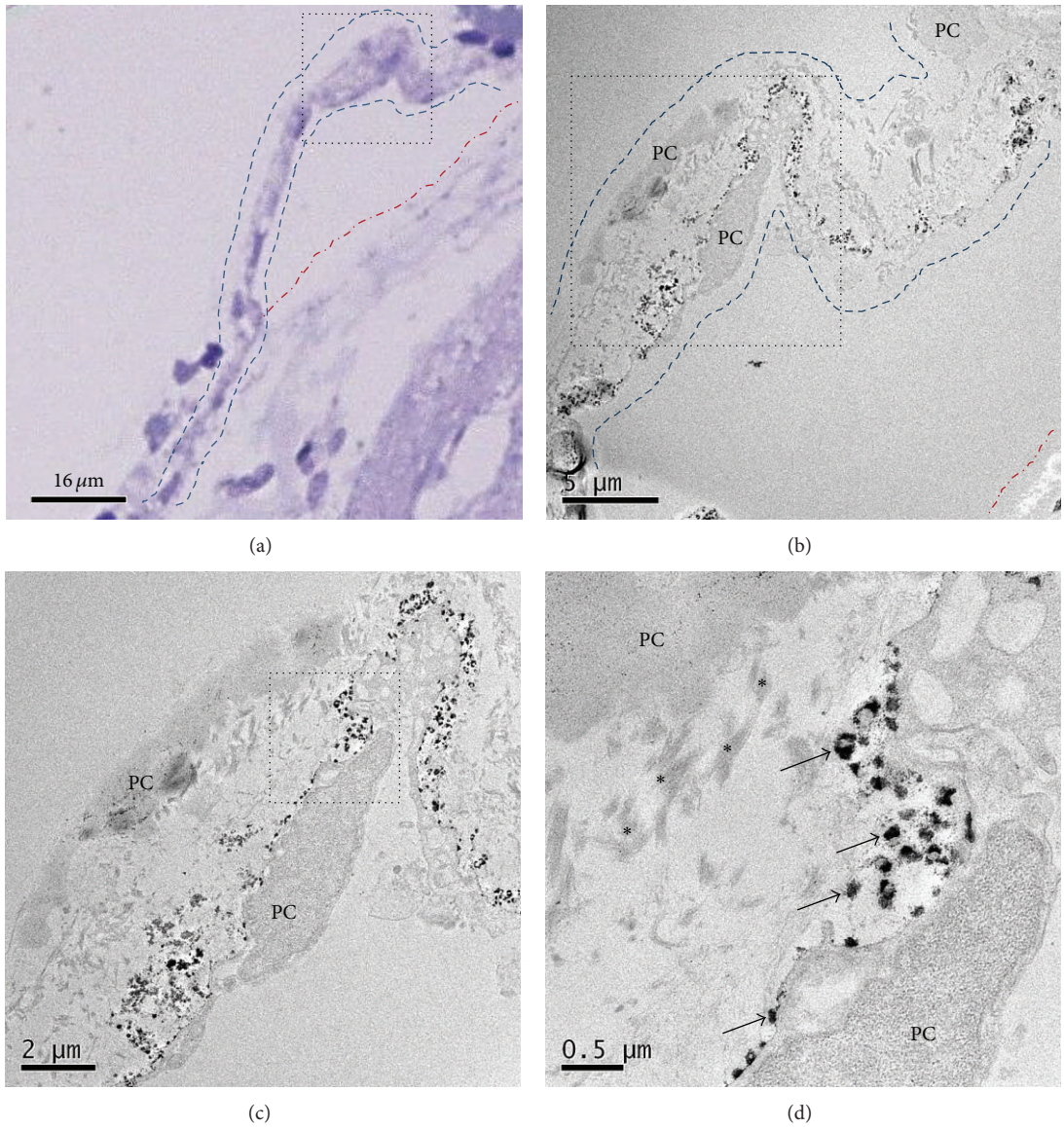

Figure 7: Light and transmission electron microscopy (TEM) images of a longitudinal sectioned PV just above the epicardium. Image (a) shows a toluidine blue-stained PV (dotted lined) above the epicardium (red-colored line). (b) TEM low-magnification view of longitudinal sectioned PV corresponding to the rectangle of image (a). Red-colored line also indicates the epicardium. Image (c) is magnified from the rectangle of (b). Image (d) shows high magnification of the rectangle of (c) in which there are high-electron-density microgranules (arrows) in the lumen of the PV. Asterisks indicate the presence of fine fibers. PC means putative endothelial cells.

the PVS to be an anatomical acupuncture meridian system, our findings, as well as those of others, should encourage both western cardiologists and oriental medical doctors to investigate the PVS above the heart in terms of both cardiology and a heart-related meridian system.

Acknowledgments

This work was supported by a National Research Foundation of Korea (NRF) Grant funded by the Korean government's Ministry of Education, Science, and Technology (MEST) in 2010 (no. 2010-0025289) and by Korean Pharmacopuncture Institute and Korea Institute of Oriental Medicine (KIOM) Grant (K13290).

References

[1] G. Krishnaswamy, O. Ajitawi, and D. S. Chi, "The human mast cell: an overview," *Methods in Molecular Biology*, vol. 315, pp. 13–34, 2006.

[2] P. Ehrlich, *Beitrage zur theorie und praxis der histologischen farburg [Thesis]*, University of Leipzig, Leipzig, Germany, 1878.

[3] H. Matsushima, N. Yamada, H. Matsue, and S. Shimada, "The effects of endothelin-1 on degranulation, cytokine, and growth

factor production by skin-derived mast cells," *European Journal of Immunology*, vol. 34, no. 7, pp. 1910–1919, 2004.

[4] P. T. Kovanen, "Mast cells in human fatty streaks and atheromas: implications for intimal lipid accumulation," *Current Opinion in Lipidology*, vol. 7, no. 5, pp. 281–286, 1996.

[5] Y. Kitamura, M. Shimada, K. Hatanaka, and Y. Miyano, "Development of mast cells from grafted bone marrow cells in irradiated mice," *Nature*, vol. 268, no. 5619, pp. 442–443, 1977.

[6] T. Edmunds and R. J. T. Pennington, "Mast cell origin of "myofibrillar protease" of rat skeletal and heart muscle," *Biochimica et Biophysica Acta*, vol. 661, no. 1, pp. 28–31, 1981.

[7] D. Zhang, G. Ding, X. Shen et al., "Role of mast cells in acupuncture effect: a pilot study," *Explore*, vol. 4, no. 3, pp. 170–177, 2008.

[8] Z. Zhu and R. Xu, "Morphometric observation on the mast cells under the acupuncture meridian lines," *Acupuncture Research*, vol. 15, no. 2, pp. 157–158, 1990.

[9] T.-F. He and Y.-F. Chen, "Advances in studies on the correlation between acupuncture-moxibustion treatment and mast cells," *Chinese Acupuncture & Moxibustion*, vol. 30, no. 1, pp. 84–87, 2010.

[10] T.-F. He, S.-H. Zhang, L.-B. Li, W.-J. Yang, J. Zhu, and Y.-F. Chen, "Effects of acupuncture on the number and degranulation ratio of mast cells and expression of tryptase in synovium of rats with adjuvant arthritis," *Journal of Chinese Integrative Medicine*, vol. 8, no. 7, pp. 670–677, 2010.

[11] F. Kagitani, S. Uchida, and H. Hotta, "Afferent nerve fibers and acupuncture," *Autonomic Neuroscience*, vol. 157, no. 1-2, pp. 2–8, 2010.

[12] A. I. Tsunikov, R. S. Megdiatov, and I. V. Grachev, "Acupuncture therapy of neuralgia of the trigeminal nerve," *Sovetskaya Meditsina*, no. 9, pp. 102–104, 1983.

[13] K. Toda, "Effect of acupuncture on afferent nerve," *Kokubyo Gakkai Zasshi*, vol. 48, no. 2, p. 251, 1981.

[14] H. M. Langevin and J. A. Yandow, "Relationship of acupuncture points and meridians to connective tissue planes," *Anatomical Record*, vol. 269, no. 6, pp. 257–265, 2002.

[15] H. M. Langevin, D. L. Churchill, J. Wu et al., "Evidence of connective tissue involvement in acupuncture," *The FASEB Journal*, vol. 16, no. 8, pp. 872–874, 2002.

[16] H. M. Langevin, D. L. Churchill, and M. J. Cipolla, "Mechanical signaling through connective tissue: a mechanism for the therapeutic effect of acupuncture," *The FASEB Journal*, vol. 15, no. 12, pp. 2275–2282, 2001.

[17] B. H. Kim, "The Kyungrak system," *Journal of the Academy of Medical Sciences of the Democratic People's Republic of Korea*, no. 6, pp. 1–38, 1965.

[18] B.-C. Lee, J. S. Yoo, V. Ogay et al., "Electron microscopic study of novel threadlike structures on the surfaces of mammalian organs," *Microscopy Research and Technique*, vol. 70, no. 1, pp. 34–43, 2007.

[19] B. S. Kwon, C. M. Ha, S. Yu et al., "Microscopic nodes and ducts inside lymphatics and on the surface of internal organs are rich in granulocytes and secretory granules," *Cytokine*, vol. 60, no. 2, pp. 587–592, 2012.

[20] W. R. Sperr, H. C. Bankl, G. Mundigler et al., "The human cardiac mast cell: localization, isolation, phenotype, and functional characterization," *Blood*, vol. 84, no. 11, pp. 3876–3884, 1994.

[21] M. Hara, K. Ono, M.-W. Hwang et al., "Evidence for a role of mast cells in the evolution to congestive heart failure," *Journal of Experimental Medicine*, vol. 195, no. 3, pp. 375–381, 2002.

[22] C. J. Mackins, S. Kano, N. Seyedi et al., "Cardiac mast cell-derived renin promotes local angiotensin formation, norepinephrine release, and arrhythmias in ischemia/reperfusion," *Journal of Clinical Investigation*, vol. 116, no. 4, pp. 1063–1070, 2006.

[23] H. S. Lee and B. C. Lee, "Visualization of the network of primo vessels and primo nodes above the pia mater of the brain and spine of rats by using Alcian blue," *Journal of Acupuncture and Meridian Studies*, vol. 5, no. 5, pp. 218–225, 2012.

[24] H. Huh, B. C. Lee, S. H. Park et al., "Composition of the extracellular matrix at lymphatic novel threadlike structure: is it keratin?" *Evidence-Based Complementary and Alternative Medicine*, vol. 2013, Article ID 195631, 6 pages, 2013.

[25] B. C. Lee, "A hypothesis for a hidden circulation system with cell-free DNA molecules, microvesicles and microparticles: the 5 primo vascular system (Bonghan system), a putative acupuncture meridian system," *Journal of Extracellular Vesicles*, vol. 2, Article ID 20826, 2013.

[26] B. C. Lee, J. W. Yoon, S. H. Park, and S. J. Yoon, "Primo Vascular System, The system of circulation and interacting extracellular DNA Microvesicles," *Evidence-Based Complementary and Alternative Medicine*. In press.

[27] V. Patella, I. Marinò, E. Arbustini et al., "Stem cell factor in mast cells and increased mast cell density in idiopathic and ischemic cardiomyopathy," *Circulation*, vol. 97, no. 10, pp. 971–978, 1998.

[28] K. Norrby, "Mast cells and angiogenesis: review article," *APMIS*, vol. 110, no. 5, pp. 355–371, 2002.

[29] A. C. Reid, R. B. Silver, and R. Levi, "Renin: at the heart of the mast cell," *Immunological Reviews*, vol. 217, no. 1, pp. 123–140, 2007.

[30] T. Williams, K. Mueller, and M. W. Cornwall, "Effect of acupuncture-point stimulation on diastolic blood pressure in hypertensive subjects: a preliminary study," *Physical Therapy*, vol. 71, no. 7, pp. 523–529, 1991.

[31] M. Krokowski, J. Hoch, A. C. Feller, H.-W. Bernd, C. Thorns, and S. Krueger, "Basal cell carcinoma with neuroendocrine differentiation arising in a scar: a case report," *Dermatology Online Journal*, vol. 15, no. 10, article 4, 2009.

[32] J. Kim, V. Ogay, B.-C. Lee et al., "Catecholamine-producing novel endocrine organ: bonghan system," *Medical Acupuncture*, vol. 20, no. 2, pp. 97–102, 2008.

[33] H. S. Lee, W. H. Park, A. R. Je, H. S. Kweon, and B. C. Lee, "Evidence for novel structures (primo vessels and primo nodes) floating in the venous sinuses of rat brains," *Neuroscience Letters*, vol. 522, no. 2, pp. 98–102, 2012.

Hindawi Publishing Corporation
Evidence-Based Complementary and Alternative Medicine
Volume 2013, Article ID 350815, 12 pages
http://dx.doi.org/10.1155/2013/350815

Research Article

Gross Morphological Features of the Organ Surface Primo-Vascular System Revealed by Hemacolor Staining

Chae Jeong Lim,[1] Jong-Hyun Yoo,[2] Yongbaek Kim,[3] So Yeong Lee,[1] and Pan Dong Ryu[1]

[1] *Laboratory of Veterinary Pharmacology, College of Veterinary Medicine and Research Institute for Veterinary Science, Seoul National University, Seoul 151-742, Republic of Korea*
[2] *Laboratory Animal Research Center, College of Pharmacy, Hanyang University, Ansan 426-791, Republic of Korea*
[3] *Laboratory of Clinical Pathology, College of Veterinary Medicine, Seoul National University, Seoul 151-742, Republic of Korea*

Correspondence should be addressed to Pan Dong Ryu; pdryu@snu.ac.kr

Received 11 February 2013; Revised 30 June 2013; Accepted 2 July 2013

Academic Editor: Walter J. Akers

The primo-vascular system (PVS), which consists of primo-vessels (PVs) and primo-nodes (PNs), is a novel thread-like structure identified in many animal species. Various observational methods have been used to clarify its anatomical properties. Here, we used Hemacolor staining to examine the gross morphology of organ-surface PVS in rats. We observed a sinus structure (20–50 μm) with a remarkably low cellularity within PNs and PVs and several lines of ductules (3–5 μm) filled with single cells or granules (~1 μm) in PV. Both sinuses and ductules were linearly aligned along the longitudinal axis of the PVS. Such morphology of the PVS was further confirmed by acridine orange staining. In PN slices, there was a honeycomb-like structure containing the granules with pentagonal lumens (~10 μm). Both PVs and PNs were densely filled with WBCs, RBCs, and putative mast cells (MCs), which were 90.3%, 5.9%, and 3.8% of the cell population, respectively. Granules in putative MCs showed spontaneous vibrating movements. In conclusion, the results show that Hemacolor, a simple and rapid staining system, can reveal the gross morphological features reported previously. Our findings may help to elucidate the structure and function of the PVS in normal and disease states in future studies.

1. Introduction

The primo-vascular system (PVS) is a novel anatomical network and new circulatory system. In the 1960s, Bong-Han Kim claimed that the PVS represented the meridians of acupuncture [1]. However, studies on the PVS have long been hampered because their isolation and identification have not been feasible. Recently, Dr. Soh's group developed several PVS-visualizing techniques and characterized the distribution, structures, and functions of the PVS [2, 3].

The PVS has been observed in small laboratory animals, such as mice, rats, and rabbits [4]. It has been consistently identified in various tissues including the surfaces of internal organs [5–8], blood vessels [9, 10], and lymphatic vessels [11] using special dyes, such as trypan blue [12, 13], acridine orange [9], and alcian blue [10, 11]. The organ-surface PVS has been primarily used in various PVS studies, as it is semitransparent, freely movable, and relatively easy to recognize with careful gross examination.

Based on various electron microscopic studies, Lee et al. [14] showed a bundle structure composed of several subducts (~10 μm) and sinuses of various diameters in primo-vessels (PVs). Ogay et al. [15] reported follicle-like formations containing clusters of immune cells and several small channels or ductules (7–15 μm) inside or near the formation in primo-nodes (PNs). Ogay et al. [15] also showed a bundle structure of several ductules (10–20 μm) exhibiting characteristic rod-shaped nuclei in whole PVs and a tissue formation containing several lumens (6–10 μm) in cross-sections of PVs.

At the cellular level, the PVS contains various types of immune cells, such as macrophages, mast cells (MCs), and eosinophils, which implies the system's potential role in immune responses [14–17]. In addition, PVS cells have been categorized into four major types based on current-voltage *(I-V)* relations recorded from the cells in PN slices [7]. Some PVS cells are much larger and rounder (10–20 μm) with granules, whereas others are much smaller and round or appear similar to red blood cells (RBCs) [7, 8].

In previous studies, diverse staining methods and light and electron microscopy have been used to identify the PVS and characterize its structures [2]. For example, trypan blue has been used to identify the PVS in situ [12, 13]. Various DNA-specific staining dyes and confocal laser scanning microscopy (CLSM) analysis have been used to identify rod-shaped nuclei, the hallmark of PVs [2, 11]. Hematoxylin and eosin (H&E) staining has been mainly used for PVS cytology [15], whereas electron microscopy has been used for the ultrastructural characterization of the PVS (e.g., ductules, bundle structure) [14, 15]. However, trypan blue staining is limited in elucidating the cytology and anatomical structure of the PVS although it is simple to use. In addition, long processing times (about 24 hours) and/or sophisticated instruments like electron microscopes and CLSM are needed in the other methods. Thus, it would be desirable to determine rapid and simple methods to identify and morphologically characterize the PVS. In this study, we tested Hemacolor reagents, a rapid staining system used in hematology and clinical cytology [18, 19], to determine whether the staining can be suitable for PVS studies, in combination with a recently developed PVS-slice preparation method [7, 8].

2. Materials and Methods

2.1. Isolation of Organ-Surface PVS. Male Sprague-Dawley rats weighing 282 ± 13 g ($n = 23$; Orientbio Inc., Kyunggi-do, Korea) were housed in a temperature-controlled environment (20–26°C) with a relative humidity range of 40–70% under a 12 h light/dark cycle; they received water and standard rodent chow *ad* libitum. All animal experiments were carried out in accordance with the guidelines of the Laboratory Animal Care Advisory Committee of Seoul National University. The rats were anesthetized with an anesthetic cocktail (Zoletil, 25 mg/kg; xylazine, 10 mg/kg) administered by intramuscular injection. The abdomen of each rat was incised, and the PVS was sampled under a stereomicroscope from the surface of the abdominal organs, according to the methods reported previously [5, 12]. Briefly, we identified the organ-surface PVS tissue based on established standards: milky colored, semitransparent, and slightly flexible tissue composed of nodes and vessels.

2.2. PVS-Slice Preparation. We prepared the PVS slices according to the published protocol [7, 8]. Briefly, the intact PVS tissues that were isolated from the surface of internal organs were taken in a Ca^{2+}-free Krebs solution supplied with O_2 (95%)-CO_2 (5%) and maintained in an ice-cooled Krebs solution (0–4°C). Meanwhile, 4% low-melting agarose (Lonza, Rockland, ME, USA) dissolved at 70°C was poured into a cubic frame (25 × 25 × 25 mm). When the agarose solution was chilled to 34–37°C, the PVS was embedded into the frame and then cooled on ice until the viscous solution was completely solidified. The agarose block was then taken out of the frame and firmly affixed to the bottom of a slicing chamber using instant glue before it was sectioned at a thickness of 200 μm using vibrating microtome (1000 Plus, Vibratome, St. Louis, MO, USA). The resulting slices were incubated for 20–30 min in the oxygenated Krebs solution composed of (in mM) NaCl (120.35), $NaHCO_3$ (15.5), glucose (11.5), KCl (5.9), $CaCl_2$ (2.5), NaH_2PO_4 (1.2), and $MgSO_4$ (1.2) followed by staining at 31°C [20].

2.3. Staining Methods for the Identification of PVS Cells. Hemacolor staining, a system of three solutions (solution 1, methanol fixative; solution 2, eosin stain; solution 3, methylene blue stain), was performed for the rapid cellular identification of PVS cell's WBCs and RBCs. The overall staining procedure of the PVS is as follows: either a PVS slice (200 μm) or the whole PVS tissue was transferred into a drop of Hank's balanced salt solution (HBSS; Sigma, St. Louis, MO, USA) on slide glass and air-dried completely without water for 1–3 min. The slide glass was then dipped into and taken out of the solution 1 ten times for 10 sec. This staining process was repeated for solutions 2 and 3 and completed within 30 sec. Each stained PVS sample was kept in a drop of phosphate buffer solution (pH 7.2) for 20 sec, dipped into a distilled water three times for 10 sec, completely air-dried for 3–5 min, and then mounted with Canada balsam (Sigma). Using a stereomicroscope, low (100x and 200x) and high (1000x) magnification digital images were obtained from the Hemacolor-stained PVS cells. We took the pictures of the PVS tissues containing a micromeasure with a minimal unit of 0.01 mm and measured the luminal diameter of the tissues from the digital images. H&E staining, a method widely used for the morphological evaluation of various tissue types, was carried out to confirm the cellular composition of PVS cells and to determine their relative abundance. The PVS tissue was initially fixed overnight in 10% neutral buffered formalin, routinely processed, embedded in paraffin, and cross-sectioned at 3 μm. The resulting PVS sections were stained with H&E as a part of the routine intake procedure. To identify DNA and RNA components in the PVS cells, each PVS sample was stained with 0.1% acridine orange solution for 15 min and then observed under a confocal laser scanning microscope (CLSM; LSM710, Carl Zeiss, Germany) in line with wavelengths of excitation and the emission of acridine orange [9, 21, 22]. To stain mast cells (MCs) in the PVS, the sample was stained with 1% toluidine blue solution for 3 min [23].

2.4. Mechanical Separation and Isolation of Single PVS Cells. For the cytological evaluation of the cellular component in the PVS, single PVS cells were prepared from intact PVS tissues as well as PVS slices on a slide glass by sprinkling the Krebs solution using a 1 mL syringe. Here, the motive power of isolating the PVS cells is solely the impact by the Krebs droplet, and trituration action was not applied to the PVS samples. The isolated cells were transferred to a slide glass followed by staining with Hemacolor in accordance with the procedure described above.

2.5. Digital Video Recording of Putative MC Movement of the PVS. One of the PVS slices in the incubation chamber was transferred to a recording chamber (0.7 mL) and was fixed with a grid of nylon threads supported by a donut-shaped

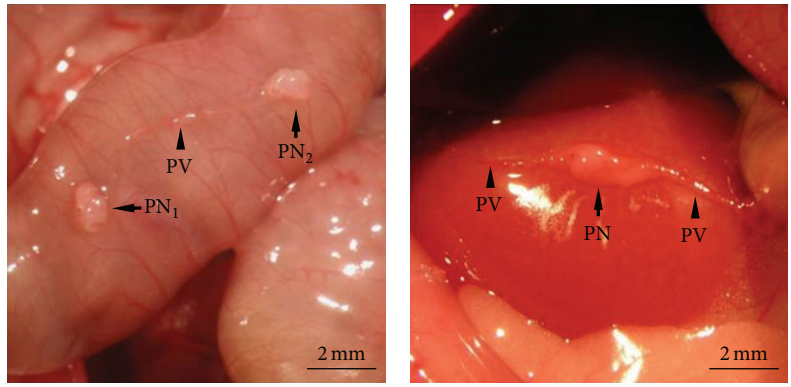

(a) (b)

Figure 1: Intact PVS tissue identified on the surface of the abdominal organs in rat. (a) Representative example of a PVS tissue composed of two PNs (arrows) and a PV (arrowhead) on the surface of the small intestine (PN_1, 1.22 × 0.86 mm; PN_2, 1.17 × 0.77 mm; PV, 0.19 mm). (b) PVS tissue composed of an enlarged PN (arrow) and a typical PV (arrowheads) on the surface of the liver (PN, 2.57 × 1.11 mm; PV, 0.17 mm).

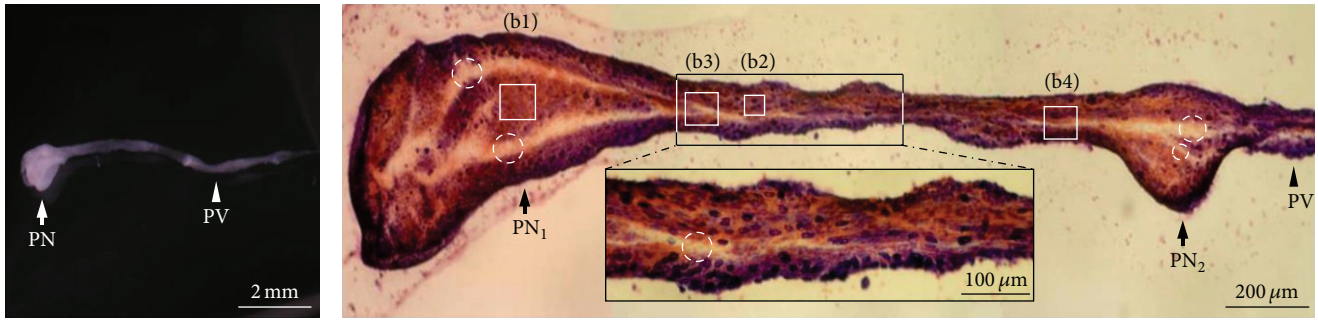

(a) (b)

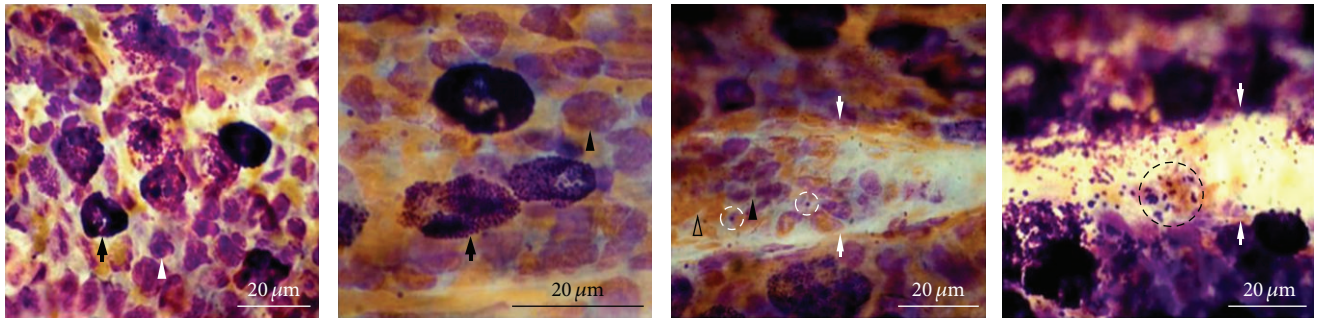

(b1) (b2) (b3) (b4)

Figure 2: Images of the whole tissue and cells of the PVS stained by Hemacolor. (a) The unstained whole PVS sample in Krebs solution. (b) Typical unsectioned longitudinal image of a whole PVS tissue composed of PNs and a PV. Note the continuous inner space structures (dotted circles) along the longitudinal axis of the PVS. There are two spaces (dotted circles, PN_1, 30–50 μm; PN_2, 10–50 μm) in the PNs and one space (dotted circle in bottom inset, 20–30 μm) in the PV. PVS cells at the edges were more abundant than in the middle of the PV. (b1) Distribution of the cells in the inner region (marked as "b1" in (b)) of the PNs. Note that most PN cells (arrow, large granular cells; arrowhead, small round cells) are round and are placed evenly and randomly. (b2) Distribution of the cells in the inner region (marked as "b2" in (b)) of the PV. Note that most PV cells (arrow, large granular cells; arrowhead, small round cells) are elliptical and horizontally arranged along the long axis of the PV. (b3 and b4) Distribution of the cells in the inner spaces (marked as "b3" and "b4" in (b)) of the PV. Note that the inner space (arrows) also contains numerous PVS cells (arrowhead, small round cells; open arrowhead, small yellowish cells; dotted circle, granules).

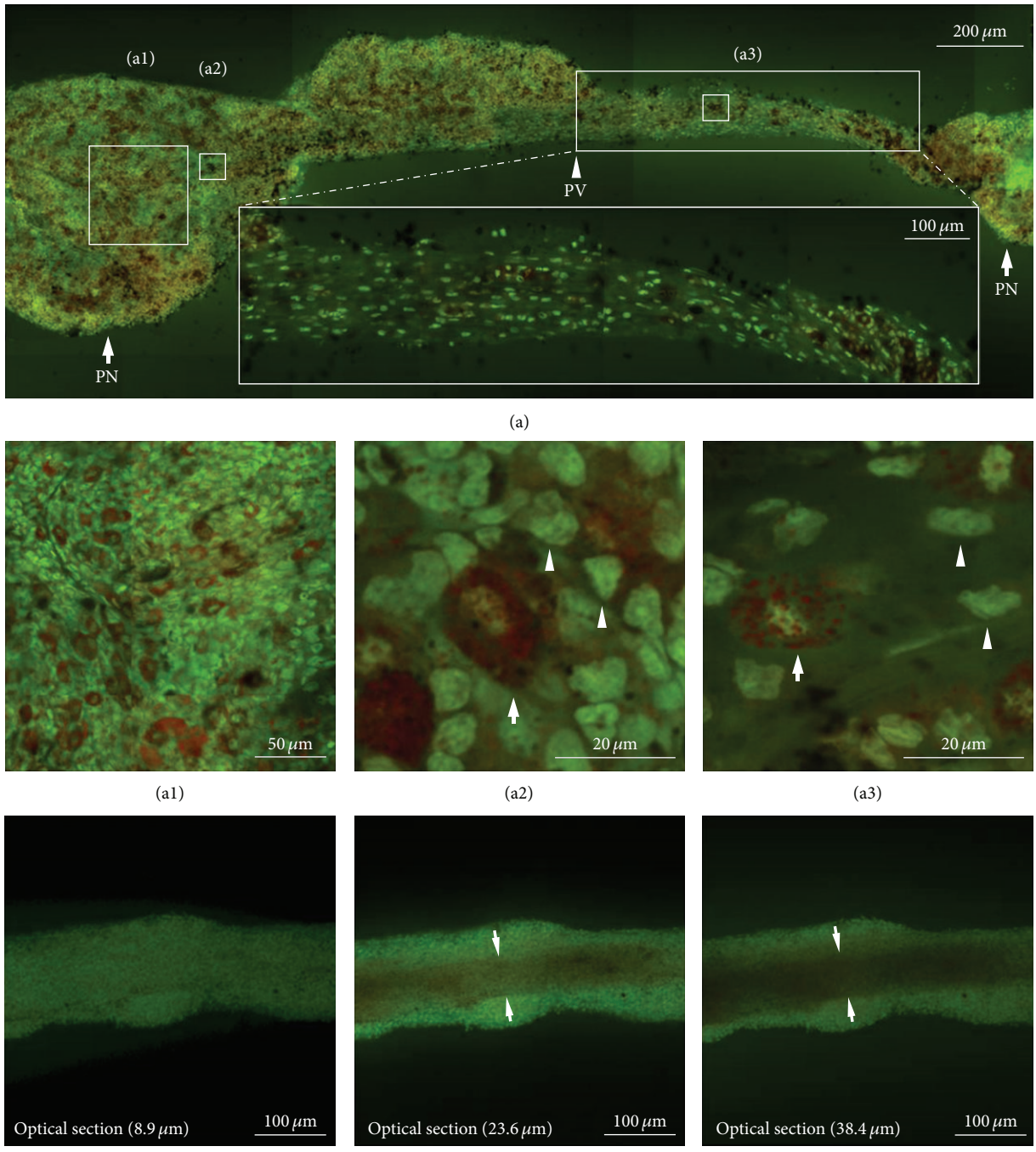

Figure 3: Confocal laser scanning microscopic images of whole PVS tissue and cells stained by acridine orange. (a) Unsectioned longitudinal image of a whole PVS composed of two PNs connected by a PV. Note that the tissue is densely filled with cells stained with green (majority) or dark brown. Some cells are linearly aligned along the longitudinal axis of the PV (bottom inset). (a1) PN cells with random distribution in the inner region (marked as "a1" in (a)). (a2 and a3) PN and PV cells at a high magnification (400x) (marked as "a2" and "a3" in (a)). Note the large cells (arrows) with granules stained red and small round cells (arrowheads) stained green in both the PNs and the PV. (b1, b2, and b3) Unsectioned longitudinal image of a whole PV showing an inner space according to depth of optical sectioning. Note that the inner space structure (arrows) devoid of cells is becoming darker with increasing depth of optical section.

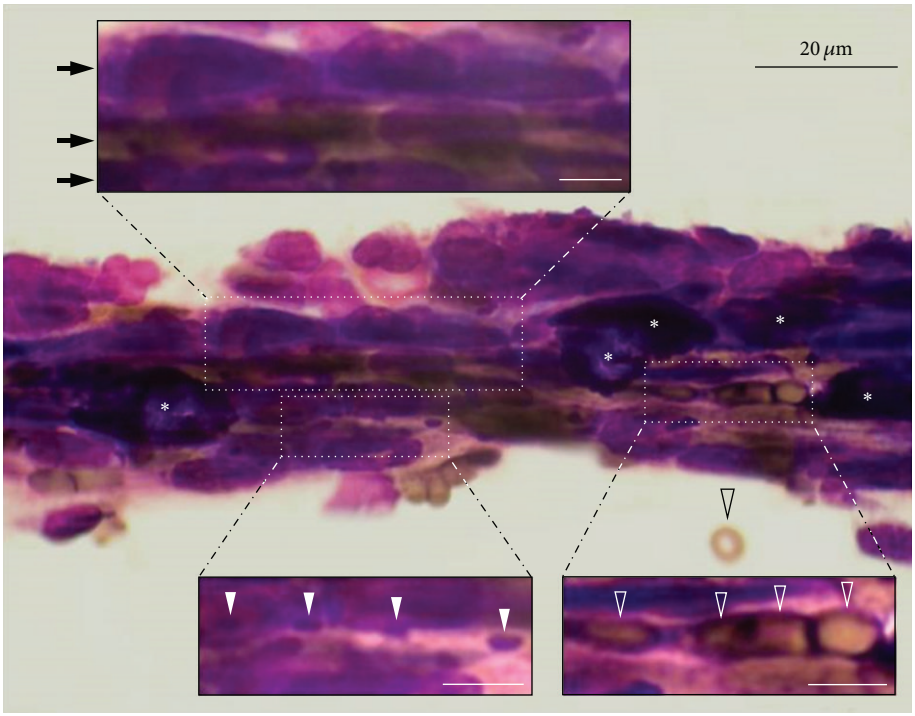

Figure 4: Longitudinal image of a thin PV stained with Hemacolor showing the multiple linear arrangement of cells (arrows in the top inset), small yellowish cells (open arrowheads in the bottom right inset), granules (arrowheads in the bottom left inset), and large granular cells (asterisks). Scale bars in the insets are 5 μm.

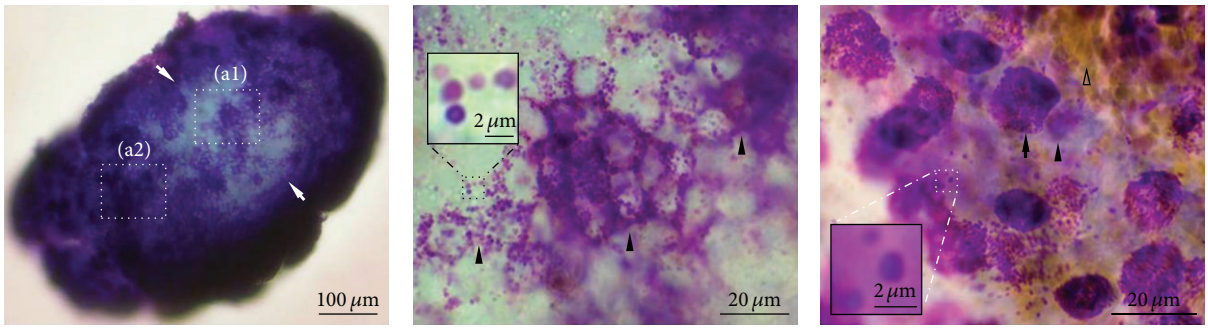

(a) (a1) (a2)

Figure 5: Honeycomb-like structure inside a PN slice (200 μm) stained with Hemacolor. (a) Cross-sectional image of the PN-slice showing the inner space structure devoid of cells (arrows). (a1) The image of the inner space in the PN slice at a higher magnification. Note the honeycomb structure (arrowheads, about 10 μm) and granules (inset) in the structure. (a2) The image of the outer part of PN slice stained with Hemacolor. Note the large granular cell (arrow), small round cell (arrowhead), small yellowish cell (open arrowhead), and the granules (inset).

silver wire weight while being perfused (3 mL/min) with oxygenated Krebs solution at 30–33°C [7, 8]. The movement of putative MC granules was observed by light microscope with differential interference contrast (BX50WI, Olympus, Tokyo, Japan) and recorded by a USB digital CCD camera series 150PIII.

2.6. PVS Cell Counting and Data Analysis. To determine the cellular composition of the PVS, individual PVS cells were counted from 25 rectangular fields (125 × 95 μm) in the images of H&E-stained PVS slices at 1000x magnification. Caution is needed when selecting these sample areas because H&E-stained PVS slices (3 μm in thickness) are very thin, and there may be some areas without cells in the edges of the slices. Considering this fact, we consistently avoided parts without cells in the PVS slices and selected only the fields filled with WBCs, RBCs, and putative MCs. Thus, we selected the representative PVS fields that showed uniform distribution of various cells. The sizes of PNs, PVs, and individual

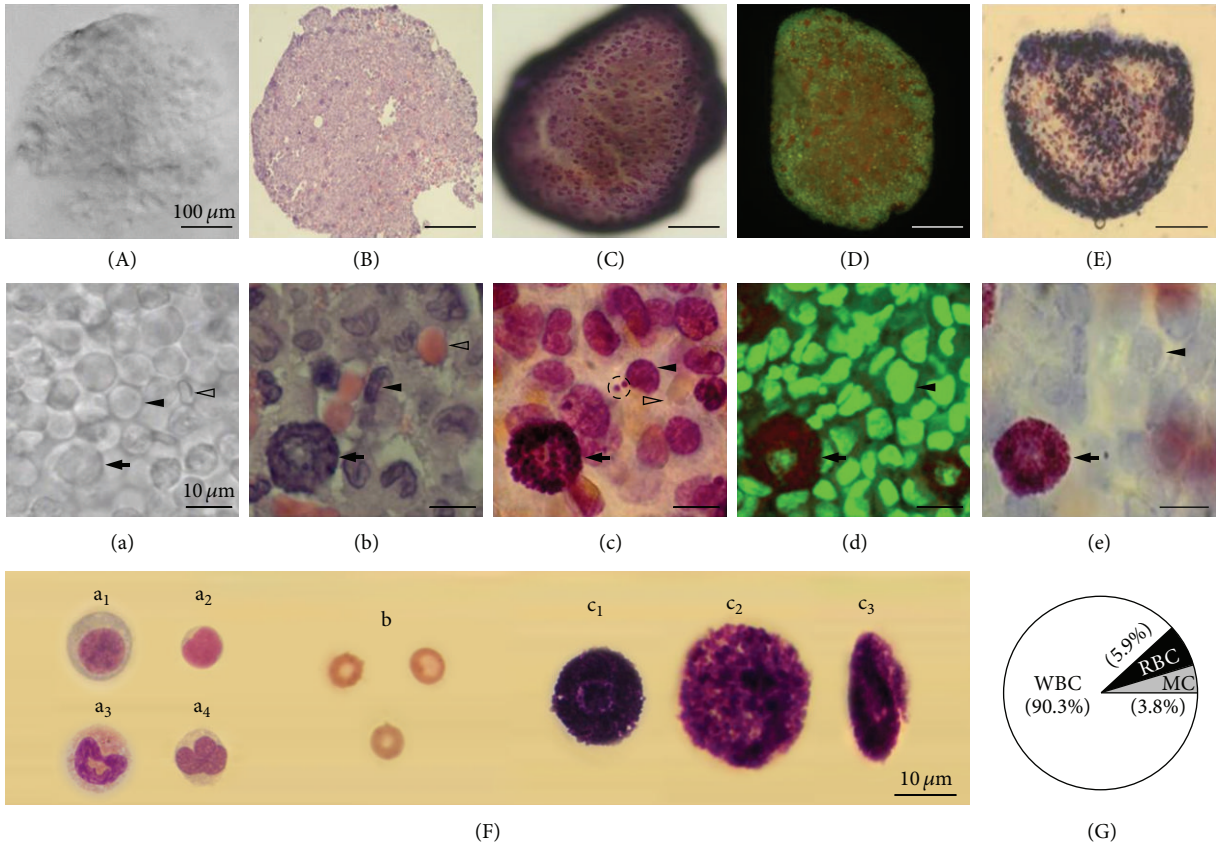

Figure 6: Three major groups of PVS cells revealed by various kinds of staining. (A and a) Unstained cross-sectional image of a PN slice with a thickness of 200 μm. Note the PN cells resembling a large round cell (arrow, 12.69 μm), a biconcave (flat)-shaped cell (open arrowhead, 7.42 μm), and a small round cell (arrowhead, 9.42 μm). (B–E) Typical cross-sectional images of the PN slice stained by H&E (B), Hemacolor (C), acridine orange (D), and toluidine blue (E). (b–e) Three groups of PN cells at a higher magnification displaying putative MCs (arrows), RBCs (open arrowheads), and WBC groups (arrowheads) which correspond to the neutrophils with lobulated nuclei. Note that the Hemacolor-stained PN slice clearly revealed the granules within putative MCs and isolated granules ((c), dotted circle). (D) and (d) are fluorescent microscopic images of acridine orange staining. (A)–(E) and (a)–(e) are images of different PVS tissues photographed at the same magnification. (F) Collection of three major groups of cells isolated from PVS tissue stained with Hemacolor. The individual PVS cells shown in ((F)-a_1–a_4) belong to the WBC group. WBC groups are composed of a plasma cell ((F)-a_1)) with eccentrically placed nucleus, lymphocyte ((F)-a_2)) with dense-staining nuclei and sparse cytoplasm, eosinophil ((F)-a_3)) with eosinophilc cytoplasmic granules, and neutrophil ((F)-a_4)) with multilobed nuclei and a lack of stained granules. The cells in ((F)-b) appeared in the group of normal mature RBCs. The cells shown in ((F)-c_1–c_3) are putative MCs (c_1, typical (10–15 μm); c_2, large (> 20 μm); and c_3, elliptical type). (G) The cellular composition of the PVS. The PVS cells were counted from 25 fields (125 × 95 μm) in images of H&E staining of PVS (n = 8) at 1000x magnification.

cells were measured using imageJ software (developed at the US National Institute of Health). All the data values were expressed as means ± standard errors, and the number of specimens or cells was represented by n.

3. Results

The results of this study were obtained from the evaluation of the 33 organ-surface PVS tissues from 23 rats. The PNs were collected mainly from the serosal surface of the small and large intestines (58.1%) and liver (35.5%) with or without PVs attached. Figure 1(a) shows a representative PVS tissue on the surface of the small intestine composing of two PNs connected by a PV of typical size. Figure 1(b) shows another example of PVS on the surface of the liver with an enlarged PN, which was even thicker than that of normal PNs. The average size of PNs was 1.26 ± 0.11 mm (major axis, 0.52–2.57 mm) and 0.73 ± 0.06 mm (minor axis, 0.34–1.50 mm, n = 27), and the average thickness of PVs was 0.25 ± 0.03 mm (n = 19).

3.1. Hemacolor Staining of the Whole PVS. To visualize the cells in the PVS, we stained the PVS with Hemacolor, a rapid staining dye widely used in hematology and clinical cytology [18, 19]. In this study, PVS cells stained by Hemacolor refer to the cells within the inside of the walls of the cells, such as WBCs, RBCS, and MCs, and do not include the cells that compose the cell walls of the PVS. Figure 2(a) shows a PVS sample isolated from the surface of internal organ in Krebs solution for staining. Figure 2(b) is a representative stereoscopic image of the whole PVS stained with Hemacolor.

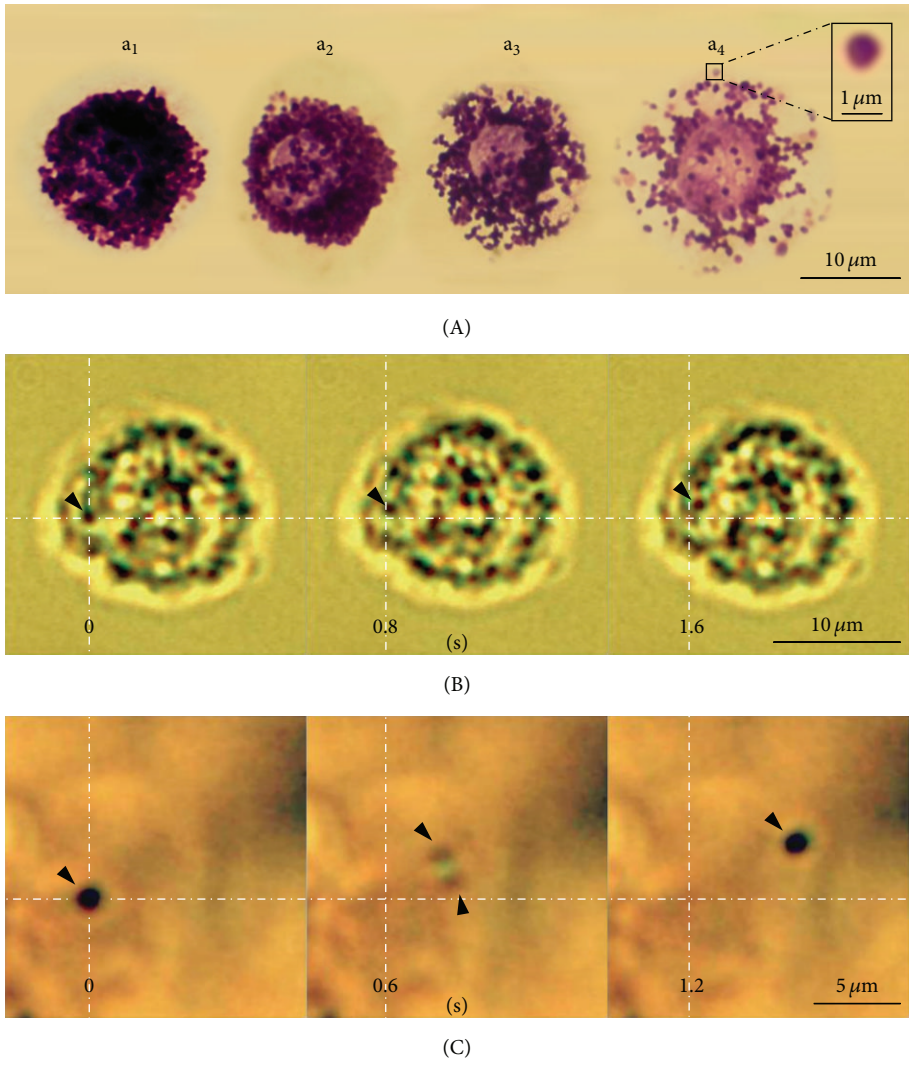

FIGURE 7: The properties of putative MCs of PVS and granules. (A) Classification of putative MCs of the PVS based on the degranulation condition. Note that the granules from a_1 (typical) to a_4 were increasingly degranulated; the granule size was about 1 μm (inset of a_4). (B) Continuous still image of granules in motion inside an MC. Note that arrowheads point to the granule that exhibits spontaneous vibrating movements on the right upper side. (C) Continuous still image of a granule with motility. Note that the granule displayed continuous vibrating movements and appeared as two divided granules for a moment (0.6 sec). This microscopy was performed on a live putative MC without any staining, which is described in the materials and methods section. The crossing points (B) and (C) of the two dotted lines indicate the location of the granule at $t = 0$. Selected frames from digital video recordings are presented.

The outer parts of the PNs and PVs were densely filled with cells, but the inner parts appearing as a white space (dotted circles in Figure 2(b)) were filled with little cells. The inner space showing low cellularity was continuous along the longitudinal axis of the PVS and had various luminal diameters depending on the location in the PVS. In general, the diameter of the space in PNs was larger than in PVs (30–50 versus 20–30 μm), and there were two spaces in PNs (dotted circles of PN_1 and PN_2 in Figure 2(b)). The inner space could be identified by its different cellular composition and high number of granules (Figures 2(b3) and 2(b4)). Hemacolor-stained PVS cells were classified into the following three major groups based on their morphological properties: small round cells (majority), large granular cells, and small yellowish cells. The PN and PV cells differed, in that the PN cells were mostly round in shape and were distributed uniformly and randomly (Figure 2(b1)). However, most PV cells, including large granular cells and small round cells, were elliptical and were arranged in parallel along with longitudinal axes of the PVs (Figure 2(b)—bottom inset and Figure 2(b2)). In PVs, the staining properties of the three major cell types are similar to those in PNs. The major cells of the PVS were also located in the inner space within PVs (Figure 2(b3)). In particular, there were a number of granules (~1 μm in diameter) in the inner space within PVs (Figure 2(b4)).

To further confirm the morphological features of whole PVS tissue, we stained the tissue sample with acridine orange,

which is DNA (green staining) and RNA- (red staining-) specific dye [21, 22], under a similar experimental condition to that in Figure 2. The cellular morphology observed in acridine orange-stained PVS tissue is similar to that obtained using Hemacolor staining. Most PV cells were stained green as shown in Figure 3(a) and were arranged in parallel along the longitudinal axis of the PV (Figure 3(a)—bottom inset and Figure 3(a3)), whereas PN cells were distributed randomly (Figures 3(a1) and 3(a2)). Most small round cells were revealed by their green color (denoting DNA) as a result of acridine orange staining, and large granular cells were revealed in green (denoting DNA) and red (denoting RNA) in nuclei and granules, respectively (Figures 3(a2) and 3(a3)) [21, 22]. The granules appeared dark brown at a low magnification (100x) (Figure 3(a)). As shown in Figure 2(b3) and Figure 2(b4), the inner space structure of the PV was also revealed by acridine orange staining according to depth of optical sectioning (Figure 3(b1–b3), see Movie S1 in supplementary material available online at http://dx.doi.org/10.1155/2013/350815).

Figure 4 shows a thin PV (30–40 μm) stained by Hemacolor. As shown in Figure 2, various PVS cells (large granular cells, small round cells, and small yellowish cells) and granules are linearly aligned within along the longitudinal axis of the PV.

To further characterize the morphology of the PVS, we stained a cross-section of a PN slice (200 μm) with Hemacolor. In general, the cellular density is higher in the outer part and lower in the inner part of the PN slice as shown in Figure 5(a), which is similar to our findings in whole PVS tissue staining (Figure 2(b)). We observed a honeycomb-like structure in the inner space, and the diameter of the individual lumens in the honeycomb was ~10 μm (Figure 5(a1)). In the honeycomb structure, granules were located within and on the borderline of each lumen. In addition, all three major cell groups were also found in the outer part of PN slices (Figure 5(a2)).

3.2. Cytomorphology of PVS Cells. Figure 6(A) shows a stereoscopic image of an unstained PN slice at a low magnification. At a higher magnification of the unstained PN slices (Figure 6(a)), the PNs are densely filled with round cells of various sizes: large round (arrow, 12–20 μm), biconcave (flat) disk-shaped (open arrowhead, 5–7 μm), and small round cells (arrowhead, 8–10 μm). Among these PVS cell groups, the small round cells were the most abundant. They were tightly packed like a cluster of grapes and evenly distributed in the area of the PN slices. Figures 6(B) and 6(b) illustrate the three groups of cells in the PN slice stained with H&E. In Figure 6(b), the large round cells were identified as putative MCs (arrow) based on their size and staining pattern in addition to their spherical nuclei and cytoplasm filled with intensely basophilic granules [24]. The small round cells stained dark blue and with round to horseshoe-shaped or multilobed nuclei (neutrophils, monocytes, and lymphocytes) were identified as WBC group (Figure 6(b), arrowhead). The biconcave-shaped cells without nucleus, yellow-stained cells by Hemacolor, were identified as RBCs (Figure 6(b), open arrowhead) [24, 25].

The three cell groups in the Hemacolor-stained PN slice (Figures 6(C) and 6(c)) had a staining pattern similar to those of H&E. In general, most PVS cells stained with Hemacolor were more clearly discernible than those stained with H&E under our experimental conditions. In particular, the images of putative MCs (Figure 6(c), arrow) and isolated granules (Figure 6(c), dotted circle) were more sharply visualized by Hemacolor staining. In the case of RBCs, however, H&E showed a staining quality superior to Hemacolor (Figure 6(b), open arrowhead).

Acridine orange staining also showed similar cytologic morphology of Hemacolor staining. The nuclei of the majority of WBCs stained by acridine orange were stained green (denoting DNA; Figure 6(d), arrowhead). In the putative MCs, the nuclei were stained green, whereas the granules were stained red (Figure 6(d), arrow), indicating the presence of DNA and RNA in nuclei and granules, respectively [21, 22]. Figures 6(E) and 6(e) illustrate the images of a PN slice stained with toluidine blue, which is known as a dye used to stain MCs [23]. The granules in these cells showed typical metachromatic staining, indicating that the large granular cells in the PVS were putative MCs.

To further characterize the morphology of single PVS cells, individual cells were isolated from the tissues and stained by Hemacolor. We identified the WBC group of PVS, including the plasma cell (Figure 6(F), a_1) with an eccentrically placed nucleus, lymphocyte (Figure 6(F), a_2) with dense-staining nuclei and sparse cytoplasm, eosinophil (Figure 6(F), a_3) with eosinophilic cytoplasmic granules, neutrophil (Figure 6(F), a_4) with multilobed nuclei and a lack of stained granules, and RBC (Figure 6(F), b) with nonnucleated red-staining and typical size [24, 25]. Putative MC of PVS could be classified into typical (Figure 6(F), c_1), large (Figure 6(F), c_2), and elliptical types (Figure 5(F), c_3) based on their morphological properties. Typical putative MCs had centrally placed nuclei and closely packed granules. As shown in Figure 2(b), the elliptical type of putative MCs was more abundantly distributed in PVs than in PNs.

The relative composition of the three groups of PVS cells, determined from the images of H&E staining (Figure 6(G)), indicated that the proportions of WBCs, RBCs, and putative MCs were 90.3%, 5.9%, and 3.8%, respectively. The average total number of the cells per PVS field (125 × 95 μm) was 167.7 ± 4.12 (158–186) in eight PNs. The numbers of putative MCs, RBCs, and WBCs per field were 6.43±0.89, 11.04±3.23, and 148.81 ± 2.64, respectively.

3.3. The Identification of Putative Mast Cells and Granules of PVS. In this study, putative MCs of the PVS contained granules of about 1 μm (inset in Figure 7(A), a_4). The degranulation stage of putative MCs differed from cell to cell (Figure 7(A), a_1–a_4). As shown in Figure 2(b4), the presence of typical putative MCs in the inner space of PVS was low, but degranulating putative MCs and isolated granules facing the inner space of the PVS were more abundant than in the outer area. We also observed that the granules

in some putative MCs of the PVS had continuous and spontaneous movements. Degranulation of the putative MC in this study was not artificially triggered, and all occurred spontaneously. Figure 7(B) illustrates a representative still image of the granules in motion within a live putative MC (see Movie S2 in supplementary material available online at http://dx.doi.org/10.1155/2013/350815). In addition, we found that some of the isolated granules had spontaneous vibrating movements in random directions (Figure 7(C), see Movie S3 in supplementary material available online at http://dx.doi.org/10.1155/2013/350815). It is interesting that one granule appeared as two divided granules at one moment while moving (Figure 7(C)-0.6 sec). The average major and minor axes of recorded MCs with vibrating granules were 15.34±1.45 (11.66–20.5 μm) and 9.69±1.01 (9.69–15.17, $n = 9$), respectively. The diameter of the putative MCs containing the granules in motion was also comparable to that of typical MCs stained with dyes as shown in Figure 6(F), c_1.

4. Discussion

In this study, using Hemacolor staining, we confirmed the channel structures composed of a few sinuses (20–50 μm) within PNs and PVs, and several lines of ductules (3–5 μm) filled with single cells or granules (~1 μm) in PVs. In a PN slice, there was a honeycomb-like structure containing granules with pentagonal lumens (~10 μm). At the cellular level, the PVS was densely filled with WBCs (90.3%), RBCs (5.9%), and putative MCs (3.8%). Granules were also found within the putative MCs at various degranulation stages, and some granules showed spontaneous vibrating movements. The results of the present study indicate that Hemacolor is a promising staining system for the rapid identification and characterization of PVS cells and structures.

Hemacolor staining revealed that the PVS had an inner space structure with a lower cellular density. It is unlikely that this is an artifact formed by the slide glass suppressing the round tissue because the tissue was mounted with Canada balsam without pressing. In addition, the inner space was further confirmed by acridine orange staining of whole PV tissue (Figure 3). This inner space contained all three major cell groups of the PVS and granules (Figure 2). In some areas, RBCs and granules are the major contents of the inner space (Figures 2(b3) and 2(b4)). The inner space is similar to the "sinus" reported from previous studies using electron microscopy [14, 26], in that the sinus contained immune cells and granules. The present study newly reveals that the sinuses are continuous inner channels along the PVS that contain various PVS cells and granules. The detailed structures and functions of the sinuses in the PVS remain to be further studied.

The most salient finding in this study is our characterization of the gross morphology of the PVS using Hemacolor staining. In general, Hemacolor staining has been used to stain and identify blood cells, such as lymphocytes, monocytes, and erythrocytes, in a short time period [18, 19]. We applied the Hemacolor staining method to the PVS for the first time and determined the most appropriate drying and staining times for the PVS. As a result, we were able to swiftly identify the cellular and structural features of the PVS. The major advantage of Hemacolor staining is that it takes just 5–10 minutes (drying time before staining: 1–3 min; Hemacolor staining for 30 sec; wash out for 30 sec; drying time after staining: 3–5 min) from the moment the whole PVS was sampled from the organ surface to the moment it was microscopically observed. In addition, by using Hemacolor staining in combination with PVS-slice preparation, we were able to identify the longitudinal part of the PVS, as well as its cross-section, within 30 min. The PVS staining method is faster and simpler than the H&E staining method, while maintaining good quality to allow the identification of the internal structure and the cellular morphology of the PVS. H&E staining, a common method to identify the PVS, takes about one day to microscopically observe the stained samples [2, 15]. Due to the short dying process involved in Hemacolor staining, we may have observed the PVS in a more natural state than that seen with previous methods. In addition, the application of Hemacolor on the PVS allows the major features of putative MCs and isolated granules in the PVS to be identified. Using Hemacolor staining, we confirmed all the previously reported immune cells stained with toluidine blue [23], H&E, and Wright Giemsa staining [14–16]. This method also allowed us to demonstrate the detailed features of the cells composing the PVS and revealed the sinuses within the PVS, ductules in PVs, and various individual cells in tissue or in isolation. Therefore, the Hemacolor staining method, combined with slice preparation, is suitable for the study of the PVS due to its fast identification of the gross and cellular morphology of the PVS.

From Hemacolor staining of the whole PVS and PN slices, we found evidence for the presence of subducts known as "ductules" in previous studies [14, 15]. The linear alignment of single cells and granules along the longitudinal axes of the PVs in this study (Figure 2(b) and Figure 4) is in good agreement with the linearly aligned elliptical or elongated cells with rod-shaped nuclei in PVs [2, 5], which have been considered a hall mark for the identification of the PVS [2]. This observation also provides evidence supporting the notion that the PVS is a circulatory channel [2, 3].

One of the novel findings of this study is the honeycomb-like structure inside the PN slice with pentagonal lumens of about 10 μn in the honeycomb (Figure 5(a1)). The size of each lumen of the honeycomb structure (~10 μm) is comparable to that of the ductules (10 μm or 7–15 μm) reported in the PV [14, 15]. In terms of its size, it is likely that each lumen of the honeycomb-like structure inside the PN may function as a ductule, as reported previously [1, 14, 15], and the channels for the flow of single cells or granules, as shown in Figure 4. The honeycomb-like structure in this study is similar to findings from prior cryoscanning electronmicroscopic studies [14, 26] in that individual lumens are tightly arranged in close contact, but distinctly different in that the size of the lumens is larger (~10 μm versus 1–5 μm) and much more homogeneous than that in the previous studies [14, 26]. This discrepancy may arise from the differences in experimental conditions and/or the types of PVS tissue tested. Further research is needed to understand the honeycomb-like structure observed in this

study and its relation with the ductules reported in previous studies [14, 26] as well as the channels for the alignment of single cells or granules shown in this study (Figure 4).

In this study, we classified PVS cells into three major groups on the basis of their cytologic morphology: WBCs, RBCs, and putative MCs comprising 90.3%, 5.9%, and 3.8% of the cell population, respectively. Our overall findings were similar to those of recent studies using H&E staining and electron microscopy that showed the presence of numerous immune cells in the PVS, such as MCs, macrophages, and neutrophils [14–17]. We attempted to observe the PVS cells in tissue as well as the single cells in isolation from PVS tissue for more decisive observation of PVS cells. Under our experimental conditions using PVS slice preparation [7, 8], we were able to directly apply Hemacolor staining to intact live PVS cells (Figure 6(a)).

The WBCs in the PVS were similar to those of typical WBCs and myeloid precursors, which are composed of neutrophils, plasma cells, eosinophils, and lymphocytes (Figure 6(F)) [24, 25]. The WBCs were consistent with the small round cells, which were further categorized into four types based on their current-voltage *(I-V)* relations recorded from cells in live PN slices in our previous electrophysiological study [7]. The presence of small clusters of RBCs in the PVS was previously reported [27]. In this study, we identified the RBCs in live PVS-slice preparation as well as in isolation as single RBCs after Hemacolor staining. The RBCs were similar to the normal mature rat RBCs in terms of the following properties: size (6–8 μm), biconcave (flat) disk-shaped, nonnucleated cells with a central region of pallor appearing in middle of cytoplasm [24, 25]. The putative MCs in the PVS appeared most outstanding in the images of Hemacolor-stained PVS and were more densely populated at the edges than other parts of the PVS. We confirmed the putative MCs in terms of their morphology, such as their large cell body of purple color, typical metachromatic granules, and staining properties using toluidine blue, a dye commonly used for the staining of MCs [23]. Our observation is consistent with previous reports [14]. In the two types of rodent MCs, connective tissue and mucosal MCs [28], the putative MCs of PVS are similar to those in connective tissues because of their large size (12–20 μm) and staining properties resulting from toluidine blue (Figure 6(e)).

In this study, we recorded the movement of granules both within cells and/or in isolation. The fact that one can observe granule movement indicates that the physiological conditions for putative MCs [29] are reasonably well preserved under our experimental conditions in live PVS slices. In addition, the granules of putative MCs of the PVS and isolated granules are similar in morphology to the primo-microcells (Sanal), which are spherical or oval in shape and have a diameter of 1-2 μm (Figure 7(A)) [2, 30, 31]. However, as the granules of the putative MCs and the primo-microcells were stained green (denoting RNA) and red (denoting DNA), respectively, by acridine orange, their components differed (Figures 3(a2) and 6(d)) [4, 32]. The critical issue of whether the granules in the putative MCs or in isolation in the PVS tissue are the primo-microcells still needs to be studied further.

It is unusual for any tissue to have such a high proportion of immune cells as in the PVS: WBCs (90.3%), RBCs (5.9%), and putative MCs (3.8%). The present study is an attempt to determine the relative composition of the PVS cells. Recently, Kwon et al. [16] reported that the proportion of MCs is 20% of the whole immune cell population in the organ-surface PVS, which indicates that the proportion of MCs is different between the two studies, 20% versus 4.0%. The discrepancy may arise from the differences in the methods and experimental conditions and needs to be studied further. Since the cellular composition of the PVS is different from that of blood (RBC of over 90%), bone marrow (MC of 2.6% ± 0.5%), and spleen (majority of lymphocytes) [26, 33], such a unique cellular composition could be a useful hallmark for the identification and comparison of the PVS in future studies.

In relation to the function of the PVS, the most salient point of the present observation is that Hemacolor staining of the PVS revealed a realistic integrated image of the PVS composed of the sinuses and the ductules reported in previous studies [14, 15]. The PVS sinuses (varying in size) and the ductules (~10 μm) observed in this study are likely to function as circulatory pathways [2] since (1) the sinuses are channel-like structures throughout PNs and PVs, (2) the sinuses contain three major types of PVS cells and granules with random arrangements, and (3) the ductules are well developed in PVs and contain lineally aligned single cells or granules. Thus, the primary function of the PVS can be thought of as a pathway for the cells, such as putative MCs, WBCs, and RBCs. In this study, the immune cells, such as MCs, neutrophils, eosinophils, and lymphocytes, accounted for the vast majority of the whole PVS cell population (~94%). The results strongly support that PVS may have a crucial role in the initiation and/or maintenance of immunological functions [14–17]. We found the degranulation of putative MCs in the sinuses of PVs, indicating that the MCs were preferentially activated in the sinuses in PVs rather than in PNs (Figure 2(b4)). It is also known that MCs are rich at the acupoints [34–38], and the effects of acupuncture are related to MCs [34, 35]. Although both the PVS and the classical acupuncture meridian system are known to be associated with MC as described above, there is a lack of sufficient evidence to directly connect them in the current stage of research, and therefore additional research is necessary.

5. Conclusion

This study shows that Hemacolor staining is useful in identifying as well as in characterizing cellular and structural properties of the PVS by confirming typical morphological features of PVs and PNs with a simple light microscope in a short time period. Our results provide two pieces of morphological evidence supporting the circulatory nature of the PVS and its roles in relation to immune functioning. (1) There are two major channel structures in the PVS: sinuses and ductules. (2) The PVS is unique in its large population of immune cells, including a cellular composition of 90.3% WBCs, 5.9% RBCs, and 3.8% putative MCs. Of note, the

MC population is high, and RBCs are present in PNs. These findings and the experimental approaches used in this study may help to elucidate the structure and function of the PVS in normal and disease states in future studies.

Authors' Contribution

C. J. Lim and J. H. Yoo contributed equally to this work.

Acknowledgments

This research was supported by Basic Science Research Program through the National Research Foundation of Korea (NRF) funded by the Ministry of Education, Science and Technology (2011-0025817).

References

[1] B. H. Kim, "On the kyungrak system," *Journal of the Academy of Medical Sciences of the Democratic People's Republic of Korea*, vol. 90, pp. 1–41, 1963.

[2] K.-S. Soh, "Bonghan circulatory system as an extension of acupuncture meridians," *Journal of Acupuncture and Meridian Studies*, vol. 2, no. 2, pp. 93–106, 2009.

[3] M. Stefanov and J. Kim, "Primo vascular system as a new morphofunctional integrated system," *Journal of Acupuncture and Meridian Studies*, vol. 5, no. 5, pp. 193–200, 2012.

[4] Z.-F. Jia, K.-S. Soh, Q. Zhou, B. Dong, and W.-H. Yu, "Study of novel threadlike structures on the intestinal fascia of dogs," *Journal of Acupuncture and Meridian Studies*, vol. 4, no. 2, pp. 98–101, 2011.

[5] H.-S. Shin, H.-M. Johng, B.-C. Lee et al., "Feulgen reaction study of novel threadlike structures (bonghan ducts) on the surfaces of mammalian organs," *Anatomical Record Part B*, vol. 284, no. 1, pp. 35–40, 2005.

[6] B.-C. Lee, S.-U. Jhang, J.-H. Choi, S.-Y. Lee, P.-D. Ryu, and K.-S. Soh, "DiI staining of fine branches of bonghan ducts on surface of rat abdominal organs," *Journal of Acupuncture and Meridian Studies*, vol. 2, no. 4, pp. 301–305, 2009.

[7] J.-H. Choi, C. J. Lim, T. H. Han, S. K. Lee, S. Y. Lee, and P. D. Ryu, "TEA-sensitive currents contribute to membrane potential of organ surface primo-node cells in rats," *The Journal of Membrane Biology*, vol. 239, no. 3, pp. 167–175, 2011.

[8] T. H. Han, C. J. Lim, J.-H. Choi, S. Y. Lee, and P. D. Ryu, "Viability assessment of primo-node slices from organ surface primo-vascular tissues in rats," *Journal of Acupuncture and Meridian Studies*, vol. 3, no. 4, pp. 241–248, 2010.

[9] B.-C. Lee, K. Y. Baik, H.-M. Johng et al., "Acridine orange staining method to reveal the characteristic features of an intravascular threadlike structure," *Anatomical Record Part B*, vol. 278, no. 1, pp. 27–30, 2004.

[10] J. S. Yoo, M. S. Kim, V. Ogay, and K.-S. Soh, "In vivo visualization of bonghan ducts inside blood vessels of mice by using an Alcian blue staining method," *Indian Journal of Experimental Biology*, vol. 46, no. 5, pp. 336–339, 2008.

[11] C. Lee, S.-K. Seol, B.-C. Lee, Y.-K. Hong, J.-H. Je, and K.-S. Soh, "Alcian blue staining method to visualize bonghan threads inside large caliber lymphatic vessels and x-ray microtomography to reveal their microchannels," *Lymphatic Research and Biology*, vol. 4, no. 4, pp. 181–189, 2006.

[12] B.-C. Lee, K. W. Kim, and K.-S. Soh, "Visualizing the network of bonghan ducts in the omentum and peritoneum by using trypan blue," *Journal of Acupuncture and Meridian Studies*, vol. 2, no. 1, pp. 66–70, 2009.

[13] B.-C. Lee and K.-S. Soh, "Visualization of acupuncture meridians in the hypodermis of rat using trypan blue," *Journal of Acupuncture and Meridian Studies*, vol. 3, no. 1, pp. 49–52, 2010.

[14] B.-C. Lee, J. S. Yoo, V. Ogay et al., "Electron microscopic study of novel threadlike structures on the surfaces of mammalian organs," *Microscopy Research and Technique*, vol. 70, no. 1, pp. 34–43, 2007.

[15] V. Ogay, K. H. Bae, K. W. Kim, and K.-S. Soh, "Comparison of the characteristic features of bonghan ducts, blood and lymphatic capillaries," *Journal of Acupuncture and Meridian Studies*, vol. 2, no. 2, pp. 107–117, 2009.

[16] B. S. Kwon, C. M. Ha, S. Yu, B. C. Lee, J. Y. Ro, and S. Hwang, "Microscopic nodes and ducts inside lymphatics and on the surface of internal organs are rich in granulocytes and secretory granules," *Cytokine*, vol. 60, no. 2, pp. 587–592, 2012.

[17] B. Sung, M. S. Kim, B.-C. Lee, S.-H. Ahn, S.-Y. Hwang, and K.-S. Soh, "A cytological observation of the fluid in the primo-nodes and vessels on the surfaces of mammalian internal organs," *Biologia*, vol. 65, no. 5, pp. 914–918, 2010.

[18] J. Walter, C. Klein, and A. Wehrend, "Comparison of eosin-thiazin and Papanicolaou-Shorr staining for endometrial cytologies of broodmares: technical note," *Tierärztliche Praxis Großtiere*, vol. 39, no. 6, pp. 358–362, 2011.

[19] Y. Keisari, "A colorimetric microtiter assay for the quantitation of cytokine activity on adherent cells in tissue culture," *Journal of Immunological Methods*, vol. 146, no. 2, pp. 155–161, 1992.

[20] N. J. Spencer, G. W. Hennig, E. Dickson, and T. K. Smith, "Synchronization of enteric neuronal firing during the murine colonic MMC," *Journal of Physiology*, vol. 564, part 3, pp. 829–847, 2005.

[21] Z. Darzynkiewicz, J. Kapuscinski, F. Traganos, and H. A. Crissman, "Application of pyronin Y(G) in cytochemistry of nucleic acids," *Cytometry*, vol. 8, no. 2, pp. 138–145, 1987.

[22] G. E. Okuthe, "DNA and RNA pattern of staining during oogenesis in zebrafish (*Danio rerio*): A Confocal Microscopy Study," *Acta Histochem*, vol. 115, no. 2, pp. 178–184, 2013.

[23] P. S. Cerri, J. A. Pereira-Júnior, N. B. Biselli, and E. Sasso-Cerri, "Mast cells and MMP-9 in the lamina propria during eruption of rat molars: quantitative and immunohistochemical evaluation," *Journal of Anatomy*, vol. 217, no. 2, pp. 116–125, 2010.

[24] M. H. Ross and W. Pawlina, *Histology: A Text and Atlas*, Lippincott Williams & Wilkins, 5th edition, 2005.

[25] V. P. Eroschenko, *DiFiore's Atlas of Histology With Functional Correlations*, Lippincott Williams & Wilkins, 11th edition, 2008.

[26] B. Sung, M. S. Kim, B.-C. Lee et al., "Measurement of flow speed in the channels of novel threadlike structures on the surfaces of mammalian organs," *Naturwissenschaften*, vol. 95, no. 2, pp. 117–124, 2008.

[27] H.-J. Han, V. Ogay, S.-J. Park et al., "Primo-vessels as new flow paths for intratesticular injected dye in rats," *Journal of Acupuncture and Meridian Studies*, vol. 3, no. 2, pp. 81–88, 2010.

[28] D. D. Metcalfe, D. Baram, and Y. A. Mekori, "Mast cells," *Physiological Reviews*, vol. 77, no. 4, pp. 1033–1079, 1997.

[29] K. Mizuno, T. Tolmachova, D. S. Ushakov et al., "Rab27b regulates mast cell granule dynamics and secretion," *Traffic*, vol. 8, no. 7, pp. 883–892, 2007.

[30] B. H. Kim, "Sanal theory," *Journal of the Academy of Medical Sciences of the Democratic People's Republic of Korea*, vol. 108, pp. 39–62, 1965.

[31] B. H. Kim, "Sanal and hematopoiesis," *Journal of the Academy of Medical Sciences of the Democratic People's Republic of Korea*, vol. 108, pp. 1–6, 1965.

[32] V. Ogay, K. Y. Baik, B.-C. Lee, and K.-S. Soh, "Characterization of DNA-containing granules flowing through the meridian-like system on the internal organs of rabbits," *Acupuncture and Electro-Therapeutics Research*, vol. 31, no. 1-2, pp. 13–31, 2006.

[33] M. C. Jamur, A. N. Moreno, L. F. C. Mello et al., "Mast cell repopulation of the peritoneal cavity: contribution of mast cell progenitors versus bone marrow derived committed mast cell precursors," *BMC Immunology*, vol. 11, article 32, 2010.

[34] D. Zhang, G. Ding, X. Shen et al., "Role of mast cells in acupuncture effect: A Pilot Study," *Explore*, vol. 4, no. 3, pp. 170–177, 2008.

[35] T.-F. He and Y.-F. Chen, "Advances in studies on the correlation between acupuncture-moxibustion treatment and mast cells," *Zhongguo Zhen Jiu*, vol. 30, no. 1, pp. 84–87, 2010.

[36] Y. C. Hwang, "Anatomy and classification of acupoints," *Problems in Veterinary Medicine*, vol. 4, no. 1, pp. 12–15, 1992.

[37] Z. Zhu and R. Xu, "Morphometric observation on the mast cells under the acupuncture meridian lines," *Zhen Ci Yan Jiu*, vol. 15, no. 2, pp. 157–158, 1990.

[38] G.-J. Wang, M. H. Ayati, and W.-B. Zhang, "Meridian studies in China: a systematic review," *Journal of Acupuncture and Meridian Studies*, vol. 3, no. 1, pp. 1–9, 2010.

Hindawi Publishing Corporation
Evidence-Based Complementary and Alternative Medicine
Volume 2013, Article ID 438079, 6 pages
http://dx.doi.org/10.1155/2013/438079

Research Article

Expression of Stem Cell Markers in Primo Vessel of Rat

Eun Seok Park,[1] Jeong Hoon Lee,[1] Won Jin Kim,[1] Jinbeom Heo,[2] Dong Myung Shin,[1,2] and Chae Hun Leem[1]

[1] *Department of Physiology, University of Ulsan College of Medicine, 88 43-Gil Olympic-Ro, Songpa-gu, Seoul 138-736, Republic of Korea*
[2] *Department of Medicine, Graduate School, University of Ulsan, 88 43-Gil Olympic-Ro, Songpa-gu, Seoul 138-736, Republic of Korea*

Correspondence should be addressed to Dong Myung Shin; d0shin03@amc.seoul.kr and Chae Hun Leem; leemch@gmail.com

Received 7 February 2013; Accepted 10 July 2013

Academic Editor: Byung-Cheon Lee

Accumulating line of evidence support that adult tissues contain a rare population of pluripotent stem cells (PSCs), which differentiate into all types of cells in our body. Bonghan microcell (primo microcells (PMCs)) discovered in 1960s was reported to have a pluripotency like a stem cell *in vivo* as well as *in vitro* condition. Here, we describe the detailed morphology and molecular features of PMCs. PMCs reside in Bonghan duct (primo vessel (PV)) reported as a corresponding structure of acupuncture points and meridian system. We found that PMCs were frequently observed in the liver surface of the rat between 300 g and 400 g from April to June, suggesting that the their detection frequency depends on the weight, the season, and the organ of rat. As reported, PMCs freshly isolated from PVs were spherical ~1-2 μm microsized cells. In contrast, a unique bithread or budding-shaped PMCs emerged during tissue culture around 8 days. RT-PCR analysis demonstrated that PVs-derived cells express the *Oct4*, the most important PSCs gene, in addition to several PSCs markers (*Sox2*, *Stella*, *Rex1*, and *Klf4*). Thus, we for the first time provide the evidence about Oct4-expressing stem-like characteristics for cells resident in PVs, a possible novel stem cell enriched niche.

1. Introduction

Continuous tissue and organ regeneration is one of the important homeostatic mechanisms of the multicellular organism. Homeostasis of adult tissues is regulated by a population of stem cells, which replace cells used up during life by undergoing self-renewal and maintaining their own pool. Stem cells are guardians of tissue/organ integrity and regulate the life span of an adult organism [1]. The most central stem cells, from a regenerative potential point of view, are pluripotent stem cells (PSCs). According to their definition, PSCs give rise to cells from all three germ layers *in vitro* and *in vivo* condition [2]. In contrast to differentiated somatic cells, PSCs commonly express pluripotent core transcription factors (TFs) such as *Oct*4, *Nanog*, and *Sox*2 that are essential to maintain their pluripotent state [2].

Typically, PSCs have been established from embryonic tissue (e.g., embryonic stem cells (ESCs)) and by the ectopic expression of reprogramming factors into the terminally differentiated adult cells (e.g., inducible PSC). However, recent evidence has accumulated demonstrating that PSCs may reside in adult tissues and are able to differentiate into tissue-committed stem cells (TCSCs) [1]. These cells have been variously described in the literature as (i) multipotent adult progenitor cells (MAPCs), (ii) marrow-isolated adult multilineage-inducible (MIAMI) cells, (iii) multipotent adult stem cell (MASCs), (iv) OmniCytes, (v) Dot cell, or (vi) very small embryonic-like (VSEL) stem cell [3–8]. It has been suggested that all these cells, described by different investigators as various names, could be closely related or could be overlapping stem cell populations. Thus, exploring their relationship could advance our understanding of biological process for their pluripotency and differentiation.

When adult stem cell research began in the 1960s, Kim claimed to discover the structures, Bonghan duct (primo vessel (PV)), and corpuscle (primo node), and reported as a corresponding structure of acupuncture points and meridian system [9]. In succession, he reported a Sanal (primo microcell (PMC)) which was spherical shape with the size of 0.8~2.4 μm containing DNA and claimed that those

cells flow in primo vessel. Most interestingly, he claimed that the Sanal had a pluripotency like a stem cell by showing the pluripotency evidenced by their dividing and differentiating into several types of tissue committed cells *in vivo* as well as *in vitro* condition [10]. Since the lack of a detailed procedure for the isolation/identification of PMCs, his results have been difficult to repeat. Thus, the Bonghan theory has been largely overlooked for many years, and PMCs were regarded just as a simple cellular debris/fragments or part of apoptotic bodies.

With advance of modern microscopy and molecular biology technologies, several researchers recently have reported the evidence for the existence of the Bonghan system inside blood or lymphatic vessels [11, 12], on the organ surface [13], and in the brain [14]. The PMCs have been also successfully isolated as DNA containing a spherical microsized (1-2 μm in diameter) cell from Bonghan systems on organ surfaces using a differential centrifugation method [15]. Observation under transmission electron (TEM) microscopy has revealed that PMCs have an inner ultrastructure of a 1.5 μm sized central region and many small 50–500 nm sized granules in the peripheral region, which are distinguished from apoptotic bodies and other microorganisms [16]. While most of PMCs were round-shaped, some of them had a unique protrusion and possible proliferation feature, as protruding threads under atomic force microscopy (AFM) [16]. However, their precise cellular and molecular natures have remained to be determined.

In this paper, we isolated the primo vessel detected in rat abdomen and tracked the cellular changes using live cell imaging. And also, we investigated whether PVs express some molecular markers for PSCs such as Oct4, Sox2, Rex1, and Stella at the mRNA level. Thus, we propose that the PVs could be a potential container for the source of Oct4 expressing adult stem cells.

2. Materials and Methods

2.1. Isolation of PVs and PMC. Sprague-Dawley rats (specific pathogen-free rat) aged 7–10 weeks were used. Procedures involving animals and their care conformed to institutional guidelines. Rats were anesthetized with intramuscular injection (Xylazine + ketamine, 1 : 4 mixture, 0.4 mL/100 g). Under the anesthesia, the abdominal wall was carefully dissected along the linea alba without any bleeding into the abdomen because the coagulation thread was easily regarded as the primo vessel [17]. Under the stereomicroscope (XTL-5, Scienscope, USA), the organ surface was thoroughly examined to find PVs with the order of liver, stomach, spleen, small intestine, large intestine, and bladder. Even though there were many studies to report PVs, until now, the confirmation criteria of PVs *in vivo* are still obscure. Therefore, firstly, we tried to find the thread-like structure on the organ surface, which was not attached and easily lifted with the forceps. If it had a node structure, it was assumed as PVs. Secondly, on the inverted microscope, the tissues were examined whether the PMCs were incorporated in the nodes. If it had the PMCs of the size of 1~2 μm, we confirmed that the isolated tissues were PVs. Sometimes, we used an alcian blue (1%) to facilitate the identification of PVs *in vivo* [18]. When the cells in PVs were cultured, high glucose DMEM (GIBCO, USA) contained 10% fetal bovine serum and 1% penicillin.

Table 1: Sequences of primers employed for RT-PCR and their anticipated PCR product size.

β-actin	For-CATGGCATTGTGATGGACT Rev-ACGGATGTCAACGTCACACT	427 bp
cMyc	For-GGGACAGTGTTCTCTGCCTCT Rev-TTCTCTTCCTCGTCGCAGAT	199 bp
Fbxo15	For-GTGGAGGAAACAGCCACA Rev-ATGTGGCCAATTTTTGTCAT	306 bp
Klf4	For-CAGTCGCAAGTCCCCTCTCTC Rev-CCTGTCGCACTTCTGGCACTG	321 bp
Nanog	For-GCCCTGAGAAGAAAGAAGAG Rev-CGTACTGCCCCATACTGGAA	356 bp
Nestin	For-AGAGAAGCGCTGGAACAGAG Rev-AGGTGTCTGCAACCGAGAGT	234 bp
Oct4_PS#1	For-GGGATGGCATACTGTGGAC Rev-CTTCCTCCACCCACTTCTC	412 bp
Oct4_PS#2	For-GATGGCATACTGTGGACCT Rev-TTCATATCCTGGGACTCCTCG	210 bp
Oct4_PS#3	For-GGCTGGACACCTGGCTTCAGA Rev-TGGTCCGATTCCAGGCCCA	204 bp
Rex1	For-TTCTTGCCAGGTTCTGGAAGC Rev-TTTCCCACACTCTGCACACAC	297 bp
Sox2	For-GGCGGCAACCAGAAGAACAG Rev-GTTGCTCCAGCCGTTCATGTG	414 bp
Stella	For-TCCTACAACCAGAAACACTAG Rev-GTGCAGAGACATCTGAATGG	304 bp

2.2. Reverse Transcriptase (RT) and Real-Time Quantitative PCR (RQ-PCR). Total RNA from the PVs was isolated using the RNeasy Mini Kit (Qiagen Inc., Valencia, CA, USA) with removal of genomic DNA using the DNA-free Kit (Applied Biosystems, Foster City, CA, USA). The mRNA (10 ng) was reverse-transcribed with TaqMan Reverse Transcription Reagents (Applied Biosystems) according to the manufacturer's instructions. The resulting cDNA PCR fragments were amplified using AmpliTaq Gold at 1 cycle of 8 min at 95°C, 2 cycles of 2 min at 95°C, 1 min at 60°C, and 1 min at 72°C and subsequently by 35 cycles of 30 s at 95°C, 1 min at 60°C, 1 min at 72°C and 1 cycle of 10 min at 72°C, by using sequence-specific primers (Table 1). All primers were designed with Primer Express software (Applied Biosystems). The PCR products were separated by 1.5% agarose gel electrophoresis.

2.3. Statistical Analysis. All the data in RQ-PCR analyses were analyzed using Student's t test or one-way ANOVA with Bonferroni posttests. We used the GraphPad Prism 5.0 program (GraphPad Software, La Jolla, CA, USA), and statistical significance was defined as $P < 0.05$ or $P < 0.01$.

3. Result and Discussion

Figure 1 showed the thread-like structures presumed PVs on organ surface such as liver, small intestine, and spleen, respectively. As shown in Figure 1, the isolated PVs, thread-like structures were easily lifted with forceps which was the most important discrimination from blood vessel or lymphatic vessel.

Next, we examined the morphologic change during maintaining the PMCs under tissue culture condition for 8 days. Most of cultured PMCs remained as spherical microsized cell (~1-2 μm sized) as similar to freshly isolated ones (Figure 2(a)). Of particular, some of the cultured PMCs showed a unique bithread shape or budding (Figure 2(b)). This transformation is similar to PMCs budding previously described by Kim [9, 10]. According to his observations, PMCs make a protrusion-like thread and produce a daughter microcell from that thread to make proliferation [9, 10]. Thus, this observation may suggest that the culture of PMCSs could promote their proliferation potency. As other expectations, this thread-like structure might be established to transfer small molecules like microvesicle [19] or to provide a polarized tension for other biological processes like migration or asymmetrical differentiation.

PMCs were not identified in all rats, and the detection rate of PMCs was 24% (39 rat detected/165 rat tested). When we performed the experiments, we felt that the detection rate of PMCs was changed depending on weight and the season. We summarized the frequency for the detection of PMCs in the condition of different weight and tissue origin in rat (Figure 3). The detection rate of PMCs was the highest in the rats weighed between 300 g and 400 g, about 32%. If the weight of rat was over 400 g, the detection rate was about 6%, and if under 300 g, the detection rate was about 17%. Moreover, we found the seasonal variation of the detection of PMCs. The PMCs were more frequently found from April to June about 40%. The PMCs were most frequently found on the liver surface more than 70% and the least found on the large intestine about 5%. The earlier results suggested the guidance of the rat choice. To facilitate finding PMCs, the rats of the weight between 300 g and 400 g were used during the spring, and the surface of liver must be firstly examined.

To better understand the molecular insight of cells in PVs, we examined the expression of PSCs-specific genes in whole extracts from PVs. First, we tried to examine the expression of *Oct4*, the most important transcription factor for maintaining stem cell pluripotency using three independent primer sets. As shown in Figure 4(a), a PCR reaction using all the primer sets amplified transcript for *Oct4* specifically in the PV, but not in cells from adult whole blood. Since PSCs also express *Nanog*, *Sox2*, and *Fbxo15*, we evaluated their expression in PVs. They express only *Sox2*, but they do not express *Nanog* and *Fbxo15* (Figure 4(b)). The *Sox2* and *Nanog* transcripts were not expressed in whole blood cells. Next, we also examine the expression level of *Stella*, *Rex1*, and *Klf4*, highly expressed in inner cell mass primitive PSCs [20]. We noticed that PVs specifically expressed these PSC markers, which all support their pluripotent character (Figure 4(c)). In contrast, the transcript of *Nestin*, a neural stem cell marker, was not detected in any PVs tested (Figure 4(d)). Of particular, the expression of cMyc was different between PVs, representing the heterogenous features for their cell proliferation potency (Figure 4(d)). Taken together, this result provides the evidence that PVs contain the Oct4 expressing stem cell-like population, which could function as a back-up/reserve source for $Oct4^+$ PSCs in adult tissues.

Lack of a detail description for the isolation and identification of PVs has been a main hurdle to get the reproducible observation of PVs. In the present study, we demonstrate that the PMCs were more frequently found from the SD rat weighed between 300 g and 400 g. Moreover, we found the seasonal variation, and most PMCs were found during the spring (April, May, and June). The liver surface was the preferred location of PMCs detection. Since we confirmed PVs when it contained microcells, PV detection rate without PMCs was not examined. Even though we did not present the detection rate during winter (from January to March), some trials during January showed that the winter season might be the worst to find PVs with PMCs (0/12 cases).

Most of PMCs prepared from PVs show the round 1-2 μm microsized morphological features, and they form the unique thread-like structure or budding during tissue culture condition. Moreover, cells resident in these PVs express the most of PSCs-specific transcripts, suggesting that they might be novel explanation about the detection of PSCs markers from adult tissues. Thus, further investigation using highly purified cells of PVs should be necessary to identify which cells in PVs could show the Oct4 expressing stem cell-like features in a molecular and cellular context, and PMCs may be the highest probable candidate having the stem cell nature.

Present study proves that the PVs express the transcripts for PSCs (Figure 4). However, several questions remain to be addressed regarding these rare microsized cells. First, their developmental origin is unresolved. It has been considered that PSCs during embryogenesis/gastrulation may become eliminated after giving rise to TCSCs, or conversely, they may survive among TCSCs and serve as a back-up/reserve source for these cells [1]. Thus, it is important to elucidate whether PMCs are functional under steady-state conditions or are merely remnants from developmental embryogenesis that loses the potency of tissue regeneration. Second, the question is about the microsize of the PMCs. Most of PMCSs were around 1-2 μm in diameter, which is smaller than normal human haploid sperm head (~2.5–3 μm). This might suggest that PMCs could contain whole parts of cell organelles. Indeed, it was reported that DNA content of PMCs was around the chromosome-sized 10^8 bps, and their DNA was fragmented [9, 10]. Thus, it is possible that PMCSs might be similar to microvesicles (MVs), small circular membrane fragments shed from the cell surface or released from the endosomal compartment.

Due to small size, MVs also have been regarded just as simple cellular debris/fragments or part of apoptotic bodies. However, accumulating lines of evidence have reported that these tiny membrane fragments play an important and underappreciated role in cell-to-cell communication [21–23]. First, MVs may stimulate target cells directly by surface-expressed ligands acting as a kind of "signaling complex."

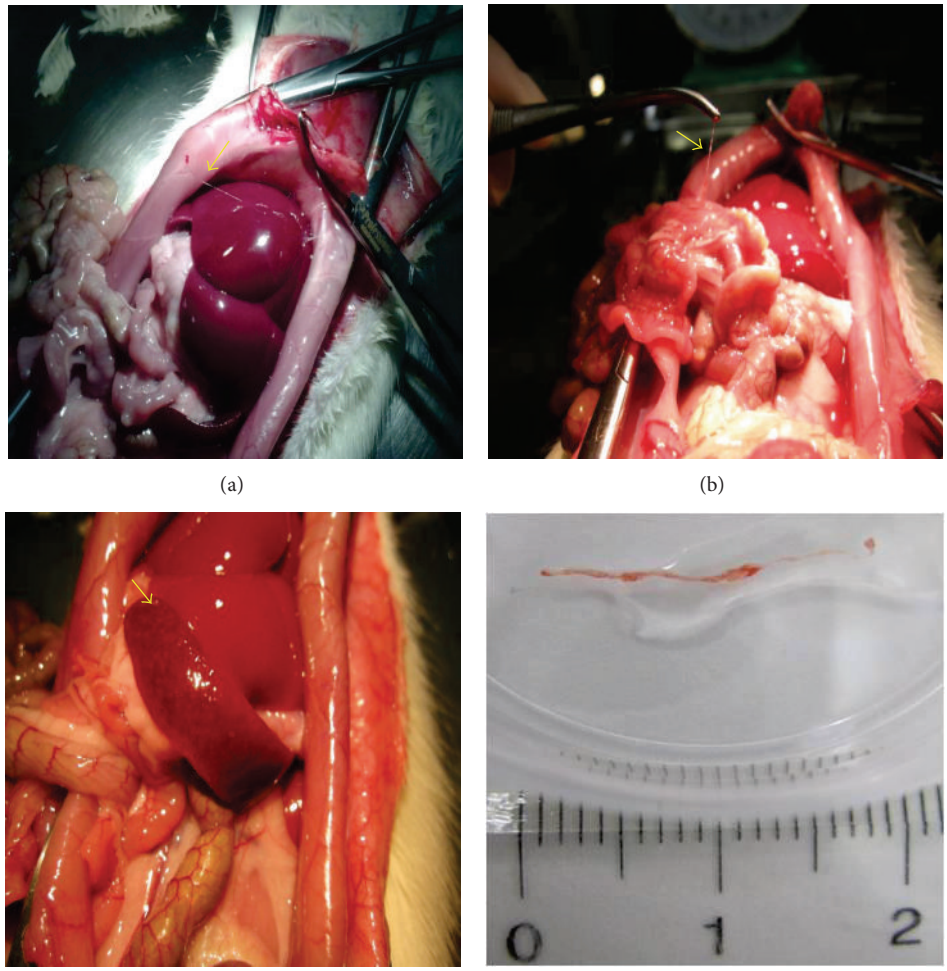

(a) (b)

(c) (d)

Figure 1: Detection of PVs on the surface of several organs. Thread-like structures presumed as PVs (arrow) were observed on organ surface such as liver (a), small intestine (b), and spleen (c). Representative photo of the isolated PV for further isolation of PMCs (d).

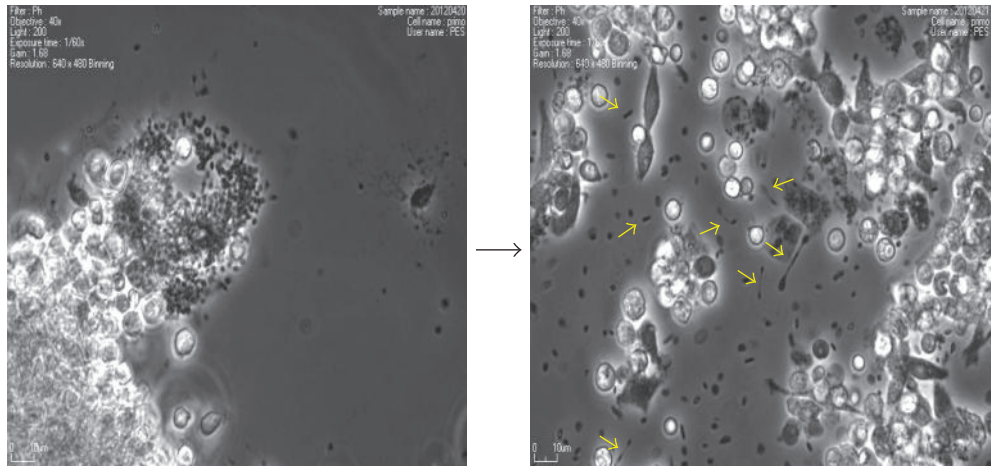

(a) (b)

Figure 2: Morphologic change during tissue culture of PMCs. Representative pictures of PMCs tissue-cultured for 1 day (a) and 8 days (b). Most of PMCs at 1 day of tissue culture remained as spherical microsized cell (~1-2 μm sized). Particularly, a unique bithread or budding-shaped PMCs (arrows in (b)) were observed after one week.

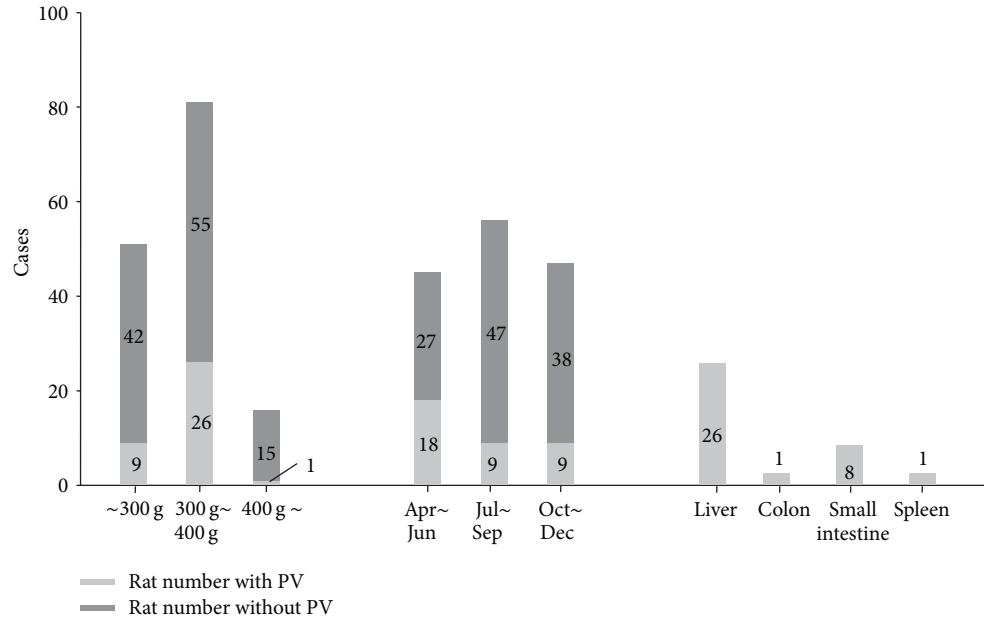

Figure 3: Detection rate of PMCs depends on rat weight and season. Frequency for detection of PMCs in the condition of the different weight, the season, and the organ in rat. Note that PMCs were frequently observed in the liver surface of the rat between 300 g and 400 g from April to June.

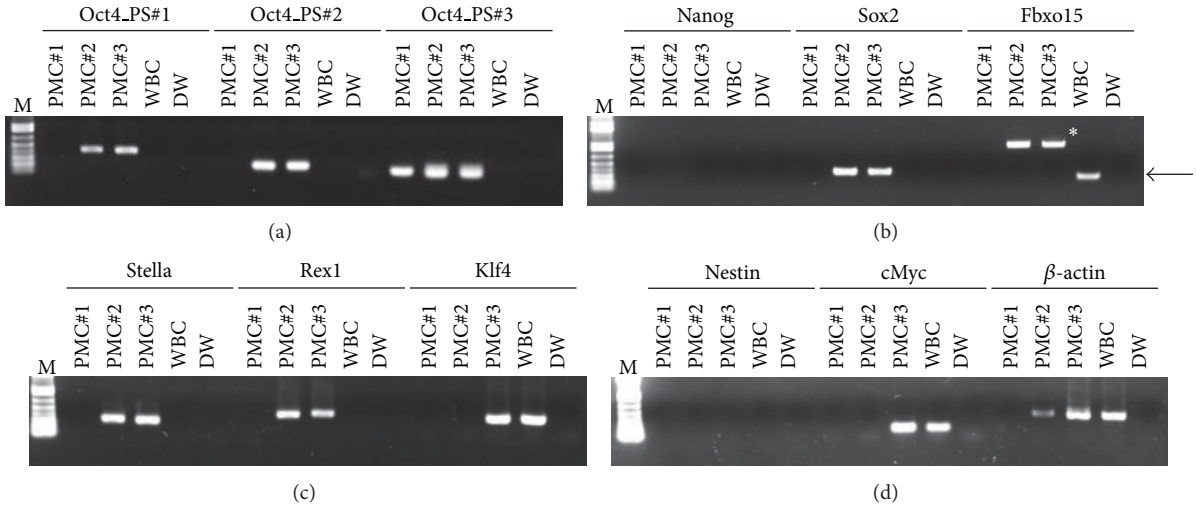

Figure 4: The expression of stem cell-related genes in PMCs. RT-PCR analysis of *Oct4* (a), PSCs (b), ICM-enriched (c), neural stem cells, and *cMyc* (d) genes in freshly isolated PMCs and whole blood cells (WBC). β-actin was used as an endogenous housekeeping gene. Control reaction was performed without template (DW, distilled water). Arrow and asterisk in Fbxo15 part represent the expectedly sized and nonspecific PCR product, respectively. M: DNA size marker.

Second, they might transform the neighboring cells by transferring surface receptors and delivering proteins, mRNA, bioactive lipids, and even whole organelles (e.g., mitochondria). Finally, they may also serve as a vehicle to transfer infectious particles between cells such as prions or HIV. Thus, investigating the relationship between PMCs and MVs could not only advance our understanding of these microsized biocomponents but also their application in stimulating the therapeutic potency of adult stem cells.

4. Conclusions

Herein, we report that PVs are frequently detected in rat grown to a weight between 300 g and 400 g. Moreover, we found the seasonal variation to detect PMC, and the spring is the best season to detect PVs. PVs were more frequently found on the liver surface than the other internal abdominal organs. And also, we provide the cellular characteristics of PMCs and the molecular characteristics of PVs.

We, for the first time, provide the evidence about Oct4-expressing stem-like characteristics for cells resident in PVs, a possible novel stem cell enriched niche. Thus, functional research about their tissue regeneration potency would be essential for providing the biological significance of PVs and PMCs, especially in the field of stem cell and cancer biology.

Conflict of Interests

The authors declare that they have no financial conflict of interests.

Acknowledgments

The authors thank Dr. Lee BC in KAIST and Professor Soh KS in SNU for the helpful advice about the primo vascular system. This research was partly supported by a grant from the Korea Institute of Oriental Medicine (K12272), by a grant from the National Research Foundation (20120009829) to C. H. Leem, and by a grant from the Korean Health Technology R&D Project, Ministry of Health & Welfare, Republic of Korea (A120301) to D. M. Shin.

References

[1] M. Z. Ratajczak, B. Machalinski, W. Wojakowski, J. Ratajczak, and M. Kucia, "A hypothesis for an embryonic origin of pluripotent Oct-4^+ stem cells in adult bone marrow and other tissues," *Leukemia*, vol. 21, no. 5, pp. 860–867, 2007.

[2] H. Niwa, "How is pluripotency determined and maintained?" *Development*, vol. 134, no. 4, pp. 635–646, 2007.

[3] Y. Jiang, B. N. Jahagirdar, R. L. Reinhardt et al., "Pluripotency of mesenchymal stem cells derived from adult marrow," *Nature*, vol. 418, no. 6893, pp. 41–49, 2002.

[4] G. D'Ippolito, S. Diabira, G. A. Howard, P. Menei, B. A. Roos, and P. C. Schiller, "Marrow-isolated adult multilineage inducible (MIAMI) cells, a unique population of postnatal young and old human cells with extensive expansion and differentiation potential," *Journal of Cell Science*, vol. 117, no. 14, pp. 2971–2981, 2004.

[5] R. R. Pochampally, J. R. Smith, J. Ylostalo, and D. J. Prockop, "Serum deprivation of human marrow stromal cells (hMSCs) selects for a subpopulation of early progenitor cells with enhanced expression of OCT-4 and other embryonic genes," *Blood*, vol. 103, no. 5, pp. 1647–1652, 2004.

[6] A. P. Beltrami, D. Cesselli, N. Bergamin et al., "Multipotent cells can be generated in vitro from several adult human organs (heart, liver, and bone marrow)," *Blood*, vol. 110, no. 9, pp. 3438–3446, 2007.

[7] M. Kucia, R. Reca, F. R. Campbell et al., "A population of very small embryonic-like (VSEL) CXCR4^+ SSEA-1^+Oct-4^+ stem cells identified in adult bone marrow," *Leukemia*, vol. 20, no. 5, pp. 857–869, 2006.

[8] M. Kucia, M. Halasa, M. Wysoczynski et al., "Morphological and molecular characterization of novel population of CXCR4^+ SSEA-4^+ Oct-4^+ very small embryonic-like cells purified from human cord blood—preliminary report," *Leukemia*, vol. 21, no. 2, pp. 297–303, 2007.

[9] B. H. Kim, "On the Kyungrak system," *Journal of Academy of Medical Sciences*, DPR Korea, pp. 1–41, 1963.

[10] B. H. Kim, "The Kyungrak system and Sanal theory," *Journal of Academy of Medical Sciences*, DPR Korea, pp. 1–62, 1965 (Korean).

[11] B.-C. Lee, K. Y. Baik, H.-M. Johng et al., "Acridine orange staining method to reveal the characteristic features of an intravascular threadlike structure," *Anatomical Record B*, vol. 278, no. 1, pp. 27–30, 2004.

[12] B.-C. Lee, J. S. Yoo, K. Y. Baik, K. W. Kim, and K.-S. Soh, "Novel threadlike structures (Bonghan ducts) inside lymphatic vessels of rabbits visualized with a Janus Green B staining method," *Anatomical Record B*, vol. 286, no. 1, pp. 1–7, 2005.

[13] H.-S. Shin, H.-M. Johng, B.-C. Lee et al., "Feulgen reaction study of novel threadlike structures (Bonghan ducts) on the surfaces of mammalian organs," *Anatomical Record B*, vol. 284, no. 1, pp. 35–40, 2005.

[14] B.-C. Lee, S. Kim, and K.-S. Soh, "Novel anatomic structures in the brain and spinal cord of rabbit that may belong to the Bonghan system of potential acupuncture meridians," *JAMS Journal of Acupuncture and Meridian Studies*, vol. 1, no. 1, pp. 29–35, 2008.

[15] V. Ogay, K. Y. Baik, B.-C. Lee, and K.-S. Soh, "Characterization of DNA-containing granules flowing through the meridian-like system on the internal organs of rabbits," *Acupuncture and Electro-Therapeutics Research*, vol. 31, no. 1-2, pp. 13–31, 2006.

[16] K. Y. Baik, V. Ogay, S. C. Jeoung, and K.-S. Soh, "Visualization of bonghan microcells by electron and atomic force microscopy," *JAMS Journal of Acupuncture and Meridian Studies*, vol. 2, no. 2, pp. 124–129, 2009.

[17] C.-J. Choi and C.-H. Leem, "Comparison of the primo vascular system with a similar-looking structure," in *The Primo Vascular System*, K.-S. Soh, K. A. Kang, and D. K. Harrison, Eds., pp. 107–113, Springer, New York, NY, USA, 2012.

[18] J. S. Yoo, M. S. Kim, V. Ogay, and K.-S. Soh, "In vivo visualization of Bonghan ducts inside blood vessels of mice by using an Alcian blue staining method," *Indian Journal of Experimental Biology*, vol. 46, no. 5, pp. 336–339, 2008.

[19] J. Ratajczak, M. Wysoczynski, F. Hayek, A. Janowska-Wieczorek, and M. Z. Ratajczak, "Membrane-derived microvesicles: important and underappreciated mediators of cell-to-cell communication," *Leukemia*, vol. 20, no. 9, pp. 1487–1495, 2006.

[20] D.-M. Shin, R. Liu, I. Klich et al., "Molecular signature of adult bone marrow-purified very small embryonic-like stem cells supports their developmental epiblast/germ line origin," *Leukemia*, vol. 24, no. 8, pp. 1450–1461, 2010.

[21] M. Z. Ratajczak, M. Kucia, T. Jadczyk et al., "Pivotal role of paracrine effects in stem cell therapies in regenerative medicine: can we translate stem cell-secreted paracrine factors and microvesicles into better therapeutic strategies?" *Leukemia*, vol. 26, pp. 1166–1173, 2012.

[22] M. Z. Ratajczak, "The emerging role of microvesicles in cellular therapies for organ/tissue regeneration," *Nephrology Dialysis Transplantation*, vol. 26, no. 5, pp. 1453–1456, 2011.

[23] R. Liu, I. Klich, J. Ratajczak, M. Z. Ratajczak, and E. K. Zuba-Surma, "Erythrocyte-derived microvesicles may transfer phosphatidylserine to the surface of nucleated cells and falsely "mark" them as apoptotic," *European Journal of Haematology*, vol. 83, no. 3, pp. 220–229, 2009.

Hindawi Publishing Corporation
Evidence-Based Complementary and Alternative Medicine
Volume 2013, Article ID 587827, 12 pages
http://dx.doi.org/10.1155/2013/587827

Review Article

50 Years of Bong-Han Theory and 10 Years of Primo Vascular System

Kwang-Sup Soh,[1] Kyung A. Kang,[2] and Yeon Hee Ryu[3]

[1] *Nano Primo Research Center, Advanced Institute of Convergence Technology, Seoul National University, Suwon 443-270, Republic of Korea*
[2] *Departments of Chemical Engineering, University of Louisville, Louisville, KY 40292, USA*
[3] *Korea Institute of Oriental Medicine, Daejon 305-811, Republic of Korea*

Correspondence should be addressed to Kwang-Sup Soh; kssoh1@gmail.com and Yeon Hee Ryu; yhryu@kiom.re.kr

Received 24 December 2012; Accepted 16 March 2013

Academic Editor: Xianghong Jing

The primo vascular system (PVS) was first introduced by Bong-Han Kim via his five research reports. Among these the third report was most extensive and conclusive in terms of the PVS anatomy and physiology relating to the acupuncture meridians. His study results, unfortunately, were not reproduced by other scientists because he did not describe the materials and methods in detail. In 2002, a research team in Seoul National University reinitiated the PVS research, confirmed the existence of PVS in various organs, and discovered new characteristics of PVS. Two important examples are as follows: PVS was found in the adipose tissue and around cancer tissues. In parallel to these new findings, new methods for observing and identifying PVS were developed. Studies on the cell and material content inside the PVS, including the immune function cells and stem cells, are being progressed. In this review, Bong-Han Kim's study results in his third report are summarized, and the new results after him are briefly reviewed. In the last section, the obstacles in finding the PVS in the skin as an anatomical structure of acupuncture meridian are discussed.

1. Introduction: A Brief Historical Review

It was in 1962 when Bong-Han Kim (hereafter BH Kim or Kim) reported his first study results on the anatomical entity of acupuncture meridians (AM) [1]. He then established and became the director of National Acupuncture Meridian Research Institute in 1963 in Pyungyang, North Korea. The Institute produced four additional reports on this new system [2–5] until October 1965, when the institute abruptly closed for some unknown reasons. His fate after the event is still unknown.

The first report was very brief and mostly about the electric response of acupoints, which was probably not considered very exciting. The second report, however, contains the discovery of a completely new system, constituting node-like anatomical structures at the acupoints and the tube-like structure (Kim claimed it to be the AM) connected to the nodes in the skin [2]. The research team named the nodes the Bonghan corpuscles (currently renamed as primo nodes) and the tubes the Bonghan ducts (primo vessels). They also found that this new system existed not only in the skin but also throughout the body, including on the surfaces of body organs and inside the blood and lymph vessels. This new discovery became the foundation of the Bong-Han theory. To publicize its scientific achievements, the North Korean government translated Kim's second report in various languages including English and disseminated it to most major libraries in the world [6]. The third report was an extension of the second one, observing the entire network of the Bong-Han system (renamed as primo vascular system (PVS)) in the mammalian body [3]. The fourth one was about the "Sanal," (renamed to be Primo-microcell (P-microcell)), whose functions, he claimed, were regeneration and/or repair, as totipotent stem cells [4]. Sanal is a Korean word and its direct translation in English is "live egg." The last (fifth) one was a brief report about the hematopoietic function of the Sanal [5]. These five publications were reports rather than journal articles, and they described mainly results with insufficient information on methods and materials. The introduction and discussion sections were very short.

Shortly after Kim's fifth report, neither he nor his publications reappeared in public for some unknown reason, and his work was completely neglected by the North Korean government. Outside the North Korea (Democratic People's Republic of Korea; DPRK), there have been several attempts to reproduce Kim's results but without success, probably because details of his methods to identify this new organ were described either in any of his reports or elsewhere. Nevertheless, until now, there has been no known serious attempts to either confirm or negate his claims, with exceptions of the following two cases: one was by Kellner, who thoroughly investigated the acupoints in a histological manner but failed to find the structure that Kim had claimed [7]. In our scientific opinion, Kellner's conventional method for histological study was not appropriate for detecting the anticipated structure in the skin, because in the cross section of the tissue containing an acupoint this new organ may not be differentiated from its surrounding tissues. Optically and histologically, both look very similar if they are seen in their cross sections. Its presence can be revealed most likely in the longitudinal view, with application of appropriate dyes, according to our own experiences for the past ten years. Another case was by Fujiwara and Yu, who partially confirmed Kim's discovery but incompletely [8]. Fujiwara, who was an assistant professor in anatomy, then, later recalled that it took about a half year of hard work to get some positive results [9]. He was able to reproduce Kim's results inside blood vessels and on the surfaces of organs, which eventually helped the research of Soh, one of the coauthors for this paper.

Soh was a professor in the Department of Physics at the Seoul National University (SNU) during 1976–2011. He formed Biomedical Physics Laboratory in 2000, initially to investigate the biological phenomena related to the acupuncture therapy using physical means, such as electricity, magnetism, acoustics, and optics. He realized that his investigation without anatomical bases would not lead to the fundamental mechanism behind the acupuncture therapy. Therefore he formed a scientific team to investigate the Bong-Han theory with Dr. BC Lee as the main experimental partner. The SNU team soon successfully confirmed the PVS presence inside the blood vessel of rabbits. However, this initial success soon faced difficulties in reproducibility. They realized that the research requires highly skilful researcher in microsurgery and optical imaging due to the extremely small size and the semitransparent nature of the organ, which frequently impeded the progress in their study.

The team, therefore, decided to seek Professor Fujiwara's help and Soh visited Dr. Fujiwara in Osaka. Fujiwara himself had experiences with failures in finding the PVS on the surfaces of internal organs for more than six months. Fujiwara was so kind to provide a movie containing the experimental procedures that he had developed in 1960s. With Dr. Fujiwara's method, the SNU team then was able to reproduce his results. Since then, the team identified the PVS floating on the surfaces of intestines, liver, stomach, and bladder of rabbits. Soon, more thorough, histological and morphological studies on PVS were performed to confirm Kim's claims. With techniques and experiences obtained for the organ-surface PVS, the team moved forward to find the PVS floating inside lymph vessels. More importantly, a technique of using Trypan blue for PVS identification was developed by Dr. BC Lee, which enabled the team to identify the PVS in other organs, such as in the bovine heart, abdominal adipose tissues, brain ventricles, and the central canal of spinal cords. The Trypan blue technique also led to the discovery of the unique characteristics of the PVS in/on cancerous tumors (cancer PVS). This may probably be one of the most significant findings in the medical science because cancer is one of the most serious, life-threatening diseases.

Until 2008, the SNU-team was the only one performing the PVS research and, therefore, the research progress was rather slow. In 2009, a review article, written by Soh, covering the PVS research progress during 2002 and 2008 was published in the Journal of Acupuncture Meridian Studies [10]. Since then several research teams in Korea participated in the PVS research, and the number of teams and their research subjects have been steadily growing. Outside Korea, the PVS gained interest as a research topic, mainly in China and USA. In September 2010, an international symposium on the PVS, The Primo Vascular System, Its Role in Cancer and Regeneration, was held in Korea, and its proceedings was published by the Springer Publishing Company in 2011 [11].

Recently, a research team led by BS Kwon at the National Cancer Center of Korea [12] confirmed that the PVS was abundant with immune cells such as macrophages and mast cells, which had been previously noticed by the SNU team [13]. In addition, primo nodes were also found to be packed with very small, embryonic stem cell- like cells. These data are consistent with the claims by BH Kim's on the properties of the PVS on regeneration and wound healing [4].

In the remaining part of the paper, we summarize the content of Kim's third report, which relates the AM system with the PVS, with our comments. His report contents are compared with the recent works reported by the SNU group and other PVS scientists. Kim's study results that were scientifically verified by the PVS researchers were described first, and then new discoveries on the PVS after Kim were introduced. The desired directions for the future PVS research were also discussed.

2. Acupuncture Meridian System

The title of Kim's third report is "The Kyungrak (經絡) System" [3], and it is officially submitted by the "Kyungrak Institute (經絡 研究院) of Democratic People's Republic of Korea," where Kim was the director. The English translation of the title is "Acupuncture Meridian System." The report covers research results on the PVS network, and the scientific standard of its content is more advanced and comprehensive than that of his previous two reports. This was, in fact, his last report relating the acupuncture meridians with the PVS. The last two of his reports were about the "Sanals" or P-microcells [4, 5], and they were published shortly before the institute was abruptly closed in 1965.

The English translated table of content of the third report was presented in Box 1 for the readers to easily capture the breadth of Kim's work. As can be seen in the box, the third

TABLE OF CONTENT

Box 1: Content of Bong-Han Kim's third report, (it should be noted that, in the box, the terms related to the Bong-Han System are translated into the terms of Primo Vascular System).

report covers not only anatomical and histological aspects of PVS but also its basic physiological aspects. The conclusion section of the report is in fact a good summary of the report, which was highly beneficial to future PVS researchers. We, therefore, translated this section (pages 36–38 of Kim's third report) with our own scientific comments, although the section by itself was already published in the book The Primo Vascular System [14]. We also added some of the important scientific progresses in the field of PVS, since Kim's publications, in subsequent sections.

2.1. English Translation of Conclusion Section of Bong-Han Kim's Third Report with Authors' Comments

2.1.1. The Bong-Han System (BHS) Is Composed of Several Subsystems

(A) These subsystems have common properties of possessing Bonghan ducts (BHDs) and Bonghan corpuscles (BHCs). All BHCs are interconnected via BHDs. BHDs connect BHCs. A BHD is composed of one to tens of Bonghan ductules.

(1) A ductule has a thin layer, composed of endothelial cells with rod-shaped nuclei. It is surrounded by an external membrane (endo-BHD), which is made of smooth muscle-like cells and fine argentaffin fibers. (Comments: Kwon et al. observed epithelial cells rather than smooth muscle-like cells [12].) The interluminal space in a BHD is filled with fibrous and amorphous materials. These ductules are wrapped together with a membrane (peri-BHD) to form a single BHD. This outer membrane is made of membranous cells. In the lumen of a ductule, basophilic the granules and nucleus-like bodies are present.

(2) The BHC is essentially formed by the enlargement, branching, or merging of the ductule. Also, the basic compositions of the BHC are the outer membrane of the ductules and the reticular fibers, extracellular matrices (ECM) between ductules. Inside the lumen of the BHD, which is extended from the BHC, basophilic granules, cell components, and chromaffin granules are present.

(B) The BHS is classified as described in the following.

(1) Intravascular BHS. This BHS class consists of the intravascular (IV) BHDs and BHCs. It is systematically distributed inside blood and lymphatic vessels along the vessel and inside the heart. (Comments: Up to now, the authors observed that the BHS is only in large caliber blood or lymphatic vessels. In the BH Kim's report, the size of the BHS-containing vessels is not clearly described.) The BHDs in this class are very fragile, and the ECM and their outer membranes (epi-BHD) are not well developed. The IV-BHC has a structure, particularly similar to hematopoietic organs. In the reticular BHS, lymphocyte series and myelocyte-like cells (cells in bone marrow) are present. Sometimes cells similar to organ parenchyma cells are gathered around.

(2) Organ surface BHS. This class of the BHS consists of the organ surface (OS) BHDs and BHCs. They freely float on the surfaces of internal organs and are not associated with blood or lymphatic vessels. For this class BHDs, the interluminal materials and the outer membrane are developed better than those for the IV-BHS. In the lumens of the BHDs and inside BHCs, there are cells possessing bright cytoplasm as well as the basophilic granules.

(3) Extravascular BHS. This BHS class made of the extravascular (EV) BHDs and BHCs. This runs along the blood and lymphatic vessels, and nerves. It is located just outside of them. It is covered with thick connective tissues. In the lumens of the BHDs and inside the BHC, many chromaffin granules are present.

(4) Nervous BHS. This class BHS is composed of the nervous (N) BHDs and BHCs, and it floats in the cerebrospinal fluid. Its branches are distributed in the parenchyma of the central nervous system and in the peripheral nervous system.

(5) Intraorgan BHS. Inside the parenchyma of internal organs, there are intraorgan (IO) BHDs and BHCs, terminal BHDs, and terminal BHCs. (Comment: the terminal BHD has only a single lumen, and it is a type of the ductule.) These are extension of the BHDs originated from IV-, EV-, or N-BHDs and present inside of the organ. Individual BHDs merge together in an IO-BHC and eventually form terminal sub-BHDs. These individual terminal sub-BHDs are directly connected to each nucleus of the organ cells. Again, these fine ductules come out from these cells.

(Comment: In summary, there are five subsystems, namely, IV-, OS-, EV-, N-, and IO-BHS). The BHS subclasses are well connected to each other. The IV-BHS is connected to the OS-BHS after coming out of the vessel wall. It is also connected to the EV-BHS via the EV-BHC. The OS-BHS is connected to the EV-BHS and the N-BHS. The communication among BHS subclasses is well established.

2.1.2. The BHS Is Made of Multiple Systems Circulating Bonghan Liquor

(A) Biochemical compositions of Bonghan liquor (i.e., liquid flowing inside the PVS) are

(1) abundant in DNA and RNA;

(2) total nitrogen content is 3.12–3.40%. Non protein nitrogen content is 0.10–0.17%. Lipid is 0.57–1.00%. Reduced sugar is 0.10–0.12%;

(3) total hyaluronic acid is 170.4 mg%;

(4) more than 19 free amino acids are present including several essential amino acids;

(5) there are more than 16 free mono nucleotides.

(B) The BHS possesses bioelectrical activities and mechanical motion.

(1) The propagation speed of the electric response from the BHD is very low and is similar to the two types of waves (ㄱ and ㄴ) displayed by the BHC. The BHD responses to electric stimuli appear in various forms. (Comment: there were two types of wave forms that Kim found: ㄱ and ㄴ; these symbols are Korean alphabet letters.)

(2) When a BHD is stimulated bioelectric signals propagate through the BHD. The speed of propagation is faster (1–3 mm/sec) for the waves with a smaller amplitude and slower for the greater.

(3) The BHD has a spontaneous motion. This motion propagates and changes when the BHD is stimulated. Its longitudinal, os-cillatory motion is either continuous or periodic. The transversal motion is vibratory. These suggest that the BHS is capable of actively circulating the Bonghan liquor.

(C) All cells are connected to the BHS.

(1) The nucleus of each cell has very small, entering and exiting terminal ductules. These ductules are connected to the BHCs in the internal organs. These IO-BHSs are connected to the cells only in their neighboring area. The IO-BHC is connected to the BHS of other classes. In other words, the BHS networks in various classes leave from and arrive at IO-BHSs.

(D) The circulatory paths observed by the radioactive P^{32} injected into various points of the BHS are as follows.

(1) The Bonghan liquor from all tissues circulates to the BHS in the skin. (Comment: The BNS in the skin may be the known acupoints and probably many unknown points.)

(2) The Bonghan liquor flows from the BHS in the skin to the BHS deep inside the body.

The fluid in the deep BHS flows to the IO-BHSs and then to the cells in the tissue. These data agree with the circulation study results obtained using dyes.

(E) The BHS circulatory path is not a singular system.

Unlike the blood circulation system, the Bonghan liquor circulatory path is not singular but multiple. These paths are connected but independent.

A dye or isotope injected into a specific network circulates only in the region of its particular network.

However, the Bonghan liquor in a particular path crosses to another one through the connecting routes between the two paths.

2.1.3. A Change in the Bonghan Liquor Condition Affects the Functions of Organs

(A) Stimulation on the BHD affects the pulsation frequency and amplitude of the heart and changes the peristaltic motion of intestines. It also affects the hysteric curves of skeletal muscles significantly.

(B) Severing a BHD significantly affects the cells of the tissues connected to the BHD.

(1) It causes the dissolution of the nuclei and consequently death of the cells.

(2) If the BHD responsible for a peripheral nerve is severed, the excitability of the nerves reduces significantly.

(3) If the BHD of a motor nerve is severed, for a certain period of time, the associated muscle does not show movement responding to the repetitive stimulations.

2.1.4. In Terms of the Stage during the Differentiation and Development. The BHS Precede Those of Blood Vessels, Nerves, and Other Organs. The typical developmental stages of BHD, for chicken egg, from incubation are: the 7–8th hours, BHD blast; the 10th hours, pre-BHD; the 15th hours, proto-BHD; and the 20–28th hours, fully developed BHD. The earlier timeline of the BHS differentiation and development suggests its roles in the development. (Comments: in the report, there is no description on its roles.)

2.1.5. BHS Exists Broadly, in All Levels of Life. The BHS is proven to exist not only in the mammalian but also in all vertebrates and invertebrates. It exists even in the plant. We conjecture that it exists in any multicellular lives

The study results on the BHS suggest that the BHS circulation rout is cells in the tissue → skin BHCs → deep BHCs → intraorgan BHCs → terminal BHSs → cells in the tissue.

The BHS is made of multiple, independent circulating systems (subsystems), which are interconnected each other, but forming a single coherent system.

All organs of the living beings are connected to and controlled by the BHS. In other words, all forms of lives have their own BHS.

3. Confirmation of BH Kim's Study Results

The nature and the scale of BH Kim's accomplishments on the PVS are enormous. Since 2002, selected parts of BH Kim's studies were repeated, and his results were confirmed to be accurate. This section summarizes BH Kim's findings that were verified fifty years later, by various scientists. Here, we briefly list the original terms and the new ones of the system, for your convenience. Bong-Han system (BHS) = primo vascular system (PVS), Bonghan duct (BHD) = primo vessel (PV), Bonghan corpuscle (BHC) = primo node (PN), Bonghan ductule = P-subvessel, Bonghan liquor = primo fluid (P-fluid), and Sanal = p-microcell.

3.1. Animal Species and Organs Studied. Animal species studied for identifying the PVS were mainly rabbits, rats, and mice. For a few cases, pigs, dogs, cows, and human placentas were also studied. Among the PVS subclasses, defined by Kim (Box 1), the IV-, OS-, and N-PVS were confirmed partially, if not completely.

The IV-PVS floating inside blood vessels was first identified in the abdominal artery and the *caudal vena cava* of rabbits [14], rats [15], and mice [16]. More importantly, the PVS in the atrium of a bovine heart was found to form a floating network [17]. The PVS in the sagittal sinus of a rat brain was recently identified [18].

The IV-PVS floating inside lymph vessels, was visualized with help of Janus Green B [19], fluorescent nanoparticles [20], Alcian blue [21] and with no contrast agent [22]. The morphological information on PVS [23] and protocols used for PVS related experiments [24] were recently published. The fact that the PNs possess large amount of cells and granules related the immune system may imply that the PVS is involved in protecting function of the body [12].

The OS-PVS floating on the surfaces of internal organs was observed in rabbits [25] rats [26], mice [27], dogs [28], and pigs [29]. The structure of this PVS subclass was characterized by the optical [25], and electron microscopy [13, 30].

The N-PVS floating in the cerebrospinal fluid (CSF) in the brain of a rabbit [31] and a rat [32] was optically observed, by use of Trypan blue. The PVS in the subarachnoidal space of the rabbit [33] and rat [34] brains, and in the spine of the rat [35] and pig [36] were also identified.

All PVS observed and listed previously were floating in the body fluid, such as blood, lymph, abdominal fluid, and CSF.

3.2. Brief Summary of Important PVS Characteristics Verified

3.2.1. Confirmation of PV Features. One of the most distinguished anatomical features of the PV is its bundle-like structure made of multiple subvessels. Figure 1(a) shows a schematic diagram of a PV prepared by Kim [3]. Throughout BH Kim's five reports, he, however, did not provide any actual image or the method to observe the PVS, corresponding to the diagram. It has been, therefore, difficult to obtain the PV image with its cross section. The image published in 2009, with hematoxylin and eosine staining, is shown in Figure 1(b) [37]. The existence of P-subvessel lumens is indeed shown in the figure, but the shape of lumens is still not clearly shown. Thanks to better techniques in the sample preparation and microscopy, imaging of a PV cross section, without severe deformation, is now possible. In one of most recent study results with an OS-PVS, a PV cross section imaged utilizing transmission electron microscopy (TEM; Figure 1(c)) [37] shows even the endothelial cell layer of a PV. The surrounding ECM is made of collagen fibers, as BH Kim claimed 3. Figure 1(d) shows confocal microscopy images of the longitudinal and cross sections of a PV sample harvested from the superior sagittal sinus of a rabbit brain [33], which clearly shows multiple lumens in a PV. We, therefore, suspect that the difficulties in appropriately preparing PV samples and in having good microscopy techniques might be the reason why BH Kim did not provide images of PV cross sections. Figure 1(e) is a schematic illustration of the PV compared with blood and lymphatic vessels displayed by Ogay et al., which summarizes most distinctive anatomical features of the PVS [37].

3.2.2. Cells inside the Primo Node. The PN is surrounded by a thin membrane, usually connected to two or more PVs (Figure 2(a)), and contains many cells (Figure 2(b)) and embryonic stem cell-like bodies (Figure 2(c)). Recent studies on PN have been mainly on the P-microcells (or Sanals) and other types of cells in it. Presence of many cells involved in immune functions was first noticed by TEM in the PN sample obtained from the rabbit organ surfaces [13]. The cell types and the ratio of the cells in the PNs harvested from the internal organ surfaces and inside the lymphatic vessels of rats are [12] mast cells (20%), eosinophils (16%), neutrophils (5%), histiocytes (53%), lymphocytes (1%), and round immature stem cells (3%). Although the presence of immune cells in PNs was not specifically mentioned in BH Kim's report, he did emphasize the abundance of chromaffin cells [3], which was confirmed by Kwon et al. [12].

The presence of BH Kim's Sanals (P-microcells) in the PVS was studied by the SNU team from its inception [25]. The cells were found to show a peculiar motion to the light in the UV-A range (360 nm) [40, 41]. Later, the budding process for cell proliferation was identified by atomic force microscopy [42–44]. An implication for these cells to be embryonic-like stem cells were made after confirming the expression of the stem cell biomarkers oct4, nanog, and CD133 [12, 38]. More studies on the Sanal are being in progress.

3.2.3. The Primo Fluid and Its Flow Direction. BH Kim's study results on the primo fluid circulation were confirmed only in a very limited level. The flow of the primo fluid in a certain path was demonstrated in the study using Alcian blue, from the rat acupoint BL-23 in the dorsal skin to the PVS on the surface of internal organs [45]. The experiment was, however, not always repeatable, and the reason for this inconsistency is still unknown.

When Chrome-hematoxylin and fluorescent nanoparticles were injected into testis they were found in the PVs on

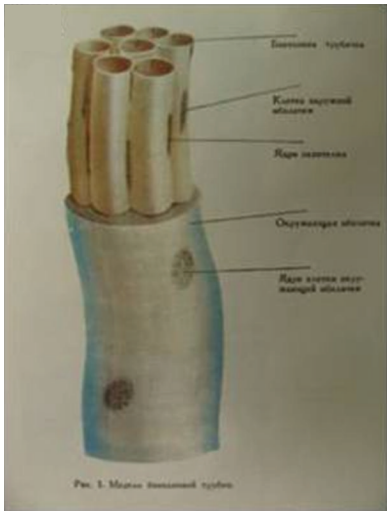

Рис 1 Модель бонхановой трубки,
Pic 1. Model of a primo vessel
Бонханова трубочка,
Primo subvessel (Bong-Han ductule)
Клетка наружной оболочки,
External membrane of cell
Ядро эндотелия,
Nucleus of endothelium
Окружающая оболочка,
Surrounding membrane
Ядро клетки окружающей оболочки,
Nucleus of surrounding membrane

(a)

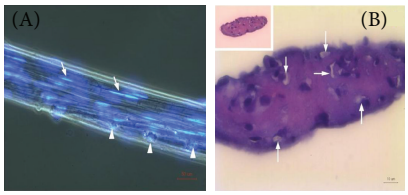

(b)

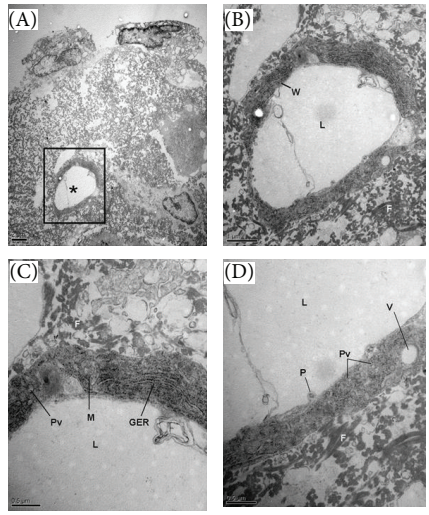

(c)

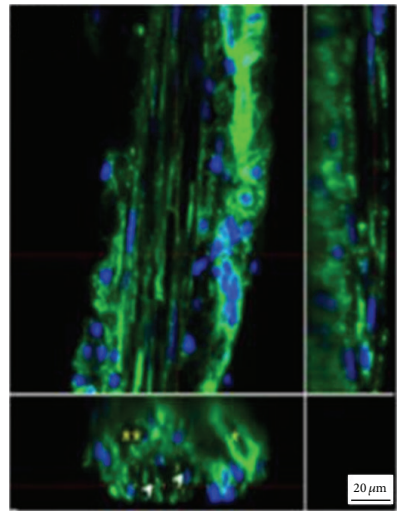

(d)

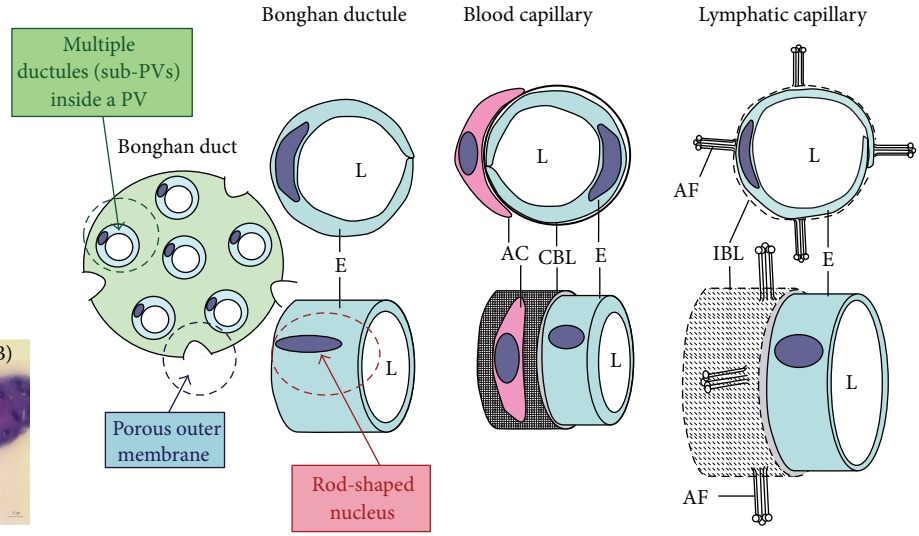

(e)

Figure 1: PV (Bonghan duct) illustrated in various publications. (a) Schematic diagram of a primo vessel, described by Bong-Han Kim with Russian terminologies. English translation of the terminology is added in bold [3]. (b) Optical images showing histological characteristics of a PV. (A) Phase-contrast image of a PV with DAPI. Several sub-PVs (arrow) with rod-shaped nuclei (light blue, arrowhead) are seen. (B) The cross section of a PV: several lumens (arrows) are seen [37]. (c) Electron microscopy of a partial cross section of a PV. (A) A lumen (asterisk) of a sub-PV can be seen. (B) Magnified image of the lumen (rectangular area in (A)). The wall (W) of the sub-PV consists of a single layer of endothelial cells surrounded by fibrin-like fibers. ((C), (D)) Magnified image of (B). L: lumen; M: mitochondria; GER: granular endoplasmic reticulum; P: cytoplasmic protrusion; PV: pinocytotic vesicles; V: vacuole; and F: fibrin-like fiber [37]. (d) Confocal laser scanning microscope image of a PV. The main panel is optical microscopy of the longitudinal section of a PV (the middle section, cells with rod-shaped nuclei in blue), accompanied by a venule and an arteriole on each side (cells with circular nuclei). The lower panel is a cross section of the PV, showing multiple lumens (open arrowheads), and the venule (asterisk) and the arteriole (two asterisks) on its each side. The PV diameter was approximately 30 μm [33]. (e) Anatomical comparisons of characteristics of the PV, blood, and lymphatic capillaries. The PV has multiple sub-PVs within, and the PV's outermost layer has large pores. The endothelial cells of the sub-PV possess rod-shaped nuclei. E: endothelium; L: lumen; AC: accessory cell; CBL: complete basal lamina; IBL: incomplete basal lamina; and AF: anchoring filaments [37].

the organ surfaces between the abdominal cavity and the abdominal wall, although farther tracing was not technically possible with optical microscopy [46]. Tracing primo fluid in the PV on rabbit organ surfaces was possible using Alcian blue, and the flow speed was measured to be 0.3 ± 0.1 mm/sec [30]. This value was consistent with the values in BH Kim's reports [3].

One of the important biochemicals in the primo fluid, which was mentioned in BH Kim's report, was catecholamine (adrenalin and noradrenalin) [3], and its presence was later

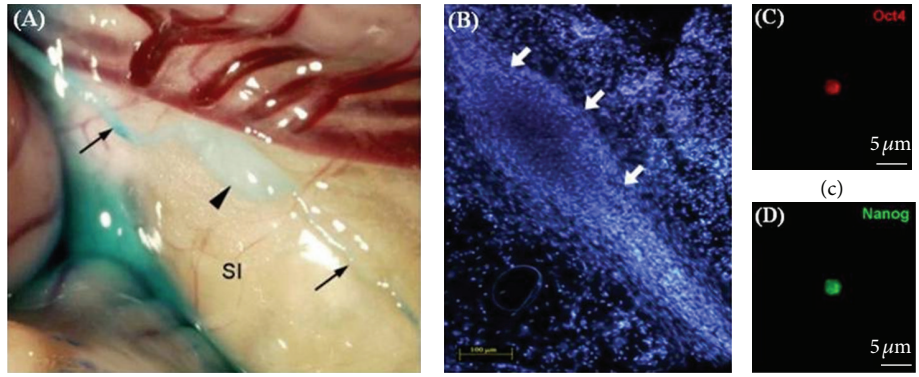

Figure 2: Images of PVS. (a) An image of a PN (Bonghan corpuscle; arrowhead) found on the rabbit small intestine, with PVs (arrows) at both ends, using methylene blue as the contrast agent [37]. (b) An image of a PN (arrows), which was identified lower part of the superior sagittal sinus of a rabbit brain [33]. DAPI staining of the nuclei of the cells inside the PN. Very small cells are packed in the PN. ((c), (d)) Immunostaining of the small cells isolated from PNs on the surfaces of rat intestine, for the embryonic stem cell markers Oct4 (red) and Nanog (green). The scale bar indicates 5 μm [38].

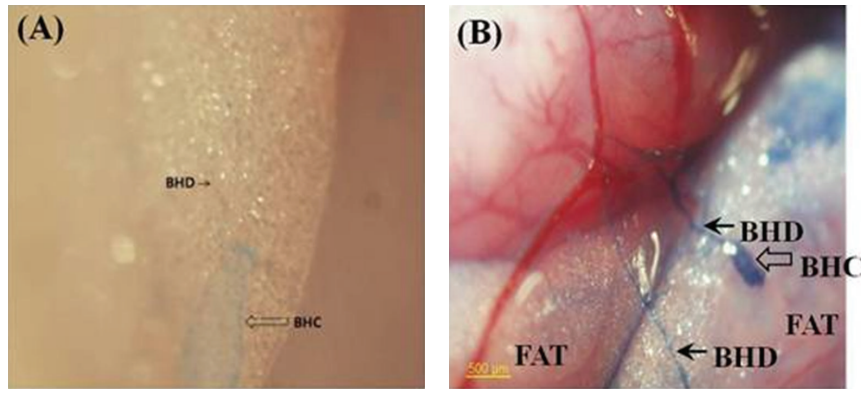

Figure 3: Images of PNs with different dyes. (a) A PN (BHC) and a PV (BHD) connected to the PN, on the adipose tissue around the rat small intestine. Alcian blue flow through the PVS left it pale blue. Notice that Alcian blue did not remain in the PVS and, therefore, *in situ* tracking of the PVS using this dye was difficult. (b) A PN and PVs, observed near the rat small intestine, stained with Trypan blue. Notice that the blood vessel and adipose tissue were not stained [39].

confirmed in the PNs on the organ surface of rabbits [47] and rats [12], using ELISA.

4. New Discoveries

Since the initiation of the PVS research, the SNU team made significant discoveries on PVS as well as developing new techniques for identifying PVS in the mammalian body. A few important and medically relevant findings are presented here.

4.1. The PVS in Adipose Tissues. The presence of the PVS entering the adipose tissues around the rat small intestine was first noticed via optical imaging using Alcian blue, which was injected intravenously at the femoral vein. The Alcian blue entering a PVS floating inside a blood vessel reached to a PN in an adipose tissue as shown in Figure 3(a). Unfortunately, the dye flowed away without showing its previous paths. Therefore, *in situ* tracking of the PVS using this dye was found to be inappropriate [39].

Trypan blue, an alternative, was, therefore, tested, and it remained inside the PVS, allowing us to visualize the system in the adipose tissue. Trypan blue was found to stain the PVS preferentially to the adipose tissues or blood vessels [39]. Figure 3(b) illustrates images of the PVS, using Trypan blue, in the adipose tissues around the small intestine of a rat. The presence of PVS in adipose tissues raises conjectures on its possible roles in connection with regeneration, obesity, and obesity-related diseases.

4.2. Cancer PVS. Existence of PVS on the surface of the tumor membranes in a xenografted mouse was first observed by Yoo et al. [48] of the SNU team. It was soon realized that PVS was more densely populated in proximity of tumors (xenografts) in various type of cancerous, human origin

tumors, and, therefore, they were easily identified [27]. More importantly, significantly large number of cancer cells was found in PVs connecting the primary to the secondary tumors [49].

Since these initial findings by the SNU team, research teams of Akers [50], Hong [51], Heo [52], Islam [53], and Kang [54] confirmed the presence of high density PVS (cancer PVS) in close proximity of cancer xenografts in mice. A PV floating inside a lymph vessel originated from the tumor xenografted in the abdominal skin of a mouse was also reported [55].

The Miller team also reported that the cells obtained from the cancer-PVS of murine xenograft of human originated lymphoma U937 expressed CD68, CD45, and lysozome. They also revealed that the immunophenotype of cells inside the cancer PVS is of U937 cell. The cells also showed hundreds to thousandsfold, upregulated KLF4, one of the human cancer stem cell specific transcription factors and an upstream regulator of NANOG, which maintain the pluripotent and undifferentiated state of stem cells [53].

4.3. Other New Findings. For the PVS studies, the SNU team has been using traditional histochemistry techniques with dyes such as Alcian blue, Trypan blue, chrome-hematoxylin. Among these the Trypan blue spraying technique invented by Dr. BC Lee was most effective for many applications. The team also adopted modern imaging techniques utilizing fluorescent nanoparticles, quantum dots, immune-affinity technique, electron microscopy [56], X-ray microscopy, and GFP expressing cells and animals, which were not available at the time of BH Kim. DAPI staining to check the shape of cell nuclei is one of the important and frequently used new techniques for the PV identification.

In Kim's reports, only white blood cells among cells and biochemicals are involved in the immune system. The concept of the stem cell, especially of the adult stem cell, was not very well known in his time, but he claimed that P-microcell (Sanal) is the main agent for wound healing and regeneration, which are the two fundamental roles of stem cells [4]. Considering that the Sanal size is very small (1–5 μm), an important question is the relation between the Sanal and the very small embryonic-like stem cells (VSEL) described by Ratajczak et al. [57], because both seem to have very similar characteristics. The budding of Sanals was previously observed by atomic force microscopy [43], and the expressions of several stem cell biomarkers on/in Sanals are confirmed. Detailed and various aspects on the Sanal should be investigated because the important nature of this particular cell. Kim also claimed that the proliferation of Sanals was affected by the light, which has not been confirmed yet, although the average movement activities of the Sanal in liquid was found to increase when the light at 360 nm (UV-A) was illuminated [40].

PVS does not express CD31 (blood vessel specific marker) and LYVE-1 (lymphatic vessel biomarker), confirming that the PVS is different from the blood or lymphatic systems. Proteomics study results on the PV and P-fluid harvested from the rabbit organ surface [58] revealed that keratin 10 was present in the PVS. Results of western blot [59] and immunohistochemistry [12] revealed that the keratin 10 was found to be from the epithelial cells of the PVS outer surface. Epithelial marker protein 3 (EMP-3) [12] was also found in the outer membrane of PVS, and von Willebrand Factor (vWF) was present in the PVS endothelial cells.

5. Concluding Remarks

Fifty years ago, BH Kim showed the relationship between the acupuncture meridian and the PVS by injecting a blue dye into an acupuncture point and by observing the dye flowing via the meridian, and concluded that the meridian system belongs to the Bong-Han system (PVS). Until now, the blue dye that BH Kim used is not known, and most of his claims on the meridian and the Bong-Han system are still to be verified, although many of his study results that could be repeated until now are found to be very important for the modern biomedical sciences. Approximately fifty years after BH Kim, the presence of the PVS inside the blood and lymphatic vessels, cerebrospinal fluids of the central nervous system, and on the surface of the various internal organs was indeed confirmed by various techniques developed by the SNU team [60]. The most significant unconfirmed part is ironically the PVS in skin, which is supposed to be the acupoint. BH Kim claimed that the acupuncture meridians extended into the PVS inside the mammalian body, which still needs to be verified because the techniques used for the PVS inside the body do not appear to work for the PVS in the skin.

A proposed detection procedure for identifying the PVS in the skin is as follows. (1) First, perform proteomics and genomics of the PVS with the PVS specimens that can be now harvested, and identify PVS specific biomarkers. (2) Then, develop these biomarker-specific, targeting biomolecules, such as antibodies or aptamers. (3) Apply the appropriate image contrast agents conjugated-targeting molecules into PNs. (4) Trace the contrast agents in appropriate image modalities to map the PVS in the entire body [61]. In this way, the entire PVS network, including the ones in the skin (acupoints), is expected to be visualized.

Currently, the main obstacles to this proposed approach are in the difficulties in obtaining sufficient quantity of pure PVS samples using the current techniques, due to the very small size of the PVS, and in identifying proper imaging modalities that can provide both sufficient sensitivity and resolution. Nevertheless once the PVS-specific biomarkers are identified, the rest is expected to be resolved with less difficulties.

We strongly believe that the thousand-year-old acupuncture therapy and traditional eastern medicine will become a true sense of the scientific medicine when the entire network of PVS and its roles in mammalian body are fully uncovered. This will then shift the level of the oriental medicine from the traditional wisdom and art with a long history to the biomedical sciences in true sense. Furthermore, it will also bring a paradigm change in the regenerative medicine, cancer, immune deficiency or hyperactivity, pain

control, stem cell therapy, and other important issues in the human health care in general.

Remaining Challenges

(1) Up to now, three of five PVS classes of BH Kim classified have been confirmed for their existence. All PVS classes need to be verified as soon as possible to fully utilize them for the medical purpose.

(2) Due to the small size and transparent nature of the PVS, identifying the system has been extremely difficult. Although there have been many progresses in PVS imaging techniques during the past ten years, which are described in this article, more user-friendly techniques, especially for beginning researchers, need to be developed.

(3) Due to the enormity of the potential that the PVS related knowledge to the future medicine, complete understanding of the system needs to be expedited. This would be feasible only by well-organized and -focused multidisciplinary research efforts.

(4) Now, with the confirmation on the existence of the PVS, is the time to vigorously pursue to elucidate the physiological roles of the PVS, both in western and eastern biomedical terms. Some of the PVS functions related to the meridian were already reported by Wang et al. [62]. The PVS on the surface of internal organs was involved neither in the inhibition of the gastric motility induced by acupuncturing at CV12 nor in the facilitation of gastric motility induced by acupuncturing at ST36, both of which are related to the subclass OS-PVS. However, the nature of the communication among the five subclass PVS networks is extremely complicated. The most important ones for the intestinal motility may be those along blood vessels (EV-PVS) and nerves (N-PVS) as implied in BH Kim's work [2]. The OS-PVS is deeply related to stem cell-like functions and immune functions [12]. The work on cancer PVS suggested that primo vessel could provide a path for metastasis [48, 49, 53]. In sum, elucidating the functional relationship between the PVS and acupuncture meridian may be one of many important ways of connecting the eastern medicine to the western.

Conflict of Interests

The authors declare no conflict of interests.

Acknowledgments

This work was supported in part by a grant from the National Research Foundation of Korea and Korea Institute of Oriental Medicine (K13290).

References

[1] B. H. Kim, "Study on the reality of acupuncture meridians," *Journal of Jo Sun Medicine*, vol. 9, pp. 5–13, 1962 (Korean).

[2] B. H. Kim, "On the acupuncture meridian system," *Journal of Jo Sun Medicine*, vol. 90, pp. 6–35, 1963 (Korean).

[3] B. H. Kim, "The Kyungrak system," *Journal of Jo Sun Medicine*, vol. 108, pp. 1–38, 1965 (Korean).

[4] B. H. Kim, "Sanal theory," *Journal of Jo Sun Medicine*, vol. 108, pp. 39–62, 1965 (Korean).

[5] B. H. Kim, "Sanal and hematopoiesis," *Journal of Jo Sun Medicine*, vol. 108, pp. 1–6, 1965 (Korean).

[6] B. H. Kim, *On the Kyungrak System; (Journal of the Academy of Medical ScienceS of the Democratic People'S Republic of Korea)*, vol. 90, 1963.

[7] G. Kellner, "Bau und Funktion der Haut," *Dtsch Zschr Akup*, vol. 15, pp. 1–31, 1966 (German).

[8] S. Fujiwara and S. B. Yu, "Bonghan theory'morphological studies," *Igaku noAyumi*, vol. 60, pp. 567–577, 1967 (Japanese).

[9] S. Fujiwara and S. B. Yu, "A follow-up study on the morphological characteristics in Bong-Han theory: an interim report," in *The Primo Vascular System: Its Role in Cancer and Regeneration*, K. S. Soh, K. A. Kang, and D. Harrison, Eds., pp. 19–22, Springer, New York, NY, USA, 2011.

[10] K.-S. Soh, "Bonghan circulatory system as an extension of acupuncture meridians," *Journal of Acupuncture and Meridian Studies*, vol. 2, no. 2, pp. 93–106, 2009.

[11] K. S. Soh, K. A. Kang, and D. Harrison, Eds., *The Primo Vascular System: Its Role in Cancer and Regeneration*, Springer, New York, NY, USA, 2011.

[12] B. S. Kwon, M. H. Chang, S. S. Yu, B. C. Lee, J. Y. Ro, and S. Hwang, "Microscopic nodes and ducts inside lymphatics and on the surfaces of internal organs are rich in granulocytes and secretory granules," *Cytokine*, vol. 60, no. 2, pp. 587–592, 2012.

[13] B.-C. Lee, J. S. Yoo, V. Ogay et al., "Electron microscopic study of novel threadlike structures on the surfaces of mammalian organs," *Microscopy Research and Technique*, vol. 70, no. 1, pp. 34–43, 2007.

[14] J. Kim, J. Jung, and M. Potroz, "Summary of Bong-Han Kim's publications," in *The Primo Vascular System*, K. S. Soh, K. A. Kang, and D. Harrison, Eds., pp. 7–17, Springer, New York, NY, USA, 2011.

[15] B.-C. Lee, K. Y. Baik, H.-M. Johng et al., "Acridine orange staining method to reveal the characteristic features of an intravascular threadlike structure," *Anatomical Record B*, vol. 278, no. 1, pp. 27–30, 2004.

[16] J. S. Yoo, M. S. Kim, V. Ogay, and K.-S. Soh, "In vivo visualization of Bonghan ducts inside blood vessels of mice by using an Alcian blue staining method," *Indian Journal of Experimental Biology*, vol. 46, no. 5, pp. 336–339, 2008.

[17] B.-C. Lee, H. B. Kim, B. Sung et al., "Network of endocardial vessels," *Cardiology*, vol. 118, no. 1, pp. 1–7, 2011.

[18] H. S. Lee, W. H. Park, A. Je, H. S. Kweon, and B. C. Lee, "Evidence for novel structures (primo vessels and primo nodes) floating in the venous sinuses of rat brains," *Neuroscience Letters*, vol. 522, no. 2, pp. 98–102, 2012.

[19] B.-C. Lee, J. S. Yoo, K. Y. Baik, K. W. Kim, and K.-S. Soh, "Novel threadlike structures (Bonghan ducts) inside lymphatic vessels of rabbits visualized with a Janus Green B staining method," *Anatomical Record B*, vol. 286, no. 1, pp. 1–7, 2005.

[20] H.-M. Johng, J. S. Yoo, T.-J. Yoon et al., "Use of magnetic nanoparticles to visualize threadlike structures inside lymphatic vessels of rats," *Evidence-based Complementary and Alternative Medicine*, vol. 4, no. 1, pp. 77–82, 2007.

[21] C. Lee, S.-K. Seol, B.-C. Lee, Y.-K. Hong, J.-H. Je, and K.-S. Soh, "Alcian blue staining method to visualize Bonghan threads

inside large caliber lymphatic vessels and X-ray microtomography to reveal their microchannels," *Lymphatic Research and Biology*, vol. 4, no. 4, pp. 181–190, 2006.

[22] B.-C. Lee and K.-S. Soh, "Contrast-enhancing optical method to observe a Bonghan duct floating inside a lymph vessel of a rabbit," *Lymphology*, vol. 41, no. 4, pp. 178–185, 2008.

[23] Y. I. Noh, M. Rho, Y. M. Yoo, S. Jung, and S. S. Lee, "Isolation and morphological features of primo vssels in rabbit lymph vessel," *Journal of Acupuncture and Meridian Studies*, vol. 5, no. 5, pp. 201–205, 2012.

[24] S. Jung, S. Y. Cho, K. H. Bae et al., "Protocol for the observation of the primo vascular system in the lymph vessels of rabbits," *Journal of Acupuncture and Meridian Studies*, vol. 5, no. 5, pp. 234–240, 2012.

[25] H.-S. Shin, H.-M. Johng, B.-C. Lee et al., "Feulgen reaction study of novel threadlike structures (Bonghan ducts) on the surfaces of mammalian organs," *Anatomical Record B*, vol. 284, no. 1, pp. 35–40, 2005.

[26] B.-C. Lee, S.-U. Jhang, J.-H. Choi, S.-Y. Lee, P.-D. Ryu, and K.-S. Soh, "DiI staining of fine branches of Bonghan Ducts on surface of rat abdominal organs," *Journal of Acupuncture and Meridian Studies*, vol. 2, no. 4, pp. 301–305, 2009.

[27] J. S. Yoo, M. Hossein Ayati, H. B. Kim, W.-B. Zhang, and K.-S. Soh, "Characterization of the primo-vascular system in the abdominal cavity of lung cancer mouse model and its differences from the lymphatic system," *PLoS ONE*, vol. 5, no. 4, Article ID e9940, 2010.

[28] Z. Jia, K. S. Soh, Q. Zhou, B. Dong, and W. Yu, "Observation of primo vascular system on intestinal fascia of dogs," in *The Primo Vascular System*, K. S. Soh, K. A. Kang, and D. Harrison, Eds., pp. 71–76, Springer, New York, NY, USA, 2011.

[29] M. A. Hossein, Y. Y. Tian, T. Huang, Y. Q. Zhang, Y. Z. Che, and W. B. Zhang, "Finding a novel threadlike structure on the intra-abdominal organ surface of small pigs by using in vivo trypan blue staining," in *The Primo Vascular System*, K. S. Soh, K. A. Kang, and D. Harrison, Eds., pp. 63–70, Springer, New York, NY, USA, 2011.

[30] B. Sung, M. S. Kim, B.-C. Lee et al., "Measurement of flow speed in the channels of novel threadlike structures on the surfaces of mammalian organs," *Naturwissenschaften*, vol. 95, no. 2, pp. 117–124, 2008.

[31] B.-C. Lee, S. Kim, and K.-S. Soh, "Novel anatomic structures in the brain and spinal cord of rabbit that may belong to the Bonghan system of potential acupuncture meridians," *Journal of Acupuncture and Meridian Studies*, vol. 1, no. 1, pp. 29–35, 2008.

[32] J. X. Dai, B.-C. Lee, P. An et al., "In situ staining of the primo vascular system in the ventricles and subarachnoid space of the brain by trypan blue injection into the lateral ventricle," *Neural Regeneration Research*, vol. 6, no. 28, pp. 2171–2175, 2011.

[33] M. H. Nam, J. K. Lim, S. H. Choi, S. C. Kim, and K. S. Soh, "A primo vascular system underneath the superior sagittal sinus in the brain of a rabbit," *Journal of Acupuncture and Meridian Studies*, vol. 5, no. 5, pp. 210–217, 2012.

[34] B. C. Lee and H. S. Lee, "Visualization of the network of primo vessels and primo nodes above the pia mater of the brain and spine of rats by using alcian blue," *Journal of Acupuncture and Meridian Studies*, vol. 5, no. 5, pp. 218–225, 2012.

[35] J. Lim, J. H. Jung, S. W. Lee et al., "Estimating the density of fluorescent nanoparticles in the primo vessels in the fourth ventricle and the spinal cord of a rat," *Journal of Biomedical Optics*, vol. 16, no. 11, Article ID 116010, 2011.

[36] S. H. Moon, R. Cha, M. S. Lee, S. C. Kim, and K. S. Soh, "Primo vascular system in the subarachnoid space of the spinal cord of a pig," *Journal of Acupuncture and Meridian Studies*, vol. 5, no. 5, pp. 226–233, 2012.

[37] V. Ogay, K. H. Bae, K. W. Kim, and K.-S. Soh, "Comparison of the characteristic features of Bonghan Ducts, blood and lymphatic capillaries," *Journal of Acupuncture and Meridian Studies*, vol. 2, no. 2, pp. 107–117, 2009.

[38] V. Ogay and K. S. Soh, "Identification and characterization of small stem-like cells in the primo vascular system of adult animals," in *The Primo Vascular System*, K. S. Soh, K. A. Kang, and D. Harrison, Eds., pp. 14–155, Springer, New York, NY, USA, 2011.

[39] B.-C. Lee, K.-H. Bae, G.-J. Jhon, and K.-S. Soh, "Bonghan system as mesenchymal stem cell niches and pathways of macrophages in adipose tissues," *Journal of Acupuncture and Meridian Studies*, vol. 2, no. 1, pp. 79–82, 2009.

[40] B. Sung, V. Ogay, J. S. Yoo et al., "UV-A induced activation of Bonghan granules in motion," *Journal of International Society of Life Information Science*, vol. 23, no. 2, pp. 297–301, 2005.

[41] B. Sung, M. S. Kim, A. Corrigan, A. M. Donald, and K.-S. Soh, "In situ microextraction method to determine the viscosity of biofluid in threadlike structures on the surfaces of mammalian organs," *Physical Review E*, vol. 79, no. 2, Article ID 022901, 2009.

[42] J. Kwon, K. Y. Baik, B.-C. Lee, K.-S. Soh, N. J. Lee, and C. J. Kang, "Scanning probe microscopy study of microcells from the organ surface Bonghan corpuscle," *Applied Physics Letters*, vol. 90, no. 17, Article ID 173903, 3 pages, 2007.

[43] K. Y. Baik, V. Ogay, S. C. Jeoung, and K.-S. Soh, "Visualization of Bonghan microcells by electron and atomic force microscopy," *Journal of Acupuncture and Meridian Studies*, vol. 2, no. 2, pp. 124–129, 2009.

[44] K. Y. Baik, C. H. Kim, S. Y. Woo, S. C. Jeoung, and K. S. Soh, "Membrane mechanical property of primo microcells," in *The Primo Vascular System*, K. S. Soh, K. A. Kang, and D. Harrison, Eds., pp. 163–170, Springer, New York, NY, USA, 2011.

[45] H.-J. Han, B. Sung, V. Ogay, and K.-S. Soh, "The flow path of alcian blue from the acupoint BL23 to the surface of abdominal organs," *Journal of Acupuncture and Meridian Studies*, vol. 2, no. 3, pp. 182–189, 2009.

[46] H.-J. Han, V. Ogay, S.-J. Park et al., "Primo-vessels as new flow paths for intratesticular injected dye in rats," *Journal of Acupuncture and Meridian Studies*, vol. 3, no. 2, pp. 81–88, 2010.

[47] J. D. Kim, V. Ogay, B.-C. Lee et al., "Catecholamine-producing novel endocrine organ: Bonghan system," *Medical Acupuncture*, vol. 20, no. 2, pp. 97–102, 2008.

[48] J. S. Yoo, H. B. Kim, V. Ogay, B.-C. Lee, S. Ahn, and K.-S. Soh, "Bonghan Ducts as possible pathways for cancer metastasis," *Journal of Acupuncture and Meridian Studies*, vol. 2, no. 2, pp. 118–123, 2009.

[49] J. S. Yoo, H. B. Kim, N. Won et al., "Evidence for an additional metastatic route: in vivo imaging of cancer cells in the primo-vascular system around tumors and organs," *Molecular Imaging and Biology*, vol. 13, no. 3, pp. 471–480, 2011.

[50] W. Akers, Y. Liu, G. Sudlow et al., "Identification of primo vascular system in murine tumors and viscera," in *The Primo Vascular System*, K. S. Soh, K. A. Kang, and D. Harrison, Eds., pp. 179–183, Springer, New York, NY, USA, 2011.

[51] M. Hong, S. S. Park, H. Do, G.-J. Jhon, M. Suh, and Y. Lee, "Primo vascular system of murine melanoma and heterogeneity

of tissue oxygenation of the melanoma," *Journal of Acupuncture and Meridian Studies*, vol. 4, no. 3, pp. 159–163, 2011.

[52] C. Heo, M. Y. Hong, A. Jo, Y. H. Lee, and M. Suh, "Study of the primo vascular system utilizing a melanoma tumor model in a green fluorescence protein expressing mouse," *Journal of Acupuncture and Meridian Studies*, vol. 4, no. 3, pp. 198–202, 2011.

[53] A. Islam, S. Thomas, K. Sedoris, and D. Miller, "Tumor-associated primo vascular system is derived from xenograft, not host," *Experimental and Molecular Pathology*, vol. 94, no. 1, pp. 84–90, 2013.

[54] K. A. Kang, "Mapping PVS by molecular imaging with contrast agents," in *The Primo Vascular System: Its Role in Cancer and Regeneration*, K. S. Soh, K. A. Kang, and D. Harrison, Eds., pp. 227–234, Springer, New York, NY, USA, 2012.

[55] S. W. Lee, J. K. Lim, Y. H. Ryu, J. M. Cha, J. K. Lee, and K. S. Soh, "Primo vessel in a lymph vessel emerging from a cancer tissue," *Journal of Acupuncture and Meridian Studies*, vol. 5, no. 5, pp. 206–209, 2012.

[56] S. Hong, S. Y. Jung, Y. H. Ju et al., "Immunohistochemical and electron microscopic study of the meridian-like system on the surface of internal organs of rats," *Acupuncture and Electro-Therapeutics Research*, vol. 32, no. 3-4, pp. 195–210, 2007.

[57] M. Z. Ratajczak, M. Kucia, J. Ratajczak, and E. K. Zuba-Surma, "A multi-instrumental approach to identify and purify very small embryonic like stem cells (VSELs) from adult tissues," *Micron*, vol. 40, no. 3, pp. 386–393, 2009.

[58] J. L. Soo, B.-C. Lee, H. N. Chang et al., "Proteomic analysis for tissues and liquid from Bonghan ducts on rabbit intestinal surfaces," *Journal of Acupuncture and Meridian Studies*, vol. 1, no. 2, pp. 97–109, 2008.

[59] S. R. Kim, S. K. Lee, S. H. Jang et al., "Expression of keratin 10 in rat organ surface primo-vascular tissues," *Journal of Acupuncture and Meridian Studies*, vol. 4, no. 2, pp. 102–106, 2011.

[60] K. S. Soh, "Current state of research on the primo vascular system," in *The Primo Vascular System: Its Role in Cancer and Regeneration*, K. S. Soh, K. A. Kang, and D. Harrison, Eds., pp. 25–40, Springer, New York, NY, USA, 2011.

[61] K. A. Kang, C. Maldonado, Perez-Aradia, P. An, and K. S. Soh, "Primo vascular system and its role in cancer metastasis," *Advances in Experimental Medicine and Biology*. In print.

[62] X. Y. Wang, H. Shi, H. Y. Shang et al., "Are primo vessels (PVs) on the surface of gastrointestine involved in regulation of gastric motility induced by stimulating acupoints ST36 or CV12?" *Based Complementary and Alternative Medicine*, vol. 2012, Article ID 787683, 8 pages, 2012.

Hindawi Publishing Corporation
Evidence-Based Complementary and Alternative Medicine
Volume 2013, Article ID 731518, 6 pages
http://dx.doi.org/10.1155/2013/731518

Research Article

Study on the Formation of Novel Threadlike Structure through Intravenous Injection of Heparin in Rats and Refined Observation in Minipigs

Yu-Ying Tian,[1] Xiang-Hong Jing,[1] Shun-Gen Guo,[2] Shu-Yong Jia,[1] Yu-Qing Zhang,[1] Wen-Ting Zhou,[1] Tao Huang,[1] and Wei-Bo Zhang[1]

[1] *Institute of Acupuncture and Moxibustion, China Academy of Chinese Medical Sciences, Beijing 100700, China*
[2] *Beijing University of Chinese Medicine, Beijing 100029, China*

Correspondence should be addressed to Wei-Bo Zhang; zhangweibo@hotmail.com

Received 22 February 2013; Revised 15 May 2013; Accepted 6 June 2013

Academic Editor: Byung-Cheon Lee

Objective. To study if the novel threadlike structure (NTS) was caused by coagulation during injecting urethane intraperitoneally and the source of NTS. *Methods*. Twenty-two SD rats were anaesthetized by urethane injected intraperitoneally. Heparin was injected at 5 minutes before the anaesthesia from femoral vein in 11 rats, and saline was given in the other 11 rats randomly. Six Chinese minipigs were carried to look for NTS. One sample was taken to be stained by DAPI/Phalloidin and observed by a laser scanning confocal microscope. *Results*. In the group of heparin, 10 rats were found to have NTS with appearance rate of 90.9%, and 9 rats were found to have NTS with the appearance rate of 80.1%. Both groups have 1.81 average numbers of NTS in each rat without significant difference ($P > 0.05$). In the observation of pigs, the NTS was found to prolong from the serous membranes of abdominal wall and organ surface. Histological observation showed elongated nuclei and alignment which is similar to the characteristics of PVS. *Conclusion*. There is no strong evidence to say that the NTS on organ surface was caused by coagulation of blood. The source of NTS might be a prolonged structure from serous membrane in abdominal cavity during the development and more or less retained after birth.

1. Introduction

Recently, a novel threadlike structure (NTS) was found on the surface of different organs in rabbits, mice, and rats by Korean team [1–4]. It was named primo-vessel system (PVS) by professor Soh as an extension of acupuncture meridians [5]. More recently, an experiment was carried by Choi and Leem that when injecting heparin intravenously at 5 min before the experiment, NTS could not be observed [6]. The rats were anaesthetized by Zoletil (50 mg/Kg) and xylazine (10 mg/kg). The author pointed out that when usually anaesthetizing rats by urethane injected intraperitoneally, it was easy to cause a slight damage of internal organs and bleeding in abdomen which may produce artifacts of NTS by coagulated string. But the author did not observe the appearance of NTS under the condition of urethane intraperitoneal anaesthesia and giving heparin before the operation. So, conclusion that NTS was caused by coagulated string when injecting urethane intraperitoneally was unclear.

The target of this study is to investigate the formation of NTS. Two methods were used around the goal. One is that we tried to damage the structure by giving heparin under the condition of intraperitoneal anaesthesia of urethane, assuming that it is formed by a coagulation of blood. The second is that we observe the structure closely on minipigs to see the continuity with other tissues or organs under the condition of both intraperitoneal anaesthesia and intramuscular anaesthesia.

2. Materials and Methods

2.1. Heparin Experiment in Rats. Twenty-two Sprague Dawley (SD) rats (male, weight from 180 g to 376 g) were carried on the experiment. The rats were anaesthetized by

intraperitoneal injection of urethane (1.5 g/kg). Then, they were randomly divided into two groups. In one group, 0.2 ~ 0.25 ml of heparin (5000 IU/mL, Sigma Co.) according to the weight was carefully injected from femoral vein, and then the place of injection was pressed for 5 minutes. In the control group, the same amount of saline was injected from femoral vein. After 5 minutes, the medial alba of the rat's abdomen was cut under deep anesthesia with the help of subcutaneous injection of small amount of xylocaine. The abdomen was then opened as much as possible to expose the internal organs. Bleeding was avoided by forcipressure. 0.4% Trypan blue solution (Sigma Co.) was obtained and was diluted to 0.1%. The 0.1% Trypan blue was further filtered through 0.22 μm pore-sized filter paper just before the experiment. After exposure of the internal organs of the rats, Trypan blue was poured evenly on the exposed organs. After about one minute, the dye was washed away with 45°C warm saline, and NTS was searched through a stereomicroscope (Nikon SMZ750). If the NTS could be seen, the images were captured by the autocollection system in the stereomicroscope. The person who did the Trypan blue stain and observed the NTS was separated from the person who did the injection of heparine or saline which was a kind of blanking method.

2.2. Observation of NTS in Minipigs. The experiment of searching NTS was also done on six Chinese minipigs in different periods. Five pigs were anaesthetized by injecting 1.5 to 2 mg/kg of 2% phenobarbital sodium solution intraperitoneally. One pig was anaesthetized by injecting phenobarbital sodium solution (0.3 mg/kg) and xylazine hydrochloride injection (0.1 mg/kg) intramuscularly. Under deep anesthesia midline incision was carefully performed, and we passed through the following structures: skin, linea alba, transversalis fascia, extraperitoneal fat, and peritoneum. The incision was extended by cutting around the umbilicus while avoiding the falciform ligament above the umbilicus. Special care was also taken for the urinary bladder. Intra-abdominal organs were exposed carefully.

In the five minipigs which were anaesthetized by phenobarbital sodium intraperitoneally, 0.4% Trypan blue solution (Sigma) was diluted to 0.1% and filtered through 0.22-μm pore-sized filter paper just before the experiment. After exposure of the internal organs, Trypan blue was applied on the exposed organs and was washed away with warm saline after about one minute. In the last minipig which was anaesthetized by phenobarbital sodium and xylazine hydrochloride injection intramuscularly, candidate NTS was searched directly without giving Trypan blue for getting the original color of NTS.

NTS was searched directly by eyes and was taken by a digital camera (Nikon D5000) with a 105 mm macro lens (Micro-Nikkor 105 mm f/2.8 G). A sample of candidate NTS from liver surface in the last minipig was harvested and fixed with 4% paraformaldehyde in 0.1 M phosphate buffered solution (PB, pH 7.4) for 2 hours at 4°C, then changed into 25% sucrose in 0.1 M PB (pH 7.4) for further examination. Serial longitudinal sections of NTS were cut at a thickness of 20 μm on a cryostat (Thermo, Microm International FSE, Germany) and mounted on silane-coated glass slides.

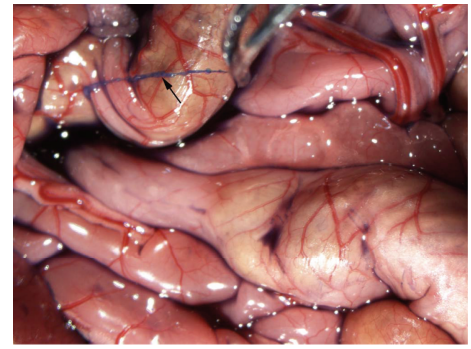

Figure 1: A blue color threadlike structure was found (↑) on the surface of intestine of a rat with intraperitoneal injection of urethane and giving heparin at 5 minutes before the incision.

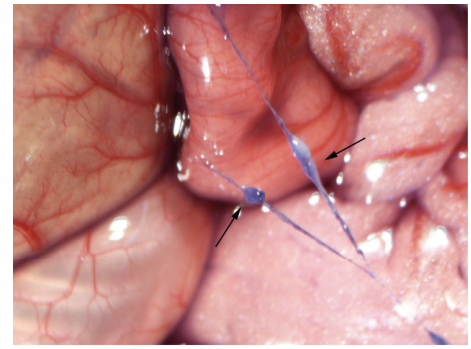

Figure 2: On enlarged sight of NTS, a node (↑) could be found on both two threadlike structures.

For staining, the mounted NTS was incubated in a solution containing 3% normal goat serum and 0.5% Triton X-100 in 0.1 M phosphate buffered solution (PB, pH 7.4) for 30 min. After 3 times rinsing with 0.1 M PB, the sample was stained with Alexa Fluor 488 Phalloidin dissolution (1 : 50; Molecular Probes, Eugene, OR, USA) for 2 h, then washed with 0.1 M PB. After that, the sample was coverslipped with DAPI (Molecular Probes, Eugene, OR, USA). In this study, Alexa Fluor 488 Phalloidin and DAPI were used for identifying the morphology of F-actin and cell nuclei.

3. Results

3.1. Heparin Experiment in Rats. The two groups of rats have similar average weights which were 260.6 g (SD = 83.7) in heparin group and 289.7 g (SD = 79.4) in saline group without significant difference ($P > 0.05$). On the group of injecting urethane, among 11 rats, 10 rats were found to have NTS on the surface of intestine or liver. Figure 1 showed one of them. The candidate NTS was blue color and can easily be separated from the surface of organ by a forceps. If we enlarged the sight by amplifying the picture, a node could be found clearly on most NTSs which was one of the criteria of discriminating NTS (Figure 2). On the control group of 11 rats, 9 rats were found to have NTS with the appearance rate of 81.8% which was similar to the appearance of heparin group.

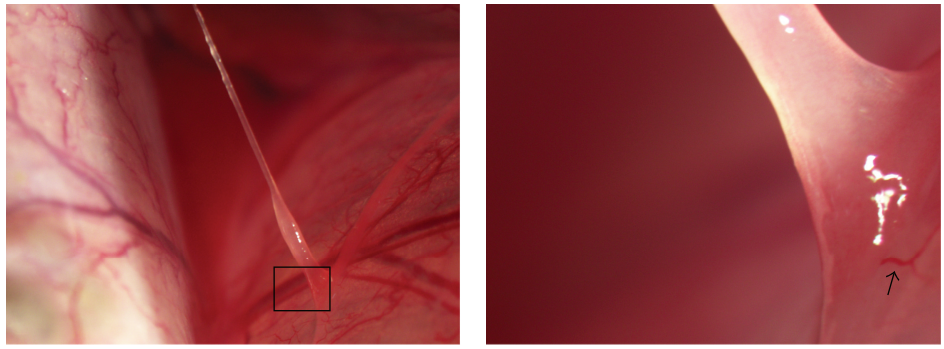

(a) (b)

Figure 3: (a) A threadlike structure was found on the surface of stomach. (b) A further enlarged picture of (a) in pane to show the connection between the NTS and the surface of the organ. A small blood vessel with red color could be seen beside the NTS (↑).

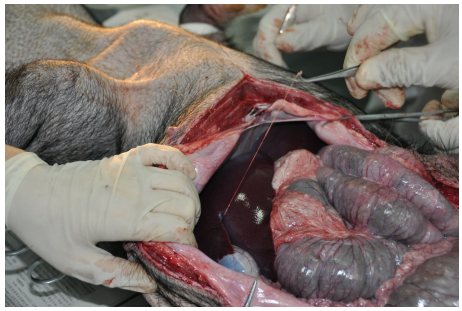

Figure 4: A threadlike structure was found on the surface of liver in one minipig with a tight connection with the liver.

We also counted carefully the numbers of NTS on the surface of organs on each rat. It was found that the mean number of NTS on heparin group was 1.82 (SD = 0.87) and 1.82 (SD = 1.17) on control group. There was no significant difference between the two groups ($P > 0.05$).

3.2. Observation of NTS in Minipigs. For the observation on minipigs, the candidate NTSs on the organ surfaces like stomach, intestine, and liver were also found. In the five minipigs anaesthetized by phenobarbital sodium intraperitoneally, some samples were stained with DAPI, and rod-shaped nuclei were found [7]. A large sample on the surface of stomach was taken, and a further enlarged picture was obtained to see the refined structure rooted on the surface of stomach (Figures 3(a) and 3(b)).

The picture showed that the connection between the NTS and the surface of stomach was firmed and continuous from a restis on the surface of stomach. The NTS had nearly no color itself compared with the red color of small blood vessel nearby and appeared semitransparent.

In the other minipig, a thick NTS was found on the surface of liver connected to the abdominal wall (Figure 4). In the last minipig which was anaesthetized by phenobarbital sodium and xylazine hydrochloride injection intramuscularly, a candidate NTS was found at a position quite similar to the last one (Figures 5(a), 5(b), and 5(c)). The connections on the surface of liver and abdominal wall were tight, and the strings were elastic.

From Figures 5(b) and 5(c), prolongations of the threadlike structure from serous membrane on the abdominal wall and surface of liver could be seen clearly.

4. Histological Observation

The tissue samples were observed and recorded with a laser scanning confocal microscope (FV1000, Olympus Co., Tokyo, Japan). Digital images were finally processed with Adobe Photoshop CS2 (Adobe Systems, San Jose, CA, USA). The result was shown in Figure 6.

From Figure 6, the cells labeled with DAPI/Phalloidin had elongated nuclei and flattened processes with alignment scene, parallel to the longitudinal direction of the sample which is similar to the characteristics of PVS and the features of fibroblasts. The distribution of nuclei and alignment is not even which showed higher density on the edge and central areas of the sample.

5. Discussion

A novel threadlike structure (NTS) was reported to be found on rabbits firstly by Bonghan Kim in North Korea in the early 1960s. As it is hard to be repeated by other scientists in other countries including China, the work had been stopped until KS Soh in South Korea claimed to find the similar structure again. The characteristics of NTS were studied extensively mainly concerning the structure, distribution, and relations with tumor, while the physiological function of NTS has not been studied intensively yet. We still do not know if it is a structure necessary for every living creature all the time or it is just a temporal structure that appeared during the development or at the pathological state. The formation of this structure is a secret. Some people thought that NST is just a coagulated string during anaesthesia or operation. An experiment was done by Liu in China to see the influence of heparin on the formation of NTS [8]. The rabbits were perfused by saline plus heparin or epinephrine through a femoral vein on one hindlimb and opened the femoral artery

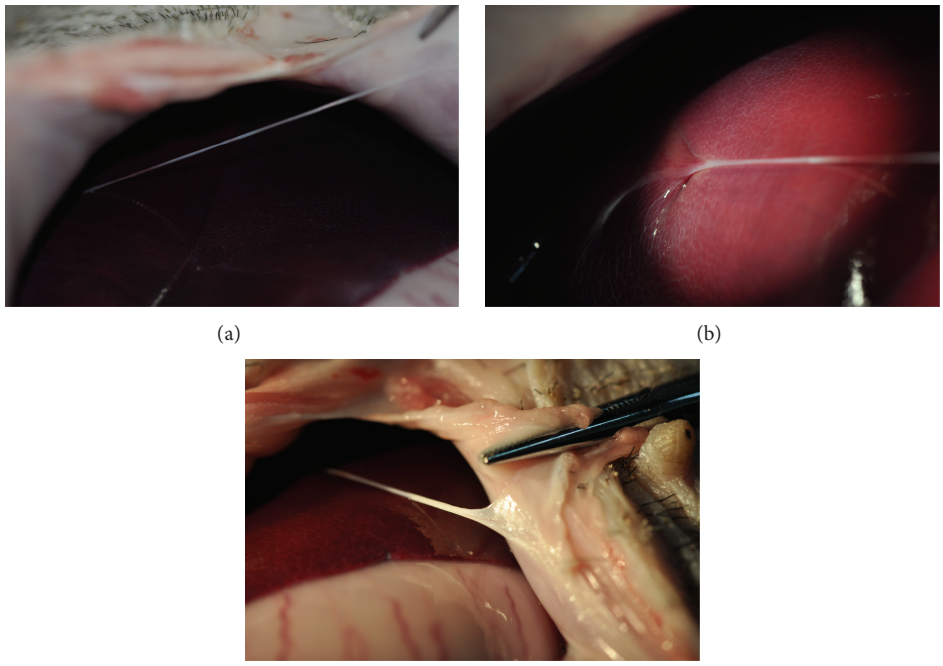

(a) (b)

(c)

Figure 5: (a) A threadlike structure was found on the last minipig at a position similar to the one in Figure 4. (b) The root structure on the surface of liver. (c) The root structure on the abdominal wall.

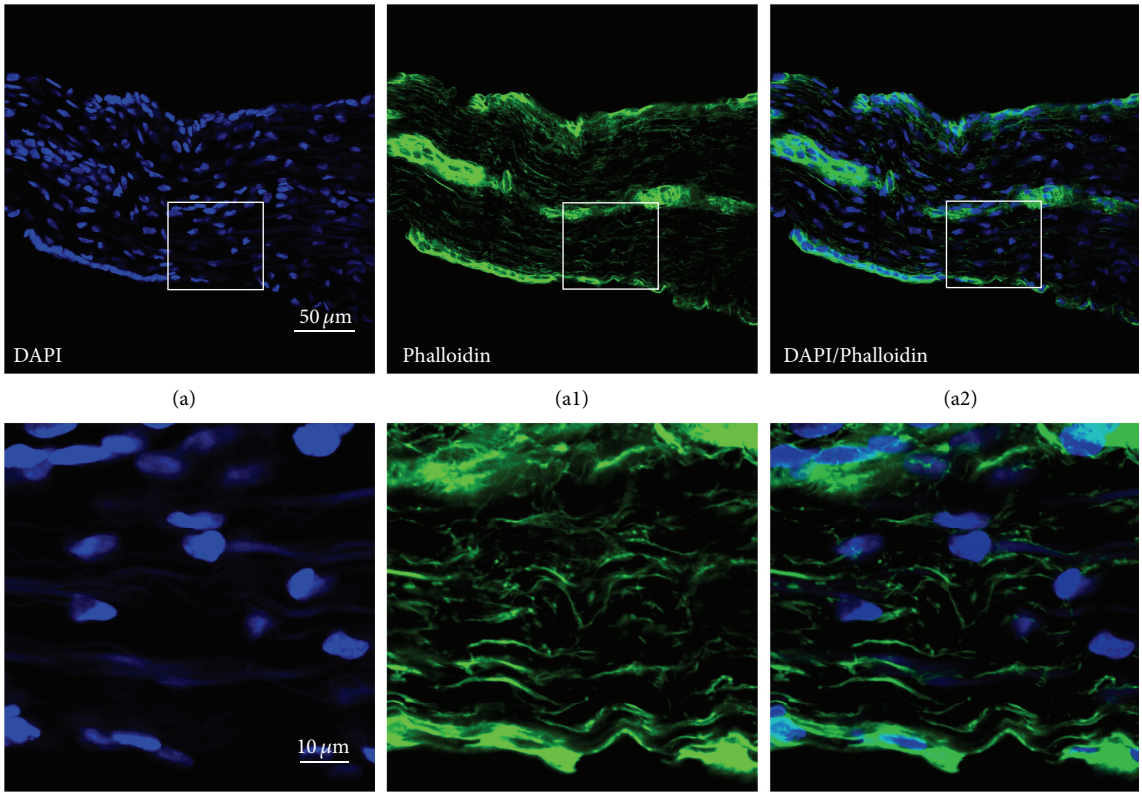

(a) (a1) (a2)

(b) (b1) (b2)

Figure 6: (a)–(a2) The structure of NTS in pig determined by fluorescent staining with DAPI (a) and Alexa Fluor 488 Phalloidin (a1) and their double labeling (a2). (b)–(b2) The magnified photos from the squares in (a)–(a2), respectively, showing the DAPI/Phalloidin-positive cells in detail. Scale bar, same for (a)–(a2) (showed in (a)) and same for (a)–(b2) (showed in (b)).

on the other hindlimb. It was found that NTS increased the length when epinephrine was given and disappeared when giving heparin. This is a good evidence to support that the NTS in blood vessel is formatted by a coagulation of blood. But outside the blood vessel, there is little chance to coagulate a string without serious bleeding. Our result showed an equal appearance of NTS on giving heparin and saline. So there is no strong evidence to say that NTS on organ surface is caused by coagulation.

Choi and Leem did observe the influence of heparin but only on the rats when injecting Zoletil and xylazine intramuscularly. There was no condition to cause the coagulating string according to the author's view. The sample he used was small, and no blanking method was taken [6]. As searching NTS was carried out by man's observation, it is easy to have bias when knowing the condition. Our blanking method can avoid the bias from the person who observed the NTS.

Also the damaged fractals from organ surface during the intraperitoneal anaesthesia are hard to form a string so quickly on the organ surface in a short time. Even if it was formed, it is impossible to form a tight connection with the internal organs or abdominal wall which has been found in minipigs. In the last minipig, intramuscular injection was used to avoid any damage on internal organs; the candidate NTS can still appear.

For the result of minipigs, the much thicker samples than those of rats and rabbits could be observed easily at anatomical lever and made it possible to observe the refined structure of NTS. Some candidate NTSs do not freely stay on the surface of organs. They are continuous from the serous membrane of internal organs or abdominal wall which implied the origination of such structure. Histological result showed that a rod nuclei structure existed on the structure [7] which is coincident with criteria of PVS, and they can be stained by Trypan blue [7]. However, the sample from the last minipig had more bundles of cells which is similar to the observation by An et al. on no-free NTS in mesentery of rats [9]. The NTS we found in minipigs which had a tight connection with organ surfaces or abdominal wall is the same type of NTS found by Ping An et al. in mesentery of rats and was recognized as PVS [9].

Although not all cellular components in NTS could be determined by DAPI/Phalloidin labeling, our results suggested that fibroblasts might be an important cellular component in the NTS of pigs which implied the similarity of NTS with the loose connective tissue or fascia.

The criteria of discriminating NTS as PVS were obtained on four aspects which were node and threadlike structure, bundle structure, rod shaped nuclei, and Trypan blue stainability [6]. As the limitation of the condition, we did not check the rod nuclei and bundle structure on all the samples. But a node threadlike structure and Trypan blue stainability are quite clear. Trypan blue can stain dead cells and is often used to discriminate the cells of living or death. The other dye, Alcian blue, which is also sensitive to NTS is often used on evaluating the density of mucopolysaccharide. Both dyes could not stain the living cells. So, a conjecture was obtained that NTS might originate from serous membrane between the abdominal wall and surface of organs during the development. There is no complete separation of serous membrane between the abdominal layer and organ layer or between the organs. Such connections might have certain functions of transporting nutrition and information from the mother through umbilical cord during the embryonic period and are more or less kept after birth, while the function is mainly replaced by self-circulatory and neural systems. This retained structure could be separated under certain unknown condition to become free style of NTS. This speculation could be tested by embryo experiment to trace the origin of NTS.

Lee et al. discussed the difference between free style and no-free style PVS and thought that they are two different tissues; namely, the no-free NTS is not a primo vessel [10]. It is quite difficult to distinguish the two things as both have rod-shaped nuclei and can be stained by Trypan blue. The differences are that free PVS has branches, node, and clear bundle, while no-free NTS has no (or less) branch, node, and clear bundle. But these differences are relative. A node may produce along a thread structure when the two ends of the thread become weak or released. For the similar reason, a bundle inside the thread may become unclear (broken) if the thread is strained and the branches may be damaged. Considering the communicating function of the tissue, a tight connection is better than loose connection on running the communication. However, two types of NTS might be the same or quite similar tissues. Study at molecular level should be done to discriminate the two styles of NTS.

6. Conclusion

NTS on internal organ surface is not formed by a coagulation of blood or damaged fractals from organ surface, while it has a close relationship with the serous membrane on abdominal cavity and organ surfaces.

Conflict of Interests

All the authors declare that they have no conflict of interests.

Acknowledgment

This work was supported by National Key Basic Research Program 973, no. 2010CB530507.

References

[1] S. J. Cho, B. S. Kim, and Y. S. Park, "Threadlike structures in the aorta and coronary artery of swine," *Journal of International Society of Life Information Science*, vol. 22, pp. 609–611, 2004.

[2] B. C. Lee, K. Y. Baik, H. M. Johng et al., "Acridine orange staining method to reveal the characteristic features of an intravascular threadlike structure," *Anatomical Record B*, vol. 278, no. 1, pp. 27–30, 2004.

[3] B. C. Lee, E. S. Park, T. J. Nam et al., "Bonghan ducts on the surface of rat internal organs," *Journal of International Society of Life Information Science*, vol. 22, pp. 455–459, 2004.

[4] K. J. Lee, S. Y. Kim, T. E. Jung, D. Jin, D. H. Kim, and H. W. Kin, "Unique duct system and the corpusclelike structures found on

the surface of the liver," *Journal of International Society of Life Information Science*, vol. 22, pp. 460–462, 2004.

[5] K.-S. Soh, "Bonghan circulatory system as an extension of acupuncture meridians," *Journal of Acupuncture and Meridian Studies*, vol. 2, no. 2, pp. 93–106, 2009.

[6] C. J. Choi and C. H. Leem, "Comparison of primo-vascular system with a similar looking structureeds," in *The Primo Vascular System*, K. S. Soh, K. A. Kang, and D. Harrison, Eds., pp. 107–114, Springer, New York, NY, USA, 2011.

[7] M. A. Hossein, Y. Y. Tian, T. Huang et al., "Finding a novel threadlike structure on the intra-abdominal organ surface of small pigs by using trypan blue," in *The Primo Vascular System*, K. S. Soh, K. A. Kang, and D. Harrison, Eds., pp. 63–70, Springer, New York, NY, USA, 2011.

[8] X. Liu, "Verification on the entity of meridians reported by Bonghan Kim," *Acupuncture Research*, vol. 34, no. 5, pp. 353–354, 2009.

[9] P. An, J. X. Dai, Z. D. Su et al., "Putative primo-vascular system in mesentery of rats," *Journal of Acupuncture and Meridian Studies*, vol. 3, no. 4, pp. 232–240, 2010.

[10] S. H. Lee, Y. H. Ryu, Y. J. Yun et al., "Anatomical discrimination of the differences between torn mesentery tissue and internal organ-surface primo-vessels," *Journal of Acupuncture and Meridian Studies*, vol. 3, no. 1, pp. 10–15, 2010.

Hindawi Publishing Corporation
Evidence-Based Complementary and Alternative Medicine
Volume 2013, Article ID 429106, 5 pages
http://dx.doi.org/10.1155/2013/429106

Research Article

Observation of a Long Primo Vessel in a Lymph Vessel from the Inguinal Node of a Rabbit

Young-Il Noh,[1] Yeong-Min Yoo,[2] Ran-Hyang Kim,[1] Ye-Ji Hong,[3] Hye-Rie Lee,[1] Min-Suk Rho,[1] and Sang-Suk Lee[1]

[1] *Department of Oriental Biomedical Engineering, College of Health Science, Sangji University, Woosan-dong, Wonju, Gangwon-do 220-702, Republic of Korea*
[2] *Department of Biomedical Engineering, College of Health and Science, Yonsei University, Wonju, Gangwon-do 220-710, Republic of Korea*
[3] *Department of Oriental Medicine, College of Oriental Medical Science, Sangji University, Woosan-dong, Wonju, Gangwon-do 220-701, Republic of Korea*

Correspondence should be addressed to Sang-Suk Lee; sslee@sangji.ac.kr

Received 28 December 2012; Accepted 29 May 2013

Academic Editor: Byung-Cheon Lee

Though primo vessels are frequently found in the lymph near the abdominal aorta of rabbit by Alcian blue dye, the reproductions are still difficult to require considerable skills and technical know-how at dissected tissue of animal species. However, in the inguinal lymph node of a rabbit we found a long-type primo vascular system (LTP) dyed with Alcian blue, from an abdominal lymph vessel to an inguinal lymph node. The length of LTP was over an average length of 9.1 cm. The average diameters of the primo and the lymph vessels were about 23.9 μm and 242 μm, respectively. The primo vessels were not floating but adhered to lymph vessels with fascial connective tissue. These primo vessels might be a functional integration in the lymph system.

1. Introduction

In the history of medical developments, discovery of the new circulating meridian system as blood vessel system and lymphatic system changed the basic paradigm of medicine. Investigation of controller for human body as an autonomic nervous system and a hormone system may be possible to develop the new approach in occurrence and treatment of diseases [1, 2]. In the perspective that the substance of meridian pipe which is path of spirit existed, the two most important things are widely known as spirit and blood in human body to be alive. If an undisclosed structures and functions of the circulating meridian system till now are revealed, it can be an intensely important research that can lead to a revolution in medicine having a bigger destructive power than any medical discovery [3, 4].

Recently, the PVS has been found as acupunctural points in mammalian internal organs, such as blood vessels, lymph vessels, spinal cords, brain ventricles, fascia, and skin, by several research groups [5, 6]. Primo vessels have been easily found, by staining with Alcian blue dye to be spread on the surfaces of all the lymphatic vessels [7]. These primo vessels are floating in lymph fluid, and the sanals that exit inside the primo vessels might have a motion property having the cell regeneration [8].

Until now, even though intensive research has been dedicated to the PVS during these years, the statistical data on primo vessels in lymph vessel have been available reported. Our group reported already the general morphological features of primo vessels in lymph vessels around the abdominal aorta [9]. The primo vessels in lymphatic vessels were identified from New Zealand white rabbits by micro dissections.

In this study, we selected lymph vessels around the caudal vena cava connected to lymphatic node in the region neighboring rabbit's inguinal region. This region included many PVS vessels, and those vessels were shown through the reproducible method from among several lymphatic systems. We were able by using the Sangji surgical protocol used on the lymphatic vessels around inguinal region of rabbits during

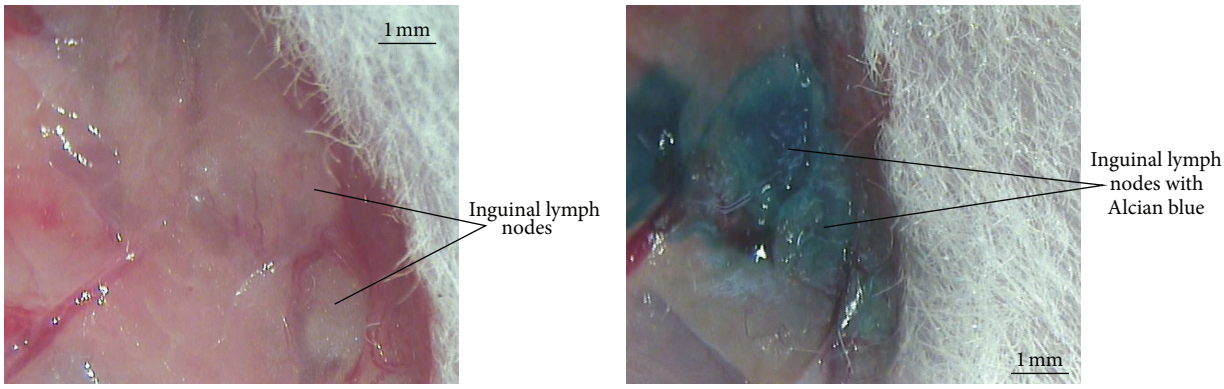

Figure 1: Rabbit's inguinal lymph nodes before (a) and after (b) Alcian blue injection.

Alcian blue staining to find enough evidence to identify easily the primo vessels under a digital stereo zoom microscope [10].

2. Materials and Methods

For the laboratory animals, five New Zealand white female rabbits (approximately 1.8 kg) were purchased from Nara-Biotech Animal Company (Seoul, Republic of Korea). All procedures conformed to the ethical regulations for animal experiments constituted by the institutional regulation board of Sangji University (approval number 2012-1). One rabbit was sacrificed for anatomy experiments in the first week, and the other 5 rabbits were sacrificed in one month. Each rabbit was kept in constant temperature and humidity conditions (23°C, relative humidity 60%), with a 12-hour light-dark cycle. All rabbits were deprived of food and water for 1 day before anatomy.

The rabbits used in the anatomical experiment were sacrificed by injecting 1.5 g/kg of urethane or zolitel intraperitoneally into the peritoneum. The adipose tissues surrounding the inferior vena cava and inguinal region of two legs were then separated and removed. Next, inside the inferior vena cava and inguinal, the PVS, which had been stained blue, was visualized [10]. Images of the PVS under a microscope image analysis system (JSZ-7XT; Samwon, Seoul, Republic of Korea) were captured using a charge coupled device camera (DP70; Olympus, Tokyo, Japan). Other processes of dissection were done with general circumstances of anesthesia [11].

Alcian blue solution was prepared from 0.1 g of Alcian blue (Sigma, St. Louis, MO, USA) in 10 mL of phosphate-buffered saline (PBS, pH 7.4) and was filtered by using a 0.45 μM membrane filter (Merck Millipore, Darmstadt, Germany) with a syringe (BD, Franklin Lakes, NJ, USA). After the sides of rabbit's inguinal region in part of two legs had been incised, Alcian blue solution, preheated to 37°C in a water bath, was injected into inguinal lymph bundles.

3. Results and Discussion

For easy reproducible isolation, we chose inguinal lymphatic vessels but did not choose abdominal lymph vessel and dark-red blood vessel, and Alcian blue staining was required for transparent lymphatic vessels. We attempted to identify large inguinal lymph vessels in the region neighboring the caudal vena cava with a digital stereo microscope. Alcian blue solution, 200 μL, was injected into inguinal lymph nodes that included a lymph vessel for *in situ* visualization of PVS's vessels [12]. Figures 1(a) and 1(b) show rabbit's inguinal lymph bundles before and after Alcian blue injection.

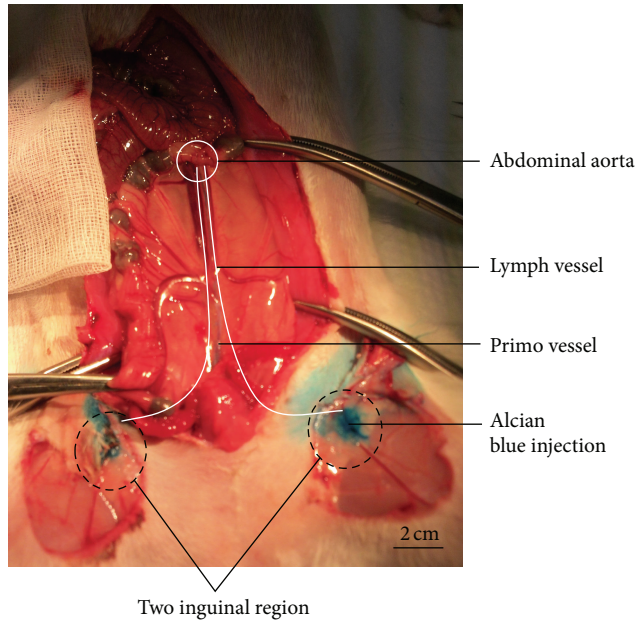

Figure 2: PVS vessel point from lymph nodes of two inguinal regions to lymph vessel of vena cava of a rabbit by injection of Alcian blue.

To investigate primo vessels from an abdominal lymph vessel to an inguinal lymph node, we injected Alcian blue into two inguinal lymph nodes. Immediately Alcian blue solution flowed into inguinal lymph vessel and arrived at an abdominal lymph vessel. This indicates that the primo vessels may be a vascular system connect an abdominal lymph node to an inguinal lymph node, as shown in Figure 2.

Table 1: Morphological analysis data of the PVS and the lymph vessels near the abdominal aorta connected to inguinal of five rabbits.

Subject number	Sex	Weight (kg)	Lymph vessel				Primo vessel	
			PV	LV	L_D (μm)	PN	P_D (μm)	l (cm)
1	F	1.9 kg	O	O	230	6	23.1	8.0
2	F	1.8 kg	O	O	255	8	22.5	9.5
3	F	1.8 kg	O	O	245	8	23.8	8.4
4	F	1.8 kg	O	O	255	6	24.9	9.5
5	F	1.9 kg	O	O	225	7	25.6	10.1
Ave.					242		23.9	9.1
S.D.					12.4		1.1	0.7

PV: primo vessel; LV: lymph vessel; L_D: diameter of lymph vessel; PN: number of primo nodes; P_D: diameter of primo vessel; l: length of primo vessel; Ave.: average value; S.D.: standard deviation.

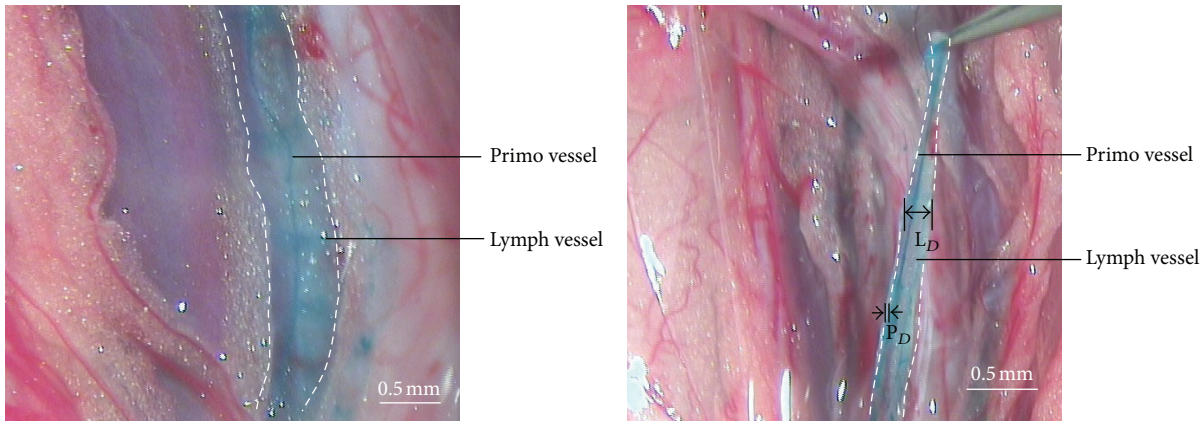

Figure 3: PVS vessels are active on the rabbit's respiration. Lymphatic primo vessels attached organs stained by Alcian blue inside the lymph vessels (a). The isolated primo vessel with lymph vessel from organ (b). White dot lines are lymph vessels.

Figure 3(a) shows lymphatic primo vessels attached organs stained by Alcian blue inside lymph vessels. Figure 3(b) shows the isolated primo vessel inside lymph vessel. The primo vessel inside the lymph vessel as a strand-like microtubular PVS stained with Alcian blue and is floating inside a lymph vessel. PVS vessels are a living tissue in the rabbit's respiration. We already identified PVS which has rod-shaped nuclei with DAPI in a previous report [9].

Table 1 shows data analysis of the morphological features, including the diameters of the lymph vessels and primo vessels observed from the 5 samples of primo vessels in lymph vessels. The number of primo vessels and the average diameter and length of a primo vessel with standard deviation are also shown in Table 1. The subject numbers are ordered according to the dates on which the experiments were performed. The observation of the diameter of a lymph vessel (L_D) and the diameter of a primo vessel (P_D) are shown in Figure 3.

Of the 5 lymph vessels observed, all had primo vessels. The average diameter of the lymph vessels inside the caudal vena cava of the 5 rabbits was 242 μm. This result is almost uniform as the size of the lymph vessels. Also, the average diameter of the primo vessels was 23.9 μm. The average diameters of the lymph vessels and the primo vessels agreed with the sizes of the lymph vessels and the primo vessels, respectively, which are similar to previously reported values (20 μm~30 μm) [9, 11, 13, 14].

We already reported that the microdissected specimens *in situ* reveal rod-shaped nuclei stained by acridine orange. Also, the blue-stained nuclei having a broken-lined stripe and a tube structure and the distance between the nuclei of two cells on neighboring aligned stripes were measured to be about 20 μm in diameter and about 5 μm~10 μm, respectively [9].

There are some of the remaining debris that still adhered to the primo vessels in the process of this experiment. The average length of the primo vessels from the lymph vessels was 9.1 mm, and this was fairly uniform throughout the samples and longer than what several primo research groups found depending on the lymph vessels and the physiological state of the subject.

Figures 4(a), 4(b), 4(c), 4(d), 4(e), and 4(f) show steps of the extraction process for a primo vessel inside the lymph vessel connected to node in the inguinal lymph of a rabbit. First, Figures 4(a) and 4(b) show images of a thick primo vessel indicated by arrows in status before and after extraction by using tweezers, respectively. Second, Figures 4(c) and 4(d) show images of two steps during the extraction of a very slender primo vessel inside the lymph vessel with pincett.

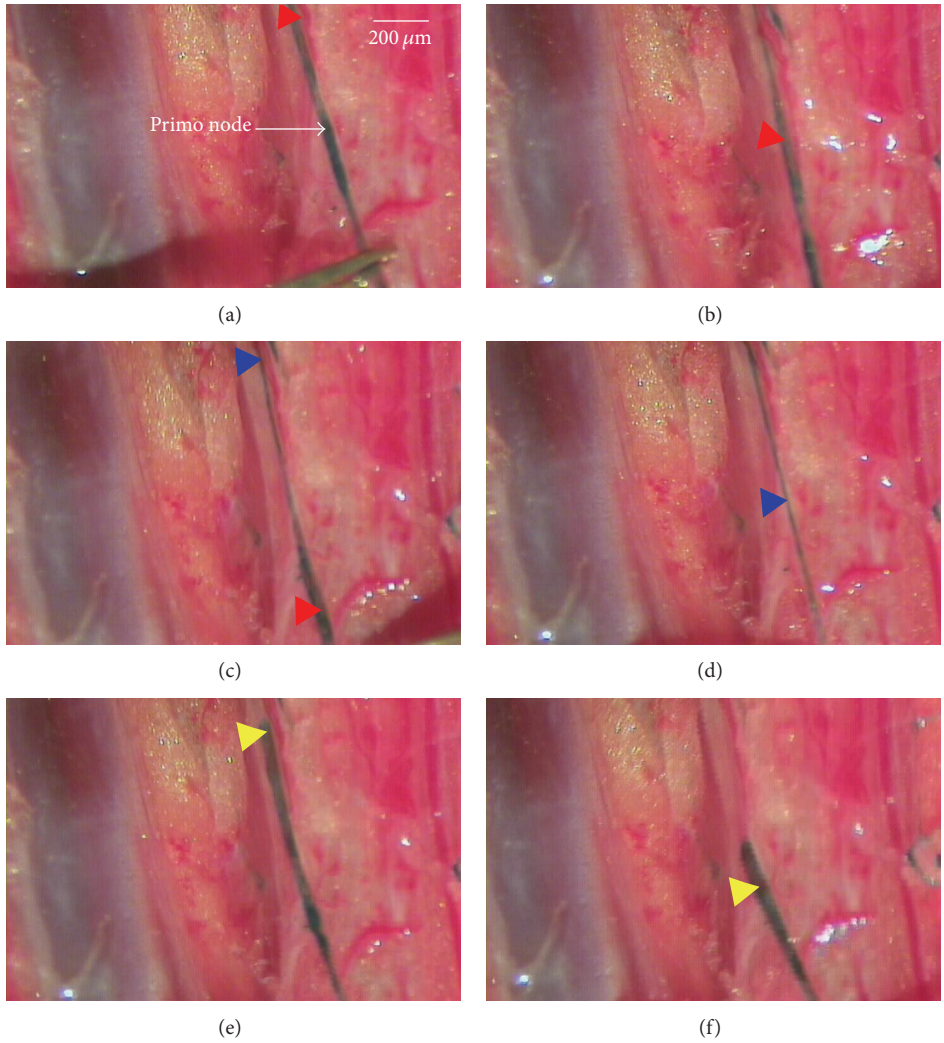

FIGURE 4: Visualization of the extraction process for a primo vessel inside the lymph vessel attached to node in the inguinal lymph of a rabbit. A thick primo vessel indicated by arrows in status before (a) and after (b) extraction by using micro-pincett. Images of two steps ((c), (d)) during the extraction of a very slender primo vessel inside the lymph vessel. Images of two steps ((e), (f)) during the extraction of a thick primo vessel indicated by arrows in status extraction by using micro-pincett.

The presence of the Bonghan system is hardly noticeable. Finally, Figures 4(e) and 4(f) show images of two steps during the extraction of a thick primo vessel indicated by arrows in status extraction by using micro-pincett. There is a long branching of the thin and thick primo vessels inside the lymph vessel having an average length above 9.1 cm. It is also significant that the primo vessel exists in the lymph attached to nearby two inguinals. The primo vessels were not floating but adhered to lymph vessels with fascial connective tissue. These attached primo vessels might be a functional integration in the lymph system [12, 15, 16].

4. Conclusion

We demonstrate that primo vessels in lymphatic vessels around the abdominal aorta connected to inguinal lymph nodes of rabbits can be simply identified under a digital stereo microscope by using Alcian blue staining. In the inguinal lymph node of a rabbit, we found a long-type primo vascular system. The length of LTP was over an average length of 9.1 cm. The average diameters of the primo and the lymph vessels were about 23.9 μm and 242 μm, respectively. The primo vessels were not floating but adhered to lymph vessels with fascial connective tissue. These adhering primo vessels might be an integrated functional system in lymph. The molecular functions and electrical characteristics of primo vessels in lymph vessels may open a new approach to treating chronic diseases such as cancer, diabetes, and cerebral apoplexy, to wound healing, and to acupuncture meridian medicine in particular.

Authors' Contribution

Young-Il Noh and Yeong-Min Yoo contributed equally to this paper.

Acknowledgments

This research was supported by the National Research Foundation of Korea (2011-0007552).

References

[1] M. Jeltsch, A. Kaipainen, V. Joukov et al., "Hyperplasia of lymphatic vessels in VEGF-C transgenic mice," *Science*, vol. 276, no. 5317, pp. 1423–1425, 1997.

[2] B.-C. Lee, J. S. Yoo, K. Y. Baik, K. W. Kim, and K.-S. Soh, "Novel threadlike structures (Bonghan ducts) inside lymphatic vessels of rabbits visualized with a Janus Green B staining method," *Anatomical Record B*, vol. 286, no. 1, pp. 1–7, 2005.

[3] J. Kwon, K. Y. Baik, B.-C. Lee, K.-S. Soh, N. J. Lee, and C. J. Kang, "Scanning probe microscopy study of microcells from the organ surface Bonghan corpuscle," *Applied Physics Letters*, vol. 90, no. 17, Article ID 173903, 2007.

[4] B.-C. Lee and K.-S. Soh, "Contrast-enhancing optical method to observe a Bonghan duct floating inside a lymph vessel of a rabbit," *Lymphology*, vol. 41, no. 4, pp. 178–185, 2008.

[5] B. H. Kim, "Study on the reality of acupuncture meridians," *Journal of Jo Sun Medicine*, vol. 9, pp. 5–13, 1962 (Korean).

[6] B. H. Kim, "Sanal theory," *Journal of Jo Sun Medicine*, vol. 108, pp. 39–62, 1965 (Korean).

[7] B. H. Kim, "On the Kyungrak system," *Journal of the Academy of Medical Sciences of the Democratic People's Republic of Korea*, vol. 90, pp. 1–35, 1963 (Korean).

[8] K.-S. Soh, "Bonghan duct and acupuncture meridian as optical channel of biophoton," *Journal of the Korean Physical Society*, vol. 45, no. 5, pp. 1196–1198, 2004.

[9] Y. I. Noh, M. Rho, Y. M. Yoo, S. J. Jung, and S. S. Lee, "Isolation and morphological features of primo vessels in rabbit lymph vessels," *Journal of Acupuncture and Meridian Studies*, vol. 5, no. 5, pp. 201–205, 2012.

[10] B.-C. Lee, K. W. Kim, and K.-S. Soh, "Visualizing the network of bonghan ducts in the omentum and peritoneum by using trypan blue," *Journal of Acupuncture and Meridian Studies*, vol. 2, no. 1, pp. 66–70, 2009.

[11] B.-C. Lee, J. S. Yoo, V. Ogay et al., "Electron microscopic study of novel threadlike structures on the surfaces of mammalian organs," *Microscopy Research and Technique*, vol. 70, no. 1, pp. 34–43, 2007.

[12] J. S. Yoo, H. B. Kim, N. Won et al., "Evidence for an additional metastatic route: in vivo imaging of cancer cells in the primo-vascular system around tumors and organs," *Molecular Imaging and Biology*, vol. 13, no. 3, pp. 471–480, 2011.

[13] B. Sung, M. S. Kim, B.-C. Lee et al., "Measurement of flow speed in the channels of novel threadlike structures on the surfaces of mammalian organs," *Naturwissenschaften*, vol. 95, no. 2, pp. 117–124, 2008.

[14] V. Ogay, K. H. Bae, K. W. Kim, and K.-S. Soh, "Comparison of the characteristic features of Bonghan ducts, blood and lymphatic capillaries," *Journal of Acupuncture and Meridian Studies*, vol. 2, no. 2, pp. 107–117, 2009.

[15] J. S. Yoo, M. H. Ayati, H. B. Kim, W.-B. Zhang, and K.-S. Soh, "Characterization of the primo-vascular system in the abdominal cavity of lung cancer mouse model and its differences from the lymphatic system," *PLoS One*, vol. 5, no. 4, Article ID e9940, 2010.

[16] S. Kato, H. Shimoda, R.-C. Ji, and M. Miura, "Lymphangiogenesis and expression of specific molecules as lymphatic endothelial cell markers," *Anatomical Science International*, vol. 81, no. 2, pp. 71–83, 2006.

Hindawi Publishing Corporation
Evidence-Based Complementary and Alternative Medicine
Volume 2013, Article ID 961957, 5 pages
http://dx.doi.org/10.1155/2013/961957

Review Article

Toward a Theory of the Primo Vascular System: A Hypothetical Circulatory System at the Subcellular Level

Byung-Cheon Lee,[1] Ji Woong Yoon,[2] Sang Hyun Park,[1] and Seung Zhoo Yoon[3]

[1] *Ki Primo Research Laboratory, Division of Electrical Engineering, KAIST Institute for Information Technology Convergence, Korea Advanced Institute of Science and Technology (KAIST), Daejeon 305-701, Republic of Korea*
[2] *Impedance Imaging Research Center and Department of Public Administration, College of Politics and Economics, Kyung Hee University, No. 1 Hoegi-dong Dongdaemun-gu, Seoul 130-701, Republic of Korea*
[3] *Department of Anesthesiology and Pain Medicine, College of Medicine, Korea University, Seoul 136-705, Republic of Korea*

Correspondence should be addressed to Ji Woong Yoon; jiwoongy@khu.ac.kr

Received 10 February 2013; Revised 27 May 2013; Accepted 4 June 2013

Academic Editor: Xianghong Jing

This paper suggests a theoretical framework for the primo vascular system (PVS), a hypothetical circulatory system, in which extracellular DNA microvesicles interact to form and break down cell structures. Since Bonghan Kim reported the existence of Bonghan ducts and the SNU research team reinvestigated and named it the PVS, there has been series of studies trying to examine its structure and functions. In this paper, we hypothesize that the PVS is the network system in which extracellular DNA microvesicles circulate and interact at the subcellular level, forming and breaking down cell structures. This idea integrates A. Béchamp's idea of microzymas and Bonghan Kim's idea of sanals. A proof of this idea may complement modern medical theory, perhaps providing an essential clue for an alternative solution dealing with modern healthcare problem.

1. Introduction

Since the Bonghan ducts were identified by Bonghan Kim in the 1960s [1–4] and renamed as Primo vascular system (PVS) by the Seoul National University (SNU) research group in 2002, the PVS has been studied by various research groups, presuming it as a new anatomic system, apart from blood and lymphatic systems [5]. The PVS has been found in various organs, and a variety of possible functions of the PVS have been proposed, based on the elements found within the PVS. The liquid carried within the PVS consists of various microparticles, such as DNA, proteins, and hormones [5]. However, the studies on the PVS are at the primitive stage showing elements flowing with the PVS and basic structures of the PVS. And it is rare to see a comprehensive discussion on a theoretical framework or approach of the PVS, trying to understand where it can stand with the modern medical theories.

Hence, this paper provides a brief overview of the PVS research up to date. And the hypothetical functions of the PVS are proposed, which may help building a theoretical framework at the subcellular level activities in the living beings. The main idea is that the PVS is a circulatory system in which microparticles, such as extracellular DNA (eDNA) microvesicles, are floating and interacting [6, 7]. Moreover, the PVS works as the primordial physical blueprint of living organisms [8], which enables eDNA to generate, and degenerate cell-like structures [9].

These hypothetical functions of the PVS are established by matching the sporadic ideas from the previous literatures at the subcellular level, which are ignored for decades. We expect to see researches that prove the hypotheses proposed in this paper in the near future. This may enable a further understanding of a new biological structure and the functions of the living beings. Furthermore, we hope that the PVS, as a primordial anatomical blueprint for living beings, can provide an eye-opening paradigm shift in the modern medical theory that treats chronic diseases, such as cancer and Alzheimer's disease.

2. What We Know about the PVS

In the 1960s, Bonghan Kim urged that he identified a new thread-like circulatory system and called that the Bonghan ducts, which is now renamed as the PVS by the SNU research group [1, 5]. Although he mainly studied rabbits and mice, Bonghan Kim mentioned that the PVS can be observed in various other mammalian species [2, 3]. He also reports that sanals flow within PVS, and sanals combine with one another, forming cells [4]. His research was suddenly shut down and he disappeared from the modern medical history, although his initial works caught some intentions from other countries [5, 6].

After several decades, to reawaken and confirm Bonghan Kim's discovery, SNU research group reinvestigated the PVS mostly in small animals since 2002. The major achievement of the group is the identification and observation of the PVS in various organs of different kinds of animals, and the advancement of technical methods for identifying the PVS. For example, the PVS was observed in the lymphatic vessels of rabbits [10, 11], in the brains and spinal cords of rabbits [12] and in the brains of rats [13]. Moreover, for the first time, the PVSs freely floating in bovine heart chambers were observed [14]. Since then, additional cases have been reported for cows [15] and dogs [16].

The structure of the PVS has been examined in more details. The PVS consists of the primo nodes (Bonghan corpuscles) and the primo vessels (Bonghan ducts). The PVS exists not only in the skin, but also is widely distributed throughout the internal organs. The PVS is classified into two parts: intravascular and extravascular. The intravascular primo vessel runs inside the blood vessel or the lymphatic vessel, while the extravascular primo vessel runs outside the vessel [10, 12, 17]. Although the intravascular primo vessel and the extravascular primo vessel take different directions from each other, there is no difference between them in structure, both having a peculiar rod shape [18].

In addition, the primo vessel comprises bundles of primo lumens. The primo lumen is very soft and has a thin wall, which consists of endothelial cells of a single layer [1]. The contents of the primo lumen often appear as granules when they are stained by a routine method. Moreover, it has been established, by cytochemical reaction, that they contain DNA vesicles [19]. The PVS has also been observed to have a web-like network structure with primo nodes connecting primo vessels, although it is not known to what extent the PVS is networked and whether that network is limited to certain organs [16, 17].

3. Hypothetical Functions of the PVS

3.1. A Third Circulatory System. The PVS is hypothesized as a third circulatory system. Various basic liquids flow within the PVS. A liquid carried by the PVS was found to be rich in basophilic granules, which can be observed individually, as well as in clusters [20]. Breaking the liquid down into its components, proteins [21], stem cell niches [22], microcells [23, 24], and hormones are identified to flow with the PVS [25, 26]. Hence, the PVS seems to function as a circulatory system conveying variety of elements which influence the whole living being.

The flow speed of the liquids in the PVS has been measured [27]. By injecting alcian blue dye in to the PVS directly, the flow speed was measured to be up to 0.3 mm/s [28] with a range of 100–800 μm/second when directly measured using radioactive tracers [29, 30]. These values are significantly higher than those measured in lymphatic vessels [20]. This supports Bonghan Kim's idea that speed of primo fluid movement depends upon various morphological features [31].

3.2. A Biological Blueprint and Channel. More specific functions of the PVS are suggested by analyzing the contents of the liquids flowing within the PVS. We hypothesize that the PVS may be a primordial circulatory system that works as a blueprint for developing and repairing the vessels and organs [32].

The PVS in the vitelline membrane in eggs has been observed within 16–24 hours of incubation, and the putative PVS clearly developed earlier than the formation of the extra-embryonic vessels, letting alone the establishment of the heart and intramembranous vessels [8]. Moreover, the primo vessels are surrounded by a membrane. The membrane has a high concentration of hyaluronic acid, and it is reported that hyaluron is responsible for cell growth and differentiation [33].

An additional function posited for the PVS is as an optical channel of biophoton emission, because collagen is involved in the photon-emitting processes. This raises the possibility that the biophotons may be the electromagnetic signals that play a key role in the processes of cell development and differentiation, or else the DNA may act as a photon store and coherent radiator [34].

3.3. A Network for the Fusion and Diversion of eDNA Microvesicles. The last hypothetical function of the PVS that we propose is that the PVS may allow eDNA microvesicles to systematically interact with one another, forming cell-like structures [7]. This function may be linked with immune system functions [35]. These activities of eDNA microvesicles at the subcellular level imply that a generation or degeneration of a cell structure may be a ramification of fusion and division at the subcellular level of the PVS.

This hypothesis was developed through several steps. First, Lee et al. attempted to demonstrate that a sanal exists and has DNA inside and grows by a budding process [36]. Then Lee et al. [37] observed about 1 μm sized extracellular vesicles, which seem quite similar to what Bonghan Kim reported in his paper [4], that cell-like structures with DNA signal in a concentric growth pattern grew in fertilized eggs [37]. In order to observe the fusion of eDNA microvesicles, Lee et al. developed a special incubating chamber equipped with a microscope, for simultaneous incubation and observation of extracellular DNA vesicles [37].

Surprisingly, it seems that this fusion of eDNA microvesicles is closely associated with recent research in the field of microvesicles, sometimes called exosomes or microparticles

[38]. Microvesicles have been shown to play a role in intercellular communication and regeneration of tissues [39]. However, studies on microvesicles do not mention systematic flow of the microvesicles nor any circulation of microvesicles. The studies are now at the level of defining the anatomical structure and basic functions of microvesicles, which are especially associated with cancer tumors [40].

4. PVS: A Network System for the Subcellular Level Activities

Building on the third hypothesis proposed in the previous section, the PVS is proposed to be a network system where fusion of eDNA vesicles occurs, which eventually form cell-like structures [7]. Observation of this phenomenon implies that the PVS could be a system allowing the interaction of eDNA vesicles to form and break down cell structures in various patterns at the subcellular level, conditional on the biological environment.

This idea of subcellular level activities in the living organ actually can be traced back to the idea of pleomorphism, which is anatomically and physiologically different from monomorphism, the modern orthodox medical paradigm. Pleomorphism, focusing on the basic living element at the subcellular level, was introduced in the mid-19th century by Béchamp, a French scientist [41]. Béchamp's idea was that the *microzyma* (*a small special class of immortal enzymes*) is the smallest living element that forms, granulates, and degrades the living cells and organs. He also showed that these microzymas were found to be present in all things, whether living or dead, and they persist even when the host dies [32]. Béchamp's idea of microzymas can be used to explain life cycle phenomena. However, he was not able to undertake experiments to prove his theory. His idea was ignored and faded away [42].

Although Béchamp's idea was lost to orthodox medicine for various reasons [41], there have been a series of medical scientists sporadically suggesting the existences of living entities at the subcellular level, which is similar to Béchamp's idea. The first one is Reich, a Norwegian medical scientist, who reports discovery of a small element, presumably one that forms the basic foundation of living organisms. Reich called this the *Bione* [35]. The second is Naessens, a French medical scientist, who also claimed to discover the *Somatid*, literally meaning *a small living element* [43], very similar to Béchamp's *microzyma*. Moreover, Lepeshinskaya, a Soviet biologist, claimed that cells need not be formed from other cells but can be formed from noncellular matter. Lepeshinskaya believed that yolk globules were source for new cells, via fusion, in chicken eggs [44].

Following the same line, Bonghan Kim further expanded the idea that a small living element is flowing through a circulatory system. Bonghan Kim found microvesicles, which he named "*Sanals*," floating in the PVS (in Korean literally meaning *living eggs*). Analysing the movement of these microvesicles, Bonghan Kim reported how the living organism works at the subcellular level. He reported that the sanals interact with one another, forming granules that eventually become cells [4].

In order to reexcavate and confirm the pioneering idea of microvesicles at the subcellular level, Lee et al. provided evidence that the fusion of eDNA microvesicles eventually forms a cell-like structure from the fertilizing eggs and the PVS of rat and mice, although the cell-like structure was not proven to be a real cell with the full range of living cell functions [7]. Lee et al. [37] hypothesize that if cell fusion is the basis of life formation, the fusion of eDNA microvesicles, named "microzymas" and "sanal," should also occur at the subcellular level [37].

5. Concluding Remarks: Toward a Theory of the PVS

In this paper, synthesizing the ideas of the pioneers, such as Béchamp and Kim, and the observations from recent research outcomes, we suggest a hypothesis that the PVS is a circulatory network system where microparticles, mainly eDNA microvesicles, interact to form and break down cell structures in response to the biological conditions at the subcellular level [9]. This idea of the PVS is integrating the idea of the Bonghan Kim's Bonghan Ducts, sanals, and Béchamp's microzymas.

Meanwhile, the exact structural boundary of the PVS is still unknown. Hence, we propose two competing hypotheses regarding the structural boundary of the PVS. One hypothesis is that the PVS is a centralized circulatory system enabling the subcellular level activities within the living being. The other hypothesis is that the PVS is a distribution network bounded by the anatomical structure in which it lies. If this is true, the PVS can be a system that can explain a living organ's response being limited to certain areas on the body.

In addition, we hypothesize that the structural density of the PVS can be limited by the evolutionary level of an animal. In other words, the density of the PVS can be high for the larger animals, compared to the smaller ones. Hence, the function of PVS can be more complex and sensitive to larger animals. Finally, we present the hypothesis that fusion and division of cell structures occur throughout life at the subcellular level [35], spontaneously to maintain the balance of conditions in a creature all through its life cycle.

The PVS has a high potential to be a seminal discovery, although it has been ignored for decades. Proving the functions and demonstrating the complete structure of the PVS, as it operates through fusion and division of cell structure based on cell-free DNA vesicles [9], challenges established views held in the modern medical community.

Although the anatomical structure and physiological function of the PVS are yet to be proven, the PVS has potential to complement the deficits in modern medicine, dealing with unknown disease causations, including those of chronic pain and cancer. Eventually, the PVS has the potential to reduce medical costs by providing a new arena of complementary or alternative medicine, based around knowledge of the functions and features of the PVS.

Conflict of Interests

The authors declare no conflict of interests.

Acknowledgments

This work was supported in part by the Industrial Strategic Technology Program of the Ministry of Knowledge Economy (10041120) and in part by the National Research Foundation of Korea (NRF) grant funded by the Korea government's Ministry of Education, Science and Technology (MEST) in 2010 (2010-0025289). The authors give special thanks to Proffessor K. S. Soh for support and advice regarding this study.

References

[1] B. H. Kim, "On the Kyungrak system," *Journal of the Academy of Medical Sciences of the Democratic People's Republic of Korea*, vol. 90, pp. 1–41, 1963.

[2] B. H. Kim, "The Kyungrak system," *Journal of Jo Sun Medicine*, vol. 108, pp. 1–38, 1965.

[3] B. H. Kim, "Sanal theory," *Journal of Jo Sun Medicine*, vol. 108, pp. 39–62, 1965.

[4] B. H. Kim, "Sanals and hematopoiesis," *Journal of Jo Sun Medicine*, pp. 1–6, 1965.

[5] K. S. Soh, "Current state of research on the primo vascular system," in *The Primo Vascular System, Its Role in Cancer and Regeneration*, K. S. Soh, K. A. Kang, and D. K. Harrison, Eds., pp. 25–39, Springer, New York, NY, USA, 2011.

[6] D. K. Harrison and P. Vaupel, "The primo vascular system: facts, open questions, and future perspectives," in *The Primo Vascular System, Its Role in Cancer and Regeneration*, K. S. Soh, K. A. Kang, and D. K. Harrison, Eds., pp. 47–54, Springer, New York, NY, USA, 2011.

[7] B.-C. Lee, H. S. Lee, J. E. Yun, and H. A. Kim, "Evidence for the fusion of extracellular vesicles with/without DNA to form specific structures in fertilized chicken eggs, mice and rats," *Micron*, vol. 44, pp. 468–474, 2013.

[8] S. Y. Lee, B.-C. Lee, K. S. Soh, and G. Jhon, "Development of the putative primo vascular system before the formation of vitelline vessels in chick embryos," in *The Primo Vascular System, Its Role in Cancer and Regeneration*, K. S. Soh, K. A. Kang, and D. K. Harrison, Eds., pp. 77–82, Springer, New York, NY, USA, 2001.

[9] B.-C. Lee, "A hypothesis for a hiddencirculation system withcell-free DNA molecules, microvesicles and microparticles: the primo vascular system (Bonghan system), a putative acupuncture meridian system," *Journal of Extracellular Vesicles (JEV)*. In press.

[10] B.-C. Lee and K.-S. Soh, "Contrast-enhancing optical method to observe a Bonghan duct floating inside a lymph vessel of a rabbit," *Lymphology*, vol. 41, no. 4, pp. 178–185, 2008.

[11] B.-C. Lee, J. S. Yoo, K. Y. Baik, K. W. Kim, and K.-S. Soh, "Novel threadlike structures (Bonghan ducts) inside lymphatic vessels of rabbits visualized with a Janus Green B staining method," *Anatomical Record B*, vol. 286, no. 1, pp. 1–7, 2005.

[12] B.-C. Lee, S. Kim, and K.-S. Soh, "Novel anatomic structures in the brain and spinal cord of rabbit that may belong to the Bonghan system of potential acupuncture meridians," *Journal of Acupuncture and Meridian Studies*, vol. 1, no. 1, pp. 29–35, 2008.

[13] B.-C. Lee, K.-H. Eom, and K.-S. Soh, "Primo-vessels and primo-nodes in rat brain, spine and sciatic nerve," *Journal of Acupuncture and Meridian Studies*, vol. 3, no. 2, pp. 111–115, 2010.

[14] B.-C. Lee, H. B. Kim, B. Sung et al., "Structure of the sinus in the primo vessel inside the bovine cardiac chambers," in *The Primo Vascular System, Its Role in Cancer and Regeneration*, K. S. Soh, K. A. Kang, and D. K. Harrison, Eds., pp. 57–62, Springer, New York, NY, USA, 2011.

[15] B.-C. Lee, H. B. Kim, B. Sung et al., "Network of endocardial vessels," *Cardiology*, vol. 118, no. 1, pp. 1–7, 2011.

[16] Z. Jia, K. S. Soh, Q. Zhou, D. Bo, and Y. Wenhui, "Observation of the primo vascular system on the fascia of dogs," in *The Primo Vascular System, Its Role in Cancer and Regeneration*, K. S. Soh, K. A. Kang, and D. K. Harrison, Eds., pp. 71–76, Springer, New York, NY, USA, 2011.

[17] A. M. Hossein, Y. Y. Tian, T. Huang, Y. Q. Zhang, Y. Z. Che, and W. B. Zhang, "Finding a novel threadlike structure on the intra-abdominal organ surface of small pigs by using in-vivo tripan blue staining," in *The Primo Vascular System, Its Role in Cancer and Regeneration*, K. S. Soh, K. A. Kang, and D. K. Harrison, Eds., pp. 63–70, Springer, New York, NY, USA, 2011.

[18] M. Stefanov, "Critical review and comments on B. H. Kim's work on the primo vascular system," *Journal of Acupuncture Meridian Studies*, vol. 5, no. 5, pp. 241–247, 2012.

[19] B.-C. Lee, J. S. Yoo, V. Ogay et al., "Electron microscopic study of novel threadlike structures on the surfaces of mammalian organs," *Microscopy Research and Technique*, vol. 70, no. 1, pp. 34–43, 2007.

[20] V. Vodyanov, "Characterization of primo nodes and vessels by high resolution light microscopy," in *The Primo Vascular System, Its Role in Cancer and Regeneration*, K. S. Soh, K. A. Kang, and D. K. Harrison, Eds., pp. 83–94, Springer, New York, NY, USA, 2011.

[21] J. L. Soo, B.-C. Lee, H. N. Chang et al., "Proteomic analysis for tissues and liquid from Bonghan ducts on rabbit intestinal surfaces," *Journal of Acupuncture and Meridian Studies*, vol. 1, no. 2, pp. 97–109, 2008.

[22] B.-C. Lee, K.-H. Bae, G.-J. Jhon, and K.-S. Soh, "Bonghan system as mesenchymal stem cell niches and pathways of macrophages in adipose tissues," *Journal of Acupuncture and Meridian Studies*, vol. 2, no. 1, pp. 79–82, 2009.

[23] J. Kwon, K. Y. Baik, B.-C. Lee, K.-S. Soh, N. J. Lee, and C. J. Kang, "Scanning probe microscopy study of microcells from the organ surface Bonghan corpuscle," *Applied Physics Letters*, vol. 90, no. 17, Article ID 173903, 3 pages, 2007.

[24] V. Ogay, K. Y. Baik, B.-C. Lee, and K.-S. Soh, "Characterization of DNA-containing granules flowing through the meridian-like system on the internal organs of rabbits," *Acupuncture and Electro-Therapeutics Research*, vol. 31, no. 1-2, pp. 13–31, 2006.

[25] J. Kim, V. Ogay, B.-C. Lee et al., "Catecholamine-producing novel endocrine organ: Bonghan system," *Medical Acupuncture*, vol. 20, no. 2, pp. 97–102, 2008.

[26] V. Ogay, S. K. Min, J. S. Hyo, J. C. Cheon, and K.-S. Soh, "Catecholamine-storing cells at acupuncture points of rabbits," *Journal of Acupuncture and Meridian Studies*, vol. 1, no. 2, pp. 83–90, 2008.

[27] M. Stefanov and J. Kim, "Primo vascular system as a new morphofunctional integrated system," *Journal of Acupuncture Meridian Studies*, vol. 5, no. 5, pp. 193–200, 2012.

[28] C. H. Lee, J. S. Yoo, H. H. Kim, J. Kwon, and K. S. Soh, "Flow of Nanoparticles inside organs-surface Bonghan ducts," in *Proceedings of the 23rd Symposium Korean Society Jungshin Science,*, vol. 23, pp. 129–134, 2005.

[29] B. Sung, M. S. Kim, B.-C. Lee et al., "Measurement of flow speed in the channels of novel threadlike structures on the surfaces of mammalian organs," *Naturwissenschaften*, vol. 95, no. 2, pp. 117–124, 2008.

[30] J. C. Daras, P. Albaredo, and P. deVernejoul, "Nuclear medicine investigations of transmission of acupuncture information," *Acupuncture in Medicine*, vol. 11, no. 1, pp. 22–28, 1993.

[31] M. Stefanov, "Critical review and comments on BH Kim's work on the primo vascular system," *Journal of Acupuncture Meridian Studies*, vol. 5, no. 5, pp. 241–247, 2012.

[32] A. Bechamp, *The Blood and Its Third Element*, Metropolis Ink, 1912.

[33] C. Lee, S.-K. Seol, B.-C. Lee, Y.-K. Hong, J.-H. Je, and K.-S. Soh, "Alcian blue staining method to visualize Bonghan threads inside large caliber lymphatic vessels and X-ray microtomography to reveal their microchannels," *Lymphatic Research and Biology*, vol. 4, no. 4, pp. 181–190, 2006.

[34] K.-S. Soh, "Bonghan duct and acupuncture meridian as optical channel of biophoton," *Journal of the Korean Physical Society*, vol. 45, no. 5, pp. 1196–1198, 2004.

[35] W. Reich, *The Bion Experiments*, Octagon Books, 1979.

[36] B.-C. Lee, D. I. Kang, and K. S. Soh, *Budding Primo Microcells (Sanals) in A Culture Medium with Fertilized Egg Albumen and RPMI Medium*, Springer, New York, NY, USA, 2012.

[37] B.-C. Lee, H. S. Lee, and D. I. Kang, "Growth of extracellular vesicles into cell-like structures in fertilized chick eggs: hypothesis for a mitosis-free alternative path-way," *Journal of Acupuncture Meridian Studies*, vol. 5, pp. 183–189, 2012.

[38] R. J. Simpson and S. Mathivanan, "Extracellular microvesicles: the need for internationally recognised nomenclature and stringent purification criteria," *Journal of Proteomics and Bioinformatics*, vol. 5, no. 2, 2012.

[39] L. Balaj, R. Lessard, L. Dai et al., "Tumour microvesicles contain retrotransposon elements and amplified oncogene sequences," *Nature Communications*, vol. 2, no. 2, article 180, 2011.

[40] J. Ratajczak, K. Miekus, M. Kucia et al., "Embryonic stem cell-derived microvesicles reprogram hematopoietic progenitors: evidence for horizontal transfer of mRNA and protein delivery," *Leukemia*, vol. 20, no. 5, pp. 847–856, 2006.

[41] D. Hume, *Bechamp or Pasteur: A Lost Chapter in the History of Biology*, BookReal, 1932.

[42] K. L. Machester, "Antoine Béchamp: père de la biologie, Oui ou non?" *Endaevour*, vol. 25, no. 2, pp. 68–72, 2001.

[43] R. Davies, "The story of Gaston Naessens," *Vision*, vol. 39, pp. 16–17, 1991.

[44] O. B. Lepeshinskaya, *The Origin of Cells From Living Substance*, Foreign Languages Publishing House, Pyongyang, Korea, 1954.

Hindawi Publishing Corporation
Evidence-Based Complementary and Alternative Medicine
Volume 2013, Article ID 536560, 5 pages
http://dx.doi.org/10.1155/2013/536560

Research Article

A Method for the Observation of the Primo Vascular System in the Thoracic Duct of a Rat

Sungha Kim,[1] Sharon Jiyoon Jung,[2,3] Sang Yeon Cho,[2] Yoon Kyu Song,[3] Kwang-Sup Soh,[2] and Sungchul Kim[1]

[1] *Department of Acupuncture & Moxibustion, Wonkwang University, Gwangju Medical Hospital, Gwangju 503-310, Republic of Korea*
[2] *Nano Primo Research Center, Advanced Institute of Convergence Technology, Seoul National University, Suwon 443-270, Republic of Korea*
[3] *Graduate School of Convergence Science Technology, Seoul National University, Suwon 443-270, Republic of Korea*

Correspondence should be addressed to Yoon Kyu Song; yksong@gmail.com and Sungchul Kim; kscndl@hanmail.net

Received 7 February 2013; Accepted 30 May 2013

Academic Editor: Walter J. Akers

Even though the primo vascular system (PVS) has been observed in large caliber lymph vessels by several independent teams, the presence of the PVS in the thoracic duct has been reported by only one team, probably because reproducing the experiment is technically difficult. This brief report presents a new, relatively straightforward method, which is a simple modification of the previous method of dye injection into the lumbar node, to observe the PVS in a thoracic duct of a rat by injecting Alcian blue into the renal node. When this new method was applied to a rat, the branching of the primo vessel in the thoracic duct was clearly displayed. Thus, this new method is expected to extend the network of the PVS from abdominal lymph ducts to thoracic ones.

1. Introduction

Observation of the primo vascular system (PVS) in the thoracic lymph ducts of rodents was reported earlier [1], but reproducing that experiment was difficult; thus, no further work by other independent groups has been performed. In this brief report, we present a different method to observe the PVS in the thoracic duct of a rat.

Our method is to inject Alcian blue staining dye into the renal lymph node near the kidney. In fact, dye injection techniques have been used to find the PVS in the lymph vessel between the lumbar and the mesenteric nodes in rabbits [2–5] and rats [6, 7]. In these previous experiments, the dye was injected into the lumbar nodes, and the stained primo vessel was traced only up to the diaphragm because the researchers were trying to observe the PVS under *in vivo* conditions. In the current work, which is still in progress, in order to expand the range of PVS observations, we opened the thoracic cavity thirty minutes after injecting the dye into the renal lymph node, and we were able to observe the PVS in the thoracic duct *in situ* but not *in vivo*.

Recently, the primo nodes in the lymph vessels of rats were found to be enriched with immune cells, such as macrophages, mast cells, and neutrophils. Thus, the PVS might play an important role in the immune mechanism [8]. Therefore, extending the network of the PVS as much as possible to obtain larger numbers of specimens would seem to be an appropriate endeavor. The current brief report is intended to serve that purpose.

2. Materials and Methods

2.1. Animals. For the laboratory animals, male Sprague-Dawley (SD) rats ($n = 7$, 9 weeks old) were purchased from DooYeol Biotech (Seoul, Korea). Rats were kept in constant temperature and humidity conditions (23°C, relative humidity: 60%) with a 12/12 light/dark cycle and were provided with water and commercial rat chow *ad libitum*. The procedures involving the animals and their care were in full compliance with current international laws and policies (Guide for the Care and Use of Laboratory Animals, National Academy Press, 1996).

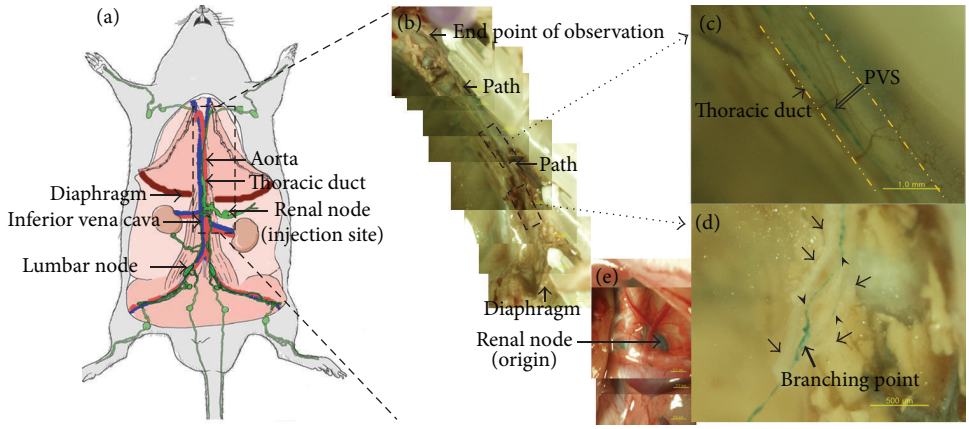

Figure 1: Anatomical location of the primo vascular system (PVS) in the thoracic duct of a rat. (a) Schematic anatomical view of the rat. Large-caliber lymph vessels are depicted with green curves and large arteries and veins with red and blue curves, respectively. (b) Stereomicroscopic image of the thoracic duct indicated with arrows. (c) Magnified view showing the primo vessel (PVS, open arrow) in the thoracic duct (arrow and two dotted lines). (d) Another magnified view showing branched primo vessels (arrow heads) in the thoracic duct (arrows). (e) Stereomicroscopic image of the left renal node (arrows) under the diaphragm. This is the injection site which became blue due to Alcian blue. The colors of panels (b) and (e) are different because (b) was taken after NBF fixing of the euthanized rat, while (e) was taken *in vivo* immediately after injection.

2.2. Surgery and Alcian Blue Injection. We anesthetized the rats by using an intramuscular injection of a mixed solution of 1.5 g/kg of urethane (or 50 mg/kg of Zoletil) and 1 mL of Rompun. With surgical scissors, we incised the outermost skin along the linea alba of the abdomen from the navel down to the symphysis pubis and again up to the ensisternum. Then, we cut the straight muscle of the abdomen to expose the internal organs and moved the organs to the side for observation of the target renal lymph node.

The Alcian blue solution was prepared from 0.1 g of Alcian blue (Sigma-Aldrich, St. Louis, MO, USA) dissolved in 10 mL of phosphate-buffered saline (PBS, pH 7.4) and was filtered by using a 0.22 μm syringe filter (Millipore, Bedford, MA, USA) with a 10 mL syringe (BD, Franklin Lakes, NJ, USA). After the rat's abdomen had been incised along the linea alba, the Alcian blue solution was preheated to 37°C in a water bath and was prepared for injection into a renal lymph node. After the staining dye had been injected into the left renal node, in order to promote the natural circulation of the lymph fluid inside the ducts for the purpose of washing the staining dye, the internal organs that had been moved to the side were replaced in their original positions, and the abdominal skin was closed with forceps. This step was necessary to raise the body temperature. The rats were sacrificed with an intracardiac injection of 0.7 mL urethane at about 30 minutes after the Alcian blue staining dye injection. The thorax of the rat was opened along the right side of the sternum, and the heart and the lungs were removed to observe the thoracic duct. For clear observation, careful incision and removal were necessary to minimize bleeding.

For *in situ* observation of the primo vessel inside the thoracic duct, we used a stereomicroscope (SZX12, Olympus, Tokyo, Japan). We put the rat in 10% neutral buffered formalin solution for one day and then washed it for two hours with tap water. We took the PVS specimen extracted from the thoracic duct, put it on a microscope slide, and examined it with a phase contrast microscope after staining.

2.3. Staining and Microscopy. We applied 4′,6′-diamidino-2-phenylindole (DAPI) and phalloidin reagents for staining of nuclei and f-actins in the cells, respectively. After a 1-hour DAPI (Invitrogen, Prolong Gold Antifade Reagent with DAPI, St. Louis, MO, USA) staining, we washed the sample three times with PBS solution. The phalloidin (Invitrogen, Rhodamine Phalloidin, St. Louis, MO, USA) staining was done in the same way as the DAPI staining.

The prepared sample was investigated under a phase contrast microscope (Olympus Model number BX51, Tokyo, Japan) in order to observe the distributions of the nuclei and the f-actin of the primo vessels that had been stained with DAPI and phalloidin, respectively. Confocal laser scanning microscopy (CLSM; Nikon, C1 plus, Tokyo, Japan) was used to examine optical sections of the threadlike primo vessel.

3. Results

The thoracic duct is a continuation of the largest-caliber abdominal lymph vessel along the caudal vena cava (Figure 1(a)). The Alcian blue was injected into the renal node, flowed into the thoracic duct, and stained the PVS floating in the thoracic duct as indicated in Figure 1(b). A magnified view of the thoracic duct (dotted line) and the primo vessel (blue curve) is given in Figure 1(c). The primo vessel was a continuous thread from the thread in the abdominal lymph vessel below the diaphragm. There were several branches and rejoins of the thoracic lymph duct, and one of them is shown in Figure 1(d). The primo vessel floating inside the thoracic lymph duct also branched and rejoined (blue curves). The thoracic lymph duct before

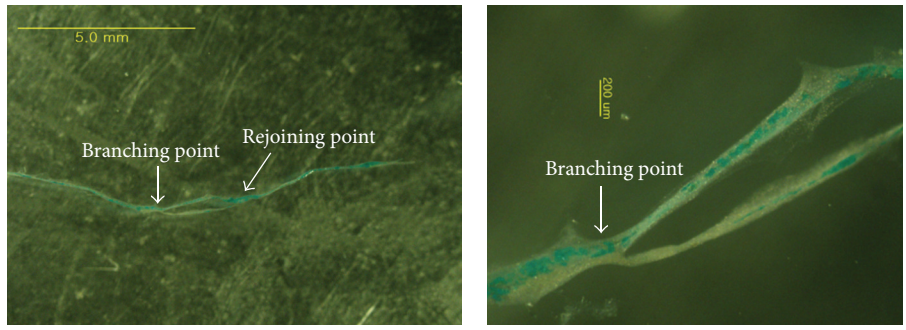

(a) (b)

Figure 2: Stereomicroscopic images of the branched primo vessels (PVS) of Figure 1(d), which were extracted from the thoracic duct and put on a slide. Panel (b) is a magnified view of (a).

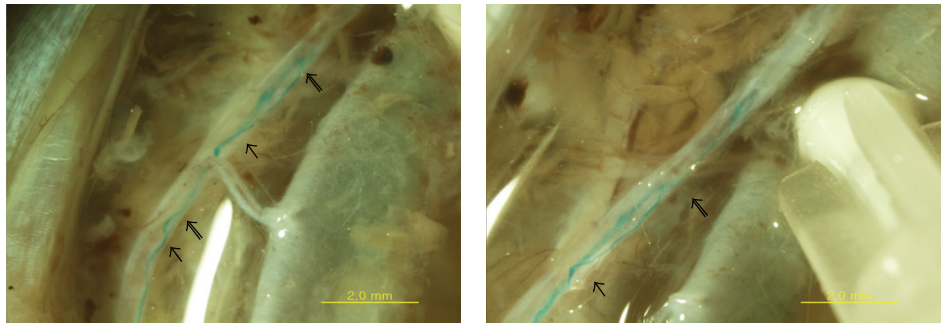

(a) (b)

Figure 3: Stereomicroscopic *in situ* image of a branched and rejoined primo vascular system (blue stained cure) in the thoracic duct of another subject rat. (a) Two regions of branching (arrows) and rejoining (open arrows) are observed, and the upper one is magnified in (b).

the branching point was stripped, and a blue primo vessel was exposed.

The branched primo vessel was extracted from the duct and put on a slide, as shown in Figure 2(a). A magnified view of the branch showed only partial Alcian blue staining (Figure 2(b)), and the reason for that partial staining is not yet understood. The branching of the thoracic duct and the primo vessel in it was a common phenomenon, as shown in Figure 3, where branching and rejoining were seen to occur twice. The image in panel (b) is a magnified view of the image in panel (a), which was taken *in situ* with a stereomicroscope.

In order to confirm that the stained threadlike structure was a primo vessel, we applied the previously established simple criteria of DAPI staining of nuclei and phalloidin staining of f-actins [9]. As shown in the DAPI image, the alignment of rod-shaped nuclei in parallel with the primo vessel was in good agreement with the criteria (Figure 4(b)). Notice that the rod-shaped nuclei were present only inside the region defined by two broken lines. Outside the region, round-shaped nuclei, which are aggregated lymphocytes, were observed. The phase contrast image more clearly showed the aggregated round-shaped lymphocytes scattered around the primo vessel whose boundaries were indicated by the two broken lines (Figure 4(a)). Also, the distribution of the f-actins in the cytoplasm was in agreement with that for a typical primo vessel and was distinctively different from that for a lymph or a blood vessel (Figure 4(c)); that is, the phalloidin signals were aligned along the vessel. The confocal laser scanning microscope image more clearly showed the rod-shaped nuclei (blue color) (Figure 4(d)).

The lengths of the nuclei were 8.3–14 μm, as expected from Bong-Han Kim's work [10]. Another important morphological datum is the diameter of the primo vessel, and it was, on average, 62 ± 28 μm. The morphological size data for the primo vessels from the thoracic ducts of the subject rats are given in Table 1.

4. Discussion

In this brief report, we presented a repeatable method for observing the PVS in the thoracic duct of a rat. Even though the thoracic duct is the largest-caliber lymph vessel, the primo vessel found in this duct is not necessarily much thicker than those found in less-large-caliber lymph vessels. The average diameter of the primo vessels in our case was 61.8 ± 28.3 μm, while the average value of the primo vessels found in the lymph vessels in abdominal cavities was 52 ± 30 μm (rat) [6]. This uniform size was also in agreement with the sizes of the primo vessels found in blood vessels and on the surfaces of internal organs [9]. In our case, the diameter was somewhat larger because of the aggregation of lymphocytes around the

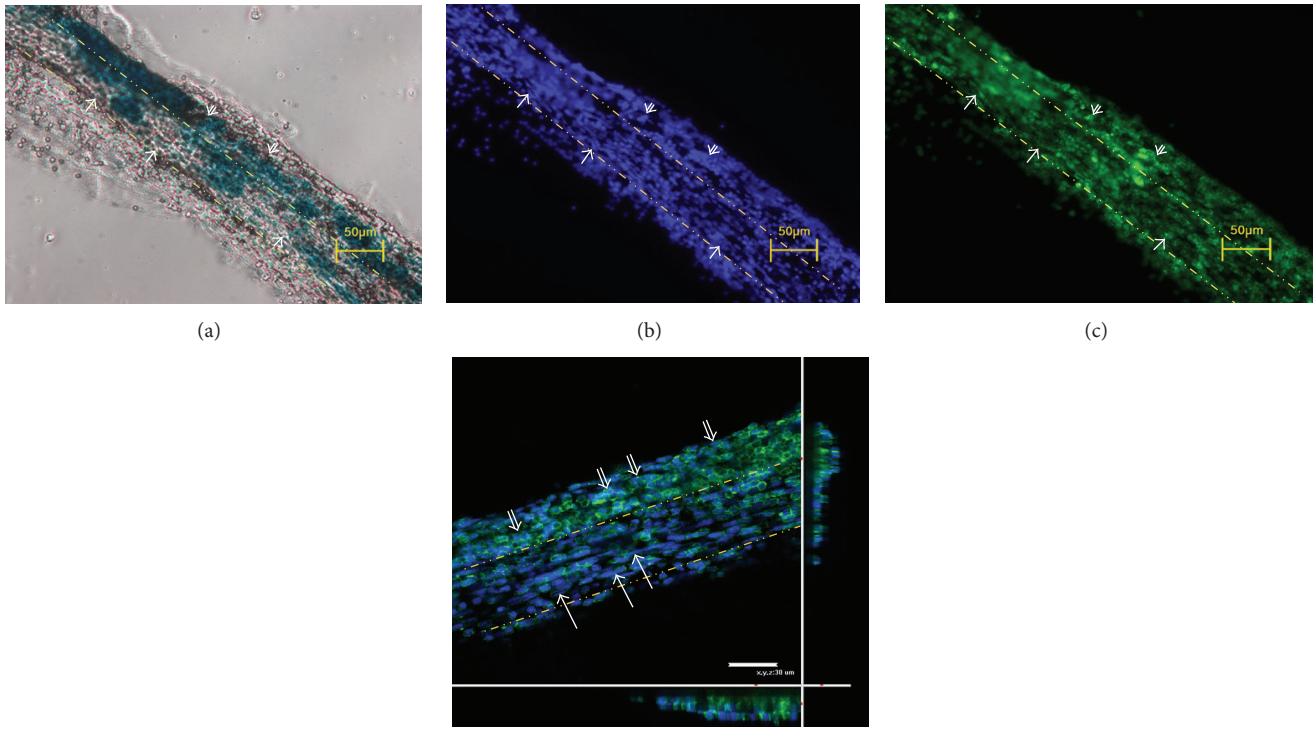

(a) (b) (c)

(d)

Figure 4: Morphological features of a primo vessel (inside the two dotted lines) in a thoracic duct. (a) Phase contrast microscopic image of the primo vessel. (b) Rod-shaped nuclei longitudinally arranged along the primo vessel (inside the yellow-lined region) stained with DAPI. (c) f-actin signals in the cell plasma of the primo vessel stained with phalloidin. (d) Confocal laser scanning microscopic (CLSM) image of the f-actin signals (green) and the nuclei (blue) of the primo vessel. The under and the side panels show cross-sectional views. Rod-shaped nuclei (arrows) are longitudinally arranged along the primo vessel, and lymphocytes (double arrows) are aggregated around the primo vessel.

Table 1: Morphological size data for the primo vessels from the thoracic ducts of seven male, nine-week-old rats.

Subject	Diameter of lymph vessel (mm)	Diameter of primo vessel (μm)
1	1.0	58.8
2	0.4	88.2
3	0.9	85.0
4	0.3	73.5
5	1.0	72.1
6	0.5	36.4
7	0.4	18.3
Average ± S.D.	0.6 ± 0.3	61.8 ± 28.3

primo vessel, as seen in Figure 4. A future task is to remove these aggregated lymphocytes to obtain pure specimens.

This work is the first report on a primo vessel seen in the whole thoracic duct in the longitudinal direction, although a cross-sectional image was presented earlier [1]. In addition, in this work, the branching and the rejoining of the thoracic duct and its associated primo vessel, as mentioned in Bong-Han Kim's work [10], were first demonstrated.

The primo vessel specimen taken from the thoracic duct showed the characteristic hallmarks of a primo vessel; namely, the DAPI images of the shapes and the distribution of nuclei and the phalloidin images of f-actins. We did not address further histological analysis in this brief report partially because the results for the basic H&E-stained specimen have already been reported [1] and partially because an immunohistochemical examination of its extended part in the abdominal lymph vessels was thoroughly done in another work [8]. Another reason was that our main purpose was to develop a repeatable method that could be reproduced by other independent groups. We were able to demonstrate that the method of injecting Alcian blue into a lumbar node could be modified to inject it into a renal node to detect a primo vessel in the thoracic duct.

Conflict of Interests

The authors declare no conflict of interests.

Authors' Contribution

S. Kim and S. J. Jung contributed equally to this work.

Acknowledgment

This work was supported in part by a grant from the Traditional Korean Medicine R&D Project, Ministry for Health & Welfare, Republic of Korea (B110076).

References

[1] I. H. Choi, H. K. Chung, and Y. K. Hong, "Detection of the primo vessels in the rodent thoracic lymphatic ducts," in *The Primo Vascular System*, K. S. Soh, K. A. Kang, and D. Harrison, Eds., pp. 121–126, Springer, New York, NY, USA, 2011.

[2] B.-C. Lee, J. S. Yoo, K. Y. Baik, K. W. Kim, and K.-S. Soh, "Novel threadlike structures (Bonghan ducts) inside lymphatic vessels of rabbits visualized with a Janus Green B staining method," *Anatomical Record*, vol. 286, no. 1, pp. 1–7, 2005.

[3] C. Lee, S.-K. Seol, B.-C. Lee, Y.-K. Hong, J.-H. Je, and K.-S. Soh, "Alcian blue staining method to visualize Bonghan threads inside large caliber lymphatic vessels and X-ray microtomography to reveal their microchannels," *Lymphatic Research and Biology*, vol. 4, no. 4, pp. 181–189, 2006.

[4] Y. I. Noh, M. Rho, Y. M. Yoo, S. Jung, and S. S. Lee, "Isolation and morphological features of primo vssels in rabbit lymph vessel," *Journal of Acupuncture and Meridian Studies*, vol. 5, no. 5, pp. 201–205, 2012.

[5] S. Jung, S. Y. Cho, K. H. Bae et al., "Protocol for the observation of the primo vascular system in the lymph vessels of rabbits," *Journal of Acupuncture and Meridian Studies*, vol. 5, no. 5, pp. 234–240, 2012.

[6] H.-M. Johng, J. S. Yoo, T.-J. Yoon et al., "Use of magnetic nanoparticles to visualize threadlike structures inside lymphatic vessels of rats," *Evidence-Based Complementary and Alternative Medicine*, vol. 4, no. 1, pp. 77–82, 2007.

[7] J. S. Yoo, H.-M. Johng, T.-J. Yoon et al., "*In vivo* fluorescence imaging of threadlike tissues (Bonghan ducts) inside lymphatic vessels with nanoparticles," *Current Applied Physics*, vol. 7, no. 4, pp. 342–348, 2007.

[8] B. S. Kwon, M. H. Chang, S. S. Yu, B. C. Lee, J. Y. Ro, and S. Hwang, "Microscopic nodes and ducts inside lymphatics and on the surfaces of internal organs are rich in granulocytes and secretory granules," *Cytokine*, vol. 60, no. 2, pp. 587–592, 2012.

[9] K.-S. Soh, "Bonghan circulatory system as an extension of acupuncture meridians," *Journal of Acupuncture and Meridian Studies*, vol. 2, no. 2, pp. 93–106, 2009.

[10] B. H. Kim, "The Kyungrak system," *Journal of Jo Sun Medicine*, vol. 108, pp. 1–38, 1965 (Korean).

Hindawi Publishing Corporation
Evidence-Based Complementary and Alternative Medicine
Volume 2013, Article ID 636081, 7 pages
http://dx.doi.org/10.1155/2013/636081

Review Article

Historical Review about Research on "Bonghan System" in China

Jun-Ling Liu, Xiang-Hong Jing, Hong Shi, Shu-Ping Chen, Wei He, Wan-Zhu Bai, and Bing Zhu

Institute of Acupuncture and Moxibustion, China Academy of Chinese Medical Sciences, Beijing 100700, China

Correspondence should be addressed to Bing Zhu; zhubing@mail.cintcm.ac.cn

Received 16 February 2013; Revised 8 May 2013; Accepted 20 May 2013

Academic Editor: M. Isabel Miguel Perez

The meridian-collateral theory is the theoretical basis of acupuncture-moxibustion therapy. Professor Bonghan Kim, a professor of the Pyongyang Medical University of the Democratic People's Republic of Korea, claimed that he found the anatomical structure of meridian-collaterals, named Bonghan corpuscles (BHCs) and Bonghan ducts (BHDs) system or primo vascular system (PVS), in 1962. From 1963 to 1965, researchers from our institute conducted a series of comparative anatomical experiments, trying to reproduce the so-called BHC- and BHD-like structures in different strains of animals. In the present paper, the authors introduced their research findings about BHC- and BHD-like structures in the young rabbit's umbilicus including its external appearance, ectoplasm and endoplasm, and about strip-like and node-like objects in the blood vessels and lymph vessels near the larger abdominal and cervical blood vessels and chromaffin tissue in the back wall of the rabbit's abdominal cavity and between the bilateral kidneys. In spite of existence of the BHC- and BHD-like structures in the rabbit, there has been no proved evidence for their association with the meridian-collateral system described in acupuncture medicine. In the present historical review, the authors also make a discussion about the significance of those findings.

1. Introduction

The theory of meridian-collateral system, established more than two thousand years ago, is the core of acupuncture medicine and the important component of traditional Chinese medicine [1]. In spite of existence of many meridian phenomena in the human body and effective guidance on clinical acupuncture practice, no any corresponding anatomical structure has been found about the main meridian running traces described in many classical works on acupuncture medicine up to now. In 1962, Bonghan Kim, a professor of the Pyongyang Medical University of the Democratic People's Republic of Korea, reported that he observed the electrical responses of acupoints [2]. In 1963, his second report titled "On the acupuncture meridian system" [3] and "On the Kyungrak (meridian) system" [4] were published, claiming that a node-like anatomical structure (Bonghan corpuscles (BHCs), current primo nodes) in the acupoints and a tube-like organ (Bonghan ducts (BHDs), current primo vessels (PVs)) were found on the skin in rabbits. This new organ exists not only in the skin or body surface but also in the internal organs including the blood vessels and lymph vessels. In 1965, his other 3 reports [5–7] were successively published, further explaining the entire network of the Bonghan system (renamed as primo vascular system (PVS)) and the "Sanal" (meaning "live egg," renamed as Primo-microcell (P-microcell)) which functions in the regeneration and/or repair and hematopoiesis [7]. This so-called greatest discovery (atomic bomb, spacecraft, and PVS) in the 20th century induced a shock to the medical circles of China and other countries in the world. A representative group of Chinese top-ranked medical scientists including anatomist, histologists, physiologists, and pathologists visited the National Acupuncture Meridian Research Institute in Pyongyang twice in 1963. In the meantime, the "Institute of Meridian-Collaterals" which is the main body of the present Institute of Acu-Moxibustion of China Academy of Chinese Medical Sciences was established in Beijing. In addition, several research groups were also founded separately in Beijing, Shanghai, Changchun, and Shenyang for verification of Kim's

work [8]. According to Kim's results and animal histological section samples, Chinese medical scientists conducted a series of comparative anatomical studies in the human corpses, rabbits, rats, guinea pigs, cats, dogs, and monkeys, trying to confirm Kim's findings. In Kim's reports and during Chinese scientists' visiting in Pyongyang, no detailed experimental materials, techniques, and histological methods were introduced. Thus, paying great efforts, Chinese medical scientists finally found the similar structure of superficial BHC-like structure in the young rabbit's umbilicus, strip-like and node-like objects in the blood vessels and lymph vessels near the larger abdominal and larger cervical blood vessels, and chromaffin tissue in the back wall of the rabbit's abdominal cavity and between the bilateral kidneys, but failed in reproducing the so-called spontaneous bioelectrical signal propagation of PVs, subcutaneous BHDs or BHCs, and so forth of the acupoint regions in the rabbit's thigh [8]. Due to some special factors at that time, these original results have not been formally published in any domestic or foreign journals until now. Nowadays, some of the Chinese principal top-ranked medical specialists have already passed away and can not see their achievements published. In order to disclose that period of history and to express our respect to their great efforts, we report their results as follows.

2. Results

2.1. Superficial BHC- and BHD-Like Structures. From the beginning of 1964, Chinese medical scientists employed routine histological perfusion, sectioning, hematoxylin and eosin (H&E) staining, and light microscope and so forth, to conduct a wide variety of experiments in the human corpses, rabbits, rats, guinea pigs, cats, dogs, and monkeys for reproducing superficial BHCs and BHDs in the acupoint regions of the body surface (more than 10 thousands tissue sections have been still reserved in our institute at present), but failed to find the similar structure. At last, they observed BHC- and BHD-like structures in the umbilici of the young rabbits.

2.1.1. Longitudinal Profile of the Rabbit's Umbilicus. Following routine transcardiac perfusion, the umbilicus tissue of the anesthetized young rabbit (about a week in age) was removed for observation under light microscope (Leitz, Germany). According to Kim's results and animal tissue section samples provided (Figure 1(b)) during Chinese medical specialists' visiting in 1963, Chinese researchers observed that the young rabbit's umbilicus was near completely the same as superficial BHCs in the external appearance including the shape, size, and arrangement of superficial blood vessels and the longitudinal structure of the umbilicus tissue sections (Figure 1(a)). The rabbit's umbilicus, about 2 cm in length, was a longitudinal cord-like organ with two intumescent endings connecting to the skin on the top and the skeleton muscle near the abdominal cavity at the bottom, respectively (Figure 1(a)).

By using a freezing microtome (Leitz, Germany), the umbilicus tissue was successively sectioned (40 μm) and observed using a light microscope. According to Professor Kim, the BHC was mainly composed of ectoplasm and endoplasm. Under microscope, the rabbit's umbilicus tissue on the longitudinal section was also composed of ectoplasm and endoplasm (Figures 2(a) and 2(b)).

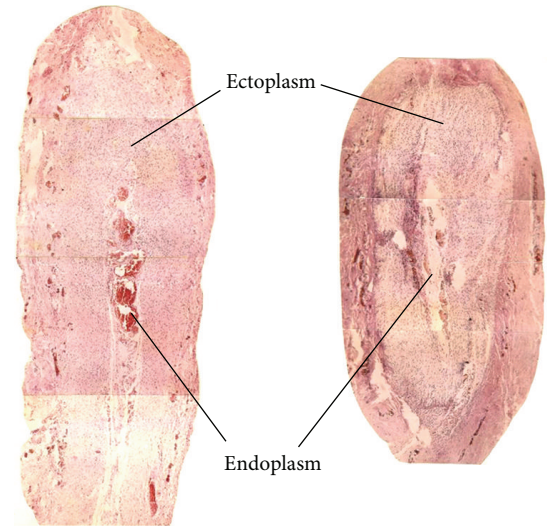

Figure 1: Comparison between the young rabbit's umbilicus observed by Chinese researchers (a) and Bonghan corpuscle (BHC) (b) in the longitudinal section. (a) A photo of hematoxylin and eosin (H&E) staining showing the longitudinal profile of the young rabbit's umbilicus (magnification, ×4), being cord-shaped in outline and about 2 cm in length. (b) A photo of the longitudinal profile of BHC presented by Northern Korean National Acupuncture Meridian Research Institute in 1963.

2.1.2. Ectoplasm of the Umbilicus. From the top to the bottom of the longitudinal umbilicus tissue, the ectoplasm contained skin layer, smooth muscles, and elastic fibrous tissue (Figure 2(b)). The smooth muscles included radiation-like smooth muscle fibers extending toward the skin (Figure 2(b), a′, a″), thinner outer-circular layer (Figure 2(b) b′, b″), thicker entolongitudinal layer between the skin and the endoplasm (Figure 2(b) c, c′, c″), and fewer muscle fibers near the skeleton muscle of the abdominal cavity. Apparently, the components of the umbilicus were basically identical to those of BHC-BHD complex. The running direction of the smooth muscle was along the longitudinal axis of the umbilicus.

These smooth muscles, encompassed by a thin layer of collagen fibers or elastic fibers, were mainly distributed in the epidermis layer near the skin of the umbilicus. The elastic fibers gradually appeared and increased in the amount on the lower end of the ectoplasm. Warthin-Starry dyeing displayed that the ectoplasm of the umbilicus also contained richer argyrophilic fibers. Feulgen staining showed that in the epidermis layer of the umbilicus, there existed some hemisphere-like cell clusters.

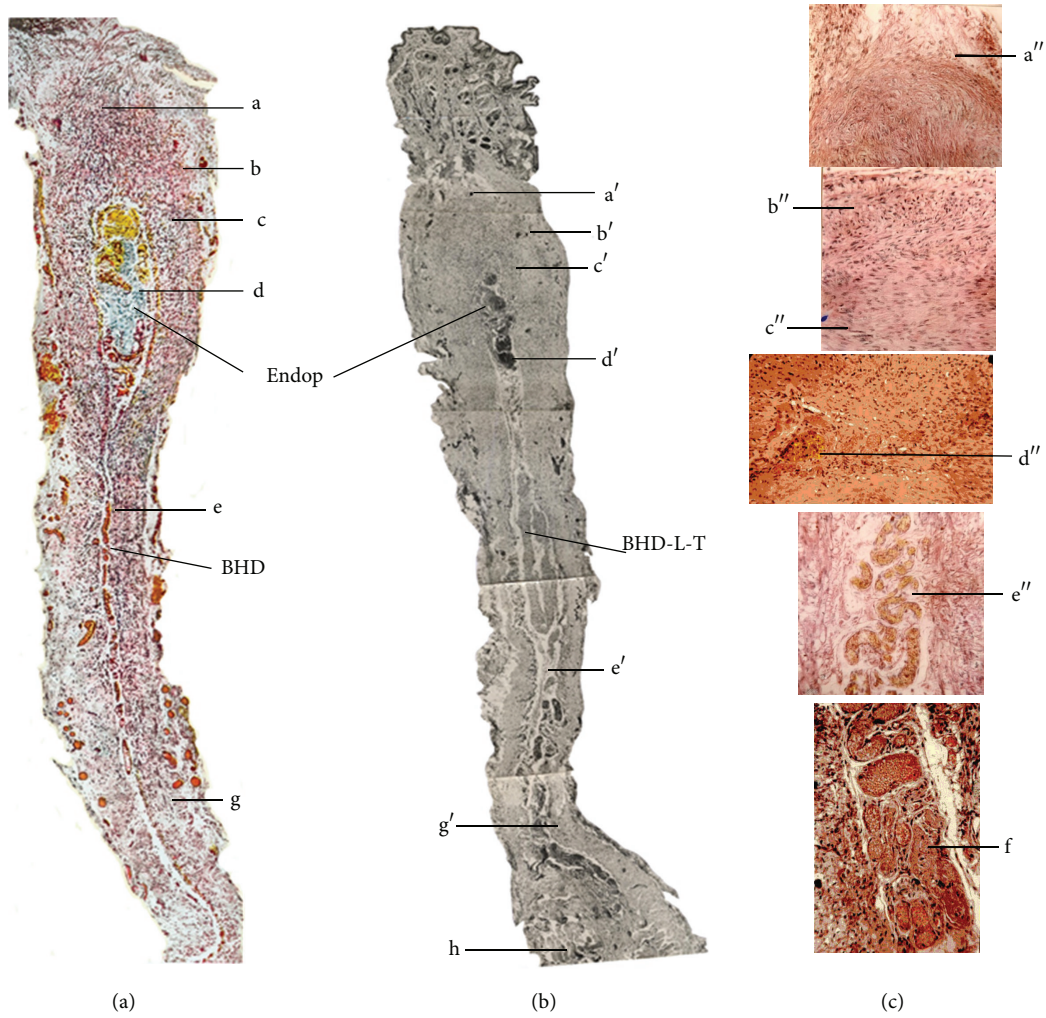

Figure 2: Comparison of histological structure of the superficial BHC (a) and the umbilicus tissue (b), (c) in rabbits. (a) Profile of BHC reported by Professor Kim (*J Jo Sun Med*, vol. 90, 1963 pages 6–35). (b) BHC-like structure of the young rabbit's umbilicus found by Chinese researchers in 1964 (an original photo unpublished) (16 × 6.3). (c) Partial components of the umbilicus (c) stained with H&E method. Both BHC and umbilicus are divided into ectoplasm (composed of smooth muscles, elastic fibers, argyrophilic fibers, etc.) and endoplasm (Endop, containing chromaffin cells, blood vessels, Fibrillenstruktur, etc.) (16 × 16). BHD: Bonghan duct, BHD-L-T: BHD-like tubule; a, a′, a″: radiation-like smooth muscle; b, b′, b″: outer-circular layer smooth muscle; c, c′, c″: entolongitudinal layer smooth muscle; d, d′, d″: chromaffin cells; e, e′, e″: blood vessels, f: Fibrillenstruktur, g, g′: elastic fibers, and h: skeleton muscle.

2.1.3. Endoplasm of the Rabbit's Umbilicus. Under light microscope, some chromaffin cells (Figure 2(c), d″), crooked blood vessels (Figure 2(c), e″), Fibrillenstruktur (Figure 2(c), f″), follicles, and smooth-muscle-like cells were observed in the endoplasm of the umbilicus. The Fibrillenstruktur was stained to be either blue (basophilia) or red (acidophilia) with H&E method. In addition, there also existed a type of cell (similar to chromaffin cell) containing a smaller nucleus and rich cytoplasma with yellow-brown granules. Further analysis showed that this type of cell is phagocyte swallowing red blood cells and so forth, and the yellow-brown granules are hemofuscin. In the neighboring part of the cavity of the follicle-like structure, some basophilia granules and smooth muscle-like cells were observed.

2.2. Bonghan Duct-Like Object in the Deep Tissues of the Rabbit. After trying various perfusion methods, Chinese researches ultimately found strip-shaped (Figure 3(a)) and node-like objects in the larger blood vessels and lymph vessels in the rabbit. Feulgen dyeing showed that these objects contained rhabdocyte nucleus and chromonucleic acid granules. After H&E staining, these intravascular rhabdocyte nuclei and chromonucleic acid granules were found to be deformed leukocyte nuclei or deciduous vascular endotheliocyte nuclei and had no chromonucleic acid granules. Following perfusion with normal saline mixed with anticoagulation reagent (heparin), these strip-shaped and node-like objects in the blood vessels disappeared. In the intravenous node-like objects, some divided hematopoietic cells were found.

2.3. Bonghan Corpuscle-Like Object in the Deep Tissues of the Rabbit. In the neighboring tissues of the larger abdominal vessels and cervical blood vessels, Chinese researchers found some node-like objects which were connected to ducts at their two ends and had no smooth muscles in the rabbit (Figure 4(a)). Following sectioning and staining, these node-like objects and their connected ducts were found to be lymph nodes and lymph vessels, respectively.

In the back wall of the rabbit's abdominal cavity and the tissues between the two kidneys, Chinese researchers observed some chromaffin cells (Figure 4(c)). Histological analysis confirmed the observed tissue to be chromaffin tissue near the paraganglion. These node-like objects and chromaffin tissue were similar to deep BHCs in the outline (Figures 4(b) and 4(d)).

3. Discussion

Just as those mentioned in the preface of the present paper, Chinese researchers tried various methods to reproduce superficial BHCs and BHDs in different strains of animals and human corpses and finally observed BHC-like structure in the young rabbit's umbilicus and deep BHD-like structure in the abdominal vessels and lymph node-like object (BHC) around the rabbit's cervical vessels. But in the young rabbit's umbilicus, no transverse BHD-like tubules along the subcutaneous tissue of the body and no rich chromonucleic acid in the BHD-like structures were found, being different to Kim's results [5]. The superficial BHC- and BHD-like structure of the rabbit's umbilicus were also not reproduced in the umbilicus of the human body and other animals. In addition, the superficial BHC- and BHD-like objects were not found in the acupoint region of the rabbit's thigh where Professor Kim claimed [3]. According to Professor Kim's reports on the schematic structure of BHCs [3, 5], the young rabbit's umbilicus was also composed of ectoplasm and endoplasm connecting to a BHD-like tubule extending toward the abdominal cavity.

The components of the ectoplasm in the umbilicus including the location or distribution and arrangement of the smooth muscles (near the skin and fibrous tissue near the abdominal muscle) and radiation-like smooth muscle fibers, the outer circular and entolongitudinal layers, thickness of the smooth muscles, the thin layer of collagen fibers or elastic fibers encompassing the smooth muscles, the distribution, shape, and size of the argyrophilic fibers, and the hemisphere-like cell clusters in the umbilicus are near completely identical to BHCs found in the acupoint and skin by Kim [3, 5].

In the endoplasm of the superficial BHCs, there was a follicle-like structure formed by several layers of cubic endothelial cells which were also observed in the young rabbit's umbilicus. The other components of the endoplasm such as the chromaffin cells, Fibrillenstruktur, follicles, smooth-muscle-like cells and crooked blood vessels, and the phagocytes containing yellow-brown granules are also the same as those of BHCs [3, 5]. In fact, the endoplasm originates from the residual collagen fibers of the degenerated blood vessels in the umbilicus.

The external appearance of the umbilicus is also very similar to that of BHC sample (provided by Kyungrak Institute of Korea in 1963 during Chinese medical scientists' visiting in Pyongyang, unpublished results of research work briefings from our institute in 1965) in the shape and blood vessel distribution. Thus, the aforementioned young rabbit's umbilicus is quite similar to BHC in the shape and structure.

Moreover, the strip- (thread-) shaped and node-like objects in the abdominal vessels and the lymph node-like objects around the larger cervical blood vessels are also consistent with those of BHDs and BHCs in the deep tissues of the rabbit [3, 5]. And the thread-like structure is also the same as the results reported by Soh and colleagues [9–11].

In spite of a similar outline between the intravascular node-like or thread-like objects and intravascular BHCs and BHDs, Chinese researchers from our institute thought that these objects were no more than some blood clots at that time. Because after perfusion with anticoagulation reagent, the node-shaped objects disappeared. This is identical to the result of Chinese Changchun research group [8] who also observed a white thread-shaped object in the rabbits' thoracic aorta (extending to the abdominal aorta) following femoral vein perfusion with normal saline. If the perfusion fluid was mixed with adrenaline which facilitates blood coagulation, the thread-shaped objects could be seen not only in the main stems of the thoracic aorta and abdominal aorta but also in their branches. If the perfusion fluid was mixed with heparin (resisting blood coagulation), the thread-shaped objects disappeared completely. Thus, Chinese researchers held that these intravascular thread-like objects were probably a fibrin bundle related to blood clotting [8]. This conclusion is not insistent to Soh and colleagues' report that the blood fibrin and PV are two different objects distinguishable by using Acridine orange staining and fluorescent microscope [12].

The deep BHC-like objects containing chromaffin cells and lymphocyte-like cells found in the rabbit's abdominal cavity and the tissues between the two kidneys were identical to BHCs reported by Kim [4]. The chromaffin cells exist mainly in the adrenal medulla, sympathetic ganglia, and so forth and function in secreting adrenaline, noradrenaline, and so forth in the human body. Whether these chromaffin cells are involved in functional activities of the meridian-collateral system or not, there have been no any reports up to now.

In 1960s, Professor Kim's work induced great attention not only in China but also in some countries of the world. Fujiwara (an assistant professor in anatomy) and Yu from Osaka City University Medical School found the superficial BHC-like structure in one rabbit and observed many BHCs inside the blood vessels and on the surface of the internal organs in the rabbit [13]. In the contemporaneity, Kellner, a histologist from Austria [14], conducted a series of animal experiments and confirmed the existence of the extremity corpuscle-like objects reported by Kim, but failed to find the structure proclaimed by Kim. He thought that these objects were merely a residual structure of embryonic development period and were impossible to have any physiological functions.

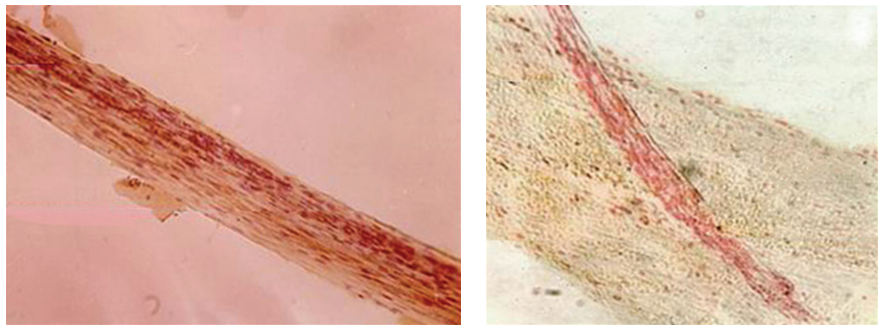

(a) (b)

Figure 3: Photos of intravascular strip-like object (a) in the rabbit's blood vessels found by Chinese researchers and extravascular BHD (b) in the rabbit's deep tissue reported by Professor Kim, being similar in the outline. (a) A photo of H&E staining showing the strip-shaped object in the rabbit's blood vessels (16 × 16). (b) Deep BHD attached to a blood vessel reported by Professr Kim.

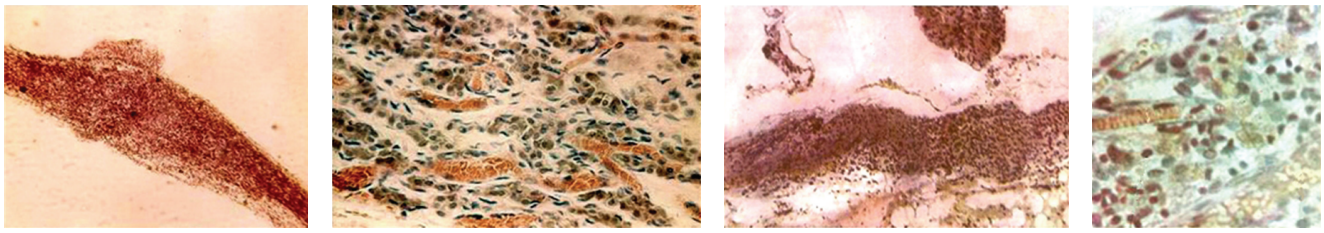

(a) (b) (c) (d)

Figure 4: Comparison of the rabbit's node-like object in the blood vessels and lymph vessels (a) and chromaffin tissue (c) in the back wall of abdominal cavity found by Chinese researchers and deep BHC (b) and chromaffin tissue (d) reported by Professor Kim. (a, c; magnification: 16 × 10).

It is very clear that all the aforementioned structures in the rabbit are known tissues or appeared under some special conditions. However, in the human body, the umbilicus is just the site of Shenque (CV8) acupoint of the conception vessel which functions in regulating borborygmus, diarrhea, edema, chronic enteritis, prolapse of the rectum, and various deficiency syndromes [15]. However, clinical effects of acupuncture or moxibustion stimulation on gastrointestinal activities and other organs rely on the integrity of the nerve system, neurotransmitters, body fluid, and gastrointestinal hormones [16]. Last year, Wang and her colleagues [17] observed that neither electrical stimulation nor section of the PVs on the surface of the stomach or intestine could affect gastric motility, and ST36-electroacupuncture (EA) stimulation induced increase of gastric systolic and diastolic activities in rats. It suggests that, at least, the thread-like structure on the surface of the gastrointestinal tract has no definite association with the effects of EA stimulation.

Furthermore, after surveying the available publications from China and other countries on the question "what is being stimulated in acupuncture?", Chan [18] held that the most convincing results indicate that expression of acupuncture effects definitely involves the nervous system. On the extremity of the body, acupuncture is equated to direct nerve stimulation. Acupuncture stimulation initiated sensory signal input from the acupoint to the brain and then the resulting processing, integration, and balancing regulation of the physiological and pathological information in the central nervous system are the basis for producing clinical effects [19, 20]. For instance, the abolition of acupuncture analgesia by injection of local anesthetics into acupoints is probably the strongest evidence to support the conclusion that neural innervation is required for the acupuncture stimulation response [21, 22]. Longhurst [23] pointed out that although additional research is warranted to investigate the role of some of the structures (such as tendinomuscular structures, primo vessels, higher- or lower-temperature traces, low skin resistance, etc.) identified, it seems clear that the peripheral and central nervous system can now be considered to be the most rational basis for defining meridians.

In the recent 10 years, analysis of PVS has been resurrected by Soh and his colleagues from the Department of Physics in the Seoul National University [24, 25] and Ma et al. from China [26]. They used Trypan blue dyeing and other techniques to show that PVs exist not only on the surface of the internal organs, but also in the nerve system, cardiovascular system, lymphatic system, fascia of the abdominal cavity, adipose tissue, generative system (testis), skin and abdominal wall, primo fluid and microcells, egg vitelline membrane, and cancer [27] in rabbits, rats, mice, dogs, and pigs. They have observed the structure of PVs by using modern instruments as electron microscope and laparoscope [28, 29] and analyzed their protein profiles of PVs tissue using proteomic technique [30], claiming that

their results will shift the level of the oriental medicine from the traditional wisdom and art with a long history to the biomedical sciences. Recently, Kwon and colleagues [11, 31] observed microscopic nodes and ducts inside lymphatics, as well as on the surface of internal organs in the rat. The nodes contain a variety of immune cells, usually enriched with mast cells, eosinophils, neutrophils and histiocytes, as well as chromaffin cells, other granule-containing cells. They guess that these ducts may be involved in the transport of secretory granules from the nodes and serve a new circulatory system.

Generally speaking, the anatomical structure always accompanies functional roles in the human body and other animals. But the conjecture about the connection between PVS and meridian-collateral system does not have any proved experimental basis. We do hope to get more proved and universally accepted evidence, particularly on its physiological functions under both normal and pathological conditions.

The meridian-collateral system theory is founded more than two thousand years ago. It highlights the close association among different parts of the body surface, and between the body surface and internal organs, functioning in regulating physiological activities of various systems of the human body via neuron-endocrine-immune networks. Despite objective existence of many meridian phenomena in the human body [32–35] and limited explanations by using current biological theories, any acupuncture intervention outcomes deviating from predominate roles of the neuron-endocrine-immune network will not be accepted by the academic circle, and the conjecture is probably unreasonable.

4. Conclusion

Chinese researchers found superficial BHC-like objects only in the young rabbits' umbilici, and also observed deep BHC- and BHD-like objects in the abdominal and cervical blood vessels. But they could not distinguish the deep BHC- and BHD-like objects from coagulation. No BHC- and BHD-like structures were found in other animals and human corpses as well as in the acupoint regions. No any proved evidence for the association between the PVS or Bonghan system and meridian-collateral system of acupuncture medicine has been found up to now.

Authors' Contributions

This work was done by Hsichun Chang, Zhaote Li, Zhili Tao, Lixia Zhu, and Chen Wen. The present paper was written by Jun-Ling Liu, Xiang-Hong Jing, Hong Shi, Shu-Ping Chen, Wei He, Wan-Zhu Bai, and Bing Zhu. Junling Liu and Xianghong Jing contributed equally to this paper.

Acknowledgments

This work was supported by the National Key Basic Research Program 973 (nos. 2010CB530507, 2013CB531904, and 2011CB505200) and National Natural Science Foundation of China (no. 81173205).

References

[1] Y. Q. Xia and C. S. Jia, "Meridian-collaterals," in *Complete Works of Chinese Acupuncture and Moxibustion*, X. T. Wang, Ed., vol. 1 of *Basis of Acupuncture and Moxibustion Science*, chapter 4, p. 57, Henan Science and Technology Press, 1988 (Chinese).

[2] B. H. Kim, "Study on the reality of acupuncture meridians," *Journal of Jo Sun Medicine*, vol. 9, pp. 5–13, 1962 (Korean).

[3] B. H. Kim, "On the acupuncture meridian system," *Journal of Jo Sun Medicine*, vol. 90, pp. 6–35, 1963 (Korean).

[4] B. H. Kim, "On the Kyungrak system," *Journal of the Academy of Medical ScienceS of the Democratic People's Republic of Korea*, vol. 90, pp. 1–41, 1963.

[5] B. H. . Kim, "The Kyungrak system," *Journal of Jo Sun Medicine*, vol. 108, pp. 1–38, 1965 (Korean).

[6] B. H. . Kim, "Sanal theory," *Journal of Jo Sun Medicine*, vol. 108, pp. 39–62, 1965 (Korean).

[7] B. H. Kim, "Sanal and hematopoiesis," *Journal of Jo Sun Medicine*, vol. 108, pp. 1–6, 1965 (Korean).

[8] X. Liu, "Review on the Replication of 'Bongham Meridian Entity'," *Zhen Ci Yan Jiu*, vol. 34, no. 5, pp. 353–354, 2009.

[9] H.-S. Shin, H.-M. Johng, B.-C. Lee et al., "Feulgen reaction study of novel threadlike structures (Bonghan ducts) on the surfaces of mammalian organs," *Anatomical Record B*, vol. 284, no. 1, pp. 35–40, 2005.

[10] K. S. Soh, K. A. Kang, and D. Harrison, Eds., *The Primo Vascular System: Its Role in Cancer and Regeneration*, Springer, New York, NY, USA, 2011.

[11] B. S. Kwon, M. H. Chang, S. S. Yu, B. C. Lee, J. Y. Ro, and S. Hwang, "Microscopic nodes and ducts inside lymphatics and on the surfaces of internal organs are rich in granulocytes and secretory granules," *Cytokine*, vol. 60, no. 2, pp. 587–592, 2012.

[12] B. C. Lee, K. Y. Baik, H. M. Johng et al., "Acridine orange staining method to reveal the characteristic features of an intravascular threadlike structure," *Anatomical Record B*, vol. 278, no. 1, pp. 27–30, 2004.

[13] S. Fujiwara and S. B. Yu, "Bonghan theory: morphological studies," *Igakuro Ayumi*, vol. 60, pp. 567–577, 1967 (Japanese).

[14] G. Kellner, "Bau und Funktion der Haut," *Dtsch Zschr Akup*, vol. 15, pp. 1–31, 1966 (German).

[15] D. Li, *Acupuncture Meridian Theory and Acupuncture Points*, Foreign Languages Press, 1st edition, 1991.

[16] S. Wu, J. Li, F. X. Liang, H. Y. Jin, and H. Wang, "Effect of acupuncture on the activity of gastrointestinal electricity," *Zhongguo Zhen Jiu*, vol. 31, no. 5, pp. 477–480, 2011.

[17] X. Wang, H. Shi, H. Shang et al., "Are primo vessels (PVs) on the surface of gastrointestine involved in regulation of gastric motility induced by stimulating acupoints ST36 or CV12?" *Evidence-Based Complementary and Alternative Medicine*, vol. 2012, Article ID 787683, 8 pages, 2012.

[18] S. H. H. Chan, "What is being stimulated in acupuncture: evaluation of the existence of a specific substrate," *Neuroscience and Biobehavioral Reviews*, vol. 8, no. 1, pp. 25–33, 1984.

[19] G. W. Lü, "Afferent fiber innervation on acupuncture points and its role in acupuncture analgesia," *Zhen Ci Yan Jiu*, vol. 12, no. 1, pp. 1–32, 1987.

[20] C. Takeshige, K. Oka, T. Mizuno et al., "The acupuncture point and its connecting central pathway for producing acupuncture analgesia," *Brain Research Bulletin*, vol. 30, no. 1-2, pp. 53–67, 1993.

[21] C. Y. Chiang and C. Chang, "Peripheral afferent pathway for acupuncture analgesia," *Scientia Sinica B*, vol. 16, pp. 210–217, 1973.

[22] B. Pomeranz and D. Paley, "Peripheral afferent pathway for acupuncture analgesia," *Experimental Neurology*, vol. 66, pp. 398–402, 1979.

[23] J. C. Longhurst, "Defining meridians: a modern basis of understanding," *Journal of Acupuncture and Meridian Studies*, vol. 3, no. 2, pp. 67–74, 2010.

[24] K.-S. Soh, "Bonghan circulatory system as an extension of acupuncture meridians," *Journal of Acupuncture and Meridian Studies*, vol. 2, no. 2, pp. 93–106, 2009.

[25] V. Ogay, K. H. Bae, K. W. Kim, and K. Soh, "Comparison of the characteristic features of Bonghan ducts, blood and lymphatic capillaries," *Journal of Acupuncture and Meridian Studies*, vol. 2, no. 2, pp. 107–117, 2009.

[26] W. Ma, H. Tong, W. Xu et al., "Perivascular space: possible anatomical substrate for the meridian," *Journal of Alternative and Complementary Medicine*, vol. 9, no. 6, pp. 851–859, 2003.

[27] K. S. Soh, "Current state of research on the primo vascular system," *The Primo Vascular System*, pp. 25–39, 2012.

[28] S. Hong, J. S. Yoo, J. Y. Hong et al., "Immunohistochemical and electron microscopic study of the meridian-like system on the surface of internal organs of rats," *Acupuncture and Electro-Therapeutics Research*, vol. 32, no. 3-4, pp. 195–210, 2007.

[29] J. Lim, M. Chae, J. Kim, J. Sohn, and K. S. Soh, "Development of a laparoscopic system for in vivo observation of the Bonghan structure," *Journal of Acupuncture and Meridian Studies*, vol. 2, no. 3, pp. 248–252, 2009.

[30] S. J. Lee, B. C. Lee, C. H. Nam et al., "Proteomic analysis for tissues and liquid from Bonghan ducts on rabbit intestinal surfaces," *Journal of Acupuncture and Meridian Studies*, vol. 1, no. 2, pp. 97–109, 2008.

[31] S. J. Jung, S. Y. Cho, K. H. Bae et al., "Protocol for the observation of the primo vascular system in the lymph vessels of rabbits," *Journal of Acupuncture and Meridian Studies*, vol. 5, no. 5, pp. 234–240, 2012.

[32] D. Z. Li and S. Z. Li, *Exploration on Secrets of Meridian-Collaterals of Chinese Medicine*, Liberation Army Press, Beijing, China, 2003.

[33] Z. G. Wang, X. Y. Lü, J. Y. Gao et al., "Study on signal transmission characteristics of meridian based on electrical network theory and experiments," *Zhongguo Zhen Jiu*, vol. 31, no. 8, pp. 705–710, 2011 (Chinese).

[34] Z. W. Meng, Z. X. Zhu, and X. L. Hu, "Progress in the research of meridian phenomena in China during the last five years," *Journal of Traditional Chinese Medicine*, vol. 5, no. 2, pp. 145–152, 1985 (Chinese).

[35] L. Chen, L. Jin, and H. Chen, "Advances and trends in the researches on meridians," *Journal of Biomedical Engineering*, vol. 25, no. 6, pp. 1470–1478, 2008 (Chinese).

Hindawi Publishing Corporation
Evidence-Based Complementary and Alternative Medicine
Volume 2013, Article ID 280418, 7 pages
http://dx.doi.org/10.1155/2013/280418

Research Article

Primo Vascular System in the Subarachnoid Space of a Mouse Brain

Sang-Ho Moon,[1,2,3] Richard Cha,[1,4] Geo-Lyong Lee,[3] Jae-Kwan Lim,[1,5] and Kwang-Sup Soh[1]

[1] *Nano Primo Research Center, Advanced Institute of Convergence Technology, Seoul National University, Suwon 443-270, Republic of Korea*
[2] *Department of Research & Development, Peace World Medical Co., Ltd., Seoul 110-775, Republic of Korea*
[3] *Nadi Primo Research Institute, Graduate School of Integrative Medicine, Sun Moon University, Asan-si 336-708, Republic of Korea*
[4] *College of Physical Education, The University of Suwon, Hwaseong-si, Gyeonggi-do 445-743, Republic of Korea*
[5] *Korea Institute of Oriental Medicine, Daejeon 305-811, Republic of Korea*

Correspondence should be addressed to Geo-Lyong Lee; leeashram@hanmail.net

Received 28 December 2012; Accepted 8 May 2013

Academic Editor: Walter J. Akers

Objective. Recently, a novel circulatory system, the primo vascular system (PVS), was found in the brain ventricles and in the central canal of the spinal cord of a rat. The aim of the current work is to detect the PVS along the transverse sinuses between the cerebrum and the cerebellum of a mouse brain. *Materials and Methods*. The PVS in the subarachnoid space was analyzed after staining with 4′,6-diamidino-2-phenylindole (DAPI) and phalloidin in order to identify the PVS. With confocal microscopy and polarization microscopy, the primo vessel underneath the sagittal sinus was examined. The primo nodes under the transversal sinuses were observed after peeling off the dura and pia maters of the brain. *Results*. The primo vessel underneath the superior sagittal sinus was observed and showed linear optical polarization, similarly to the rabbit and the rat cases. The primo nodes were observed under the left and the right transverse sinuses at distances of 3,763 μm and 5,967 μm. The average size was 155 μm × 248 μm. *Conclusion*. The observation of primo vessels was consistent with previous observations in rabbits and rats, and primo nodes under the transverse sinuses were observed for the first time in this work.

1. Introduction

The primo vascular system (PVS) was proposed by Kim as a third circulatory system that corresponded to and extended the acupuncture meridians [1]. In various parts of an animal's body, the PVS was confirmed [2], especially in blood vessels [3], the heart [4], lymph vessels [5, 6], and on the surfaces of internal organs [7] of mice, rats, and rabbits.

The PVS in the central nervous system was first observed in the 4th ventricle of the brain and the central canal of the spinal cord of a rabbit by using a staining dye, chrome hematoxylin [8], and subsequently in the 3rd ventricle of a rat brain by using Trypan blue dye [9]. Fluorescent nanoparticles were injected into the lateral ventricle of a rat to detect the PV in the fourth ventricle and the spinal cord of a rat [10]. The PVS in the subarachnoid space of a rat spine [11] and in the sciatic nerve of a rat [12] has also been reported. The function of the PVS with respect to nerve regeneration and acupuncture is not yet studied [13, 14].

Recently, the PVS was observed on the pia mater of a rat brain by using Alcian blue [15]. Primo vessels (PVs) and primo nodes (PNs) were found underneath the superior sagittal sinus (SSS) in the sagittal fissure of a rabbit [16]. The PV underneath the SSS was also found in a rat, and it showed a strong linear optical polarization.

Thus, an investigation as to whether the PV in the falx cerebri underneath the SSS also exists in mice and exhibits a similar polarization effect is needed. Another pending effort is to find PNs in a mouse brain. The present work reports observations of a PV underneath the SSS and its optical polarization and observations of PNs on the transverse sinuses instead of the SSS.

2. Materials and Methods

2.1. Animal Preparation. Eleven adult ICR mice (female, 10 weeks old, 33 g) were purchased from Dooyeol Biotech Co., Ltd., (Seoul, Korea). Animals were housed in the laboratory animal facility at 25°C and 60% relative humidity under a 12-hour light/dark cycle. Procedures involving the animals and their care were in full compliance with current international laws and policies (Guide for the Care and Use of Laboratory Animals, National Academy Press, 1996). All surgical procedures were performed under general anesthesia (25-mg/kg Zoletil and 10-mg/kg Rompun administered by intramuscular injection).

2.2. Brain Specimen Preparation. After the mouse had been sacrificed by overanesthetizing, the mouse was decapitated, and the head was fixed by putting it in paraformaldehyde (PFA, Sigma-Aldrich, USA) for one week in the refrigerator (2°C). The head was opened one hour before the experiment and was washed with running tap water. After the skull had been separated from the brain by using tweezers, we carefully kept the dura mater and the pia mater of the brain intact. Before peeling the dura mater off the brain, as a preparation for detection of primo nodes and primo vessels with the features of nuclei distribution, we sprayed 4′,6-diamidino-2-phenylindole (DAPI) solution on the surface of the dura mater and the pia mater of the brain. Because the dura mater had a high density of nuclei, discerning the features of the nuclei distribution in the PVS that was covered by the dura mater was difficult. Therefore, we developed techniques to peel the dura mater off the brain meninges. In this method, we were able to discern the PNs, PVs on the pia mater of the brain.

2.3. Staining and Observations with Microscopes. We applied DAPI and phalloidin reagents for staining of nuclei and f-actin molecules in the cells, respectively. After a one-hour DAPI (Invitrogen, ProLong Gold Antifade Reagent with DAPI, USA) staining, we washed the sample with phosphate based saline (PBS) three times. After that, the phalloidin (Invitrogen, Rhodamine Phalloidin, USA) staining was done for one hour, and the PBS washing was done three times.

After the samples had been washed, we dried them and poured on Neomount (M1289-10 mL, Sigma-Aldrich, USA) solution on the brain with care not to make bubbles and noise so that the Neomount would not become too thick for analysis of the primo vessels with a high-magnification microscope. We gently placed the cover glass on the sample; the cover should be maintained level for high-magnification observation.

The stained specimens were investigated with a phase-contrast microscope (BX51, Olympus, Japan) and polarization microscope (KSM-BA3, Samwon, Korea) to search for loose connective tissues, such as blood capillaries, nerve tissues, and bundles of PVs and PNs. A fluorescent microscope (MVX10, Olympus, Japan) was used to investigate the characteristic features of the nuclei and the F-actin distributions of the PVs and the PNs with DAPI and phalloidin staining, respectively. Confocal laser scanning microscopy (C1 plus, Nikon, Japan) was used to optically scan the threadlike PVs to uncover the characteristic bundle structure of the PVs.

3. Results

A schematic illustration and a real specimen of the mouse brain are shown in Figures 1(a) and 1(b), respectively. The falx cerebri houses the superior sagittal sinus. The PV was located in the falx cerebri and could be detected because of its strong polarization signal, as shown in Figures 1(c) and 1(d). We confirmed the representative features of a PV by staining the sample with DAPI and phalloidin to reveal the nuclei and the f-actin distributions. The results are presented in Figures 2(a), 2(b), and 2(c). The confocal laser scanning microscope image shows the presence of rod-shaped nuclei and multiple bundle of channels, as shown with the asterisk ⊛ in the lower panel of Figure 2(c).

We observed PNs at two locations in the subarachnoid space between the pia mater and the arachnoid mater of a mouse brain: the first location, named as the H-point, is under the transverse sinus at the boundary between the hemisphere and the vermis of the cerebellum. The second location, named as the P-point, is further outside along the transverse sinus near the end of the hemisphere of the cerebellum. The average distances from the H-point and the P-point to the λ (lambda) point were 3,763 μm and 5,967 μm (Figure 1(a)).

As shown in Table 1, we did experiments with eleven mice and found six PNs at the left H-point, six at the right H-point, three at the left P-point, and three at the right P-point. The average distances from the λ point and the average size were as follows:

3,925 μm (distance); 125 μm (short axis) × 230 μm (long axis), the left H-point,

3,600 μm; 120 μm (short axis) × 205 μm (long axis), the right H-point,

5,533 μm; 177 μm (short axis) × 350 μm (long axis), the left P-point, and

6,400 μm; 197 μm (short axis) × 207 μm (long axis) the right H-point.

Remarkably PNs of fairly distinguishable shapes (Figures 3, 4, and 5) were repeatedly observed at the H-points and the P-points along the transverse sinuses.

A detailed description of a PN at the H-point is shown in Figure 3. The location in the dura mater was determined under a stereomicroscope (Figure 3(a)), and the PN specimen was observed with a phase-contrast microscope equipped for fluorescence. The observation after DAPI and phalloidin staining revealed cells and nuclei packed in the PN, as expected (Figures 3(b), 3(c), 3(d), 3(e)). A more realistic view was obtained with a confocal laser scanning microscope as presented in Figure 3(f). The PV attached to the PN showed rod-shaped nuclei aligned along the PV (Figure 3(g)).

Another case of a PN at the H-point is presented to show that its apparent shape is different from the previous shape (Figures 4(b), 4(c), and 4(d)). In this example, we exposed

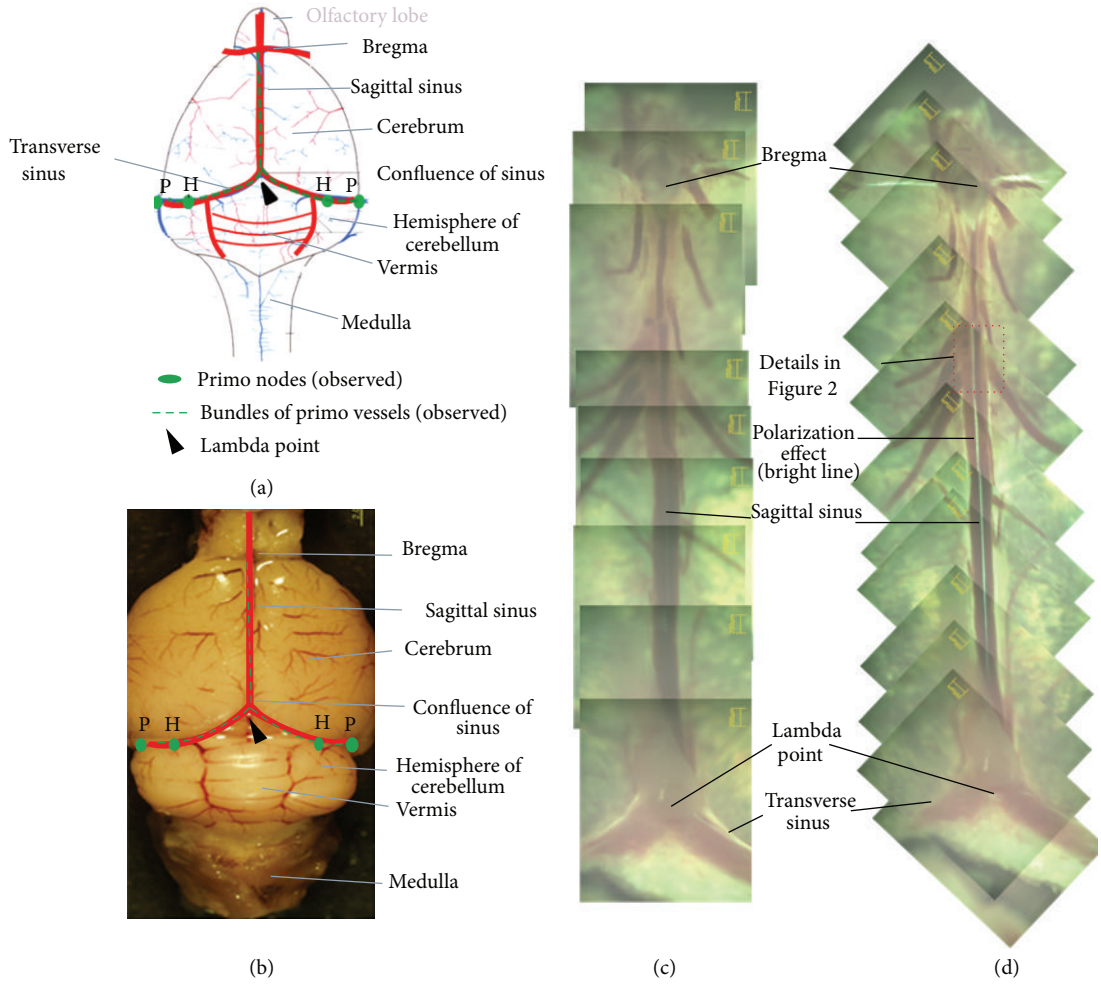

FIGURE 1: (a) Schematic illustration of the cranial view of a mouse brain. The sagittal sinus branches to two transverse sinuses at the confluence of sinuses where the λ point (arrow head) lies. The primo vessels ran along the sagittal sinus and branches and then along the two transverse sinuses (dotted line). The primo nodes were observed at the points designated as H and P on two sides of the brain. H is at the point where the hemisphere of the cerebellum and the vermis meet along the transverse sinus. P is further outside, along the transverse sinus near the end of the hemisphere of the cerebellum. The distances from the λ point to the H-point and the P-point were 3,763 μm and 5,967 μm, respectively. (b) Stereo microscopic image of the cranial view of a mouse brain. The symbols are the same as in (a). (c) Polarization microscope image of brain meninges complex of the dura and the pia mater peeled off from the brain and put on a slide with the pia mater side down. (d) Polarization microscope image of the same specimen rotated 45 degrees relative to (c). There appeared a strong polarization signal along the midline of the sagittal sinus. The polarization image was in agreement with those in the rabbit and the rat brains. The image shows a primo vessel in the falx cerebri under the dura mater of the superior sagittal sinus.

the PN and its attached PV by removing the surrounding dura and pia maters (Figures 4(e) and 4(f)). The DAPI signals showed packed nuclei in the PN and rod-shaped nuclei in the PV.

A PN at the P-point was observed, as indicated with the dotted circle in Figure 5(a). Its shape was oval, and its size was 230 μm × 460 μm. Its phase-contrast, DAPI-stained, MVX-10, and phalloidin-stained images (Figures 5(d), 5(e), 5(f), and 5(g), resp.) were similar to those for the PNs at the H-points. A PN at the H-point is indicated with a circle in Figure 5(a). Figures 5(b) and 5(c) demonstrate a strong polarization signal along the PV attached to the PN.

4. Discussion

The PV in the falx cerebri embedded in the dura mater under the sagittal sinus was first observed in a rabbit brain [15] and subsequently in a rat brain. The current work confirmed the presence of a similar PV in a mouse brain. The thicknesses of the PVs were 55.7 μm, 56.7 μm, and 31 μm in the cases of rabbits, rats, and mice, respectively. The distributions of rod-shaped nuclei and the bundle structures of the multiple channels were similar.

The linear polarization of the PV that was previously observed in a rat brain was also clearly visible in the mouse

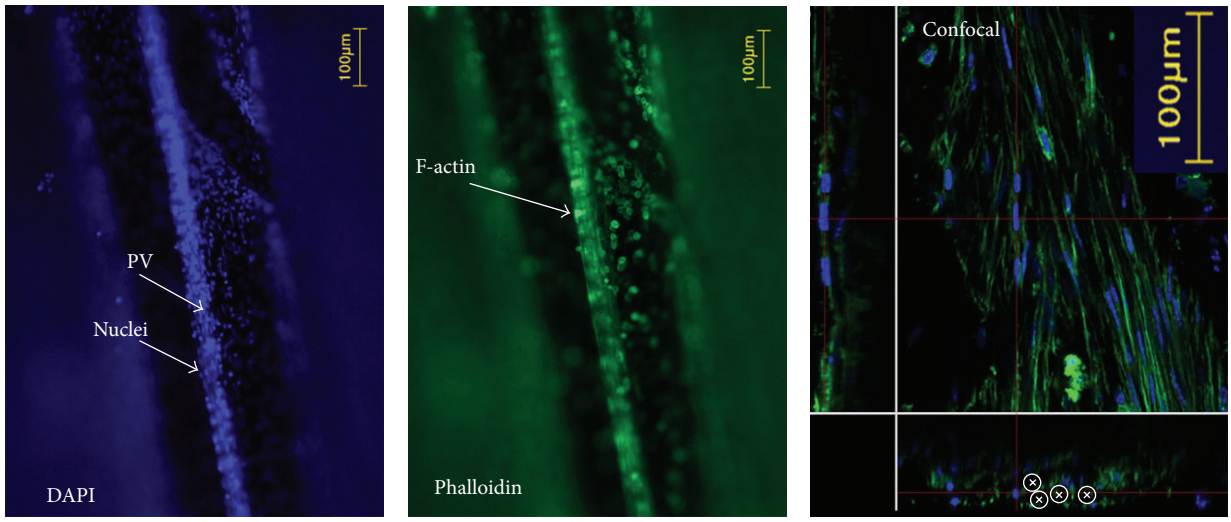

(a) (b) (c)

Figure 2: (a) Nuclei distribution in the primo vessel in the falx cerebri stained with DAPI. The dark neighboring background is the sagittal sinus. The specimen is the dotted box area of Figure 1(d). (b) F-actin distribution in the same specimen stained with phalloidin. (c) Confocal laser scanning microscope image of the same specimen. The left column shows a longitudinal section, which reveals rod-shaped nuclei. The bottom panel shows a transversal section of the primo vessel, which reveals multiple channels ⊗. These two features are in agreement with data obtained from rabbit and rat brains.

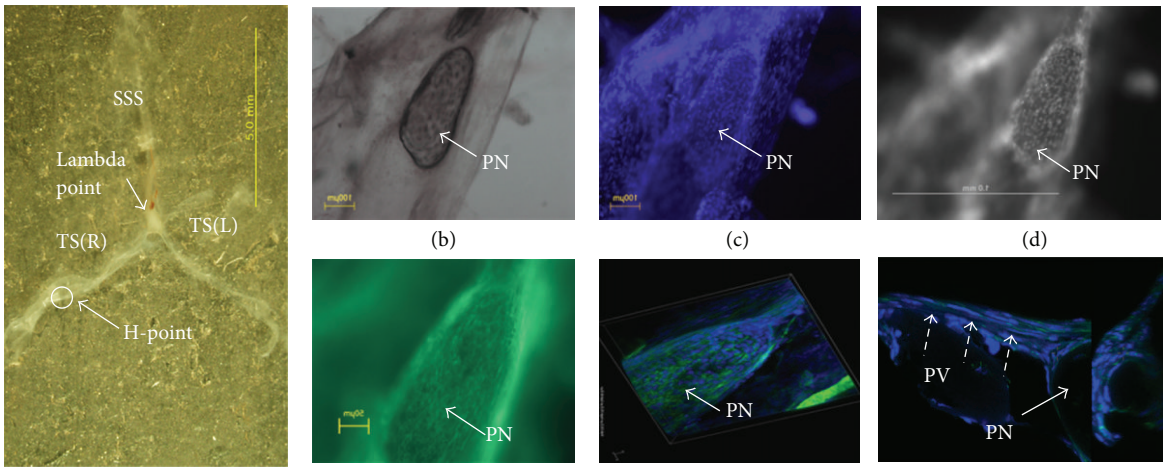

(a) (b) (c) (d) (e) (f) (g)

Figure 3: (a) Stereomicroscopic image of the dura mater taken from the mouse brain. The PN is indicated with a circle that is 3,900 μm from the λ point (arrow). The specimen is sample no. 10 in Table 1. PV: primo vessel, PN: primo node, SSS: superior sagittal sinus, and TS (R, L): transverse sinus right, left, respectively. (b) Phase-contrast microscopic image of the PN. It has an eggplant shape, and its size is 180 μm × 420 μm. (c) Fluorescent image of the nuclei distribution of the same PN after DAPI staining. The DAPI staining was not clearly seen with the phase-contrast microscope because the PN was too thick. (d) The fluorescence microscope with tissues MVX-10 showed a better image of the DAPI staining. (e) The f-actins of cells in the same PN are shown with phalloidin staining. (f) A 3D image of the PN stained with DAPI and phalloidin taken with a confocal laser scanning microscope. (g) The primo vessel (PV) attached to the PN is shown. Primo vessel (dotted arrow).

case. This optical property was useful in detecting the PNs along the transverse sinus, as shown in Figure 5.

The presence of a PN in the brain was noticed in the case of a rabbit at the confluence of the transverse sinuses, that is, near the λ point [15]. However, no PN was detected at a similar location in mice. In our experiment, PNs were observed at completely different positions, the left and the right H-points and the left and the right P-points along the transverse sinuses. The sizes of the PNs were 286 μm × 503 μm and 155 μm × 248 μm in rabbits and mice, respectively. The PNs of both animals were packed with many cells inside.

PNs packed with various cells were a common feature. Especially, immune cells were abundant in the PNs on the

Table 1: Primo nodes in the mouse brain observed in this experiment.

Subject		Locations and Primo nodes		Sizes
No.	Weight (g)	Location	Distance from λ point (μm)	Short (μm) × long (μm)
1	32	Left H-point	3,600	120 × 190
2	34	Left H-point	4,000	170 × 300
		Right H-point	3,500	200 × 270
3	35	Right H-point	3,500	50 × 80
4	32	Left H-point	3,700	30 × 110
		Right H-point	3,300	50 × 80
5	31	Right P-point	7,800	250 × 400
6	32	Left H-point	3,750	130 × 220
7	35	Left H-point	3,700	100 × 160
		Left P-point	5,500	80 × 190
8	32	Right H-point	3,800	120 × 180
		Right P-point	5,900	190 × 230
9	34	Right H-point	3,600	120 × 200
		Left P-point	5,400	230 × 460
10	31	Right H-point	3,900	180 × 420
		Left P-point	5,700	220 × 400
		Right P-point	5,500	150 × 180
11	31	Left H-point	4,800	200 × 400
Average	33	Left H-point	3,925	125 × 230
		Right H-point	3,600	120 × 205
		Left P-point	5,533	177 × 350
		Right P-point	6,400	197 × 207

The subjects were 10-week-old female ICR mice. The primo nodes had cucumber or oval shapes; short and long axes were measured.

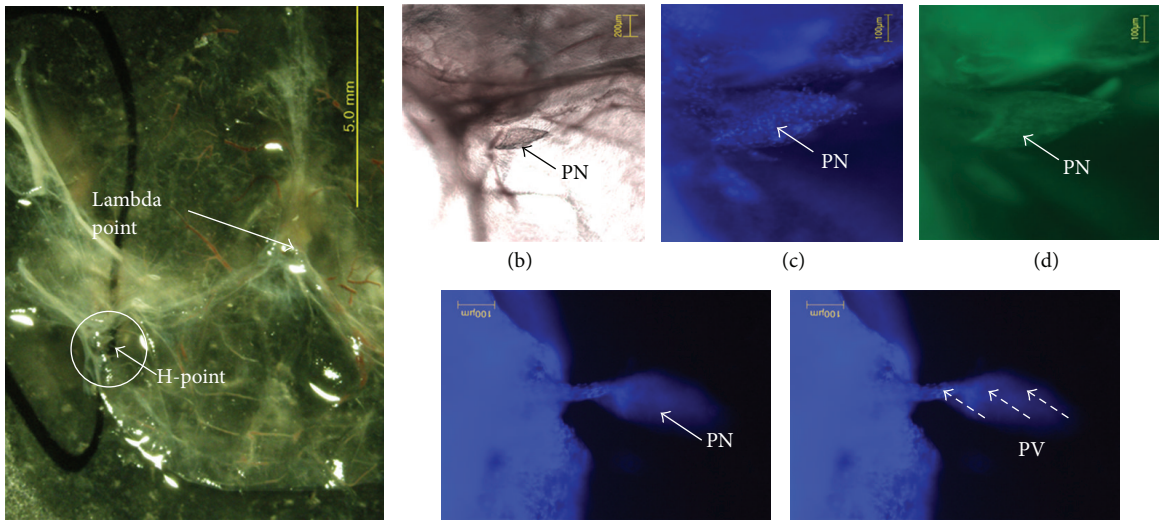

Figure 4: (a) Another specimen of the PN located in the circle shown in the stereomicroscopic image of the dura mater and the pia mater of a mouse brain (sample no. 11 in Table 1). It was located 4,800 μm from the λ point. (b) Phase-contrast microscope images of the PN. It had a fusiform shape, and its size was 200 μm × 400 μm. (c) and (d) Fluorescence images of the PN with DAPI and phalloidin staining, respectively. (e) and (f) Fluorescence images of the PV attached to the PN with DAPI and phalloidin staining, respectively. The pia mater that covered the PV was removed to reveal the PV. Rod-shaped nuclei and f-actin distributions were noticed.

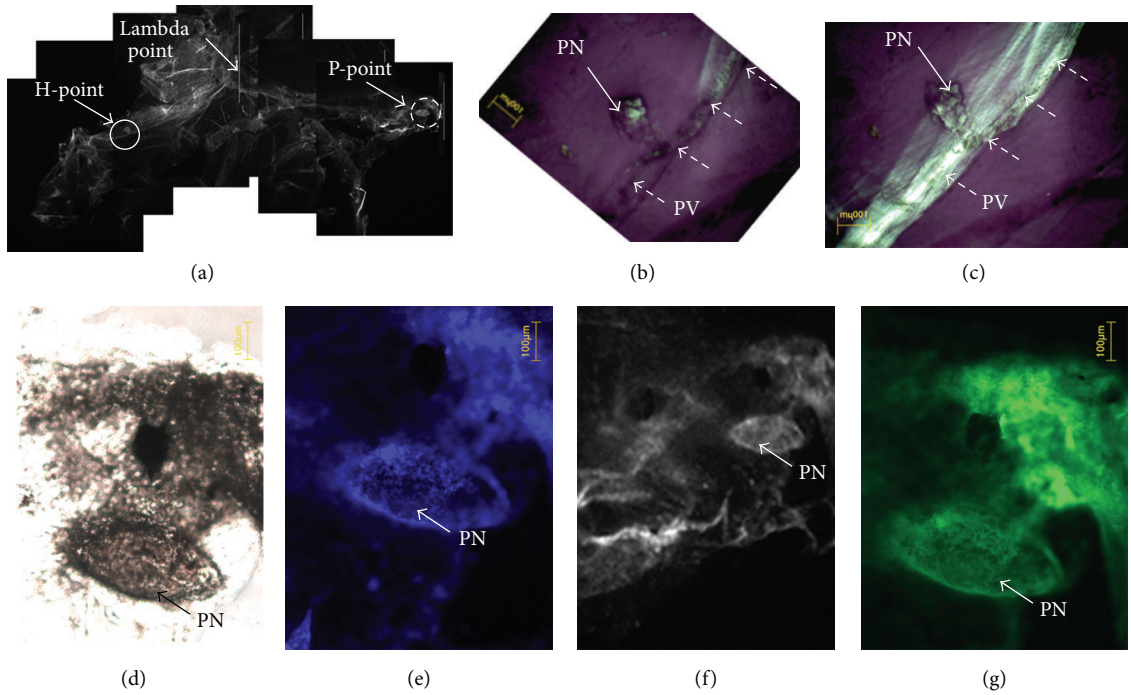

Figure 5: (a) Stereo microscopic image of a dura mater with two PNs indicated with solid and dotted circles, which were 3,600 μm and 5,400 μm from the λ point (arrow), respectively. (b) Polarization microscopic images at a 45-degree rotation. The image in (c) has bright polarization signals along the transverse sinus, as seen in Figure 1(d). (d)–(g) Phase-contrast, DAPI-stained, MVX-10, and phalloidin-stained PN images, respectively, of the PN in the dotted circle. Its shape was oval and its size was 230 μm × 460 μm.

surfaces of internal organs [17] and inside lymph vessels [18]. Immunohistochemical data also suggested the presence of embryonic-like stem cells in the PNs on the surfaces of internal organs and inside the lymph vessels [18]. Furthermore, observations of cancer stem cells in the PNs of xenografted cancer mice were recently reported [19].

In the current work, we were not able to isolate and analyze the cells from the brain PNs. It remains an important question whether the PNs in brain contain abundant immune cells and/or stem cells as observed in the PNs on the surfaces of internal organs. There are also critical works against the acupuncture relevance of the PVS [20]. These medically critical features are worthy of more future work.

Authors' Contribution

Sang-Ho Moon and Richard Cha contributed equally to this work.

Conflict of Interests

The authors listed above declare no conflict of interests.

Acknowledgments

This work was supported in part by a Grant from Korea Institute of Oriental Medicine (K13290) and National Research Foundation (Career Scientist Program 2013). The authors thank the animal care service of the WOOJUNG BSC, Inc.

References

[1] B. H. Kim, "The Kyungrak system," *Journal of Jo Sun Medicine*, vol. 108, pp. 1–38, 1965.

[2] M. Avijgan, "Can the primo vascular system (Bong Han Duct System) be a basic concept for qi production?" *International Journal of Integrative Medicine*, vol. 1, no. 20, pp. 1–10, 2013.

[3] H. M. Johng, *Observation method for threadlike structures inside blood and lymph vessels and on organ surfaces. Study on extracurriculum teaching model of biophysics [Ph.D. thesis]*, Seoul National University, Seoul, Korea, 2005.

[4] B. C. Lee, H. B. Kim, B. Sung et al., "Network of endocardial vessels," *Cardiology*, vol. 118, no. 1, pp. 1–7, 2011.

[5] Y. I. Noh, M. Rho, Y. M. Yoo, S. Jung, and S. S. Lee, "Isolation and morphological features of primo vessels in rabbit lymph vessel," *Journal of Acupuncture and Meridian Studies*, vol. 5, no. 5, pp. 201–205, 2012.

[6] I. Choi, H. K. Chung, and Y. K. Hong, "Detection of the primo vessels in the rodent thoracic lymphatic ducts," in *The Primo Vascular System: Its Role in Cancer and Regeneration*, K. S. Soh, K. A. Kang, and D. Harrison, Eds., pp. 121–126, Springer, New York, NY, USA, 2011.

[7] K. J. Lee, S. Kim, T. E. Jung, D. Jin, D. H. Kim, and H. W. Kim, "Unique duct system and the corpuscle-like structures found on the surface of the liver," *Journal of International Society of Life Information Science*, vol. 22, pp. 460–462, 2004.

[8] B. C. Lee, S. Kim, and K. S. Soh, "Novel anatomic structures in the brain and spinal cord of rabbit that may belong to the Bonghan system of potential acupuncture meridians," *Journal of Acupuncture and Meridian Studies*, vol. 1, no. 1, pp. 29–35, 2008.

[9] J. X. Dai, B. C. Lee, P. An et al., "*In situ* staining of the primo vascular system in the ventricles and subarachnoid space of the brain by trypan blue injection into the lateral ventricle," *Neural Regenerational Research*, vol. 6, pp. 2171–2175, 2011.

[10] J. K. Lim, *Visualization of primo vascular system in brain and spinal cord with fluorescent nanoparticles [Ph.D. thesis]*, Seoul National University, Seoul, Korea, 2011.

[11] I. H. Lee, Z. Su, K. W. Kim, B. C. Lee, and K. S. Soh, "Visualization of the primo vascular system by using trypan blue in the subarachnoid space of rats," in *The Primo Vascular System: Its Role in Cancer and Regeneration*, K. S. Soh, K. A. Kang, and D. Harrison, Eds., pp. 133–138, Springer, New York, NY, USA, 2011.

[12] Z. F. Jia, B. C. Lee, K. H. Eom et al., "Fluorescent nanoparticles for observing primo vascular system along sciatic nerve," *Journal of Acupuncture and Meridian Studies*, vol. 3, no. 3, pp. 150–155, 2010.

[13] I. A. Chang and U. Namgung, "Induction of regenerative responses of injured sciatic nerve by pharmacopuncture therapy in rats," *Journal of Acupuncture and Meridian Studies*, vol. 6, no. 2, pp. 89–97, 2013.

[14] E. S. Park, H. Y. Kim, and D. H. Youn, "The primo vascular structures alongside nervous system: its discovery and functional limitation," *Evidence-Based Complementary and Alternative Medicine*, vol. 2013, Article ID 538350, 5 pages, 2013.

[15] H. S. Lee and B. C. Lee, "Visualization of the network of primo vessels and primo nodes above the pia mater of the brain and spine of rats by using alcian blue," *Journal of Acupuncture and Meridian Studies*, vol. 5, no. 5, pp. 218–225, 2012.

[16] M. H. Nam, *Investigation of the primo vascular system underneath the superior sagittal sinus in the brain [M.S. thesis]*, Kyung Hee University, Seoul, Korea, 2013.

[17] B. C. Lee, J. S. Yoo, V. Ogay et al., "Electron microscopic study of novel threadlike structures on the surfaces of mammalian organs," *Microscopy Research and Technique*, vol. 70, no. 1, pp. 34–43, 2007.

[18] B. S. Kwon, M. H. Chang, S. S. Yu, B. C. Lee, J. Y. Ro, and S. Hwang, "Microscopic nodes and ducts inside lymphatics and on the surfaces of internal organs are rich in granulocytes and secretory granules," *Cytokine*, vol. 60, no. 2, pp. 587–592, 2012.

[19] A. Islam, S. Thomas, K. Sedoris, and D. Miller, "Tumor-associated primo vascular system is derived from xenograft, not host," *Experimental and Molecular Pathology*, vol. 94, no. 1, pp. 84–90, 2012.

[20] X. Y. Wang, H. Shi, H. Y. Shang et al., "Are primo vessels(PVs) on the surface of gastrointestine involved in regulation of gastric motility induced by stimulation acupoints ST36 or CV 12?" *Evidence-Based Complementary and Alternative Medicine*, vol. 2012, Article ID 787683, 8 pages, 2012.

Hindawi Publishing Corporation
Evidence-Based Complementary and Alternative Medicine
Volume 2013, Article ID 195631, 6 pages
http://dx.doi.org/10.1155/2013/195631

Research Article

Composition of the Extracellular Matrix of Lymphatic Novel Threadlike Structures: Is It Keratin?

Hyub Huh,[1] Byung-Cheon Lee,[2] Sang-Hyun Park,[2] Ji Woong Yoon,[3] Soo Jae Lee,[4] Eun Jung Cho,[1] and Seung Zhoo Yoon[1]

[1] *Department of Anesthesiology and Pain Medicine, College of Medicine, Korea University, Seoul 136-705, Republic of Korea*
[2] *Ki Primo Research Laboratory, Division of Electrical Engineering, KAIST Institute for Information Technology Convergence, Korea Advanced Institute of Science and Technology (KAIST), Daejeon 305-701, Republic of Korea*
[3] *Impedance Imaging Research Center & Department of Public Administration, Kyung Hee University, Seoul 130-701, Republic of Korea*
[4] *Nanotechnology Research Center, Konkuk University, Chungju 380-701, Republic of Korea*

Correspondence should be addressed to Seung Zhoo Yoon; yoonsz70@gmail.com

Received 12 February 2013; Accepted 2 May 2013

Academic Editor: Yeonhee Ryu

Background. The lumen of novel threadlike structures (NTSs) is enclosed by a single layer of endothelial cells surrounded by extracellular matrix (ECM). We hypothesized that collagen may be a component of the ECM associated with lymphatic NTSs. *Methods*. Six female New Zealand white rabbits were anesthetized, and the NTS structures within lymphatic vessels were identified by contrast-enhanced stereomicroscopy or alcian blue staining. Isolated NTS specimens were stained with acridine orange, YOYO-1, and 1,1′-dioctadecyl-3,3,3′,3′-tetramethylindocarbocyanine perchlorate (DiI). The structural and molecular composition of the ECM was investigated using transmission electron microscopy (TEM), electrospray ionization-mass spectrometry, and proteomic analysis. *Results*. The lymph vessel wall was stained red by DiI, and rod-shaped nuclei were stained green by YOYO-1. The area surrounding the NTS was also stained red and contained green rod-shaped nuclei. TEM images showed that the NTS consisted of many ECM fibers and the ECM fibers appeared to be ~100 nm in diameter and had narrowly spaced striated bands. Proteomic analysis of the lymphatic NTS-associated ECM identified 4 proteins: keratin 10, cytokeratin 3, cytokeratin 12, and soluble adenylyl cyclase. *Conclusion*. The TEM study suggested that the lymphatic NTS-associated ECM did not contain collagen. This was confirmed by proteomic analysis, which showed that keratin was the major component of the ECM.

1. Introduction

In 2003, Jiang et al. [1] established the existence of intravascular novel threadlike structures (NTSs). Their study was inspired by the Bong-Han theory, which was first introduced by Kim in 1963 [2]. Jiang et al. reinvestigated the Bong-Han theory using modern techniques, and consequently, NTSs were discovered in various organs, including rabbit blood vessels [1], rat lymphatic vessels [3], bovine heart [4], rabbit central nervous system [5], and on the surface of rat abdominal organs (liver, stomach, and hollow viscus) [6, 7]. NTSs have also been called Bonghan ducts or primo vessels by Jiang et al.

Histologically, the structure of the NTS appeared to be a simple bundle of several ductules with characteristic rod-shaped nuclei (10–20 μm long), which were clearly visible by phase contrast microscopy. In cross section, the NTS presents as a tissue containing several small lumens, 6–10 μm in diameter. The ductule lumen is lined by a single layer of endothelial cells surrounded by extracellular matrix (ECM) [8]. However, there have been few studies of the fibrous elements that make up the NTS-associated ECM.

A previous study, using fluorescent magnetic nanoparticles and in vivo imaging techniques, identified NTSs inside lymphatic vessels [9]. The ECM was shown to consist of loosely packed and randomly distributed collagen fibrils. In a recent report, Jung et al. [10] examined the ECM composition of NTSs at the serosal surface of the large intestine and the liver capsule in rabbits and concluded that the ECM is probably collagen. NTSs associated with the endocardial

surface of cattle and the serosal and adventitial surfaces of the rat colon were also reported to contain collagen. In that study, however, the authors did not examine the composition of the ECM in lymphatic NTSs. However, conflicting results were reported by Lee et al. [11]. They examined cross sections of an NTS stained with Masson's trichrome, which is widely used to detect collagen fibers in tissue specimens. Although strong staining was observed in mural cells and the matrix surrounding the lymphatic vessel, the NTS was not stained, suggesting that the lymphatic vessel, but not the NTS, contained collagen.

In this study, we sought to determine if the ECM of lymphatic NTSs is composed of collagen. We identified NTS structures in rabbits by stereomicroscopy using a contrast-enhancing optical method or alcian blue staining. Isolated NTS specimens were stained with acridine orange, YOYO-1, or 1,1′-dioctadecyl-3,3,3′,3′-tetramethylindocarbocyanine perchlorate (DiI) to identify the nuclei, membranes, and ECM. The composition of the ECM was further investigated using TEM, electrospray ionization-mass spectrometry (ESI-MS), and proteomic analysis.

2. Materials and Methods

2.1. Preparation of Rabbit Tissues. Six female New Zealand white rabbits (~1.8 kg) were housed under conditions of constant temperature and humidity (23°C, 60% relative humidity), with a 12 h light-dark cycle. The rabbits were fasted for 12 h before surgery and then anesthetized by an intraperitoneal injection 1.5 g/kg of urethane or Zoletil. The care and handling of animals were in full compliance with institutional regulations and current international laws and policies (Guide for the Care and Use of Laboratory Animals, National Academy Press, 1996).

The adipose tissue surrounding the inferior vena cava was separated and removed. The lymph vessels inside the caudal vena cava were located, and the NTSs were visualized with a contrast-enhanced optical method using a stereomicroscope (SZX12; Olympus, Tokyo, Japan). Alcian blue solution was added when necessary to distinguish the NTS. The NTS specimens were isolated from the lymphatic vessels and fixed in 4% (wt/vol) paraformaldehyde (PFA) or 10% (vol/vol) neutral-buffered formalin (NBF) for up to 2 days. Specimens were stored at 4°C until further analysis.

2.2. Microscopic Identification of Extracellular Matrix. After fixation, the tissues were stained with acridine orange, YOYO-1, or DiI to discriminate between the NTS and lymphatic vessels. The sections were then incubated with antifade reagent (Molecular Probes, Grand Island, NY, USA) and mounted for microscopy. Acridine orange-stained sections were visualized using differential interference contrast microscopy, and sections stained with YOYO-1 and DiI were examined by confocal laser scanning microscopy (LSM 500, Zeiss, Germany).

2.3. Transmission Electron Microscopy (TEM). For examination by TEM, tissues were fixed in 2.5% PFA and 2.5% glutaraldehyde in a neutral 0.1 M phosphate buffer for 1 h. Tissues were postfixed for 1 h in 1% (wt/vol) osmic acid in phosphate-buffered saline (PBS), dehydrated in a graded ethanol series, and embedded in Epon812 (EMS, Fort Washington, PA, USA). Semithin (1 mm) sections were stained with 1% (wt/vol) toluidine blue in 1% borax, observed under a light microscope (Axiophot, Carl Zeiss, Germany) to study the gross morphology, and photographed. Ultrathin sections were cut and mounted on nickel grids and then double stained with uranyl acetate followed by lead citrate. The sections were examined with a JEOL 100 CX-II TEM (Tokyo, Japan).

2.4. LC-MS/MS Analysis of Lymphatic NTS. LC-MS/MS analysis of the lymphatic NTS structures was performed as previously described [12]. The isolated lymphatic NTSs were homogenized and sonicated. Samples of 10 μg of homogenate were resolved by 4–12% gradient Tris-glycine PAGE (Invitrogen, Carlsbad, CA, USA). The gel was then sliced into 10 pieces from the bottom to the top of the gel, and in-gel digestion was performed by incubation of slices with 10 ng/μL sequencing grade modified trypsin (Promega, Madison, WI, USA) in 50 μL of 50 mM NH_4HCO_4 buffer (pH 8.0) at 37°C overnight, as previously described [13]. The tryptic peptides were then loaded onto a fused silica microcapillary C18 column (75 μm × 10 cm). LC separation was conducted under a linear gradient as follows: 0 min, 3% B; 5 min, 3% B; 75 min, 40% B; 80 min, 90% B; 90 min, 90% B; 91 min, 3% B; 110 min, 3% B. The initial solvent was 3% B, and the flow rate was 200 nL/min. Solvent A was 0.1% formic acid in H_2O, and solvent B was 0.1% formic acid in acetonitrile. The separated peptides were subsequently analyzed using a linear ion trap mass spectrometer (LTQ; Thermo Finnigan, San Jose, CA, USA). The electrospray voltage was set at 2.0 kV and the threshold for switching from MS to MS/MS was 250. All spectra were acquired in data-dependent mode and each MS scan was followed by MS/MS scans of the 3 main peaks from each MS scan.

All MS/MS spectra were searched against the rabbit whole protein database using the SEQUEST algorithm. Dynamic modifications were permitted for oxidized methionine (+16 Da) and carboxyamidomethylated cysteine (+57 Da). The SEQUEST criteria for identifying peptides included *Xcorr* values of at least 1.8, 2.3, and 3.5 for the +1, +2, and +3 charged peptides, respectively.

3. Results

Lymphatic vessels containing NTSs were identified by stereomicroscopy using a contrast-enhanced optical method or alcian blue staining. The contrast-enhanced optical method was used for 2 rabbits, and the NTS could be observed moving up and down in rhythm with the breathing pattern (Figure 1(a), movie available in Supplementary Materials). For the remaining 4 rabbits, alcian blue dye was injected into the lymphatic vessels around the caudal vena cava. In Figure 1(b), the blue-colored NTS can be seen within the lymph vessel in 2 segments (Figure 1(b)).

Sections of the lymphatic vessels containing the NTS were stained with acridine orange, YOYO-1, and DiI dyes to

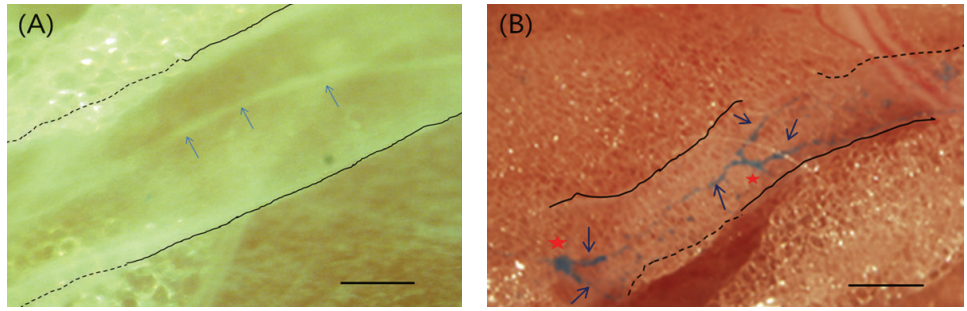

(a) (b)

Figure 1: Stereoscopic images of a novel threadlike structure (NTS) in a rabbit lymphatic vessel: (a) contrast-enhanced optical image, (b) alcian blue-stained image. (a) The outermost wall of the lymphatic vessel is indicated by solid black lines (exposed portion) and dotted lines (embedded in fat). The contrast-enhanced NTS (arrows) is freely movable within the lymphatic vessel of the anesthetized rabbit (see movie in Supplementary Material available online at http://dx.doi.org/10.1155/2013/195631). (b) NTS visualized after injection of alcian blue into the rabbit lymphatic vessel. The NTS (arrows) is floating inside the lymphatic vessel, indicated by black lines as in (a). Note the 2 branch points (red asterisks) within the lymphatic vessel. Scale bars in (a) and (b) are 100 μm and 200 μm, respectively.

visualize the nuclei and membranes. Sections stained with acridine orange were examined by confocal laser scanning microscopy (Figure 2). The specimen was optically sectioned into 4 serial images from the top of the lymph vessel. The images of NTS inside the lymph vessels were gradually clarified toward the bottom. Figure 3 shows a cross section of the specimen stained with YOYO-1 and DiI fluorescent dyes. The lymph vessel wall is stained red by DiI, and the green rod-shaped nuclei (YOYO-1) are visible along the lymph vessel wall (Figure 3(a)). At higher magnification (Figure 3(b)), we observed that the tissue surrounding the NTS is also stained red and contains green rod-shaped nuclei.

To examine the structure of the NTS-associated ECM, we performed TEM imaging on the same specimen. The TEM images show an NTS composed of many ECM fibers and a highly electron-dense structure in the sinus (Figure 4). This structure corresponds to the image shown in Figure 3(b). Under high magnification, the ECM fibers appear to be ~100 nm in diameter and contain narrowly spaced striated bands (Figure 4(c)).

We performed proteomic analysis of a lymphatic NTS homogenate to identify the protein components of the ECM. We identified 4 proteins: keratin 10 (GI number 87045985), cytokeratin 3 (GI number 75059267), cytokeratin 12 (GI number 3183048), and soluble adenylyl cyclase (GI number 126723185). These proteins were identified using high stringency cutoff *Xcorr* values and consensus scores as criteria for the identification of peptides and proteins, respectively. Only proteins with a consensus score greater than 10.1 were selected. The small number of proteins found may have been due to the very small amount of protein (total 1.682 μg) available for analysis.

4. Discussion

We hypothesized that collagen may be one component of the lymphatic NTS ECM. Unexpectedly, our results suggest that this is not the case.

The main difficulty associated with identifying the NTS in vivo and in situ is discriminating between the threadlike structure and fibrin strings. With acridine orange staining, however, fluorescence microscopy can be used to identify nuclei and thus distinguish the NTS from the fibrin strings. The nuclei of the NTS tissue are rod shaped, 10–20 μm long, and are aligned in a broken line. In contrast, the cell nuclei associated with the fibrin strings are globular and randomly scattered; these are actually the nuclei of fibrin-associated white blood cells. This method of positively identifying the NTS is a major breakthrough that allowed us to identify and firmly establish the existence of the NTS inside blood vessels.

The fine network structure of the NTS was not obvious with the alcian blue or acridine orange stains but was clearly revealed by DiI, a highly lipid-soluble cell membrane dye that has been used extensively as a retrograde and anterograde tracing agent in nerve tissue [14]. The tracing property of DiI occurs by a process of lateral diffusion [15]. The DiI labeling of fine networks and terminal arborizations of NTS observed in this study were likely to be due to the mode of action of DiI and not by lateral diffusion in the proximal region of the NTS, because the DiI fluorescence was not continuous and restrained within the sinuses or in the spaces surrounding the sinuses. Given its minimal cytotoxicity and long-term stability restrained to within sinuses or surrounding spaces in animals, DiI appears to be a promising dye for the analysis of the fine morphology and functions of NTSs [16].

The main limitation of DiI is that it cannot stain DNA. The alignment of rod-shaped nuclei along the major axis of the NTS is one of the characteristics that can discriminate the NTS from other similar-looking tissues or artifacts. Therefore, we simultaneously stained the specimens with the DNA-specific dye YOYO-1. As shown in Figure 3, the rod-shaped nuclei are visible along the lymph vessel wall, and rod-shaped nuclei in the NTS were observed at higher magnification (Figure 3(b)). These findings provided confidence that the specimen analyzed by TEM was indeed the ECM of a lymphatic NTS.

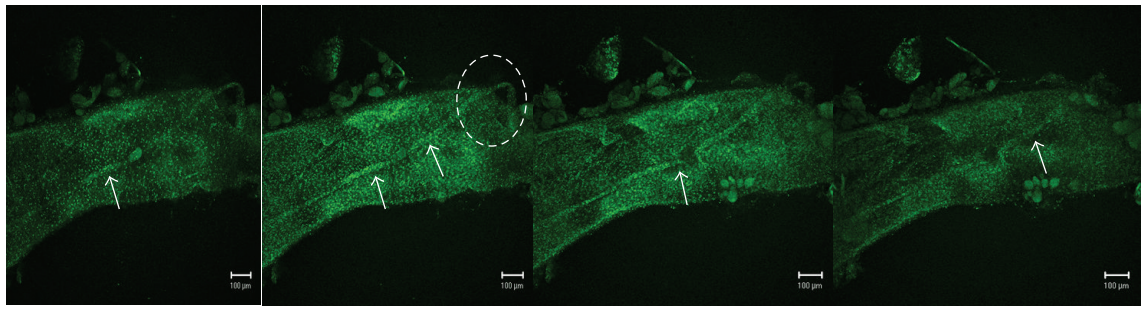

(a) (b) (c) (d)

Figure 2: Confocal laser scanning microscopic images of a novel threadlike structure (NTS). Images show serial optical sections (panels (a–d); 1 μm thick) of an NTS-containing lymphatic vessel stained with acridine orange. The arrows indicate the NTS within the lymphatic vessel. Panel (b) shows the distinct protrusion of the NTS from the lymphatic vessel (dotted oval). Scale bar in all panels is 100 μm.

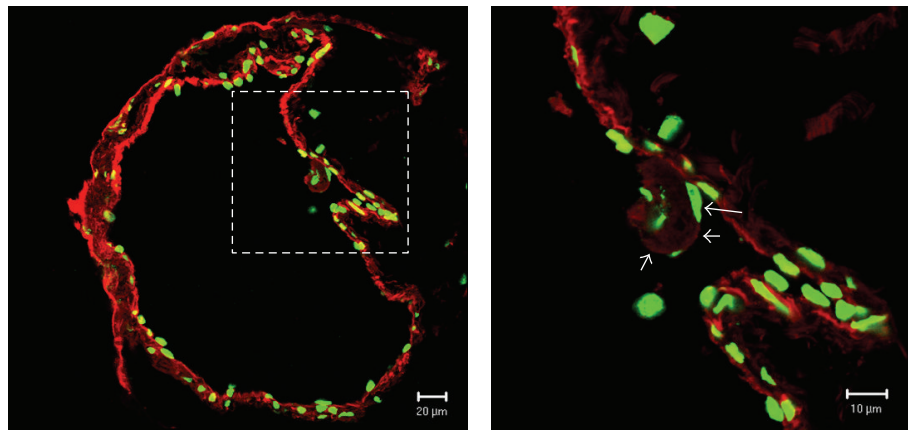

(a) (b)

Figure 3: Confocal laser scanning microscopic images of cross sections of a novel threadlike structure (NTS) within a rabbit lymphatic vessel. (a) The lymphatic vessel wall is stained red (DiI), and the rod-shaped nuclei (YOYO-1; green) are visible along the vessel wall. The dotted square is magnified in (b). (b) The long arrow indicates the nucleus in the outermost membrane, and the 2 short arrows and the asterisk indicate the NTS-associated outermost membrane and nucleus, respectively. Scale bars in (a) and (b) are 20 μm and 10 μm, respectively.

Transmission electron microscopy (TEM) is a technique whereby a beam of electrons is transmitted through an ultrathin specimen, interacting with the specimen as it passes through. TEM is capable of imaging at a significantly higher resolution than light microscopy, owing to the small de Broglie wavelength of electrons. This enables examination of detail as small as a single column of atoms, which is tens of thousands of times smaller than the smallest object resolvable by light microscopy. Images of collagen fibrils obtained by TEM have shown that collagen monomers align parallel to the main axis of the fibril in a staggered manner. In negatively stained TEM images of collagen fibrils, the banding pattern is ascribed to stain penetration and deposition into vacant spaces between monomers, and thus, the periodic dark bands along these fibrils are commonly referred to as "gap" regions or zones. The banding periodicity of alternating dark and light bands of collagen have been shown to be ~67 nm and ~ 70 nm, respectively [17]. However, the ECM fibers shown here (Figure 4(c)) show a pattern of narrowly spaced striations that are distinct from the pattern observed in TEM images of known collagen fibrils.

What, then, is the main component of lymphatic NTS ECM? Our results suggest that it may be keratin. Although we identified only 4 proteins, due to the small amount of protein available, 3 of the proteins were keratins (Krts): Krt10, cytokeratin 3, and cytokeratin 12. Our results are consistent with a recent proteomic study [12] that identified 3 keratins in the NTS tissues: Krt3, Krt10, and Krt12. Keratins are cytoskeletal proteins important for the integrity and stability of epithelial cells and tissues [18]. Krt10, which is the most abundant of the 3 keratins detected in NTS tissue, pairs with Krt1, a type II keratin, to form dense bundles that are features of suprabasal epidermal keratinocytes in humans. These Krt10/Krt1 pairs provide mechanical integrity to the epidermis. Krt10 is normally expressed in postmitotic keratinocytes, where it inhibits keratinocyte proliferation and cell cycle progression and reduces skin tumorigenesis [19]. In addition, Krt10 is a duct-specific marker in normal

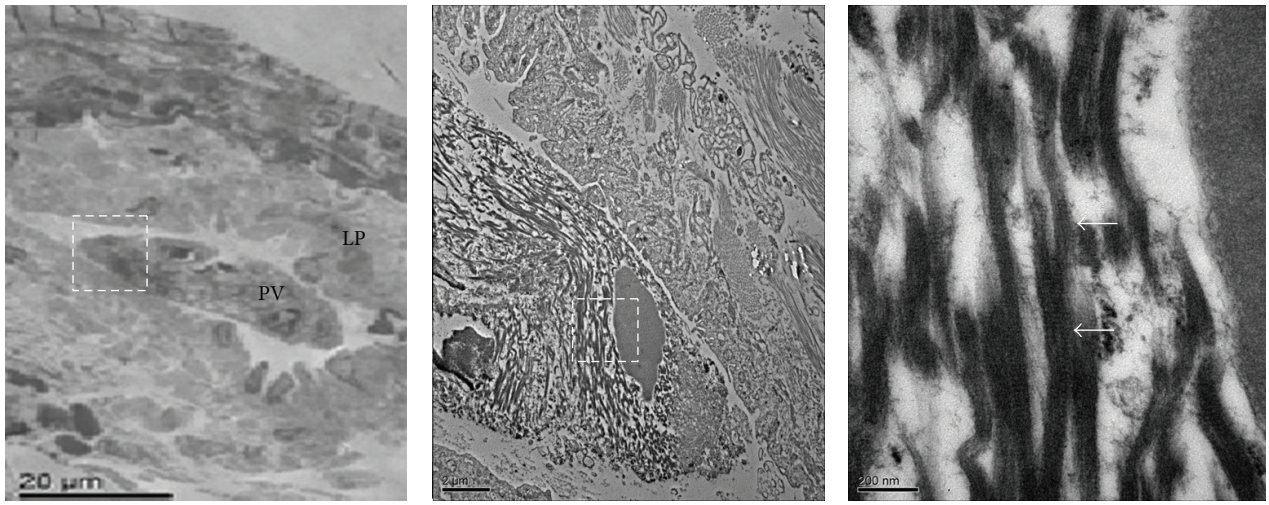

(a) (b) (c)

Figure 4: Transmission electron microscopic image of cross sections of a novel threadlike structure (NTS) within a rabbit lymphatic vessel. (a) A low-magnification image of an NTS contained within the lymphatic vessel. The dotted square is magnified in (b). (b) The NTS consists of many extracellular fibers (asterisks). Note the nucleus-like highly electron-dense structure (arrow) in the sinus. This structure corresponds to the asterisk in Figure 3(b). (c) High-power magnification of the dotted square in (b), which shows distinctive fibers (~100 nm in diameter) with narrowly spaced striations (arrows). Scale bars in (a), (b), and (c) are 20 μm, 2 μm, and 200 nm, respectively.

eccrine sweat glands [20]. In a subsequent study, Kim et al. [21] also demonstrated Krt10 expression in NTS tissues on the surface of abdominal organs in the rat. Krt10 was visualized in patchy spots around single cells or in follicle-like structures containing groups of cells but was not detected on the external membranes of NTS nodes. Krt10 was also identified in blood and lymphatic vessels, but its distribution was diffused.

5. Conclusion

The results of our TEM study suggested that the lymphatic NTS-associated ECM might not contain collagen, as was suggested by previous studies using trichrome staining. Instead, our proteomic analysis suggests that keratin is present. Although the proteomic study was limited by the small amount of protein analyzed (1.682 μg), it is very meaningful to share the same implication with TEM images, however, to further functional research of lymphatic NTS because this is the first try to identify the proteins in lymphatic NTS.

Conflict of Interests

The authors declare no conflict of interests.

Authors' Contribution

H. Huh and B.-C. Lee contributed equally to this work.

Acknowledgments

This work was supported, in part, by the Industrial Strategic Technology Program of the Ministry of Knowledge Economy (10041120) and a National Research Foundation of Korea (NRF) Grant funded by the Korean government's Ministry of Education, Science and Technology (MEST) in 2010 (no. 2010-0025289). The authors give special thanks to Professor K. S. Soh for support and advice during this study. Professor S. Z. Yoon pays homage to Professor K. S. Soh for his great achievements since 2002.

References

[1] X. Jiang, H. K. Kim, H. S. Shin et al., "Method for observation intravascular Bonghan ducts," *Korean Journal of Oriental Preventive Medical*, vol. 6, pp. 162e–166e, 2002.

[2] B. H. Kim, "On the Kyungrak system," *Journal of the Academy of Medical Sciences of the Democratic People's Republic of Korea*, vol. 90, pp. 1–35, 1963.

[3] H. M. Johng, J. S. Yoo, T. J. Yoon et al., "Use of magnetic nanoparticles to visualize threadlike structures inside lymphatic vessels of rats," *Evidence-Based Complementary and Alternative Medicine*, vol. 4, no. 1, pp. 77–82, 2007.

[4] B. C. Lee, H. B. Kim, B. Sung et al., "Network of endocardial vessels," *Cardiology*, vol. 118, pp. 1–7, 2011.

[5] J. Lim, J. H. Jung, S. Lee et al., "Estimating the density of fluorescent nanoparticles in the primo vessels in the fourth ventricle and the spinal cord of a rat," *Journal of Biomedical Optics*, vol. 16, Article ID 116010, 2011.

[6] H. S. Shin, H. M. Johng, B. C. Lee et al., "Feulgen reaction study of novel threadlike structures (Bonghan ducts) on the surfaces of mammalian organs," *Anatomical Record B*, vol. 284, no. 1, pp. 35–40, 2005.

[7] B. C. Lee, J. S. Yoo, V. Ogay et al., "Electron microscopic study of novel threadlike structures on the surfaces of mammalian organs," *Microscopy Research and Technique*, vol. 70, no. 1, pp. 34–43, 2007.

[8] V. Ogay, K. H. Bae, K. W. Kim, and K. S. Soh, "Comparison of the characteristic features of Bonghan ducts, blood and lymphatic capillaries," *Journal of Acupuncture and Meridian Studies*, vol. 2, no. 2, pp. 107–117, 2009.

[9] J. S. Yoo, H. M. Johng, T. J. Yoon et al., "*In vivo* fluorescence imaging of threadlike tissues (Bonghan ducts) inside lymphatic vessels with nanoparticles," *Current Applied Physics*, vol. 7, no. 4, pp. 342–348, 2007.

[10] J. H. Jung, B. Sung, and K. S. Soh, "Fine structure of extracellular fibers in primo-nodes and vessels," *Connective Tissue Research*, vol. 52, pp. 487–495, 2011.

[11] C. Lee, S. K. Seol, B. C. Lee, Y. K. Hong, J. H. Je, and K. S. Soh, "Alcian blue staining method to visualize Bonghan threads inside large caliber lymphatic vessels and X-ray microtomography to reveal their microchannels," *Lymphatic Research and Biology*, vol. 4, no. 4, pp. 181–189, 2006.

[12] J. L. Soo, B. C. Lee, H. N. Chang et al., "Proteomic analysis for tissues and liquid from Bonghan ducts on rabbit intestinal surfaces," *Journal of Acupuncture and Meridian Studies*, vol. 1, no. 2, pp. 97–109, 2008.

[13] S. J. Lee, K. H. Kim, J. S. Park et al., "Comparative analysis of cell surface proteins in chronic and acute leukemia cell lines," *Biochemical and Biophysical Research Communications*, vol. 357, no. 3, pp. 620–626, 2007.

[14] C. Köbbert, R. Apps, I. Bechmann, J. L. Lanciego, J. Mey, and S. Thanos, "Current concepts in neuroanatomical tracing," *Progress in Neurobiology*, vol. 62, no. 4, pp. 327–351, 2000.

[15] M. J. Swift, P. E. Crago, and W. M. Grill, "Applied electric fields accelerate the diffusion rate and increase the diffusion distance of DiI in fixed tissue," *Journal of Neuroscience Methods*, vol. 141, no. 1, pp. 155–163, 2005.

[16] B. C. Lee, S. U. Jhang, J. H. Choi, S. Y. Lee, P. D. Ryu, and K. S. Soh, "DiI staining of fine branches of Bonghan ducts on surface of rat abdominal organs," *Journal of Acupuncture and Meridian Studies*, vol. 2, no. 4, pp. 301–305, 2009.

[17] A. C. Lin and M. C. Goh, "Investigating the ultrastructure of fibrous long spacing collagen by parallel atomic force and transmission electron microscopy," *Proteins*, vol. 49, no. 3, pp. 378–384, 2002.

[18] R. Moll, M. Divo, and L. Langbein, "The human keratins: biology and pathology," *Histochemistry and Cell Biology*, vol. 129, no. 6, pp. 705–733, 2008.

[19] M. Santos, J. M. Paramio, A. Bravo, A. Ramirez, and J. L. Jorcano, "The expression of keratin k10 in the basal layer of the epidermis inhibits cell proliferation and prevents skin tumorigenesis," *The Journal of Biological Chemistry*, vol. 277, pp. 19122–19130, 2002.

[20] M. Ban, K. Yoneda, and Y. Kitajima, "Differentiation of eccrine poroma cells to cytokeratin 1- and 10-expressing cells, the intermediate layer cells of eccrine sweat duct, in the tumor cell nests," *Journal of Cutaneous Pathology*, vol. 24, no. 4, pp. 246–248, 1997.

[21] S. R. Kim, S. K. Lee, S. H. Jang et al., "Expression of keratin 10 in rat organ surface primo-vascular tissues," *JAMS Journal of Acupuncture and Meridian Studies*, vol. 4, no. 2, pp. 102–106, 2011.

Hindawi Publishing Corporation
Evidence-Based Complementary and Alternative Medicine
Volume 2013, Article ID 439508, 9 pages
http://dx.doi.org/10.1155/2013/439508

Review Article

The Meanings and Prospects of Primo Vascular System from the Viewpoint of Historical Context

Jongwook Jeon and Sanghun Lee

Acupuncture, Moxibustion, Meridian Research Group, Korea Institute of Oriental Medicine, 1672 Yuseong-daero, Yuseong-gu, Daejeon 305-811, Republic of Korea

Correspondence should be addressed to Jongwook Jeon; lovejnj@kiom.re.kr and Sanghun Lee; ezhani@kiom.re.kr

Received 8 February 2013; Revised 3 April 2013; Accepted 5 April 2013

Academic Editor: Byung-Cheon Lee

The aim of this overview is to evaluate the primo vascular system research in the context of the history of meridian theory and the modern meanings of it. The 12 meridian systems were naturally presupposed in the conventional study of the meridians and acupuncture. But the excavations of Mawang-tui old documents and Sichuan Mianyang wooden puppet revealed the primordial concepts of meridians uncolored by the numerological cosmology of Han era. Further, the meridian map of horse, cow and hawk show another resemblance to the primordial type of meridians. Modern meridian theory has been challenged by the material based scientific theory and the primo vascular theory presents the most radical answer for it. It aims to reveal the anatomical entity of meridians. However, the study of primo vascular system is unexpectedly opening the new horizon of scientific integration of East and West beyond the mere searching for anatomical entity of meridians. Conclusions we have drawn from the historical reviews are, (1) the surface structure of the body reflects the physiopathological changes of inside the body, (2) by stimulating specific sites on the surface, it is possible to acquire therapeutic effects of certain symptoms, and (3) numbers and locations of meridian acupoints are variable among traditional meridian theories.

1. Introduction

Bonghan Kim, a medical scientist in Democratic People's Republic of Korea, was announced to identify the anatomical entities corresponding to the meridian system of Oriental medicine in 1963 [1]. It was known as the discovery of a third circulatory system and received worldwide attention at the time. Though following experiments from several countries was deployed, the original paper contains no detailed information about the process of the experiment. So the verifying experiments were very difficult to reproduce. After Bonghan Kim's sudden deposition and death, the authorities' strict closure of information was overthrown and it remained forgotten history [2].

Meanwhile, in 2002, Professor Kwangseop Soh in the Republic of Korea, performed reexcavation research to the reality of the meridian systems to revive Bonghan's achievements using advanced experimental apparatus. He newly named primo vascular system for Bonghan's system to express more fundamental system than others. At the end of 10 years' effort to identify the reality of meridian system, he held the first international primo vascular conference with leading scholars of the field. In this paper, we briefly review historical aspect of meridian systems which had been presupposed in the system of Bonghan Kim or Professor Kwangseop Soh. After Bonghan Kim announced that he had discovered the anatomical entities of the meridian system, meaningful historical excavations were performed showing a prototype of the meridian systems quite different from the conventional. And secondly, the stark dichotomy between Oriental medicine and Western medicine is being challenged on multiple layers of readjustment by the contemporary atmosphere of fusion research [3]. Only after considering seriously these two apparent situations, we can open a wider horizon for future researches and make constructive debates for the primo vascular system (or Bonghan system).

2. Mawang-Tui Old Documents and Mianyang Wooden Puppet Unearthed

It is well known that the present twelve line meridian system had been based on Huang Di Nei Jing (The Yellow Emperor's

(a)

(b) (c)

Figure 1: (a) Mawang-tui old documents on medicine. It was described on Yin-Yang eleven meridians for moxibustion and Foot-Arm eleven meridians for moxibustion. (b) Drawings of traditional meridians (part). (c) Meridians carved in stone in Ming dynasy, preserved in royal library in Japan(明正統石刻銅人经脉图, 日本宫内厅藏).

Internal Medicine; 黄帝内经) which was established in Han empire era (B.C. 206~A.D. 220) and made a great influence on the literature of Oriental medicine for 2000 years. But about 200 years earlier than Huang Di Nei Jing, a remarkable excavation of old documents was made in the Mawang-tui [4]. Fourteen kinds of the old documents contained medicinal resource, and 2 kinds of them described old type of meridian system (Figure 1(a)). Unearthed in 1973, the old documents revealed that it was quite different from that of Huang Di Nei Jing (Figure 1(b)) or other later one (Figure 1(c)). Admittedly, these Mawang-tui old documents had been made around B.C. 168 delivering direct information of medicine of the time, such as "Yin-Yang eleven meridians for moxibustion" and "Foot-Arm eleven meridians for moxibustion." Considerable researches have been made in the relevant academia, so a brief conclusion widely recognized would be helpful. Characteristics common to the two kinds of meridians on Mawnag-tui old documents are just like the followings [5, 6].

(1) Meridians are mainly used for the moxibustion and pyaemia emissions (biensi, 砭石) therapy rather than needling acupuncture therapy.

(2) There are only descriptions of meridian line but none about the acupoints.

(3) Number of meridians are not twelve but eleven.

(4) Among the eleven, only 2 or 3 have connections between meridians and viscera.

(5) Meridians are independent each other, not like the unified circulatory system consisting of 12 meridians in Huang Di Nei Jing.

Though there are more detailed differences between them, I want to check these five things first. Distinctions become clear by these five points. Conventional concept of meridians is a certain energy (qi, 氣) route that consisted of acupoints which are certain places under the skin for acupuncture therapy. But in Mawang-tui old documents acupoints (穴) were not present in the meridian pathway, and the meridian itself was not for acupuncture but for moxibustion therapy or pyaemia emissions treatment. Number of meridians and the names are also different from conventional twelve meridians (Table 1). Primitive type of naming is seen such as the shoulder meridians (肩脈), ear meridians (耳脈), and tooth meridians (齒脈), which used particular parts of the body. Furthermore, it attempts only a couple of connections between organ and meridians, and the meridians are described as isolated lines independent of the others. It is just a connecting line between one part of the body and the other, an one-to-one-relation line. According to modern multidisciplinary researchers, the meridians in Mawang-tui old documents did indicate specific palpation site of human body rather than the long pathway of qi. So it is proposed that the pulsing signals of eleven meridian system of Mawang-tui were the prototype of the later twelve meridians diagnosing method [4]. Collectively, different from the present meridians, it is just a pulse site which indicates health status of body and a place for therapeutic treatment at the same time.

Moreover, in 1993, a wooden puppet was unearthed in Mianyang City of Sichuan Province [7]. On this lacquer painted wooden puppet, drawings of human meridian path were found (Figure 2(a)). Compared with Mawang-tui old documents, it had the one meridian that Mawang-tui did not have at the moment and added the dorsal median meridian (督脈). Instead, the puppet lacks three yin meridians on the hand and also has no acupoints. There are connections between meridian lines which are faintly seen on the wooden surface (Figure 2(b)), and so this puppet is estimated to show an important step forward the whole unified concept of body, including the addition of the dorsal median meridian. It is the reason why this puppet is considered as an intermediate step of Mawang-tui and the following Huang Di Nei Jing [5, 8].

These excavated relics are shocking to the experiment researchers who had believed the theory of Huang Di Nei Jing. Where is the acupuncture meridian we know?

Table 1: Names of meridians in Mawang-tui and Mianyang in comparison with Huang Di Nei Jing. Arrows show historical changes of meridian or equivalent names from Mawang-tui to Huang Di Nei Jing. Red arrows indicate no equivalent names in Mianyang wooden puppet.

Yin-Yang eleven meridians for moxibustion (足臂十一脈灸經)	Foot-Arm eleven meridians for moxibustion (陰陽十一脈灸經)	Sichuan Mianyang wooden puppet (四川綿陽木人形)	The Yellow Emperor's Internal Medicine (靈樞經脈)
Foot-greater-yang meridian 7	Greater-yang meridian 7	Foot-greater-yang meridian 7	Hand-greater-yin meridian of lung 1
Foot-lesser-yang meridian 11	Lesser-yang meridian 11	Foot-lesser-yang meridian 11	Hand-bright-yang meridian of large intestine 2
Foot-bright-yang meridian 3	Bright-yang meridian 3	Foot-bright-yang meridian 3	Foot-bright-yang meridian of stomach 3
Foot-lesser-yin meridian 8	Shoulder meridian 6	Hand-greater-yang meridian 6	Foot-greater-yin meridian of spleen 4
Foot-greater-yin meridian 4	Ear meridian 10	Hand-lesser-yang meridian 10	Hand-lesser-yin meridian of heart 5
Foot-reverting-yin meridian 12	Tooth meridian 2	Hand-bright-yang meridian 2	Hand-greater-yang meridian of small intestine 6
Arm-greater-yin meridian 1	Greater-yin meridian 4	Hand-greater-yin meridian 1	Foot-greater-yang meridian of urine bladder 7
Arm-lesser-yin meridian 5	Reverting-yin meridian 12	Hand-lesser-yin meridian 5	Foot-lesser-yin meridian of kidney 8
Arm-greater-yang meridian 6	Lesser-yin meridian 8	Hand-reverting-yin meridian 9*	Hand-reverting-yin meridian of pericardium 9
Arm-lesser-yang meridian 10	Arm-greater-yin meridian 1	Dorsal medial meridian*	Hand-lesser-yang meridian of triple energizers 10
Arm-bright-yang meridian 2	Arm-lesser-yin meridian 5		Foot-lesser-yang meridian of gall bladder 11
			Foot-reverting-yin meridian of liver 12

*Denotes the meridian only appeared in Mianyang wooden puppet.

3. The Numerological Cosmology of Han Empire and the Meridian Theory

Meanwhile, the following interpretations are gaining strength by the evidence collected along these excavations [4, 8, 9]. There had been a variety of therapeutic theories and practices in various areas around China, prior to gaining ultimate legitimacy. But with the establishment of the Han empire (B.C. 206~A.D. 220), the integration of each theory was rapidly accelerated in every field of thought and society. Yin-Yang and five elements theory as the representative convergence, affected by numerological cosmology of the Han empire, made huge influence on the following history. It is interpreted as systematic corresponding system in a modern version. The human body has come to share the verge of the law penetrating the entire universe, which means not only the surrounding nature (mountains, rivers) but also the operation of the national management system (bureaucracy), the flow of economic products, and the movements of heavenly bodies [9]. From the initial clue of connection between rustic old meridian and a couple of viscera, a full-fledged systematic corresponding system of twelve viscera/entrails and twelve meridians were completed finally. Since then, a systematic corresponding system of the Han empire lasted for two thousand years without major change at least in acupuncture meridian theory. But in a more advanced interpretation, it seems that Mawang-tui meridian system preserves the original meanings of meridians, not wholly colored by the unified concept of Yin-Yang Wu-Xing (陰陽五行) cosmology, which is later invention of numerological intellectuals of Han empire [8].

In Oriental medicine twelve meridian theory based on Yin-Yang Wu-Xing has got the self-consistency and metaphysical power for long time [9]. It is accepted now as the core of the Oriental medicine. Still in many clinics using Oriental medicine, they show successful treatments for patients with the concept of qi-flowing meridians. However, it is not sufficient. It must be reminded that the mainstream treatments should be grounded on the explanatory framework of our time of science [3].

4. Mixing of Practice and Theory in the History of Oriental Medicine

The paradigm of the Han empire so formed gives a significant impact on us until now. According to this paradigm, diseases come from an imbalance of yin and yang or interference with the circulation of the qi, and the four diagnostic methods are presented to catch the state: (1) visual inspection, (2)

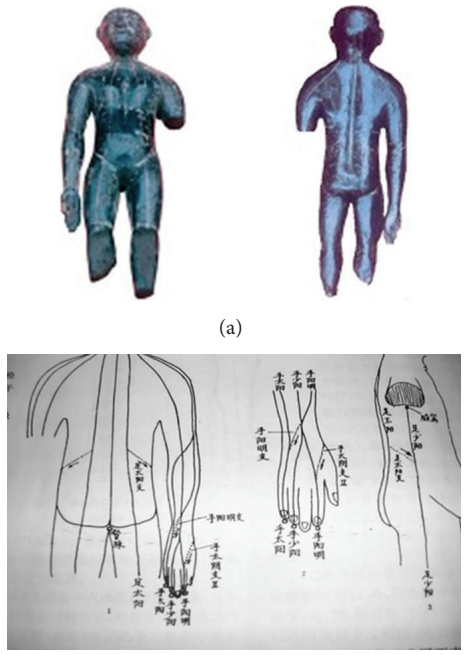

(a)

(b)

Figure 2: (a) Sichuan Mianyang lacquered wooden puppet. It is believed to be made in B.C. 179~B.C. 141, slightly later or contemporary to Mawang-tui. (b) There are ten meridians, no acupoints, with several connections of meridians.

listening/smelling, (3) questioning, and (4) touching (mainly palpation). Thus obtained data are connected to each other in a regular pattern to understand the disease or symptoms [10]. This patternization of symptoms (bian zheng; 辨證) in Oriental medicine has been argued for a long time because they cannot be understood as conventional scientific thought. Also treatments consisting of acupuncture and herbal medicine are linked to the bian-zheng (pattern of symptoms). It is like a synchronicity of the events of the world, in the modern terms. A disease occurs as a disharmony of Yin-Yang and five elements of the body because the universe is connected to each other with the concept of systematic correspondence. Oriental medicine has been characterized by this cosmology of Yin-Yang and five elements, so the medical experience and treatments were understood as functional perspective (i.e., systematic correspondence), which is strikingly different from the Western perspective (i.e., causality) [3, 9].

But is this integration of Han empire, as alleged, an immovably robust system? Or is it an incomplete, vulnerable one and needed to revise itself continuously? We are now forced to put stress on the latter; it had problems and cracks around the system from the beginning. In the first place, though focused much on the theoretical tidiness or completion of twelve meridian systems, there had been little evidence based on clinical effectiveness [6]. In fact, when acupoints have been added over a hundred of new comers until 361, for example, expansion criteria of the number of acupoints, their major effectiveness to certain symptoms was never discussed or explained [6]. And later, that the dorsal median meridian (*dumai*, 督脈) takes two branches is never explained but just described [6]. This important addition or revision has no specific theoretical explanation or clinical evidence by responsible writers or doctors. This shows an inevitable weakness of meridian theory based on the mainstream ideology of the Han empire, and now we need new methodology to organize the new findings and experiences in a modern setting.

When it comes to herbal medicine, it is a more obvious failure. From the first full-scale pharmacology text, Herbal Medicine of Divine Farmer (*Shennong Bencao Jing* 神農本草經), the systematic correspondence model could not harmoniously incorporate the various herbs with respect to Yin-Yang and five elements, rather just using the scale of hot or cold using Yin-Yang only [9]. By the 12th century, four great physicians of Jin and Yuan dynasties (金元四大家) attempted a meaningful try of integration, but also to an incomplete and sloppy end [9]. It means the cosmological integration of herbal medicine in Oriental medicine was incomplete, so it was vulnerable to other competitive cosmologies through the history. Therefore it seems natural that herbal medicine might easily be disseminated by the Western methodology, especially by pharmacology.

In respect to acupuncture meridian theory, Mawang-tui discovery itself reveals the distinct process of changes of the meridian theory. It features a rustic anatomical view based on actual observations, just a blood vessel, and in a respect shows mechanical view of what looked to be in their senses. In consensus of the field, it was described that the Mawang-tui meridians (脈) have three complex meanings [8].

(1) Meridian (mai, 脈) was blood vessels in the original sense.

(2) Meridian (mai, 脈) was Pulsation in the own character. In diagnostic process, they could pick out other forms of Pulsation in comparison with the normal pulsation.

(3) Meridian (mai, 脈) was also a treatment site to achieve a therapeutic effect by stimulations including moxibustion initially or acupuncture and both later. These three aspects of the meanings of meridians have been changed through the history until now (Table 2).

5. Primo Vascular System on the Dynamic Rebuilding of Oriental Medicine

A number of multifaceted researches have been performed to identify meridians and to explain them anatomically. Spotlighted are the recent active researches using fMRI equipment. Their conclusions are that the effect of acupuncture relies a significant portion on neurotransmitter systems. Though this neural hypothesis that the peripheral and central nervous systems play an important role in acupuncture effect is getting scientific basis for defining meridians [11], others oppose this interpretation. They contend that effect of acupuncture appears after a certain period of time and that acoustic shear wave in the tissue of human body fits

Table 2: Primo vascular system in comparison with meridians in the history of Oriental medicine.

	Mawang-tui documents (B.C. 168)	Sichuan Mianyang puppet (B.C. 170~140)	Shiji by Sima Qian (B.C. 109)	Huang Di Nei Jing (A.D. 100?)	Bonghan system (1963)	Primo vascular system (2002~)
Primary meridians (number & type)	11 line No AP	10 line No AP	12 line? AP	12 line AP	12 line? BD/BC	Sponge-like form BD/BC
Diagnostics	Pulse	?	Pulse	Pulse	?	?
Therapeutics (Local & systemic)	M, PE	A?	A M?	A, M	A, EA	A, EA

AP: acupoints; PE: pyaemia emissions; A: acupuncture; M: moxibustion; EA: electroacupuncture; BD: bonghan duct; BC: bonghan corpuscle.

well with both the effect of acupuncture and the image of the meridian [12]. Both have considerable support and experimental evidence. Overall the effect of acupuncture might encompass these phenomena. But these experimental setups presuppose that meridian system should be understood via other structures of human body. In respect to that point, primo vascular system seems to provide a very unique one unlike others. Researchers on primo vascular system just focus on revealing the exact factual structure, which has never been presented to us by visual sense, a new anatomical circulatory system [13].

They try to show or explain a tube (with the diameter of 10~30 μm) connecting the whole body which corresponds to the meridians or corpuscles which correspond to the acupoints, independent of the other circulatory (vascular or lymph) systems or nerve systems. In this point primo vascular system researchers authentically follows the study of North Korea's Bonghan Kim [2, 14]. They are trying to demonstrate the structure and function of the primo vascular system in terms of sophisticated modern terminology based on various animal experiment, daring in front of the establishment of physiological knowledge [15–20]. In particular, Bonghan Kim argued that Bonghan duct can be found in every vertebrate in common [1] (Figure 3), which fits with the long tradition of acupuncture treatment on the diseases of horse and cattle, and hawk for hunting [21]. And interestingly, the meridians of these animals are more similar to those of Mawang-tui or Mianyang wooden puppet. It is highly necessary to take a close look on the remaining prototypes of meridians.

It is interesting that the twelve meridians of horse have their main acupoint name at the head of names (Figure 4).

It may be another support that the meridians first served as diagnostic and therapeutic sites. Also it seemed to start first not as a long line of acupoints with similar functions but as a relevant place to other parts of horse body, likely to the inner organs. Moreover, there remains "theory on the relation of spot to pain (*dian-tung lun* 點痛論)" which presents 45 specific signs or movements with the pain sites of the horse [21]. Several examples are as follows.

(1) Walking with straight legs is the sign of pain of the upper knee.

(2) Not moving with the head up is because of the pain in the hoofs.

(3) Walking with head nodding is because of the pain of hind limbs.

(4) Walking with head shaking is because of shoulder pain.

(5) Poor moving of the hind legs is because of kidney pain.

(6) Choppy breathing is due to the pain of the lung meridian.

(7) Urgent wake-up and urgent lie-down is due to the pain of spleen meridian.

(8) Walking with upraised tail is due to the pain of large intestine.

(9) Walking with rolled tail is due to the pain of small intestine.

We can compare the fragmental knowledge of diagnoses and therapies with the original notions of meridians in the Mawang-tui and Mianyang wooden puppet. With the accumulation of evidence of site-to-site relations of the body, the generalized concept of interconnected meridians, such as viscera-limbs, inner-outer, and upper-lower, might have its mature conditions. Though there are multiple dimensions on the way of generalization, we do consider that these pieces of evidence are worth of advanced investigation in the course of meridian research.

This is the time to consider whether the primo vessel (or Bonghan duct) is the anatomical structure of the meridians. Though tentative, we are in the negative position when we see in line with the history of meridian theories and the remaining fragmental knowledge about the vertebrates. It sounds reasonable saying that anatomical structures of meridians are more reliable in the old documents of Mawang-tui in the respect of reality, because the meridian theory of Huang Di Nei Jing had been deeply colored by theoretical cosmology, that is, a kind of ideological generalization in Han empire era [9]. After wards, twelve meridian theory of the Huang Di Nei Jing was neither physically based nor fully explained until the recent day. Meridians are more of a cosmological image than a factual reality, though the pulsation-organ relationship remains alive in part [6].

Some primo vascular system researchers recently do not just try to meet it with the traditional meridian theory along with these notions. Further they try to reveal that the

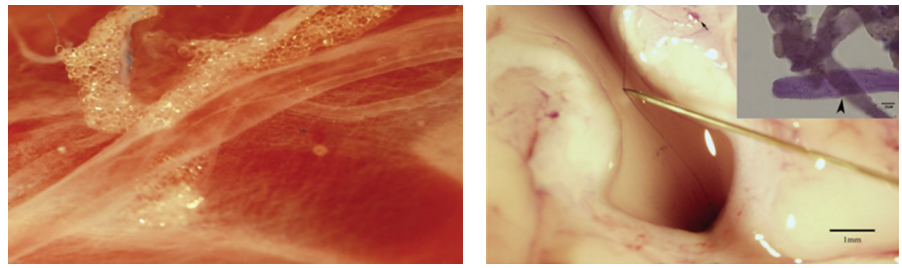

Figure 3: Bonghan duct (primo vessel) floating in lymphatic vessel of rabbit (Lt) and rabbit ventricle (Rt). Bonghan duct is increasingly recognized as the anatomical entity of acupuncture meridians. It runs every part of living body both in human and other vertebrate animals.

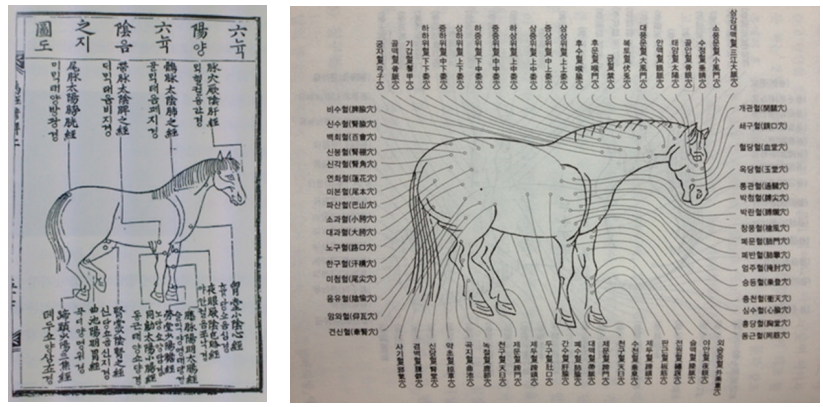

Figure 4: Lt. Drawing of meridians of a horse in the book *Newly Edited Horse Disease Therapy Regimen* in 1399, early Joseon dynasty. The meridians are a common phenomenon in vertebrates. Rt. Acupoints of horse with relation to meridians. Meridian names do have one of the name of its major acupoints.

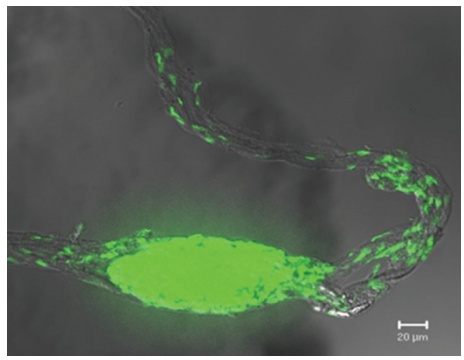

Figure 5: Sanal cells with dense DNA appear bright green on fluorescence staining in bovine heart corpuscle (visible part).

relationship of stem cells, new function of DNA, and the possibility of cell therapy are main concerns of the field [22–24].

Even the meridian-oriented informing system is also a range of research areas expanding, especially in that Sanal matures when it receives light, and Bonghan duct has features of bundle structure, which reflects the characteristic of plants (Figure 5). Some researchers contend that the primo vascular tube is regarded as fiber-optic cable with high-speed flow inside of it. Like Western medicine is backed upon medical physics, this new medicine might be grounded on electromagnetic power, light, and biophoton which is detectable by photo-multiplier tube [25].

On the other hand, as a unique part in Oriental medicine, meditation and respiration training may have an impact on the circulation of the fluid with rhythmical stimulation of Bonghan duct in the multiple layer of abdominal fascia [26]. During the respiration, respiratory-related effect on primo vascular system is expected in the rhythmic contraction and relaxation along with continuous peritoneal muscle activity.

Lee Byung-cheon, researcher of primo vascular system, presented a new generalized model of more than 10 years of experimental research on primo vascular system. He shows a sponge model of human body which well represents the primo vessel running in and outside of the blood vessels around the body, in and outside of the organs, and all the musculoskeletal or connective tissues like a loofah sponge (Figure 6) [27, 28]. This is estimated to provide the imaginative basis of a new research direction on the network of primo vascular pathway and on the mechanisms of the regeneration of wounded tissue [22, 29]. Interestingly, this model has common aspects with the author of Energy Medicine, James L. Oschman, who suggests that the meridians penetrate all the organs of the human body, including cells and cellular organelles [30].

Thus the most promising area of primo vascular system's future development might be the research of self-organized circulatory system that encompasses the energy and information. This means that they are trying to answer on the role of

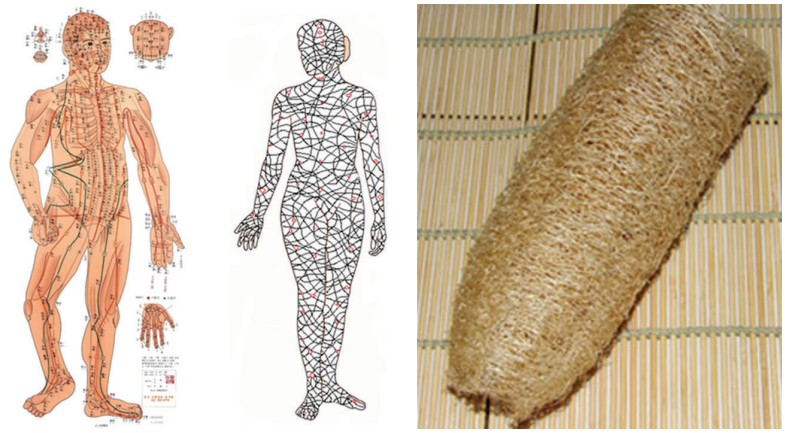

Figure 6: Loofah sponge model of primo vascular system (Bonghan-Fascia Model, Lee and Soh, 2009 and 2011).

the primo vascular system in respect to developmental, healing, and regenerating functions to which modern medicine is most vulnerable [31].

6. Discussion

In the ancient Chinese book Mencius is stated, "What is inside your body, necessarily disclose itself (有諸内形諸外)" [32]. In the book Great learning is stated, "When others easily watch me like looking into the five viscera, it is useless trying to hide (人之視己 如見其肺肝 然則何益矣)" [33]. This way of thinking seems deeply rooted among ancient Chinese. And it is likely that the ancient Chinese thought that it was very easy to look inside the body because the inner side of human body must be throwing a signal to some areas outside of the body. It has been identified in the human body, so to speak, "theory of three sites and nine diagnoses (三部九候論)", and nine pulsation sites of the surface of human body were conceived to regulate all the problems of human body like remote-controller [8]. And these original concepts of human body were systematically combined with numerological cosmology which unified the body and the universe with systematic correspondence mainly of the Han empire.

Could the 12 meridians be regarded as ultimate anatomical system of Oriental medicine? On which empirical evidence had the theory been established? We recall again the historical fact that Bonghan's theory was released in 1963. It is obvious that Bonghan Kim had in his mind the conventional 12 meridian system as anatomical entities known at that time. However, Mawang-tui old documents were excavated in 1973. Newly found old documents strikingly influenced almost all the relevant fields of academia. In Mawang-tui the meridians of the human body were not 12 but 11 without acupoints. Twenty years later in the mountains of Sichuan Mianyang province lacquered puppet was excavated with meridians drawn on the surface of the body and 10 meridians are identified. The discovery of the two was a big turning point for researchers especially in medical history. Until then it was accepted without a doubt that there had been acupoints first, and later the meridian line was formed by the grouping of similar acupoints. Those excavations, however, transformed the old concepts dramatically. In addition, the formation of the 12 meridian system seems to have been influenced by various routes and practices, and it is increasingly admitted that we should carefully winnow sophisticated historical literature to understand the true empirical phenomena of meridians [4]. Specifically, beyond the conventional study, we first should separate the reality of meridians (pulsation, diagnosis, and treatment) from the philosophical structures (numerology, philosophy of systematic correspondence). A newly refined model of meridians should be presented, adapted to the scientific progress in the 21st century. This is why the current researchers on meridians also need to be aware of the advanced knowledge from historical excavation.

Does the primo vascular system belong to Oriental medicine or Western medicine? The answer indulges in a dilemma because the definition of the term already has various deflects. Oriental medicine persistently made an attempt to mangle various disparate elements or practices from its departure, and it is such a dynamic structure allowing active influx, acceptance, and generalization with all the contradictions, inconsistencies, eventually to a different way of systematization or reconstruction. The case of New York Times journalist Reston, in 1971, and "auricular acupuncture" is representative examples. Western medicine also openly applied Galen's theory of fluids in the clinics until modern medicine methodology was established by Pasteur and Koch [10]. When considering that Western medicine and Oriental medicine also made their way with a ceaseless acceptance and reconfiguration of heterogeneous elements, and due to the imperfect explanatory framework, the effort of modification and systematization is still under process; the primo vascular system in its present form might be the most fierce contact and conversation between the two medical systems [3].

The target of Oriental medicine or Western medicine is the same "human body." However, both emphasize the heterogeneity, respectively, focusing on the usefulness of each approach which is either holistic or analytical. Maintaining a dichotomic view that human body is divided into matter and energy, they cause frictions in terms of qi (气) and meridians whether they should be defined as a tangible presence or just

a functional phenomenon. However, when you look back on the process of formation of the initial meridian theory, we cannot deny blood vessels and blood circulation in substance had been recognized as the meridians. Surely meridian theory was formed by combining clinical experience of the specific effect of certain stimuli on existential objects and theorized complying on the zeitgeist of ancient Han era. After that, even though there are some changes historically in meridian theories, the consistent thought in meridian theories to control diseases by stimulation of the body surface has been unchanged. This might be served as a guideline primo vascular system researchers can consider with all the differences of meridian systems in history, that is, number of the meridians, the location of acupuncture points, the pathways of meridians, and connections between the meridians and the viscera. Though primo vascular system is a powerful theory to explain the mechanism and the entity of the meridians, the conventional meridian theories were considerably affected by the spirit of the times. So it is required that we should clarify the core meanings of meridians from other cultural products. From those analyses we can derive free and creative premises for the primo vascular researches, which may be a completely new modern meridian theory. We expect that it may be the starting point that reflects the modern zeitgeist not only integrating the matter and spirit but also connecting the Eastern and Western perspective of the human body.

7. Conclusion

Based on the historical research on the old documents and practices, the implicit premises of conventional meridian studies should be modulated with a certain transformation. Though Bonghan's theory was set out clearly away with previous conventional idea, it was under the impact of long-standing tradition of meridian theory. But we think primo vascular system was apparently sparked by the meridian theory in Oriental medicine; the results might be a completely new intellectual discovery never known to us. It is increasingly likely to act as a prelude to mobilize a new medicine in the disciplines of all ages and countries, which belongs neither to Western nor to Oriental. We expect that it is just a probable vision upon the historical perspective of Oriental medicine.

Authors' Contribution

Jongwook Jeon coordinated this work and Sanghum Lee provided a revised version of the original paper.

Conflict of Interests

The authors declare no conflict of interests.

Acknowledgments

This work was partly supported by Grant K13210 awarded to the Korea Institute of Oriental Medicine (KIOM) from the Ministry of Education, Science and Technology (MEST), the Republic of Korea, and by the Bio & Medical Technology Development Program of the National Research of Korea. And the authors thank professor DW Shin at KAIST, Daejeon, Republic of Korea, for providing horse acupuncture data and other advice on animal acupunctures.

References

[1] B. H. Kim, "On the Kyungrak system," *Journal of Academy of Medical Sciences*, vol. 90, pp. 1–61, 1963.

[2] K.-S. Soh, "On the meridians and Bonghan theroy," in *Thought on Science*, pp. 189–217, 2004.

[3] J. Kim, "Beyond paradigm: making transcultural connections in a scientific translation of acupuncture," *Social Science and Medicine*, vol. 62, no. 12, pp. 2960–2972, 2006.

[4] Y. Zhou, *Medical Culture in the Mawang-Tui*, Chuangsi, Beijing, China, 1993.

[5] W. Jung, "The origin of Jingmai: through the investigation into some important hypotheses," *Korean Journal of Medical History*, vol. 19, no. 2, pp. 433–458, 2010.

[6] C. S. Yin and H. G. Koh, "What's the original concept of meridian and acupuncture point in oriental medicine?" *Uisahak*, vol. 14, no. 2, pp. 137–150, 2005.

[7] J. Ma, "Acupuncture meridians on the laquered wooden puppet unearthed in th tombs of Han," 1996.

[8] J. Li, *Mai and the Development of Medical Knowledge in Early China*, Academia Sinica, Beijing, China, 2007.

[9] P. Unschuld, *Medicine in China: A History of Ideas*, University of California Press, Berkeley, Calif, USA, 1985.

[10] J.-Y. Kim, "Oriental medicine as a He terogeneous ensemble," *Uisahak*, vol. 10, no. 2, pp. 103–123, 2001.

[11] J. C. Longhurst, "Defining meridians: a modern basis of understanding," *JAMS Journal of Acupuncture and Meridian Studies*, vol. 3, no. 2, pp. 67–74, 2010.

[12] E. S. Yang, P. W. Li, B. Nilius, and G. Li, "Ancient Chinese medicine and mechanistic evidence of acupuncture physiology," *Pflugers Archiv*, vol. 462, no. 5, pp. 645–653, 2011.

[13] K. S. Soh, "Bonghan circulatory system as an extension of acupuncture meridians," *JAMS Journal of Acupuncture and Meridian Studies*, vol. 2, no. 2, pp. 93–106, 2009.

[14] B. Kim, *On the Kyungrak System*, vol. 90, 1963.

[15] B. C. Lee, K. W. Kim, and K. S. Soh, "Characteristic features of a nerve primo-vessel suspended in rabbit brain ventricle and central canal," *JAMS Journal of Acupuncture and Meridian Studies*, vol. 3, no. 2, pp. 75–80, 2010.

[16] B. C. Lee, S. Kim, and K. S. Soh, "Novel anatomic structures in the brain and spinal cord of rabbit that may belong to the Bonghan system of potential acupuncture meridians," *JAMS Journal of Acupuncture and Meridian Studies*, vol. 1, no. 1, pp. 29–35, 2008.

[17] B. C. Lee and K. S. Soh, "Contrast-enhancing optical method to observe a Bonghan duct floating inside a lymph vessel of a rabbit," *Lymphology*, vol. 41, no. 4, pp. 178–185, 2008.

[18] B. C. Lee, J. S. Yoo, K. Y. Baik, K. W. Kim, and K. S. Soh, "Novel threadlike structures (Bonghan ducts) inside lymphatic vessels of rabbits visualized with a Janus Green B staining method," *Anatomical Record B*, vol. 286, no. 1, pp. 1–7, 2005.

[19] H. S. Shin, H. M. Johng, B. C. Lee et al., "Feulgen reaction study of novel threadlike structures (Bonghan ducts) on the surfaces of mammalian organs," *Anatomical Record B*, vol. 284, no. 1, pp. 35–40, 2005.

[20] V. Vodyanoy, "Demonstration of Bonghan corpuscles and ducts in rabbits and rats by Korean scientists," *Journal of Acupuncture and Meridian Studies*, vol. 2, no. 2, p. 169, 2009.

[21] S. Dw, "History of horse medicine in Korea," 2004.

[22] B. C. Lee, K. H. Bae, G. J. Jhon, and K. S. Soh, "Bonghan system as mesenchymal stem cell niches and pathways of macrophages in adipose tissues," *JAMS Journal of Acupuncture and Meridian Studies*, vol. 2, no. 1, pp. 79–82, 2009.

[23] S. S. Yi, I. K. Hwang, M. S. Kim, K. S. Soh, and Y. S. Yoon, "The origin of endothelial cells in novel structures, Bonghan ducts and Bonghan corpuscles determined using immunofluorescence," *JAMS Journal of Acupuncture and Meridian Studies*, vol. 2, no. 3, pp. 190–196, 2009.

[24] J. S. Yoo, H. B. Kim, V. Ogay, B. C. Lee, S. Ahn, and K. S. Soh, "Bonghan ducts as possible pathways for cancer metastasis," *JAMS Journal of Acupuncture and Meridian Studies*, vol. 2, no. 2, pp. 118–123, 2009.

[25] L. Ruby, "Popp in the research of three professors".

[26] B. C. Lee, K. W. Kim, and K. S. Soh, "Visualizing the network of bonghan ducts in the omentum and peritoneum by using trypan blue," *JAMS Journal of Acupuncture and Meridian Studies*, vol. 2, no. 1, pp. 66–70, 2009.

[27] B. C. Lee and K. S. Soh, "A novel model for meridian: bonghan systems combined with fascia (Bonghan-Fascia Model)," in *Proceedings of the Fascia Research II: Basic Science and Implications for Conventional and Complementary Healthcare*, p. 144, Elsevier, Amsterdam, The Netherlands, 2009.

[28] B. C. Lee, "Interrelationship between primo vascular system and fascia system," in *Proceedings of the 17th International Symposium Anniversary of KIOM Current Research Trends in Traditional Medicine*, pp. 257–270, 2011.

[29] B. C. Lee, H. S. Lee, and D. I. Kang, "Growth of microgranules into cell-like structures in fertilized chicken eggs: hypothesis for a mitosis-free alternative pathway," *Journal of Acupuncture and Meridian Studies*, vol. 5, no. 4, pp. 183–189, 2012.

[30] J. L. Oschman, *Energy Medicine*, Churchill and Livingstone, Philadelphia, Pa, USA, 2000.

[31] V. Ogay, K. Y. Baik, B. C. Lee, and K. S. Soh, "Characterization of DNA-containing granules flowing through the meridian-like system on the internal organs of rabbits," *Acupuncture and Electro-Therapeutics Research*, vol. 31, no. 1-2, pp. 13–31, 2006.

[32] J. Legge, *The Works of Mencius*, Dover Books, Mineola, NK, USA, 1990.

[33] J. Legge, *Confucian Analects, the Great Learning, and the Doctrine of the Mean Oxford*, Clarendon Press, New York, NY, USA, 2006.

Hindawi Publishing Corporation
Evidence-Based Complementary and Alternative Medicine
Volume 2013, Article ID 279176, 7 pages
http://dx.doi.org/10.1155/2013/279176

Review Article

Review and Comment on the Relationship between Primo Vascular System and Meridians

Ding-Jun Cai,[1] Ji Chen,[2] Yi Zhuang,[1] Mai-Lan Liu,[1] and Fan-Rong Liang[1]

[1] *Chengdu University of Traditional Chinese Medicine, Sichuan, Chengdu 610075, China*
[2] *Foreign Languages School, Chengdu University of Traditional Chinese Medicine, Sichuan, Chengdu 610075, China*

Correspondence should be addressed to Fan-Rong Liang; acuresearch@126.com

Received 11 February 2013; Revised 3 April 2013; Accepted 10 April 2013

Academic Editor: Xianghong Jing

This paper aims to summarize the recent progress of researches on the primo vascular system (PVS) and to analyze characteristics between PVS and traditional Chinese meridians. With the distribution, position features, identification and origin of PVS, and its function related to meridians elaborated on, we propose that there is still a lack of enough evidence to support the correlation between PVS and traditional Chinese meridians.

1. Introduction

Acupuncture therapy boosts a good clinical efficacy worldwide. According to the traditional Chinese medicine theories, acupuncture owes its favorable effect to the regular and diversified meridians. The meridians are interconnected to form a fundamental system, which are the channels distributing all over the human's body to circulate *qi* and blood and to connect internal viscera with the external part. However, there has emerged little scientific biological evidence to support this traditional theory, since the key problem of meridians seems that what the material basis of the meridians is, which has always been a puzzle for many researchers. The researchers who focus on this problem have labored to expose the structure of meridians in terms of anatomical and physiological methods.

There were some studies providing few clues to uncover this conundrum. In the early 1960s, Prof. Kim in North Korea proposed that he found the anatomic and physiological basis for the meridians. He stained out some special ducts and nodes in the subcutaneous tissue, organ surface, and nerve tissue, entitled as Bonghan ducts and Bonghan corpuscle, with a novel dye and revealed the morphologic features and function of Bonghan ducts and Bonghan corpuscle in his research [1–6]. However his studies were ignored for almost forty years due to the lack of details in his research protocol, and others failed to reproduce his outcomes. Recently, Prof. Soh's group has carried out a series of studies stemmed from Kim's conjecture of meridians in traditional oriental medicine, which also declared that they had found some structures as primo vascular system (PVS) which was just alike to Prof. Kim's claims. Prof. Soh even pointed out that Bonghan circulatory system serves as an extension of acupuncture meridians [7]. However, as it refers to the relationship between the PVS and meridians, it should be careful due to a few key issues of their distributions, positions, and physiological functions.

This review is to summarize the recent progress of researches on PVS and to analyze the most important distinguishing characteristics between PVS and traditional meridians.

2. On Universality of PVS Distribution

The PVS is composed of the small primo vessels (PVs) and primo nodes (PNs). It is reported that the PVs are semitranslucent thread-like structures whose diameter is about 0.1 mm connecting the PNs. The PVs away from the PN branch out into 2-3 smaller vessels with fine terminal arborizations [8]. In the past ten years, increasing researches focused on finding out PVS. Various staining techniques, such as Trypan blue techniques [9], Alcian blue dyeing [10],

and Janus green B staining method [11] among others, were applied to detect the PVs and PNs, which appeared in most parts of an animal's body. The PVs and PNs were found in nervous system, instance in venous sinuses of rat brains [12], around the perineurium in the spinal cord and in the epineurium, perineurium, and endoneurium of a rat sciatic nerve [9]. They also emerged on the surface of internal organs, for example, stomach, intestine, liver, bladder, and heart [13–17]. In addition, in circulatory system, the PVs and PNs were detected inside the various large blood vessels [18–23] and lymphatic vessels [11, 24–26]. Moreover, the PVs and PNs were observed in the superficial tissues. An example can be found in the hypodermis of rat by using Trypan blue [27]. Besides, beyond the Prof. Kim's hypothesis, in the adipose tissues, PVS was detected [28]. And more interestingly, some researchers reported that the PVs and PNs were not isolated and intermittent, but connected to form a novel network. A significant report stated that the existence of an entire network above the pia mater of the brain and spine of rats was proved with two approaches, spraying Alcian blue into the pia mater of the rat brain and injecting Alcian blue into the lateral ventricle [29]. A similar work also declared that the network of Bonghan ducts (PVs) was noticed in the omentum and peritoneum by using Trypan blue [30]. On the layer of the stratum fibrosum in the superficial fascia of rat hypodermis, the networks of threadlike structures composed of primo nodes and vessels could be found in which the fluorescent nanoparticles existed [31]. The researchers even proposed that the network of PVS in the fascia might be helpful for acupuncture [32]. Those research findings are in accordance with Prof. Kim's conception of the Kyungrak system (meridians) that PVS is an independent functional morphological system in which the superficial PVs and extravascular PVs are connected with superficial nodes, and the deep PVs are connected between them with intravascular PVs, deep PNs, and organ nodes [2]. Based on the above, it seemed that the novel PVS could be considered to have a special relationship with acupuncture meridians due to its distribution features. Unfortunately, a big difference of distribution still lies in PVS and meridians. As it is well known in the oriental traditional medicine, the meridians distribute widely in various parts of the body, and different individuals have a similar distribution of the meridian pathway. Although the above researches have suggested that PVS was observed in most parts of the body, it seems absent in the structures of the organs in head or face. However, according to the classic meridian theory, the six *yang* meridians travel to the head and face and connect with their corresponding body orifices on the head. At the same time, lung and pericardium are important viscera connected with the *yin* meridians. But there has been no reports which stated that the structures of PVS were found in the lung and pericardium. In addition, by carefully analyzing the results of studies that PVS was concerned, it can be found that the PVs and PNs were not observed in all experimental animals, and there even exited gender differences detected in a same experiment [33]. Thus, it seems that there still exists difference in the distribution between the existing research findings on PVS and traditional meridians. Fortunately, some interesting studies may help to answer this question. Primo nodes were observed at CV12, CV10, and CV8, and basic histological study with H&E and Mason's trichrome revealed that they were different from lymph nodes. And after injecting FNP into the primo nodes, it traced the flow of nanoparticles along the CV line to the ligament wrapping the bladder in the primo vessels [34]. After injecting Alcian Blue (AB) dye into the rat acupoint BL23, AB-stained PVS were also observed on the surface of internal organs in right abdominal cavity [35]. In addition, after the subcutaneous injection of fluorescent nanoparticles into the acupoint ST36, the PVs and PNs were found from the knee to the middle of tibia, around the location of the classical "stomach meridian," of which tracing region was a maximum of 1-2 cm away from the diffusion area [31]. Therefore, despite of the distinct difference of the distribution universality between the PVS and traditional meridians, there is not enough evidence to negate a possible link between these two concepts. In order to discover the relationship between them based on the distribution features, intensive researches should be carried out in future which focus on confirming the existence of PVS in the skin and the ubiquity of the connection between skin PVS, especially acupoints and PVS of internal organs.

3. On Stability of PVS Location

Currently most studies of PVS revealed the existence of PVs and PNs in the animal's body. But the PVs and PNs were floating in liquid. In the blood system, the PVs and PNs were observed floating in the venous sinuses of rats [12], in blood vessel of mice and rats [36], and inside the bovine heart [17]. In the lymph system, the PVs also were floating in the lymphatic vessels. The researchers isolated the floating PVs with diameters of 20~30 μm from abdominal lymph vessels of rabbits by Alcian blue staining [37]. In the nervous system, PVS was not attached to the wall of the ventricle, but acted as a freely floating structure in the cerebrospinal fluid (CSF), and it ran along the central canal of the spinal cord by using fluorescent nanoparticles that were injected into the lateral ventricle [38]. Even on the surface of the internal organs, the PVs and PNs were not adhered to the surface of organs, but were floating in peritoneal fluid [39]. The floating phenomenon indicates that the position of PVS is unfixed and irregular which leads up to irregular observation and hardly reproduction at the same time. However, in accordance with the descriptions of meridians in medical classics, it is not difficult to find that the position of meridians is fixed, stable, and symmetrical under the physiological condition. The irregularly free-floating state of the PVs and PNs was a little bit contradictory to traditional meridian theory. Fortunately, some recent studies dedicated that a fixed PVS of well-defined location was found underneath the superior sagittal sinus in the sagittal fissure of rabbit, and its characteristics were the same as observed in other organs [40]. Moreover, the PVs were irregularly fixed on the stratum fibrosum in the subcutaneous fascia [31]. These findings may be helpful for exploring the fixed PVS in other parts of body and also be

beneficial for studying the relationship between PVS and meridians.

4. On Identification and Origin of PVS

Since the novel tread-like structures were observed in the animals, the intensive researches were conducted on the field which distinguished those semitransparent tread-like structures from other tissues. Because, inside an organism, there are many similar tread-like structures, especially under certain special experimental conditions. In both Prof. Kim' and Prof. Soh' researches, the method of blood perfusion was adapted to study PVS in the blood vessels. Injecting a 10% dextrose solution into the left femoral vein to replace blood, the retaining PVs in the vessels were observed which were longitudinal tread-like structures floating in the transparent fluid [18–20]. Some researchers also found some similar fibrous string in the vessels through blood perfusion by giving 0.9% NaCl solution into femoral vein of rabbit on one side. However, their further studies suggested that the fibrous strings were coagulated composed by bundle of fibrin because of distinct difference of tracing rate between injecting hypercoagulable and hypocoagulable perfusion fluid [41]. Meanwhile, with careful analysis on the method of Soh's research team, some researchers found that PVS on a visceral organ surface was frequently observed in phenylhydrazine- (PHZ-) induced anemic rats [7]. But phenylhydrazine is known to cause hypercoagulability. They designed to investigate PVS on PHZ-induced anemic and bleeding-induced anemic rat models. The tread-like structures were only detected on PHZ-induced anemic and the phenomena were blocked when heparin was administered [42]. It is well known that even slightly bleeding could make it easy to find tread-like structures on the internal organs. Since it is badly difficult in avoiding bleeding during surgical operation, it is crucial to identify PVS from coagulate string. Concerned with Prof. Kim's hypothesis, Prof. Soh's research group confirmed PVS by some distinctive characteristics, such as tread-like structures connected with node, multiple tubular structure, trypan blue sustainability, and rod-shaped nuclei. But the rod-shaped nuclei are absent in fibrin [43]. Conversely, research results stated that the tread-like structures detected under hypercoagulability and blocked by heparin also have the four hallmarks of the PVs [42].

There is another condition to which the special attention should be attracted. The visceral peritoneum is easily damaged by mechanical and chemical factors during the operation. Therefore, it is necessary to distinguish the internal organ-surface PVS from torn peritoneum and the debris of peritoneum. Using stereoscopic and microscopic observation, some researchers discriminated internal organ-surface primo vessels from torn mesentery, which is considered as a similar and potentially confusing tissue [44]. Both of them are milky-white-colored and string-like observed by a stereoscope. But there are distinguishing features between them. The internal organ-surface PVs were weakly connected to the organ surface, connected to corpuscles, and branched onto the surface of other organs. While torn mesentery tightly attaches to the organ surface with a fan-shape membrane, which is strong enough to withstand force sufficient to lift the organ, and does not branch. Moreover, the PVs were bundle patterns, while irregular patterns were seen in torn mesentery tissue under an optical microscope. To our knowledge, some anesthetics, such as urethane, can lead up to injury of visceral peritoneum by IP injection. In most studies of PVS on organs' surface, animal models were usually anesthetized by administrating anesthetic directly into abdominal cavity. Thereby, the debris of visceral peritoneum should be considered. A research revealed that the debris of visceral peritoneum caused by urethane was thread-like structures in the peritoneal fluid, which also had the above four characteristics of PVS [42]. The research results seemed controversial, as this may be due to the loose criteria of PVS. According to the Kim's conception and traditional meridian theory, PVS and meridians should be continuous and form a certain network, and the tread-like structures in the peritoneal fluid were always fragment, which might be considered to be the segmental structures from the allover of PVS in the peritoneum and omentum. Hence, there is a need to develop more suitable methods to identify PVS from these similar tissues.

Furthermore, one more easily confusing tissue is the lymph vessel. Both lymph vessels and the PVs are transparent vessels. But there are many characteristics of the PVs different from the lymphatic vessels [26, 37, 45, 46]. The first and most importance is that the PV has a multiple tubular structure and is filled with fibrous material, while the lymph vessel is a single tube. Secondly, the PV reveals rod-shaped nuclei stained by Acridine orange and 4′,6-diamidino-2-phenylindole and dihydrochloride (DAPI). And the blue-stained nuclei, which are distributed in a broken-lined stripe, form a tube structure. Thirdly, the size of them is different. For example, the average diameter of the lymph vessels inside the caudal vena cava of the rabbits was 258.5 μm and the average diameter of the primo vessels was 26 μm. Fourthly, the PV is easy to lift from internal organ surface, while the lymphatic vessel is fixed in the organ. Fifthly, the PV has some sinuses through which some liquid and granules flow. Last but not the least, by applying immunostaining with a lymphatic marker of lymphatics, LYVE-1, the lymphatic endothelial cells with strong positive staining are clearly located at the inner boundary of the lymphatic vessel whereas no LYVE-1 positive cells were detected in the PV. In addition, compared with the blood vessel, the PV has distinguished features which are multilumen structure from the rod-shaped nuclei of endothelial cells [46]. All of these research findings revealed that PVS was a novel and independence structure in the animal's body although some uncertain conflict still existed.

Moreover, a question concerned is what the origin of PVS is. However, the current research results seemed to be contradictory. Using double-labeled, positive green fluorescence and Trypan blue staining, a research finding stated that PVS in the induced tumor in a green fluorescence protein- (GFP-) expressing mouse originated from endogenous sources rather than from exogenous cells, because PVS shared the genetic characteristics of the host animal. At the same time, with the fluorescence microscopy employed to investigate the PVs

in the epidermis under the skin in the normal GFP mouse, an extensive length of the PV line and a PN was clearly observed, which was surrounded with abundant adipose tissue. Combined the finding in the normal GFP mouse, it would be more certain that PVS is endogenous [47]. On the contrary, a research in 2013 suggested a different view. Through immunostaining with antibodies against human CD3 (T lymphocyte), CD20 (B lymphocyte), CD45 (histiocyte), CD68 (macrophage), and lysozyme, it was found that the cells in the PNs of the mice with human U937 tumor were strongly immunoreactive to lysozyme and modestly immunopositive for CD45 and CD68. The author pointed out that the high expression of lysozyme, which was specific for histiocytic lymphoma, in PVS cells strongly suggested that PVS was not of host origin but derived from the xenografted tumor cells. Meanwhile, qRT-PCR analysis of mRNA isolated from PVS cells also revealed a striking predominance of human, rather than mouse, sequences [48]. According to Kim's hypothesis, PVS would vary in different conditions, which is in accordance with the classic meridian theory. But this change does not alter the feature that the meridians or PVS belong to an inherent structure of body. Given that PVS is a basis of traditional meridians, it should be an intrinsic structure in any states. It seemed that the last research did not support the above opinion. However, combined with these two researches, the results benefited us to understand the origins of the different components of PVS. The primo vessels originated from endogenous sources. The cells in the primo nodes might change in different conditions, just like the physical and chemical features of the acupoints would vary under pathological condition [49]. And more interestingly, the finding of the research focused on the markers of the epithelium and endothelium is that the PN and PV (BHC/D) from within lymphatics and those on organ surfaces have the same wall structure, suggesting that they have the same developmental origin [50]. This is also valuable for regarding PVS all over the body as a whole like meridians.

5. On Function of PVS Related to Meridian

A series of PVS studies suggested that PVS has certain physiological functions. According to Prof. Kim [2–5], the functions of PVS (Kyungrak system) included many aspects, for example, (1) the circulatory function of PVS; (2) PVs with bioelectrical activity, excitatory conductivity, and mechanical motility; (3) hematopoietic function for the intravascular PVS; (4) the biochemical function of the primo fluid; (5) the regeneration of damaged function of primo microcells (Sanals). The researcher also has summarized the functions of PVS in his article, including carrying a fluid, immune action, a potential effect of cells, and development and differentiation of organs [51]. In traditional meridian theory, the significant function of meridians is to convey *qi* and blood and to receive stimulus to regulate the functions of organism. Therefore, the function of PVS which might be associated with these two aspects will be discussed further.

Based on the morphological studies, it is confirmed that the PVs are bundle pattern of tubules filled with primo fluid [16, 52–54]. By injecting fluorescent nanoparticles into a PN (BH corpuscle), the experiment showed a one-way flow, but the flow speed was not measured properly because of the limitation of experimental conditions [55]. Another research measured the flow speed by injecting Alcian blue into the PN (BHC) on the surface of rabbit's liver. The flow was unidirectional whose distance was up to 12 cm, and the speed was measured as 0.3 ± 0.1 mm/s [16]. The results were consistent with the Prof. Kim' work. According to traditional theory of meridians, the meridians perform the function to carry *qi* and blood to organs and tissues. And the research on propagated sensation along meridians also revealed the transmission with low-speed characteristics [56]. Therefore, from this perspective, PVS and meridians are considered to link with each other potentially.

The principal function of meridians and acupoints is to receive stimulation and induce therapeutic effect, especially after receiving appropriate stimulations. Provided the established connection between the external stimulation and internal organ's effect, PVS might be like a foundation of meridians. Fortunately, a few researchers have devoted themselves to solving this issue. A research team focused on the electrophysiological characteristics of PVS. Applying extracellular recording method, the researchers recorded two types of pulses generated by the primo vessels on the internal organ surface: type I pulses' feature was with fast depolarizing and repolarizing phases, and type II pulses' characteristic was with fast depolarizing phase and gradually slowing repolarizing phase. And moreover, basing on the sharp top and larger amplitude of the pulses induced by stimulating primo vessels, the researchers could distinguish them from the pulses generated by smooth muscle [57]. Using intracellular recording method, others found that the electrical potential rose slowly by an average of 10.5 ± 8.4 mV in 18.1 ± 14.0 seconds to a steady resting potential, and irregular bursts of spontaneously evoked spikes occurred in the resting potential with an average duration of 16.6 ± 14.9 seconds. The average amplitude of the spikes was 1.2 ± 0.6 mV, and the average duration of the spikes was 0.8 ± 0.8 seconds while the full width at half height was 0.27 ± 0.19 seconds. These results implied that the resting potential of a PN not only was merely to be smooth-muscle-like, but also acted as the irregular burst pattern of nerve tissue [58]. A morphological work which found the presence of nerve-like structures confined to the PNs also supported the above result [48]. Further research suggested that there are different types of cells in PVs and PNs and some of them were excitable [59]. All of these researches suggested that PVS was excitable, which had capability of receiving stimulation and generating a certain reaction. This function might benefit information transfer induced by external stimuli through PVS.

However, whether this kind of electrophysiological reaction generated by the PVs on the internal organ surface could be induced by subcutaneous PV and PN or acupoints is still uncertain. This point is highly important for acupuncture treatment. Hence, another research focused on the relation between the PVs on the internal organ surface and acupoints through detecting the modulation of gastric motility by stimulating the PVs on the surface of stomach or intestine,

as well as acupoints *Zusanli* (ST36) and *Zhongwan* (CV12). The researchers based the view that the PVs on the surface of stomach or intestine did not mediate the regulation of gastric motility induced by stimulating at the acupoints ST36 or CV12 on the fact that electric stimulation of the PVs had no effect on the gastric motility and on the fact that the effect of stimulating at CV12 or at ST36 is no significant difference between the PVS-intact and the PVS-cut rats [60]. Combined with the above research works, it is conceived that lacking the function of the PVs induced by stimulating acupoints makes it fail to support the relationship between PVS and meridians even though PVS could be excitable. However, there are some researches contributing a different view. They suggested that the PVs and PNs on the surface of organs formed a closed circulatory system, within which there were many kinds of immune cells, such as mast cells (20%), eosinophils (16%), neutrophils (5%), and histiocytes (53%) [50]. Therefore, they proposed that the main function of PVS on the organs' surfaces was to regulate immune function, which was in accordance with Prof. Kim's claim. But based on Prof. Kim's conception, all the nuclei of tissue cells are connected with fine terminal subducts and these subducts are connected to the primo vessels for the organs. Acupuncture may regulate organs' function by simulating exterior PVs and PNs through the exterior tissue cells. The proteomic analysis of the PVs also showed that the PVs had some protein whose duty was responding to stimulus [61]. Furthermore, the histological research of PV and PN also showed that there was abundant fibrillar material composed of thread-like structures suggestive of collagen and/or elastic fibers. It is known that the connective tissue is the carrier of the mechanical stimulation induced by acupuncture [62, 63]. Hence, further researches on acupuncture regulating organs' functions through the exterior-interior PVS should be conducted in future. Only by establishing the functional connection of the exterior-interior PVS between the stimulus of acupoints and responds of organs could PVS be a basis for meridians.

6. Conclusions

We reviewed the features of PVS in light of its distribution, which suggested that PVS covered the massive parts of the body. However, the relevant skin PVS has not been studied completely, and only few researches revealed some cues. Thus, a comparison between acupuncture meridians and PVS leaves nothing rigorous but a mist. BH Kim's claim on the observation of acupuncture meridians remains to verified in future. We analyze the position stability, identification, and origin of PVS. The data demonstrate that PVS is a novel and distinctive structure, but the criteria of it are still needed to develop. The locations of the PVS subsystems floating in fluid are not fixed, and those fixed-location PVS subsystems like intraorgan PVS are not yet observed. The origin of the primo vessels and nodes associated with xenografted tumor is the host animal, but cells like the histiocytes in the primo node are from the tumor. We pay more attention to the function of PVS related to meridians. The study with PVS on the organ surface showed that they are not involved with acupuncture stimulations, and further studies with skin PVS and extra PVS are required to find out the functional relation with acupuncture. In conclusion, there is still a lack of enough evidence to ensure PVS as a fundamental substance of traditional meridians. In order to verify the hypothesis of the relationship between PVS and meridians, further researches on the skin PVS, extra PVS, and the functional connection between them and organs' function should be carried out in the near future.

Acknowledgments

This study was supported by the National Basic Research Program of China (973 Program, nos. 2012CB518501 and 2010CB530501) and National Natural Science Foundations of China (no. 30930112).

References

[1] B. H. Kim, "Study on the reality of acupuncture meridian," *Journal of Jo Sun Medicine*, no. 9, pp. 5–13, 1962.

[2] B. H. Kim, "On the Kyungrak system," *Journal of Academy of Medical Sciences*, no. 90, pp. 1–41, 1963.

[3] B. H. Kim, "The Kyungrak system," *Journal of Jo Sun Medicine*, no. 108, pp. 1–38, 1965.

[4] B. H. Kim, "Sanal theory," *Journal of Jo Sun Medicine*, no. 108, pp. 39–62, 1965.

[5] B. H. Kim, "Sanals and hematopoiesis," *Journal of Jo Sun Medicine*, no. 108, pp. 1–6, 1965.

[6] B. H. Kim, "Developmental and comparative biological study of primo vascular system," *Journal of Acupuncture and Meridian Studies*, vol. 5, no. 5, pp. 248–255, 2012.

[7] K. S. Soh, "Bonghan circulatory system as an extension of acupuncture meridians," *Journal of Acupuncture and Meridian Studies*, vol. 2, no. 2, pp. 93–106, 2009.

[8] B. C. Lee, S. U. Jhang, J. H. Choi, S. Y. Lee, P. D. Ryu, and K. S. Soh, "DiI staining of fine branches of bonghan ducts on surface of rat abdominal organs," *Journal of Acupuncture and Meridian Studies*, vol. 2, no. 4, pp. 301–305, 2009.

[9] B. C. Lee, K. H. Eom, and K. S. Soh, "Primo-vessels and Primo-nodes in Rat Brain, spine and sciatic nerve," *Journal of Acupuncture and Meridian Studies*, vol. 3, no. 2, pp. 111–115, 2010.

[10] S. J. Jung, S. Y. Cho, K. H. . Bae SH Hwang et al., "Protocol for the observation of the primo vascular system in the lymph vessels of rabbits," *Journal of Acupuncture and Meridian Studies*, vol. 5, no. 5, pp. 234–240, 2012.

[11] B. C. Lee, J. S. Yoo, K. Y. Baik, K. W. Kim, and K. S. Soh, "Novel threadlike structures (Bonghan ducts) inside lymphatic vessels of rabbits visualized with a Janus Green B staining method," *Anatomical Record B*, vol. 286, no. 1, pp. 1–7, 2005.

[12] H. S. Lee, W. H. Park, A. R. Je, H. S. Kweon, and B. C. Lee, "Evidence for novel structures (primo vessels and primo nodes) floating in the venous sinuses of rat brains," *Neuroscience Letters*, vol. 522, no. 2, pp. 98–102, 2012.

[13] M. S. Kim, J. Y. Hong, S. Hong, B. C. Lee, C. H. Nam, and H. J. Woo, "Bong-Han corpuscles as possible stem cell niches on the organ-surfaces," *Journal of Korean Pharmacopuncture Institute*, vol. 11, pp. 5–12, 2008.

[14] J. Kim, V. Ogay, B. C. Lee et al., "Catecholamine-producing novel endocrine organ: Bonghan system," *Medical Acupuncture*, vol. 20, no. 2, pp. 97–102, 2008.

[15] H. M. Johng, H. S. Shin, J. S. Yoo, B. C. Lee, K. Y. Baik, and K. S. Soh, "Bonghan duct on the surface of rat liver," *Journal of International Society of Life Information Science*, vol. 22, no. 2, pp. 469–472, 2004.

[16] B. Sung, M. S. Kim, B. C. Lee et al., "Measurement of flow speed in the channels of novel threadlike structures on the surfaces of mammalian organs," *Naturwissenschaften*, vol. 95, no. 2, pp. 117–124, 2008.

[17] B. C. Lee, H. B. Kim, B. Sung et al., "Structure of the sinus in the primo vessel inside the bovine cardiac chambers," in *The Primo Vascular System: Its Role in Cancer and Regeneration*, K. S. Soh, K. A. Kang, and D. K. Harrison, Eds., pp. 57–62, Springer, New York, NY, USA, 2011.

[18] X. W. Jiang, H. K. Kim, H. S. Shin et al., "Method for observing intravascular Bonghan duct," *Korean Journal of Oriental Preventive Medical Society*, no. 6, pp. 162–166, 2002.

[19] H. S. Shin and K. S. Soh, "Electrical method to detect a Bonghan duct inside blood vessels," *New Physics*, vol. 45, pp. 376–378, 2002 (Korean).

[20] B. C. Lee, K. Y. Baik, S. Cho, C. Min, H. M. Johng, and J. Hahm, "Comparison of intravascular Bonghan ducts from rats and mice," *Korean Journal of Oriental Preventive Medical Society*, vol. 7, pp. 47–53, 2003.

[21] K. Y. Baik, B. C. Lee, H. M. Johng, T. J. Nam, B. Sung, and K. S. Soh, "Long threadlike structure inside the blood vessels of rats," *The Newest Medical Journal*, vol. 47, pp. 18–22, 2004.

[22] J. S. Yoo, M. S. Kim, V. Ogay, and K. S. Soh, "In vivo visualization of Bonghan ducts inside blood vessels of mice by using an Alcian blue staining method," *Indian Journal of Experimental Biology*, vol. 46, no. 5, pp. 336–339, 2008.

[23] B. C. Lee, K. Y. Baik, H. M. Johng, B. Sung, K. Soh, and D. I. Kang, "Fluorescent method for observing intravascular Bonghan duct," *Journal of the Korean Institute of Herbal Acupuncture*, no. 8, pp. 5–9, 2005.

[24] B. C. Lee and K. S. Soh, "Contrast-enhancing optical method to observe a Bonghan duct floating inside a lymph vessel of a rabbit," *Lymphology*, vol. 41, no. 4, pp. 178–185, 2008.

[25] C. Lee, S. K. Seol, B. C. Lee, Y. K. Hong, J. H. Je, and K. S. Soh, "Alcian blue staining method to visualize Bonghan threads inside large caliber lymphatic vessels and X-ray microtomography to reveal their microchannels," *Lymphatic Research and Biology*, vol. 4, no. 4, pp. 181–189, 2006.

[26] H. M. Johng, J. S. Yoo, T. J. Yoon et al., "Use of magnetic nanoparticles to visualize threadlike structures inside lymphatic vessels of rats," *Evidence-Based Complementary and Alternative Medicine*, vol. 4, no. 1, pp. 77–82, 2007.

[27] B. C. Lee and K. S. Soh, "Visualization of acupuncture meridians in the hypodermis of rat using trypan blue," *Journal of Acupuncture and Meridian Studies*, vol. 3, no. 1, pp. 49–52, 2010.

[28] B. C. Lee, K. H. Bae, G. J. Jhon, and K. S. Soh, "Bonghan system as mesenchymal stem cell niches and pathways of macrophages in adipose tissues," *Journal of Acupuncture and Meridian Studies*, vol. 2, no. 1, pp. 79–82, 2009.

[29] H. S. Lee and B. C. Lee, "Visualization of the network of primo vessels and primo nodes above the pia mater of the brain and spine of rats by using Alcian blue," *Journal of Acupuncture and Meridian Studies*, vol. 5, no. 5, pp. 218–225, 2012.

[30] B. C. Lee, K. W. Kim, and K. S. Soh, "Visualizing the network of bonghan ducts in the omentum and peritoneum by using trypan blue," *Journal of Acupuncture and Meridian Studies*, vol. 2, no. 1, pp. 66–70, 2009.

[31] B. C. Lee, Z. D. Su, B. Sung et al., "Network of the primo vascular system in the rat hypodermis," in *The Primo Vascular System*, K. S. Soh, K. A. Kang, and K. Harrison David, Eds., pp. 139–146, Springer, New York, NY, USA, 2011.

[32] R. Schleip, W. Klingler, and F. Lehmann-Horn, "Active fascial contractility: fascia may be able to contract in a smooth muscle-like manner and thereby influence musculoskeletal dynamics," *Medical Hypotheses*, vol. 65, no. 2, pp. 273–277, 2005.

[33] Z. F. Jia, B. C. Lee, K. H. Eom et al., "Fluorescent nanoparticles for observing primo vascular system along sciatic nerve," *Journal of Acupuncture and Meridian Studies*, vol. 3, no. 3, pp. 150–155, 2010.

[34] K. H. Eom, *Imaging of the primo vascular system in the conception vessel line by using fluorescent nanoparticles, [M.S. thesis]*, Seoul National University, Seoul, Korea, 2010.

[35] H. J. Han, B. Sung, V. Ogay, and K. S. Soh, "The flow path of alcian blue from the acupoint BL23 to the surface of abdominal organs," *Journal of Acupuncture and Meridian Studies*, vol. 2, no. 3, pp. 182–189, 2009.

[36] B. C. Lee, J. S. Yoo, K. Y. Baik, B. Sung, J. Lee, and K. S. Soh, "Development of a fluorescence stereomicroscope and observation of Bong-Han corpuscles inside blood vessels," *Indian Journal of Experimental Biology*, vol. 46, no. 5, pp. 330–335, 2008.

[37] Y. I. Noh, M. Rho, Y. M. Yoo, S. J. Jung, and S. S. Lee, "Isolation and morphological features of primo vessels in rabbit lymph vessels," *Journal of Acupuncture and Meridian Studies*, vol. 5, no. 5, pp. 201–205, 2012.

[38] J. Lim, J. H. Jung, S. Lee et al., "Estimating the density of fluorescent nanoparticles in the primo vessels in the fourth ventricle and the spinal cord of a rat," *Journal of Biomedical Optics*, vol. 16, no. 11, pp. 116010–116017, 2011.

[39] H. S. Shin, H. Johng, B. C. Lee et al., "Feulgen reaction study of novel threadlike structures on the surface of rabbit livers," *The Anatomical Record B*, vol. 284, no. 1, pp. 35–40, 2005.

[40] M. H. Nam, J. Lim, S. H. Choi, S. Kim, and K. S. Soh, "A primo vascular system underneath the superior sagittal sinus in the brain of a rabbit," *Journal of Acupuncture and Meridian Studies*, vol. 5, no. 5, pp. 210–217, 2012.

[41] X. Liu, "Validating research on Kim Bong-Han's meridian phenomenon," *Acupunture Research*, vol. 34, no. 5, pp. 353–354, 2009 (Chinese).

[42] B. C. Lee, Z. D. Su, B. Sung et al., "Comparison of the primo vascular system with a similar-looking structure," in *The Primo Vascular System*, K. S. Soh, K. A. Kang, and D. K. Harrison, Eds., pp. 107–112, Springer, New York, NY, USA, 2011.

[43] B. C. Lee, K. Y. Baik, H. M. Johng et al., "Acridine orange staining method to reveal the characteristic features of an intravascular threadlike structure," *Anatomical Record B*, vol. 278, no. 1, pp. 27–30, 2004.

[44] S. Lee, Y. Ryu, Y. Yun et al., "Anatomical Discrimination of the Differences Between Torn Mesentery Tissue and Internal Organ-surface Primo-vessels," *Journal of Acupuncture and Meridian Studies*, vol. 3, no. 1, pp. 10–15, 2010.

[45] Z. F. Jia, K. S. Soh, Q. Zhou, B. Dong, and W. H. Yu, "Study of novel threadlike structures on the intestinal fascia of dogs," *Journal of Acupuncture and Meridian Studies*, vol. 4, no. 2, pp. 98–101, 2011.

[46] J. S. Yoo, M. Hossein Ayati, H. B. Kim, W. B. Zhang, and K. S. Soh, "Characterization of the primo-vascular system in the abdominal cavity of lung cancer mouse model and its differences from the lymphatic system," *PLoS ONE*, vol. 5, no. 4, Article ID e9940, 2010.

[47] C. Heo, M. Y. Hong, A. Jo, Y. H. Lee, and M. Suh, "Study of the primo vascular system utilizing a melanoma tumor model in a green fluorescence protein expressing mouse," *Journal of Acupuncture and Meridian Studies*, vol. 4, no. 3, pp. 198–202, 2011.

[48] M. A. Islam, S. D. Thomas, K. J. Sedoris, S. P. Slone, H. Alatassi, and D. M. Miller, "Tumor-associated primo vascular system is derived from xenograft, not host," *Experimental and Molecular Pathology*, vol. 94, no. 1, pp. 84–90, 2013.

[49] Y. Q. Li, B. Zhu, P. J. Rong, H. Ben, and Y. H. Li, "Effective regularity in modulation on gastric motility induced by different acupoint stimulation," *World Journal of Gastroenterology*, vol. 12, no. 47, pp. 7642–7648, 2006.

[50] B. S. Kwon, C. M. Ha, S. Yu, B. C. Lee, J. Y. Ro, and S. Hwang, "Microscopic nodes and ducts inside lymphatics and on the surface of internal organs are rich in granulocytes and secretory granules," *Cytokine*, vol. 60, no. 2, pp. 587–592, 2012.

[51] M. Stefanov and J. Kim, "Primo vascular system as a new morphofunctional integrated system," *Journal of Acupuncture and Meridian Studies*, vol. 5, no. 5, pp. 193–200, 2012.

[52] B. C. Lee, J. S. Yoo, V. Ogay et al., "Electron microscopic study of novel threadlike structures on the surfaces of mammalian organs," *Microscopy Research and Technique*, vol. 70, no. 1, pp. 34–43, 2007.

[53] S. Y. Jung, S. K. Min, B. Sung et al., "Cribriform structure with channels in the acupuncture meridian-like system on the organ surfaces of rabbits," *Acupuncture and Electro-Therapeutics Research*, vol. 32, no. 1-2, pp. 130–132, 2007.

[54] V. Ogay, K. H. Bae, K. W. Kim, and K. S. Soh, "Comparison of the characteristic features of Bonghan ducts, blood and lymphatic capillaries," *Journal of Acupuncture and Meridian Studies*, vol. 2, no. 2, pp. 107–117, 2009.

[55] C. Lee, J. S. Yoo, H. H. Kim, J. Kwon, and K. S. Soh, "Flow of nanoparticles inside organs-surface Bonghan ducts," in *Proceedings of the 23rd Symposium Korean Society Jungshin Science*, pp. 129–134, 2005.

[56] S. G. Yu and B. Xu, *Science of Experimental Acupuncture*, People's Medical Publishing House, Beijing, China, 2012.

[57] S. J. Cho, S. H. Lee, W. Zhang et al., "Mathematical distinction in action potential between primo-vessels and smooth muscle," *Evidence-Based Complementary and Alternative Medicine*, vol. 2012, Article ID 269397, 6 pages, 2012.

[58] S. H. Park, B. C. Lee, C. J. Choi et al., "Bioelectrical study of bonghan corpuscles on organ surfaces in rats," *Journal of the Korean Physical Society*, vol. 55, no. 2, pp. 688–693, 2009.

[59] J. H. Choi, T. H. Han, C. J. Lim, S. Y. Lee, and P. D. Ryu, "Basic electrophysiological properties of cells in the organ surface primo vascular tissues of Rats," in *The Primo Vascular System*, K. S. Soh, K. A. Kang, and K. Harrison David, Eds., pp. 243–249, Springer, New York, NY, USA , 2011.

[60] X. Wang, H. Shi, H. Shang et al., "Are primo vessels (PVs) on the surface of gastrointestine involved in regulation of gastric motility induced by stimulating acupoints ST36 or CV12?" *Evidence-Based Complementary and Alternative Medicine*, vol. 2012, Article ID 787683, 8 pages, 2012.

[61] J. L. Soo, B. C. Lee, H. N. Chang et al., "Proteomic analysis for tissues and liquid from Bonghan ducts on rabbit intestinal surfaces," *Journal of Acupuncture and Meridian Studies*, vol. 1, no. 2, pp. 97–109, 2008.

[62] H. M. Langevin, D. L. Churchill, and M. J. Cipolla, "Mechanical signaling through connective tissue: a mechanism for the therapeutic effect of acupuncture," *FASEB Journal*, vol. 15, no. 12, pp. 2275–2282, 2001.

[63] H. M. Langevin, N. A. Bouffard, G. J. Badger, D. L. Churchill, and A. K. Howe, "Subcutaneous tissue fibroblast cytoskeletal remodeling induced by acupuncture: evidence for a mechanotransduction-based mechanism," *Journal of Cellular Physiology*, vol. 207, no. 3, pp. 767–774, 2006.

Hindawi Publishing Corporation
Evidence-Based Complementary and Alternative Medicine
Volume 2013, Article ID 949245, 6 pages
http://dx.doi.org/10.1155/2013/949245

Research Article

Primo Vascular System Accompanying a Blood Vessel from Tumor Tissue and a Method to Distinguish It from the Blood or the Lymph System

Jaekwan Lim,[1] Sungwoo Lee,[1] Zhendong Su,[2] Hong Bae Kim,[1] Jung Sun Yoo,[1] Kwang-Sup Soh,[1] Sungchul Kim,[3] and Yeon Hee Ryu[4]

[1] *Nano-Primo Research Center, Advanced Institutes of Convergence Technology, Seoul National University, Suwon 443-270, Republic of Korea*
[2] *Chinese Traditional Veterinary Laboratory, Department of Animal Medicine, Northeast Agriculture University, Harbin 150-030, China*
[3] *Center of Amyotrophic Lateral Sclerosis, Wonkwang University Hospital, Gwangju 503-310, Republic of Korea*
[4] *Department of Acupuncture, Korea Institute of Oriental Medicine, Daejeon 305-811, Republic of Korea*

Correspondence should be addressed to Sungchul Kim; kscndl@hanmail.net and Yeon Hee Ryu; yhryu@kiom.re.kr

Received 24 December 2012; Accepted 17 March 2013

Academic Editor: Byung-Cheon Lee

A primo vessel was observed in the abdominal cavity in the lung cancer mouse model, and its function as an extra metastatic path was observed. In this work, we found a primo vessel accompanying a blood vessel emanating from a tumor in the skin. We also presented simple and efficient criteria to distinguish a primo vessel from a blood or a lymph vessel and from a nerve. The criteria for using DAPI and Phalloidin will be useful in clinical situations to find and identify the primo vessels among the blood vessels, lymph vessels, or nerves in the tissue surrounding a tumor such as a melanoma or breast cancer.

1. Introduction

Primo vessels were recently reported as additional paths of cancer metastasis besides blood or lymph vessels [1–3]. They were originally found as a novel circulatory system corresponding to acupuncture meridians [4]. Even though primo vessels accompanying blood vessels were expected from the general theory of primo vessels [5], none had previously been observed in the area of a tumor.

In this paper, we present a simple method to observe primo vessels accompanying blood vessels emerging out of tumor tissue by using a staining technique with Phalloidin and $4'$, 6-diamidino-2-phenylindole (DAPI). This method was effectively used to distinguish primo vessels from blood vessels or lymph vessels in the mesentery of mice [6] and was partially used in earlier work [3]. Phalloidin shows the F-actin distribution of cells, and DAPI reveals the shape of the nuclei. Blood, lymph, and primo vessels turn out to show distinctive patterns in Phalloidin and DAPI images [3, 6]. We specifically studied the primo vessels and the blood vessels in the myofascia under the hypodermis around a tumor that was xenografted into the dorsal skin of a nude mouse.

A primo vessel is transparent and too thin to be detected with a stereomicroscope. Ordinary histological examination with hematoxylin and eosin is not effective in revealing this novel structure, because the structure is filled with collagenous fibers and is indistinguishable from the surrounding connective tissue. Therefore, our technique should be very useful for detecting this elusive novel conduit of cancer metastasis. It is especially convenient to distinguish a primo vessel from lymph vessels without having to use the time-consuming immunohistochemical method of LYVE-1 to make the distinction, which was essential in previous work [3].

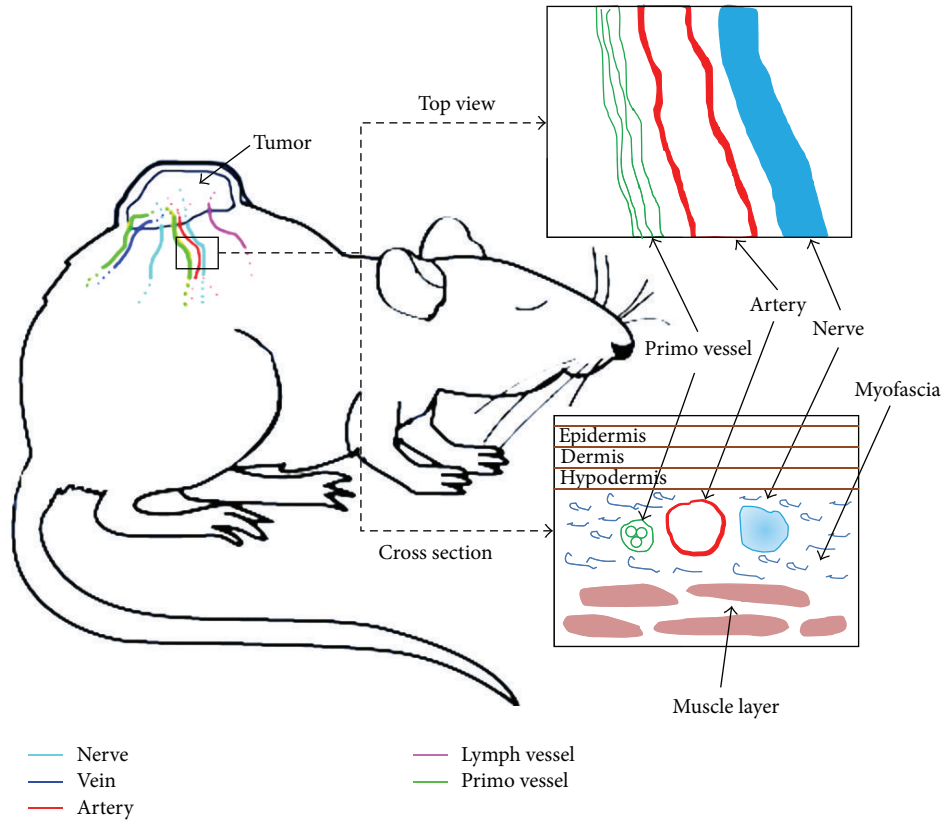

Figure 1: Illustration of primo vessels observed along a blood vessel. A primo vessel was found with a blood vessel or a nerve bundle inside the myofascia of the skin. The surrounding tissue around a xenografted tumor in the skin of the dorsal lumbar area (the boxed region near the tumor) was illustrated with the top view and the cross-sectional view. The nerve, artery, and primo vessel in the myofascia on the muscle layer were shown by arrows. The myofascia became thicker and squishier compared to normal skin.

2. Materials and Methods

2.1. Cell Culture. NCI-H460 human lung cancer cells were purchased from the Korean Cell Line Bank (Seoul, Republic of Korea). Cancer cells were cultured in a RPMI-1640 medium (GIBCO, USA) supplemented with 1% penicillin-streptomycin and 10% fetal bovine serum (GIBCO, USA). Cancer cells were incubated in 95% air and 5% CO_2 at 37°C.

2.2. Animal Cancer Model. Female athymic nude mice (BALB-c-nu/nu, 5 weeks, weight = 15–20 g; DooYeol Biotech, Seoul, Republic of Korea) were used. The mice were inoculated subcutaneously in the dorsal skin with 2×10^6 NCI-H460 human lung cancer cells (in a 0.2-mL RPMI-1640 medium) to form tumors under the skin. All research involving the animals was approved by the Institute of Laboratory Animal Resources of Seoul National University.

2.3. Method to Find a Primo Vessel around a Tumor. After four to eight weeks of inoculation of the cancer cells, the mouse was anesthetized using a Zoletil/Rompun intraperitoneal (IP) injection. The epidermis, dermis, and hypodermis around the tumor tissue were incised carefully at 3~5 mm from the boundary of the tumor tissue under a stereomicroscope (SZX12, Olympus, Japan). We tried to find a primo vessel along the blood vessel, but it was almost impossible to find a primo vessel under the stereomicroscope without any special treatment. The distribution of primo, blood, and lymph vessels and nerves was photographed with a CCD camera (DP70, Olympus, Japan). Several parts of primo, blood, and lymph vessels and nerves in the myofascia around the tumor tissue were taken and fixed in 10% neutral buffered formalin (NBF) for 1 hour to prevent DNA from flowing out of the nuclei during long Phalloidin treatment. After fixation, samples were stained with Alexa Fluor 568 Phalloidin (Molecular Probes, USA) for more than 15 hours and were then treated with Prolong Gold Antifade Reagent with DAPI (Molecular Probes, USA) for 2 hours to counterstain for nuclei. Finally, samples were mounted with a cover slip and photographed with a phase-contrast fluorescent microscope and a CCD camera with the inscribed scale bar. The diameters of the blood vessel, lymph vessel, nerve, and the primo vessel were measured with the scale bar.

3. Results

As illustrated in Figure 1, well-developed blood vessels, lymph vessels, primo vessels, and nerves emanated from the tumor tissue on the dorsal skin of a nude mouse. We studied

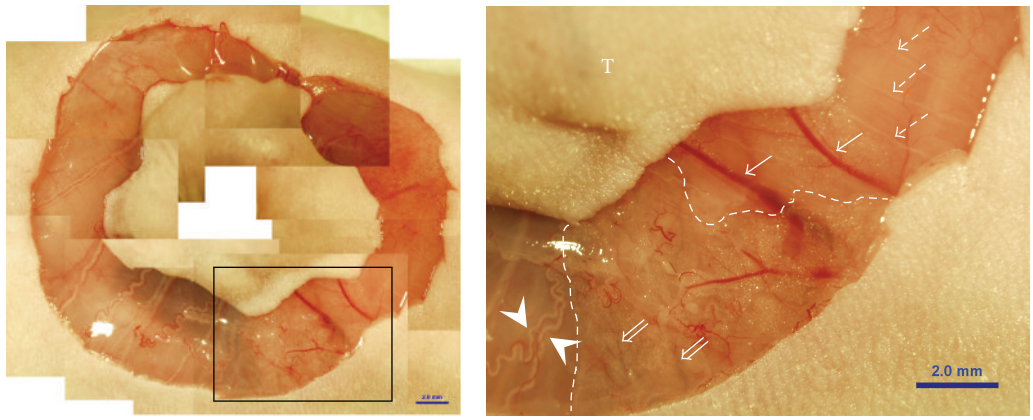

(a) (b)

Figure 2: Stereoscopic image of a tumor and its surrounding area. (a) The skin was incised, and blood, lymph, and nerves in the myofascia were exposed. The rectangular area is magnified in (b). (b) Blood vessels (arrows), lymph vessels (double arrows), nerves (dotted arrows), and bundles of blood vessels and nerves (arrowheads) are seen connected to tumor tissue. They came out from the tumor (T) in radial direction. A lymphatic network that develops in adipose tissue (area between the dotted lines) can also be seen. Primo vessels accompanying blood vessels were not detectable with a stereomicroscopic image.

Table 1: Size of tumors, blood vessels, lymph vessels, primo vessels, and nerves.

Subject no.	Shape and size of tumor (cm, width × length × height)	Diameter of blood vessel (μm)	Diameter of lymph vessel (μm)	Diameter of primo vessel (μm)	Diameter of nerve (μm)	Site of primo vessel
1	Not recorded	190	60	20	120	Along BV
2	Oval shape (2.5 × 3.0 × 2.5)	40	×	20	150	Along BV
3	Irregular shape (3.5 × 2.5 × 2.0)	160	×	10	×	Along BV
4	Irregular shape (3.1 × 2.8 × 1.0)	25	100	15	110	Along BV
5	Irregular shape (2.6 × 2.4 × 1.5)	30	×	10	320	Along BBN
6	Irregular shape (not recorded)	110	×	16	390	Along BBN

×: not observed; BV: blood vessel; BBN: bundle of blood vessel-nerve.

these vessels and nerves in the myofascia covering the muscle layer under the skin.

The skin around the tumor was incised, and the myofascia layer was exposed, as shown in the stereomicroscopic image in Figure 2(a). The rectangular area in Figure 2(a) was magnified (Figure 2(b)) to reveal the blood vessels (*arrows*), lymph vessels (*double arrows*), nerves (*dotted arrows*), and a bundle of blood vessels and nerves (*arrowheads*). Primo vessels were not detectable with a stereomicroscope.

As shown in Table 1, we studied six mice and observed the primo vessels accompanying blood vessels or bundles of blood vessels and nerves. The diameters of the primo vessels were rather uniform and were in the range of 10–20 μm.

The DAPI and Phalloidin techniques [6], which can distinguish a primo vessel from a blood or a lymph vessel, were applied to detect the primo vessel, as shown in Figure 3. The blood vessels (*dotted arrows*) showed transverse patterns, whereas the primo vessels (*arrows*) had longitudinal patterns of Phalloidin stains (Figure 3(a)). In addition, the longitudinal alignment of the rod-shaped nuclei in the primo vessels is a clear indicator to distinguish a primo vessel from a blood vessel, as shown in Figures 3(b), 3(c), and 3(d). The rod-shaped nuclei (*arrows*) are distinct in the magnified view (Figure 3(d)) of the merged image of the Phalloidin and the DAPI signals (Figure 3(c)).

The Phalloidin and the DAPI images of a lymph vessel are presented in Figure 4. The Phalloidin pattern and irregular nuclei distribution are manifestly different from those of blood and primo vessels. Nerves showed less F-actin distribution (Figure 5(a)) and some longitudinally distributed nuclei (Figure 5(b)). Nerves can be easily distinguished from blood, lymph, or primo vessels with a stereomicroscope.

The current work did not provide immunofluorescence proof that the primo vessel was different from blood or lymph vessels, because this was already provided in previous work [2, 3]. Nevertheless, for reader convenience, we provided a CD31 and LYVE-1 test of the primo vessels, arteries, veins, and lymph nodes as in the Supplementary Information (see Figures S1 and S2 available online at http://dx.doi.org/10.1155/2013/949245).

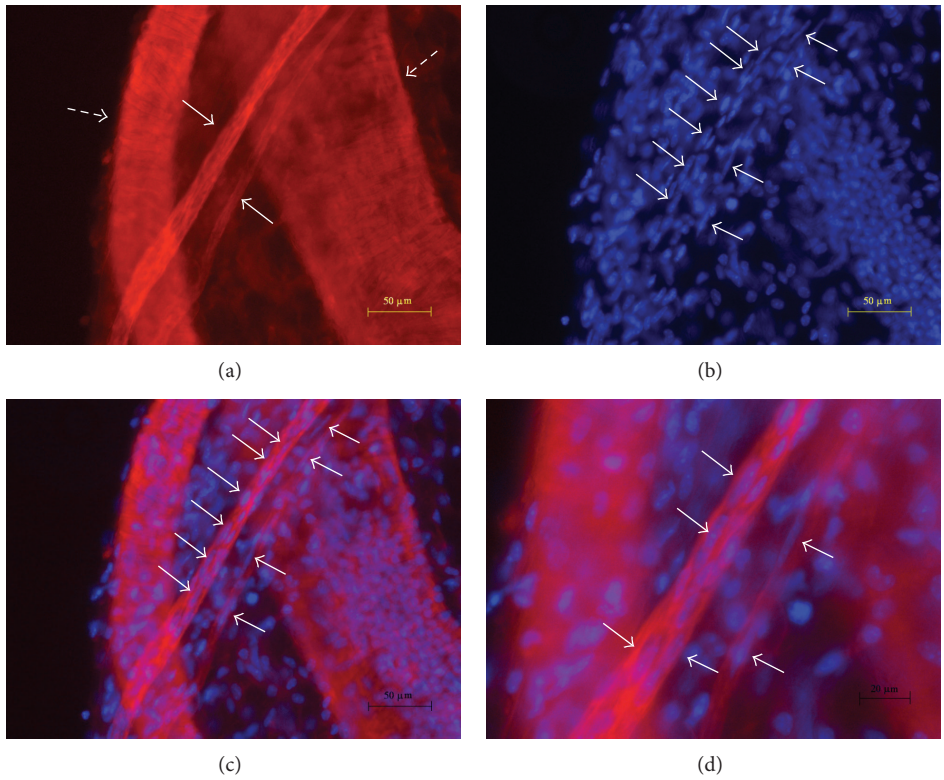

(a) (b)

(c) (d)

Figure 3: Images of blood vessels with accompanying primo vessels stained with DAPI and Phalloidin. (a) Fluorescent images of primo vessels (arrows) and blood vessels (dotted arrows) stained with Phalloidin. Blood vessels have a smooth muscle structure, whose Phalloidin signal pattern of F-actins had many transversal components to the blood vessel direction. The pattern of F-actins of the two primo vessels (arrows) was only longitudinal and therefore distinct from the patterns of the blood vessels. (b) Fluorescent image of the same sample as that in (a) with DAPI staining of nuclei. Primo vessels have rod-shaped nuclei (arrows). (c) A merged image of (a) and (b). (d) A magnified view of (c). Rod-shaped nuclei (arrows) are clearly seen in the primo vessels which are demonstrably different from the nearby blood vessels.

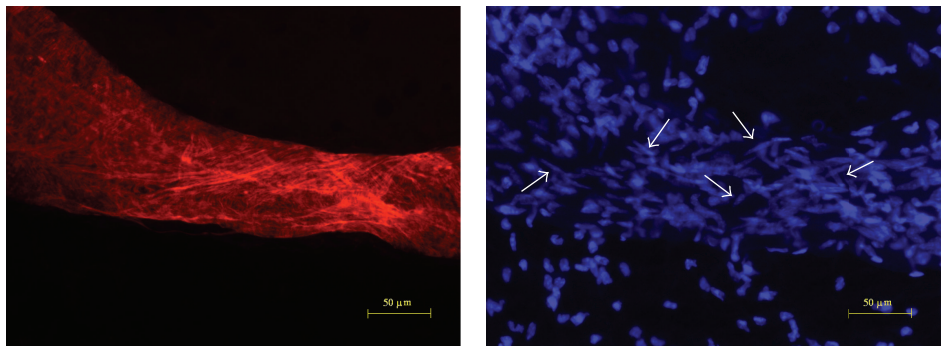

(a) (b)

Figure 4: DAPI and Phalloidin images of a lymph vessel. The patterns of red-stained F-actins shown by Phalloidin (a) and blue-stained nuclei shown by DAPI (b) of a lymph vessel were irregular and readily distinguishable from blood vessels or primo vessels.

4. Discussion

The purpose of this study was to present simple and efficient criteria to discern primo vessels from blood vessels, lymph vessels, and nerves in the myofascia under the skin around a tumor. In previous work [1–3], primo vessels were observed in the abdominal cavity or on the surface of the hypodermis of a xenografted tumor in a mouse or rat but not in the pathologically developed, thick, and squashy myofascia that developed around the tumor. The rationale is based upon our previous work of immunofluorescence analysis verifying the primo vessels amongst blood vessels and lymph vessels [2, 3].

We confirmed the existence of primo vessels near the adventitia of blood vessels emerging from tumor tissue. These primo vessels could be distinguished from blood or lymph vessels using simple techniques of staining with Phalloidin

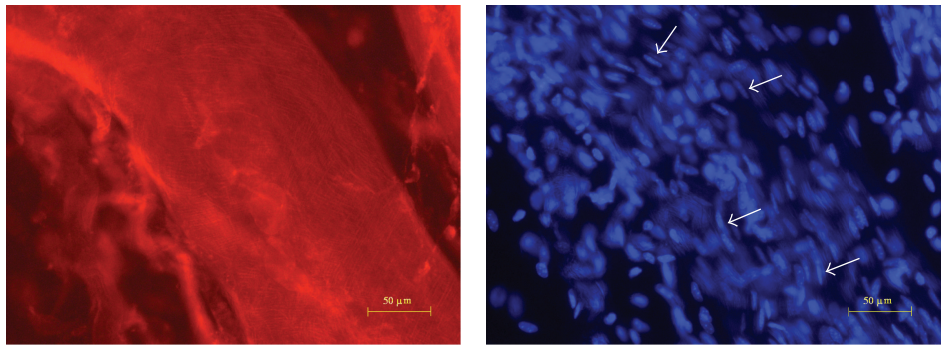

(a) (b)

Figure 5: DAPI and Phalloidin images of a nerve. The F-actin distribution (a) of the nerve is much less than that of blood or primo vessels. The nuclei distribution is denser than that of primo vessels. Nuclei (blue) are of various shapes and scattered around, while the nuclei of a primo vessel is mainly rod-shaped and arranged in broken lines.

and DAPI and reading the resultant patterns. This new technique is different from the Trypan blue method, which until now was the only published method to find and identify the primo vessels. The Trypan blue technique is applicable only to live tissue and therefore is limited to *in vivo* situations. The current technique with Phalloidin and DAPI is applicable to tissue samples whether or not they are biologically fixed. This new technique can be useful in dealing with clinical melanoma or breast cancer situations where tissues around a tumor are available for examination of metastasis through blood, lymph, or primo vessels.

The importance of blood vessels and angiogenesis in cancer biology, especially with respect to growth [7] and metastasis [8, 9], does not need to be emphasized. However, no one has noticed the presence of another circulatory conduit near the adventitia of blood vessels. The suggested functions of the primo vessels, in general, include a path for neurotransmitter hormones [10], a circulatory path [11] for primo-fluid-containing stem-cell-like microcells [12], and proteins related to stem cell differentiation [13]. Evidence also exists for cancer metastasis through the primo vessel [2]. These functions may have some relevancy in the primo vessel accompanying a blood vessel emerging from tumor tissue. A blood vessel with accompanying primo vessels may be more active in metastasis than previously understood.

Our research may remind readers of the discovery by Hendrix of vasculogenic mimicry [14] which is a new conduit different from blood or lymph vessels related to cancer events. This vessel was formed by a reversion of tumor cells to an undifferentiated phenotype and recapitulated embryonic vasculogenesis. Elucidating the relationship between primo vessels and vasculogenic mimicry as networks between the inside and the outside of tumor tissue remains to be done.

In conclusion criteria to find and identify by using Phalloidin and DAPI staining the primo vessels that were developed along the blood vessels emanating from a tumor tissue in the myofascia underneath mouse skin were presented. This method was based upon the different patterns of nuclei and F-actin distribution in the primo vessels, blood vessels, lymph vessels, and nerves.

Acknowledgments

This work was supported in part by a Grant from the Traditional Korean Medicine R&D Project, Ministry for Health and Welfare, Republic of Korea (B110076), and Department of Acupuncture, Republic of Korea Institute of Oriental Medicine, Daejeon, Korea (K12272).

References

[1] J. S. Yoo, H. B. Kim, V. Ogay, B. C. Lee, S. Ahn, and K. S. Soh, "Bonghan ducts as possible pathways for cancer metastasis," *Journal of Acupuncture and Meridian Studies*, vol. 2, no. 2, pp. 118–123, 2009.

[2] J. S. Yoo, H. B. Kim, N. Won et al., "Evidence for an additional metastatic route: in vivo imaging of cancer cells in the primo-vascular system around tumors and organs," *Molecular Imaging and Biology*, vol. 13, no. 3, pp. 471–480, 2011.

[3] J. S. Yoo, M. H. Ayati, H. B. Kim, W. B. Zhang, and K. S. Soh, "Characterization of the primo-vascular system in the abdominal cavity of lung cancer mouse model and its differences from the lymphatic system," *PLoS ONE*, vol. 5, no. 4, Article ID e9940, 2010.

[4] B. H. Kim, "On the Kyungrak system," *J. Academy of Medical Sciences of the Democratic People's Republic of Korea*, vol. 90, pp. 1–41, 1963.

[5] K. S. Soh, "Bonghan circulatory system as an extension of acupuncture meridians," *Journal of Acupuncture and Meridian Studies*, vol. 2, no. 2, pp. 93–106, 2009.

[6] P. An, J. Dai, Z. Su et al., "Putative primo-vascular system in mesentery of rats," *Journal of Acupuncture and Meridian Studies*, vol. 3, no. 4, pp. 232–240, 2010.

[7] J. Folkman, "The role of angiogenesis in tumor growth," *Seminars in Cancer Biology*, vol. 3, no. 2, pp. 65–71, 1992.

[8] L. A. Liotta, P. S. Steeg, and W. G. Stetler-Stevenson, "Cancer metastasis and angiogenesis: an imbalance of positive and negative regulation," *Cell*, vol. 64, no. 2, pp. 327–336, 1991.

[9] N. Weidner, J. P. Semple, W. R. Welch, and J. Folkman, "Tumor angiogenesis and metastasis—correlation in invasive breast carcinoma," *The New England Journal of Medicine*, vol. 324, no. 1, pp. 1–8, 1991.

[10] J. Kim, V. Ogay, B. C. Lee et al., "Catecholamine-producing novel endocrine organ: bonghan system," *Medical Acupuncture*, vol. 20, no. 2, pp. 97–102, 2008.

[11] B. Sung, M. S. Kim, B. C. Lee et al., "Measurement of flow speed in the channels of novel threadlike structures on the surfaces of mammalian organs," *Naturwissenschaften*, vol. 95, no. 2, pp. 117–124, 2008.

[12] K. Y. Baik, V. Ogay, S. C. Jeoung, and K. S. Soh, "Visualization of bonghan microcells by electron and atomic force microscopy," *Journal of Acupuncture and Meridian Studies*, vol. 2, no. 2, pp. 124–129, 2009.

[13] S. J. Lee, B. C. Lee, C. H. Nam et al., "Proteomic analysis for tissues and liquid from bonghan ducts on rabbit intestinal surfaces," *Journal of Acupuncture and Meridian Studies*, vol. 1, no. 2, pp. 97–109, 2008.

[14] A. J. Maniotis, R. Folberg, A. Hess et al., "Vascular channel formation by human melanoma cells in vivo and in vitro: vasculogenic mimicry," *The American Journal of Pathology*, vol. 155, no. 3, pp. 739–752, 1999.

Hindawi Publishing Corporation
Evidence-Based Complementary and Alternative Medicine
Volume 2013, Article ID 205951, 10 pages
http://dx.doi.org/10.1155/2013/205951

Research Article

Discovery of Endothelium and Mesenchymal Properties of Primo Vessels in the Mesentery

An Ping,[1] Su Zhendong,[2] Dai Jingxing,[3] Liu Yaling,[1] Kyung-Hee Bae,[4] Tan Shiyun,[1] Luo Hesheng,[1] Kwang-Sup Soh,[4] Yeon Hee Ryu,[5] and Sungchul Kim[6]

[1] *Renmin Hospital of Wuhan University, Wuhan 430-060, China*
[2] *Chinese Traditional Veterinary Laboratory, Department of Animal Medicine, Northeast Agriculture University, Harbin 150-030, China*
[3] *Department of Human Anatomy, Southern Medical University, Guangzhou 510-515, China*
[4] *Nano Primo Research Center, Advanced Institutes of Convergence Technology, Seoul National University, Suwon 443-270, Republic of Korea*
[5] *Department of Acupuncture, Korea Institute of Oriental Medicine, Daejeon 305-811, Republic of Korea*
[6] *Center of Amyotrophic Lateral Sclerosis, Wonkwang University Hospital, Gwangju 503-310, Republic of Korea*

Correspondence should be addressed to Yeon Hee Ryu; yhryu@kiom.re.kr and Sungchul Kim; kscndl@hanmail.net

Received 27 November 2012; Revised 22 January 2013; Accepted 30 January 2013

Academic Editor: M. Isabel Miguel Perez

Recent evidences demonstrated that endothelial-to-mesenchymal transition (EndMT) has a crucial role in cancer and is recognized as a unique source of cancer-associated fibroblasts (CAFs). Primo vascular system (PVS) is a new circulatory system which may play an important role in cancer metastasis and regeneration. In the current study, we applied previously established time-saving method to identify primo vessels and further investigated the immunocytochemical properties of primo vessels. Both primo vessels and primary primo vessel cells in the mesentery expressed endothelial markers and fibroblast markers. Double-labeling experiments demonstrated that endothelial and fibroblast markers are coexpressed in primo vessels. In addition, under the stimulation of TGF-β1 *in vitro,* primary primo vessel cells differentiated into fibroblasts. Therefore, we found that primo vessels in the mesentery had a transitional structure between endothelium and mesenchymal. This is a new finding of EndMT in normal postnatal animals.

1. Introduction

Recently, growing evidence manifested that endothelial cells could be triggered to acquire a mesenchymal phenotype (fibroblast-like cells and loss of cell-cell contacts), obtain mesenchymal biological properties (invasive and migratory capabilities), and gain mesenchymal markers [1–4]. These studies indicated that there existed a unique population of cells that coexpressed both endothelial marker CD31 (also known as platelet endothelial cell adhesion molecule-1 (PECAM-1)) and fibroblast markers, such as PDI, MTS1 (S100A4, also known as FSP1), and procollagen I. Researchers supposed that these recruit fibroblasts mainly arose from endothelial cells and categorized this process as endothelial-to-mesenchymal transition (EndMT). EndMT was first detected in embryonic heart development and later was observed in a variety of pathologic procedures, including cancer, chronic kidney fibrosis, cardiac fibrosis, chronic pulmonary hypertension, atherosclerosis, and wound healing [4–13]. Although the function and precise molecular mechanisms of EndMT in some postnatal diseases have not yet been determined, their determinant role in cancer was conclusively established. Now EndMT was recognized as a crucial source of cancer-associated fibroblasts (CAFs) which modulated cancer progression and played a definitive role in cancer metastasis, microenvironment and angiogenesis [4, 12, 14–21]. EndMT was a critical process and mechanism contributed to a setting of pathological diseases [5, 11, 22]. Does EndMT also occur in normal postnatal states? Till now, no answer can be found.

Primo Vascular System (PVS) is a new kind of circulatory system beyond vascular and lymphatic system [23]. On International Symposium of Primo Vascular System 2010 (ISPS2010), the functional role of PVS in cancer, especially in tumor metastasis, and regeneration was extensively discussed [24, 25]. In this work, we investigated cellular properties of the PVS in the mesentery with immunocytochemistry by studying the primo vessels and their primary cultured cells with endothelial and mesenchymal antibodies. In previous studies [23], there were much work with DAPI and phalloidin to establish the histological characteristics of PVS which we repeated in this work for searching and identifying the PVS in the mesentery specimens. Because thorough immunocytochemical study with the endothelial antibodies and mesenchymal antibodies to characterize the primo vessel was lacking, the EndMT was not noticed before. Furthermore, no study was ever performed with primary cultured cells of the PVS. By performing this study, we found not only the immunocytochemical properties of endothelial and mesenchymal cells of the PVS in the mesentery but also a novel case of EndMT in a normal postnatal animal.

Our study showed that primo vessels in the mesentery coexpressed endothelial markers (CD31, VE-cadherin, vWF) along with fibroblast markers (PDI, MTS1, procollagen I). Primary primo vessel cells also coexpressed these markers and showed a fibroblast-like phenotype. Further investigation revealed that over 14 days culture *in vitro*, primo vessel cells differentiated into fibroblasts and showed increased levels of collagen α1(I) mRNA and protein secretion. We deduced primo vessels in the mesentery as a unique structure consisting of EndMT cells. To our knowledge, this might be the first evidence to validate a transitional structure between endothelium and mesenchymal in normal postnatal animals. We believe that this discovery will enrich the recognition and concept of EndMT which maybe exist in normal tissues and conductive to angiogenesis.

2. Materials and Methods

2.1. Animals. Seven-week-old male and female Sprague-Dawley rats, weighing 200–250 g (Jung-Ang Laboratory Animal Company, Seoul, Korea), were used in this study. For each separate experiment, three rats of each gender were used. Animal care, maintenance, and surgery were performed in accordance with the international laws and policies of the Care and Use of Laboratory Animals, National Academy Press (1996).

2.2. Sample Preparation. Rats were anaesthetized with urethane (1.5 g/kg) (Sigma, MO) i.m., and then the abdomens were opened. Under a stereomicroscope (SZX12, Olympus, Japan), primo vessels in the mesentery between the colon and the root of mesentery and between the colon and the small intestine were carefully detected. Primo vessels with a characteristic appearance of semitransparent, white thread-like lines were taken out and were carefully checked under the stereomicroscope to avoid the involvement of vascular vessels and lymphatic vessels. For immunofluorescent study, vascular vessels and lymphatic vessels were chosen as controls. After embedding in OCT (Sakura Finetek, CA), all the tissues were rapidly frozen over liquid nitrogen and stored at −80°C until processed.

2.3. Phalloidin and DAPI Staining in Tissue Samples and Cryosections. To confirm the role of phalloidin combined with 4′,6-diamidino-2-phenylindole (DAPI) staining in distinguishing primo vessels from vascular vessels and lymphatic vessels, we performed phalloidin (Invitrogen, CA) and DAPI (Invitrogen, CA) staining in tissue samples and cryosections at first. The main procedure was as follows. Fresh tissues or 10 μm-thickness cryosections were fixed in 3.7% formaldehyde at room temperature (RT) for 10 min. After being washed with 0.1 M phosphate buffered saline (PBS) three times, the samples were further treated with 0.2% Triton-X100 for 5 min. Then, the tissues were washed in PBS and incubated with Alexa Fluor 568 phalloidin (1 : 50) for 2 h in the dark at room temperature (RT). After PBS washing, DAPI (0.1 mg/mL) was added and incubated for 30 min, and then tissues were mounted with prolong gold antifade reagent (Invitrogen, CA). Staining was analyzed independently by two investigators using a fluorescence microscope (BX51, Olympus, Japan).

2.4. Isolation of Primary Primo Vessel Cells and Cell Culture. Primary primo vessel cells were obtained from 7-week-old SD rats according to the following procedures. Briefly, primo vessels in the mesentery were gently washed three times with PBS, moved into a cell culture dish, and minced with a disposable surgery knife for approximately 2 min. Tissues were incubated in a solution of 1% collagenase type I (Sigma, MO) dissolved in Hank's balanced salt solution at 37°C for 2 h. Then, the suspension was centrifuged (1200 g for 3 min), and the cells were seeded in a six-well cell culture plate at the desired density (2.5 to 5 × 10^5 cells per well) and cultured in Dulbecco's modified Eagle's medium (DMEM, Gibco by Invitrogen, CA) supplemented with 10% fatal bovine serum (FBS, Gibco by Invitrogen, CA), 100 U/mL of penicillin (Gibco by Invitrogen, CA), and 100 μg/mL of streptomycin sulfate (Gibco by Invitrogen, CA) at 37°C in a 5% CO_2 incubation. After 30 min of incubation, suspension cells were removed, and adherent primo vessel cells were cultured in the above medium. Cell cultures were observed by phase contrast microscopy to verify growth, and viability was routinely checked by a trypan blue exclusion assay (Sigma, MO). Cultures showing viability over 95% were used. Culture medium was replaced every 3 d.

The murine fibroblast NIH3T3 cell line and the rat fibroblast BHK-21 cell line were chosen as controls in this study. They were obtained from SNU cell bank (Seoul, Korea) and were cultured in DMEM supplemented with 10% FBS, 100 U/mL of penicillin, and 100 μg/mL of streptomycin sulfate.

2.5. Immunohistochemistry and Phalloidin Staining. Tissue samples were cut into 10 μm longitudinal cryosections for

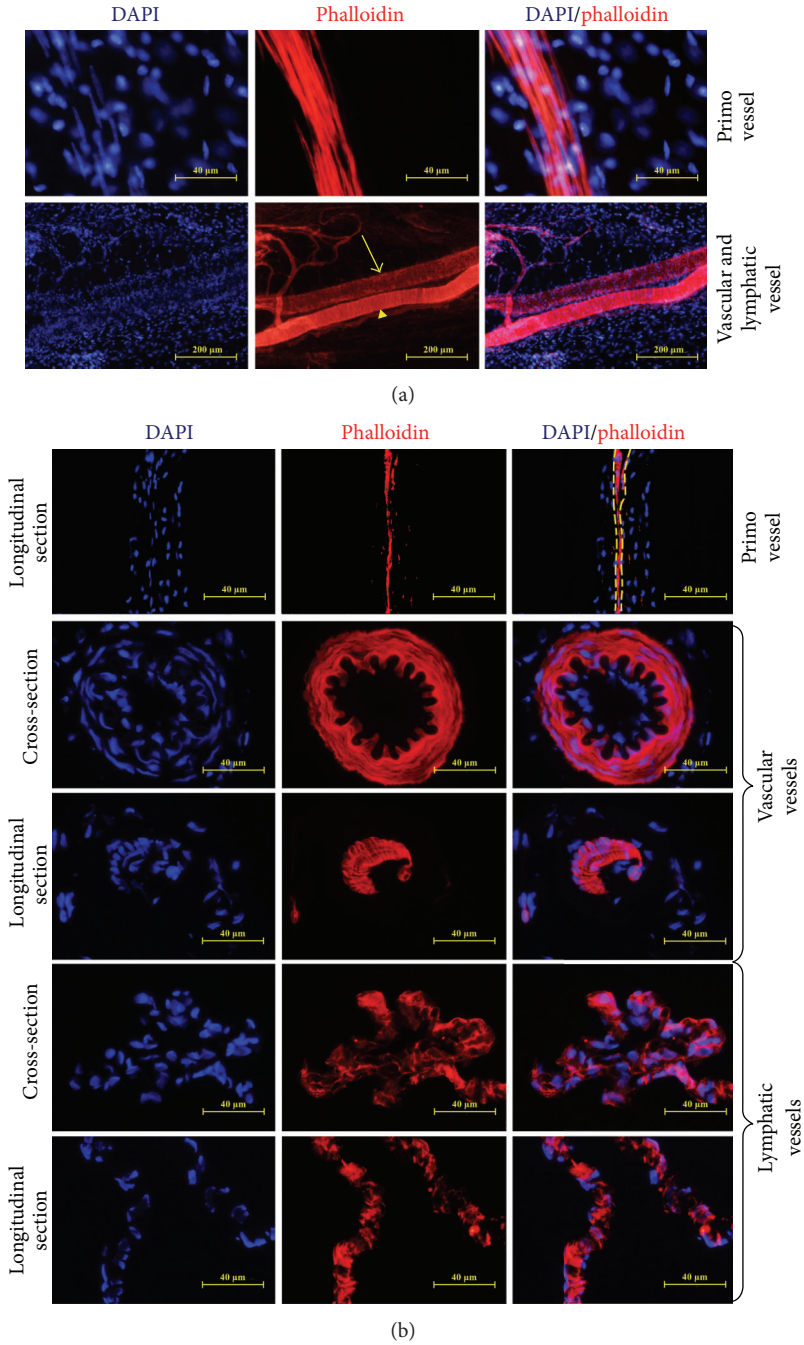

Figure 1: Primo vessels in the mesentery in fresh tissues and cryosections by phalloidin and DAPI staining. (a) The differences among primo vessels, vascular vessels, and lymphatic vessels. Primo vessels consist of phalloidin positive cells with characteristic rod-shaped nuclei, linear arrangements paralleling with the vessels. Vascular smooth muscle cells were also sensitive to phalloidin but showed thoroughly different appearances (yellow arrowheads). In lymphatic vessel, the endothelial cells formed the vessels in a network way (yellow arrows). (b) The differences among primo vessels, vascular vessels, and lymphatic vessels in cryosections. Phalloidin positive cells with rod-shaped nuclei; linear arrangements in longitudinal sections were primo vessels (yellow dashed area). Vascular vessels showed smooth muscular cells circulating the vessels and lymphatic vessels were formed in a network way.

immunofluorescence staining. In single staining, sections of primo vessels were rinsed in PBS and fixed in 4% PFA at 4°C for 10 min. After washing (3 × 10 min in PBS), fixed sections were permeabilized with 0.1% Triton X-100 in PBS for 15 min. Nonspecific binding was blocked by incubation with serum solution for 2 h at room temperature. Then, sections were incubated with primary antibodies overnight at 4°C at the following dilutions: monoclonal anti-CD31 antibody (mouse

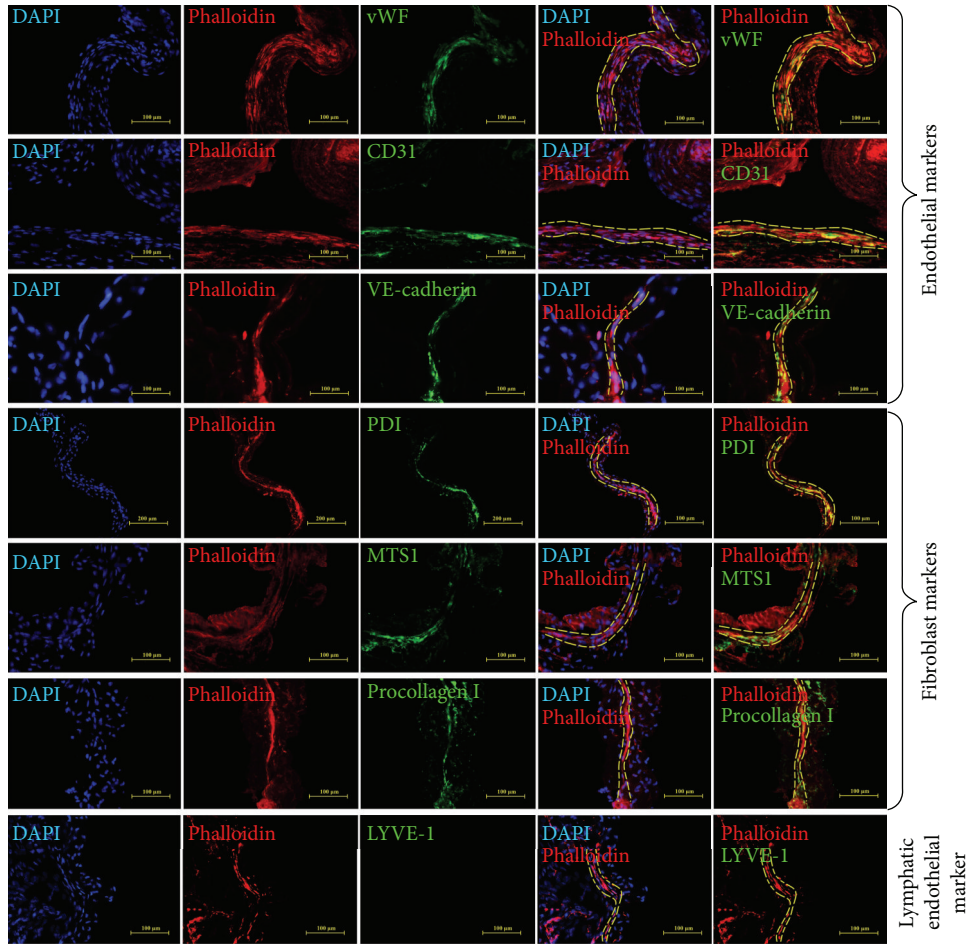

Figure 2: Immunofluorescent staining of primo vessels in the mesentery with endothelial markers, fibroblast markers, and phalloidin in longitudinal sections. Endothelial and fibroblast markers expressed in primo vessels in the mesentery. Antibodies to endothelial markers (vWF, CD31, VE-cadherin), fibroblast markers (PDI, MST1, procollagen I), and lymphatic endothelial marker (LYVE-1) (green) were used. DAPI (blue) and phalloidin (red) were used to identify primo vessels (yellow dashed area). Both of endothelial markers and fibroblast markers (green) were expressed in primo vessels. Lymphatic endothelial marker was negative in primo vessels.

anti-rat) at 1 : 200, polyclonal anti-vWF antibody (rabbit anti-rat) at 1 : 200, monoclonal anti-PDI antibody (mouse anti-rat) at 1 : 400, polyclonal anti-FSP1 antibody (rabbit anti-rat) at 1 : 200, polyclonal anti-VE-cadherin antibody (rabbit anti-rat) at 1 : 200, polyclonal anti-procollagen I antibody (rabbit anti-rat) at 1 : 400, and polyclonal rabbit anti-LYVE-1 (rabbit anti-rat) at 1 : 200 (Santa Cruz Biotechnology, CA). To detect immunofluorescence, sections were washed and incubated with Alexa Fluor 488- (1 : 400) or 594- (1 : 400), (Invitrogen, CA) for 2 h in the dark at RT. After washing in PBS, sections were incubated with Alexa Fluor 488 phalloidin or Alexa Fluor 568 phalloidin (1 : 50) for 2 h. Counterstaining was performed with DAPI, and the glass coverslips were mounted on the slides with prolong gold antifade reagent. As negative controls, the primary antibody was replaced with nonimmune IgG. Staining was analyzed independently by two investigators using a fluorescence microscope and further processed with Adobe Photoshop CS5 extended computer software.

2.6. Immunocytochemistry. For cell immunofluorescent staining, cells were washed in PBS for three times and fixed with pure Acetone for 20 min at −20°C. Then, cells were blocked with serum solution and incubated with the primary antibodies overnight at 4°C. After rinsed again, immunostaining cells were incubated for 45 min at room temperature with Alexa Fluor 488- and 594-conjugated secondary antibodies and mounted with prolong gold antifade reagent with DAPI.

2.7. Double Immunofluorescent Labeling. For a double immunofluorescence procedure, we incubated the sections and cells with two primary antibodies at 4°C overnight. We blocked samples with 10% donkey serum for 2 h at room temperature. The primary antibodies were anti-CD31 (1 : 200), anti-vWF (1 : 200), and anti-PDI (1 : 200). After washing in PBS, the sections and cells were incubated in the dark with a mixture of two secondary antibodies as described already.

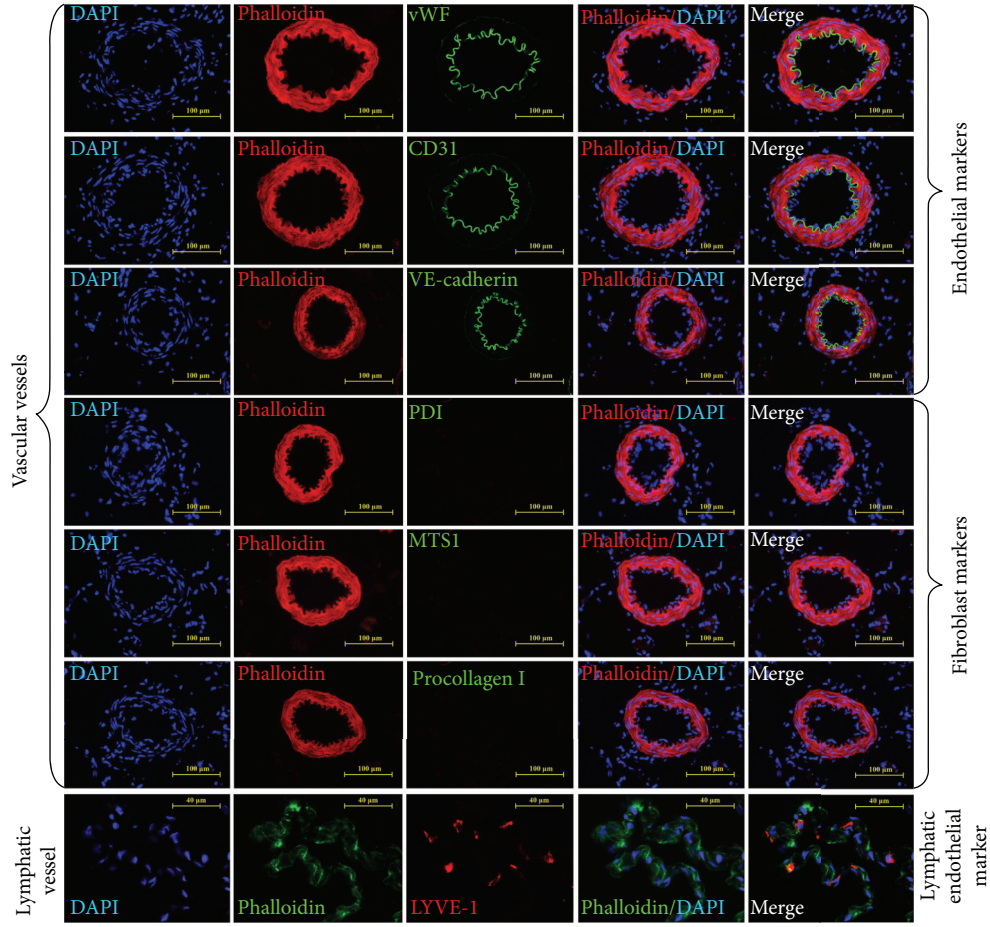

Figure 3: Controls for immunofluorescent staining of primo vessels in the mesentery. Vascular vessels were tested for endothelial (vWF, CD31, VE-cadherin) and fibroblast markers (PDI, MTS1, procollagen I). LYVE-1 was chosen to mark lymphatic endothelial cells.

Table 1: The sequences of the primers.

Primer	Sequences (5′-3′)	Size
Rat collagen α1(I)	Forward: TTCCCTGGACCTAAGGGTACT Reverse: TTGAGCTCCAGCTTCGCC	113 bp
Rat GAPDH	Forward: TGGCCAAGGTCATCCATGAC Reverse: GAGTGGCAGTGATGGCATGG	75 bp

2.8. Assessment of the Differentiation Capacity of Primo Vessel Cells In Vitro. The differentiation capacity of primo vessel cells was further tested *in vitro*. After cultured in DMEM with or without 5 ng/mL TGF-β1 (Pierce, Rockford, IL, USA) stimulation for indicated days, endothelial markers (vWF, CD31, VE-cadherin), and fibroblast markers (PDI, MTS1, procollagen I) expression in primo vessel cells were determined by immunocytochemistry. Culture media was refreshed every 3 days.

2.9. mRNA Isolation and Real-Time PCR. Total RNA was extracted from cultured primo vessel cells using the Trizol reagents according to the protocol provided by the manufacturer (Invitrogen, Carlsbad, CA, USA). The RNA content was measured spectrophotometrically. Then, total RNA (2 μg) was treated with DNase I followed by synthesis of the first strand of DNA using reverse transcription system. Real-time PCR was performed in 25 μL of reaction mixture containing 0.4 μM primers, 2 μL of cDNA product, 5 mM dNTPs, 0.75 units of Taq polymerase (Invitrogen, CA, USA), and 1 μL of iQ-SYBR green supermix reagent (Bio-Rad, CA, USA). Fold changes of target gene mRNA levels relative to the endogenous glyceraldehyde-3-phosphate dehydrogenase (GAPDH) control were calculated. The sequences of the primers were listed in Table 1. The mRNA levels were expressed as fold changes after normalization.

2.10. ELISA Analysis. For collagen α1(I) secretion in primo vessel cells culture media, it was measured using ELISA method. Primo vessel cells were cultured in six-well plates

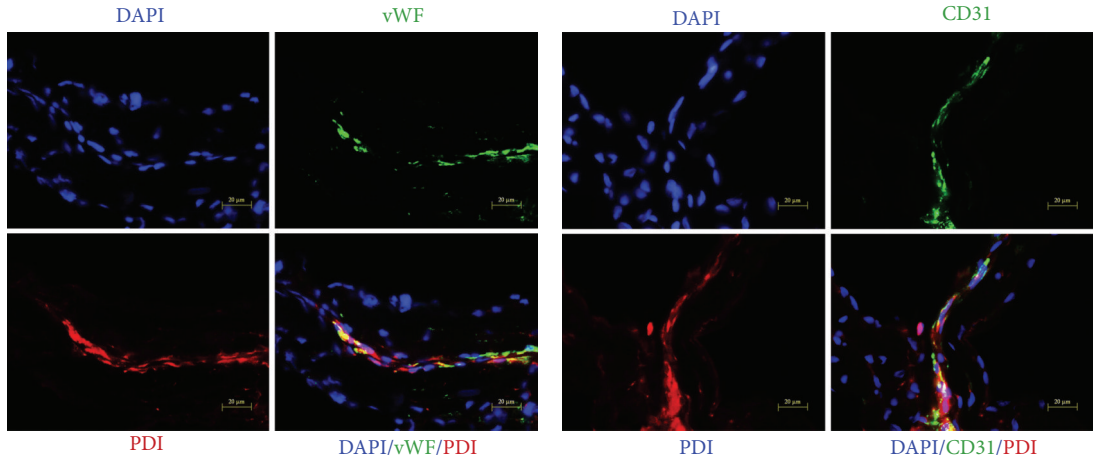

Figure 4: Double labeling of primo vessels in the mesentery with vWF/PDI and CD31/PDI. (a) Fluorescent microscopy of cryosections double-labeled with antibodies to vWF (green) and PDI (red). DAPI was used for labeling of nuclei (blue). In addition to the single-color panels, the pictures were merged. Primo vessel cells with rod-shaped nuclei and linear alignments were labeled positive for both vWF and PDI (yellow, white arrows). (b) CD31/PDI double labeling of primo vessels in the mesentery. Fluorescent microscopy of cryosections double-labeled with antibodies to CD31 (green) and PDI (red). DAPI was used for labeling of nuclei (blue). Accumulation of CD31/PDI positive cells (yellow, white arrows) correlated with areas of primo vessels with rod-shaped nuclei, linear alignments.

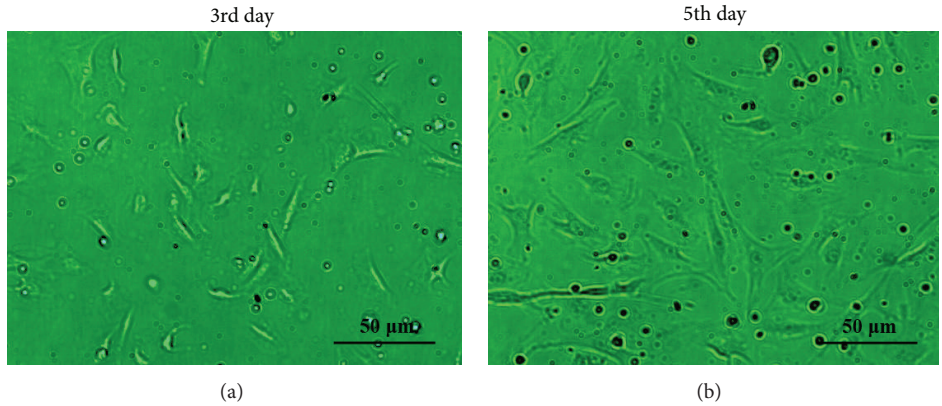

Figure 5: Primary primo vessel cell culture and identification. Primary primo vessel cells on 3rd and 5th day. Primo vessel cells started to spread on the 3rd day and showed a fibroblast-like phenotype on the 5th day.

at a density of 5×10^3 cells/well for indicated days. Then, supernatants were collected, and a sandwich ELISA for collagen α1(I) (Santa Cruz Biotechnology, CA) was performed. Optical densities were measured using an ELISA plate reader at 450 nm. Results are expressed as fold increases of collagen α1(I) secretion compared with cells without TGF-β1 stimulation.

2.11. Statistics. All results were expressed as the means ± SE of at least three independent experiments. A one-way ANOVA was used to evaluate differences between groups ($P < 0.05$ was considered significant).

3. Results and Discussion

3.1. Identification of Primo Vessels in the Mesentery in Fresh Tissues and Cryosections. Our previous studies have demonstrated that primo vessels located in the mesentery of rats [26]. They had prominent histological features such as rod-shaped nuclei with linear alignments, multiple-sinus, and collagen fibers inside the structures, and sometimes outer membranes were observed. We also found that using phalloidin (specific to F-actin) and DAPI staining, the cells' shape and arrangements of primo vessels were clearly detected. Here, we applied this method in distinguishing primo vessels from vascular vessels and lymphatic vessels.

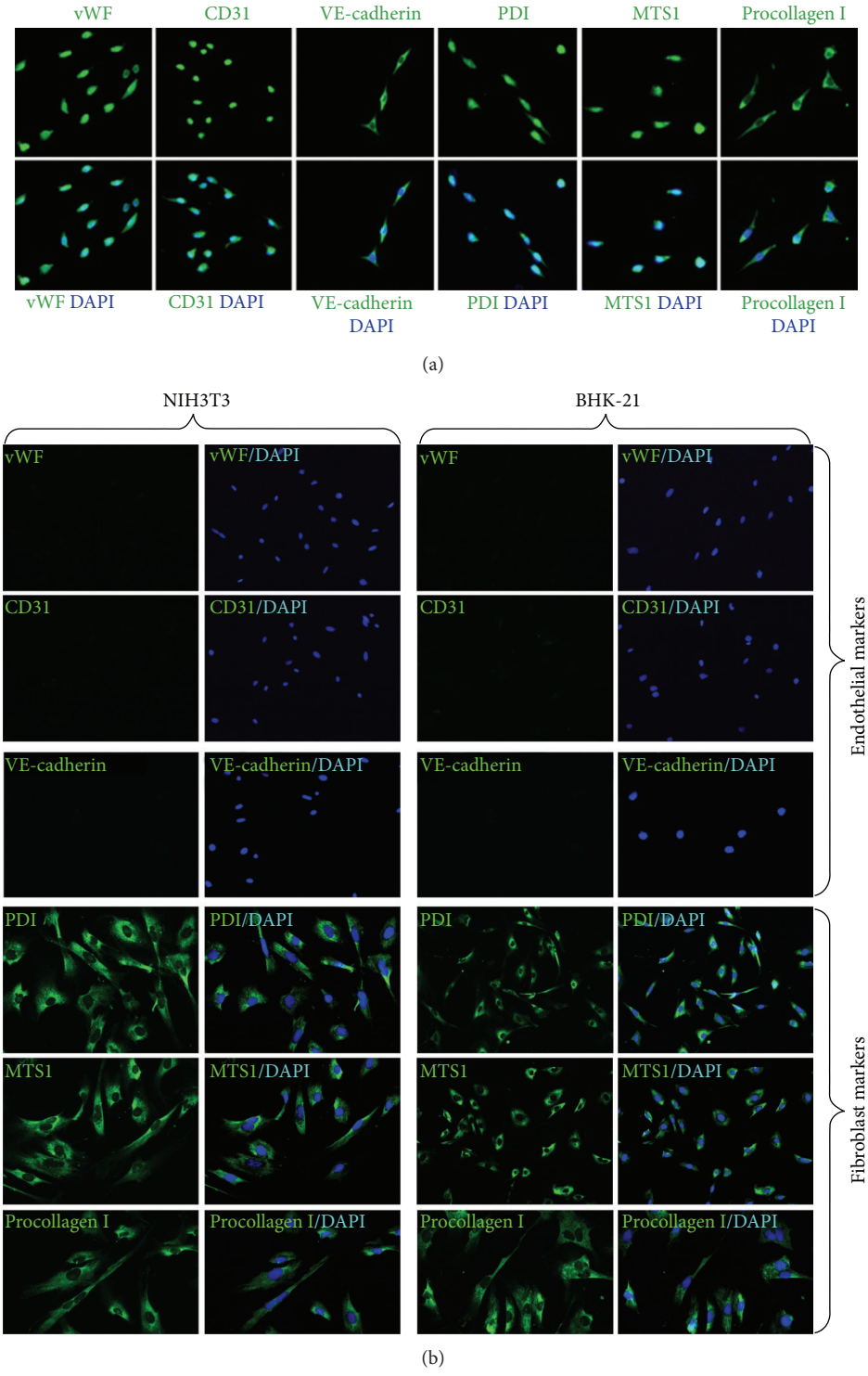

Figure 6: Immunofluorescent staining of primary primo vessel cells with endothelial markers and fibroblast markers. (a) Labeling of primo vessel cells with endothelial and fibroblast markers. Antibodies to endothelial markers (vWF, CD31, VE-cadherin) and fibroblast markers (PDI, MST1, procollagen I) (green) were used. Fluorescent microscopy revealed that both of endothelial markers and fibroblast markers (green) were expressed in primo vessel cells. (b) Controls for immunofluorescent staining of primo vessel cells. NIH3T3 cells and BHK-21 cells were positive to fibroblast markers (PDI, MTS1, procollagen I) (green) whereas negative to endothelial markers (vWF, CD31, VE-cadherin).

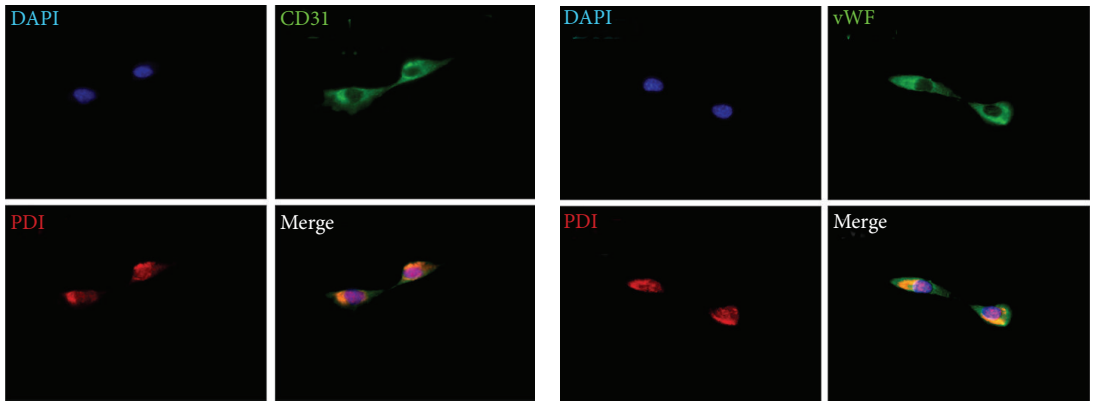

Figure 7: Double labeling of primary primo vessel cells with vWF/PDI, CD31/PDI. (a) Fluorescent microscopy of primo vessel cells double-labeled with antibodies to vWF (green) and PDI (red). DAPI was used for labeling of nuclei (blue). In addition to the single-color panels, the pictures were merged. Primo vessel cells were labeled positive for both vWF and PDI (orange). (b) CD31/PDI double labeling of primo vessel cells in the mesentery. Fluorescent microscopy of primo vessel cells double-labeled with antibodies to CD31 (green) and PDI (red). DAPI was used for labeling of nuclei (blue). Primary primo vessel cells coexpressed CD31/PDI (yellow).

As shown in Figure 1(a), primo vessel cells had characteristic rod-shaped nuclei with linear arrangements, and their regular arrays along the vessels were clearly detected with phalloidin staining. Vascular smooth muscle cells were also sensitive to phalloidin but showed thoroughly different arrangement from primo vessels (Figure 1(a), arrowheads). As for lymphatic vessels, the endothelial cells were weakly positive to phalloidin and showed as a network structure (Figure 1(a), arrows). On the basis of phalloidin/DAPI double staining in reliably distinguishing primo vessels, vascular vessels, and lymphatic vessels in fresh tissues, we further employed this method in cryosections. As shown in Figure 1(b), in longitudinal cryosections, the structures with rod-shaped nuclei in linear alignments, and positive phalloidin expression (yellow dashed area) were considered as primo vessels. This method established in previous researches [23, 24, 26] was used in the current work as a time-saving method to detect primo vessels not only in tissue samples but also in longitudinal cryosections.

3.2. Endothelial and Fibroblast Markers Expressed in Primo Vessels in the Mesentery. To investigate the biological properties of primo vessels, we first examined their endothelium features. Our results revealed that endothelial markers (vWF, CD31, VE-cadherin) were positive in primo vessels (Figure 2, green) and indicated their endothelium properties. Then, we performed fibroblasts markers (PDI, MTS1, procollagen I) in our experiments. As shown in Figure 2, primo vessels also positively expressed fibroblast markers (green). We concluded that primo vessels in the mesentery also possessed mesenchymal features. In addition, primo vessels negatively expressed a lymphatic endothelial cell marker, LYVE-1. As a control, endothelial markers (vWF, CD31, VE-cadherin) and fibroblast markers (PDI, MTS1, procollagen I) were also tested in vascular vessels (Figure 3). Next, we performed double-labeling experiments with endothelial and fibroblast markers to verify the possible properties of both endothelium and mesenchymal in primo vessels. The colocalization of vWF/PDI and CD31/PDI in primo vessels (Figure 4(a)) demonstrated that primo vessels are a transitional structure between endothelium and mesenchymal.

3.3. Endothelial and Fibroblast Markers Expressed in Primary Primo Vessel Cells. To further demonstrate our observation of endothelial and fibroblast markers in primo vessels, we isolated and cultured primary primo vessel cells in rat mesentery. According to the potential biological features of fibroblasts in primo vessel cells, we performed collagenase digestion method in primary primo vessel cell isolation. Our data showed that on the 3rd and 5th day, primo vessel cells showed fibroblast-like shapes (Figure 5). We stained primo vessel cells with antibodies to endothelial markers (vWF, CD31, VE-cadherin) and fibroblast markers (PDI, MST1, procollagen I) (Figure 6(a)). The results revealed that all these markers positively expressed in primo vessel cells. NIH3T3 cell line and BHK-21 cell line were selected as controls and only positive to fibroblast markers (PDI, MST1, procollagen I) (Figure 6(b)). Double labeling with vWF/PDI and CD31/PDI supported the conception that primo vessel cells were ascribed to a phenotype between endothelial cells and fibroblasts (Figure 7).

3.4. Differentiation of Primo Vessel Cells into Fibroblasts In Vitro. Our results indicated that in the mesentery, primo vessels were a unique transitional structure possessing both endothelial and mesenchymal properties. We deduced that primo vessel cells had differentiation potential. Under different stimulations, they might be induced and perform endothelial cells or fibroblasts functions. To verify this deduction, we studied the plasticity of primo vessel cells *in vitro*. We found that with the induction of TGF-β1, primo vessel cells transformed into fibroblasts over 5 days. Endothelial

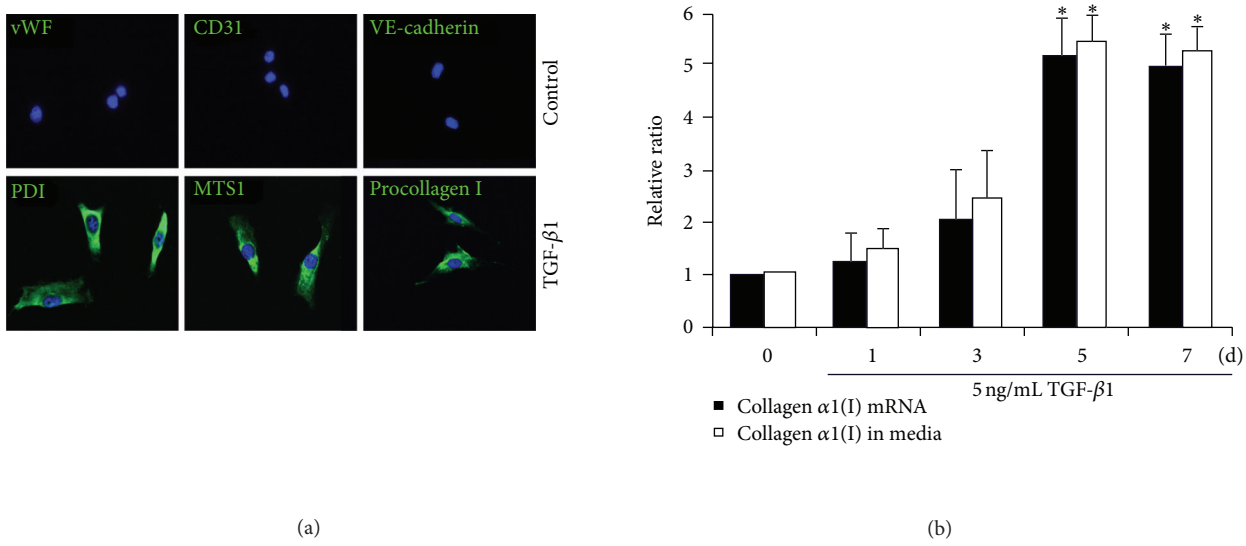

Figure 8: Assessment of differentiation of primo vessel cells *in vitro*. (a) Primary primo vessel cells were cultured in DMEM supplemented with or without 5 ng/mL TGF-β1 for 5 days, and then endothelial markers (vWF, CD31, VE-cadherin) and fibroblast markers (PDI, MTS1, procollagen I) were tested by immunocytochemistry. (b) Primary primo vessel cells were cultured in DMEM supplemented with or without 5 ng/mL TGF-β1 for indicated days collagen α1(I) mRNA was examined by real-time PCR, and collagen α1(I) secretion in culture media was detected by ELISA. $^{*}P < 0.01$ versus TGF-β1-simulated primo vessel cells (the first column on the left in each group).

markers (vWF, CD31, VE-cadherin) diminished, and just fibroblast markers (PDI, MTS1, procollagen I) were positive in these cells (Figure 8(a)). One of the important functions of fibroblasts is to synthesize and produce extracellular matrix (ECM), especially collagen α1(I) [27, 28]. We found that in contrast to primo vessel cells, both the collagen α1(I) mRNA and protein secretion obviously increased in cells with TGF-β1 stimulation (Figure 8(b)). These data demonstrated that primo vessel cells differentiated into fibroblasts. Primo vessel cells are a new source of fibroblasts.

4. Conclusions

In conclusion, our research demonstrated that primo vessels in the mesentery were a special transitional structure between endothelium and mesenchymal. Primo vessel cells had the capability of differentiation into fibroblasts *in vitro*. It is a new finding of EndMT in normal postnatal states.

Acknowledgments

This work was supported in part by a grant from the Traditional Korean Medicine R&D Project, Ministry of Health & Welfare, Republic of Korea (B110076), Department of Acupuncture, Korea Institute of Oriental Medicine, Daejeon, Republic of Korea (K12272), and Natural Science Foundation of Hubei Province, China (2012FKB04432).

References

[1] J. D. Potts and R. B. Runyan, "Epithelial-mesenchymal cell transformation in the embryonic heart can be mediated, in part, by transforming growth factor β," *Developmental Biology*, vol. 134, no. 2, pp. 392–401, 1989.

[2] Y. Nakajima, T. Yamagishi, S. Hokari et al., "Mechanisms involved in valvuloseptal endocardial cushion formation in early cardiogenesis: roles of transforming growth factor (TGF)-beta and bone morphogenetic protein (BMP)," *Anatomical Record*, vol. 258, pp. 119–127, 2000.

[3] E. J. Armstrong and J. Bischoff, "Heart valve development: endothelial cell signaling and differentiation," *Circulation Research*, vol. 95, no. 5, pp. 459–470, 2004.

[4] H. S. Shin, H. M. Johng, B. C. Lee et al., "Feulgen reaction study of novel threadlike structures (Bonghan ducts) on the surfaces of mammalian organs," *Anatomical Record B*, vol. 284, no. 1, pp. 35–40, 2005.

[5] R. R. Markwald, T. P. Fitzharris, and F. J. Manasek, "Structural development of endocardial cushions," *American Journal of Anatomy*, vol. 148, no. 1, pp. 85–119, 1977.

[6] X. Mao, Y. Fujiwara, and S. H. Orkin, "Improved reporter strain for monitoring Cre recombinase-mediated DNA excisions in mice," *Proceedings of the National Academy of Sciences of the United States of America*, vol. 96, no. 9, pp. 5037–5042, 1999.

[7] E. Gustafsson, C. Brakebusch, K. Hietanen, and R. Fässler, "Tie-1-directed expression of Cre recombinase in endothelial cells of embryoid bodies and transgenic mice," *Journal of Cell Science*, vol. 114, no. 4, pp. 671–676, 2001.

[8] E. M. Zeisberg, S. E. Potenta, H. Sugimoto, M. Zeisberg, and R. Kalluri, "Fibroblasts in kidney fibrosis emerge via endothelial-to-mesenchymal transition," *Journal of the American Society of Nephrology*, vol. 19, no. 12, pp. 2282–2287, 2008.

[9] E. M. Zeisberg, O. Tarnavski, M. Zeisberg et al., "Endothelial-to-mesenchymal transition contributes to cardiac fibrosis," *Nature Medicine*, vol. 13, no. 8, pp. 952–961, 2007.

[10] E. M. Zeisberg, S. Potenta, L. Xie, M. Zeisberg, and R. Kalluri, "Discovery of endothelial to mesenchymal transition as a source for carcinoma-associated fibroblasts," *Cancer Research*, vol. 67, no. 21, pp. 10123–10128, 2007.

[11] P. Zhu, L. Huang, X. Ge, F. Yan, R. Wu, and Q. Ao, "Transdifferentiation of pulmonary arteriolar endothelial cells into smooth muscle-like cells regulated by myocardin involved in hypoxia-induced pulmonary vascular remodelling," *International Journal of Experimental Pathology*, vol. 88, no. 2, pp. 127–128, 2007.

[12] S. Potenta, E. Zeisberg, and R. Kalluri, "The role of endothelial-to-mesenchymal transition in cancer progression," *British Journal of Cancer*, vol. 99, no. 9, pp. 1375–1379, 2008.

[13] J. G. Lee and E. P. Kay, "FGF-2-mediated signal transduction during endothelial mesenchymal transformation in corneal endothelial cells," *Experimental Eye Research*, vol. 83, no. 6, pp. 1309–1316, 2006.

[14] J. C. Tse and R. Kalluri, "Mechanisms of metastasis: epithelial-to-mesenchymal transition and contribution of tumor microenvironment," *Journal of Cellular Biochemistry*, vol. 101, no. 4, pp. 816–829, 2007.

[15] L. Selek, M. Dhobb, B. Van Der Sanden, F. Berger, and D. Wion, "Existence of tumor-derived endothelial cells suggests an additional role for endothelial-to-mesenchymal transition in tumor progression," *International Journal of Cancer*, vol. 128, no. 6, pp. 1502–1503, 2011.

[16] R. Kalluri and M. Zeisberg, "Fibroblasts in cancer," *Nature Reviews Cancer*, vol. 6, no. 5, pp. 392–401, 2006.

[17] E. Olaso, A. Santisteban, J. Bidaurrazaga, A. M. Gressner, J. Rosenbaum, and F. Vidal-Vanaclocha, "Tumor-dependent activation of rodent hepatic stellate cells during experimental melanoma metastasis," *Hepatology*, vol. 26, no. 3, pp. 634–642, 1997.

[18] I. Cornil, D. Theodorescu, S. Man, M. Herlyn, J. Jambrosic, and R. S. Kerbel, "Fibroblast cell interactions with human melanoma cells affect tumor cell growth as a function of tumor progression," *Proceedings of the National Academy of Sciences of the United States of America*, vol. 88, no. 14, pp. 6028–6032, 1991.

[19] E. Olaso, C. Salado, E. Egilegor et al., "Proangiogenic role of tumor-activated hepatic stellate cells in experimental melanoma metastasis," *Hepatology*, vol. 37, no. 3, pp. 674–685, 2003.

[20] M. T. Dimanche-Boitrel, L. Vakaet, P. Pujuguet et al., "*In vivo* and *in vitro* invasiveness of a rat colon-cancer cell line maintaining E-cadherin expression: an enhancing role of tumor-associated myofibroblasts," *International Journal of Cancer*, vol. 56, no. 4, pp. 512–521, 1994.

[21] A. Orimo, P. B. Gupta, D. C. Sgroi et al., "Stromal fibroblasts present in invasive human breast carcinomas promote tumor growth and angiogenesis through elevated SDF-1/CXCL12 secretion," *Cell*, vol. 121, no. 3, pp. 335–348, 2005.

[22] J. P. Thiery, H. Acloque, R. Y. J. Huang, and M. A. Nieto, "Epithelial-mesenchymal transitions in development and disease," *Cell*, vol. 139, no. 5, pp. 871–890, 2009.

[23] K. S. Soh, "Bonghan circulatory system as an extension of acupuncture meridians," *JAMS Journal of Acupuncture and Meridian Studies*, vol. 2, no. 2, pp. 93–106, 2009.

[24] J. S. Yoo, M. Hossein Ayati, H. B. Kim, W. B. Zhang, and K. S. Soh, "Characterization of the primo-vascular system in the abdominal cavity of lung cancer mouse model and its differences from the lymphatic system," *PLoS ONE*, vol. 5, no. 4, Article ID e9940, 2010.

[25] J. S. Yoo, H. B. Kim, N. Won et al., "Evidence for an additional metastatic route: *in vivo* imaging of cancer cells in the primo-vascular system around tumors and organs," *Molecular Imaging and Biology*, vol. 13, no. 3, pp. 471–480, 2011.

[26] P. An, J. Dai, Z. Su, J. S. Yoo, R. Qu, S. W. Lee et al., "Putative primo-vascular system in mesentery of rats," *Journal of Acupuncture and Meridian Studies*, vol. 3, pp. 232–240, 2010.

[27] J. J. Tomasek, G. Gabbiani, B. Hinz, C. Chaponnier, and R. A. Brown, "Myofibroblasts and mechano: regulation of connective tissue remodelling," *Nature Reviews Molecular Cell Biology*, vol. 3, no. 5, pp. 349–363, 2002.

[28] G. Parsonage, A. D. Filer, O. Haworth et al., "A stromal address code defined by fibroblasts," *Trends in Immunology*, vol. 26, no. 3, pp. 150–156, 2005.

Hindawi Publishing Corporation
Evidence-Based Complementary and Alternative Medicine
Volume 2013, Article ID 538350, 5 pages
http://dx.doi.org/10.1155/2013/538350

Review Article

The Primo Vascular Structures Alongside Nervous System: Its Discovery and Functional Limitation

Eun-sung Park,[1,2] Hee Young Kim,[3] and Dong-ho Youn[1]

[1] *Department of Oral Physiology, School of Dentistry, Kyungpook National University, Daegu 700-412, Republic of Korea*
[2] *Department of Quality Control, Koatech, Pyeongtaek, Gyeonggi-do 451-864, Republic of Korea*
[3] *Department of Physiology, College of Korean Medicine, Daegu Haany University, Daegu 706-060, Republic of Korea*

Correspondence should be addressed to Hee Young Kim; hykim@dhu.ac.kr and Dong-ho Youn; dyoun@knu.ac.kr

Received 9 January 2013; Revised 8 March 2013; Accepted 15 March 2013

Academic Editor: Xianghong Jing

The primo vascular structures comprising primo nodes and vessels (originally called Bonghan corpuscles and ducts, resp.) have recently been suggested to be the anatomical correlate of acupuncture, a therapeutic technique used in oriental medicine. Although the primo vascular structures have been observed in many parts of animals, including the nervous system, using anatomical methodologies, its physiological functions are still unclear. This paper summarizes the reports on the primo vascular structures, particularly in the nervous system and its surroundings, as well as the electrophysiological properties of cells in the primo nodes. In addition, recent reports examining the potential roles of the primo vascular structures in acupuncture are discussed. This review raises some fundamental questions and, at the same time, highlights the potential physiological roles of the primo vascular structures in acupuncture.

1. Introduction

Acupuncture is a centuries-old therapeutic technique in oriental medicine, but its therapeutic mechanism is unclear. Currently, acupuncture is becoming popular in Western countries, and NIH (National Institutes of Health, USA) has also agreed that acupuncture is effective or at least useful in the treatment of 13 conditions, including low back pain, fibromyalgia, and stroke rehabilitation [1]. During acupuncture, fine needles are inserted through the skin and muscle at certain acupuncture points (so-called "acupoints") on the body of the patient, which are located mainly along the "meridians" [2]. In addition to the different principles used in oriental medicine, many studies using modern scientific (Western style) methodologies have attempted to define the anatomical structures of the acupoints and meridians that make the unique oriental technique work both physiologically and clinically in the bodies of humans or animals [2]. Soh's group has examined the primo vascular structures, which was originally coined by Kim Bonghan in 1963, as potential anatomical structures for the acupoints and meridians. By appreciating the various conventional staining or advanced microscopic imaging methods (Table 1), the existence of the primo vascular structures was reported in various areas of the body, including the nervous system [3]. The primo vascular structures, which consist of primo nodes (previously called Bonghan corpuscles) and primo vessel (previously called Bonghan duct) [3], were categorized according to its location as follows: superficial (in the skin), intravascular, extravascular, organ-surface, intraorgan, and neural primo vascular systems. The neural primo vascular system is designated when it exists inside or adjacent to the brain and spinal cord and is accompanied by the outer surface of peripheral nerves [3].

This paper summarizes the discovery of the primo vascular structures alongside central and peripheral nervous

Table 1: Primo nodes and vessels in the surroundings of the peripheral and central nervous system.

Areas	Species and sites	Dyes
3rd or 4th ventricles	Rat [3, 4]; rabbit [5, 6]	Fluorescent nanoparticles, hematoxylin, Acridine orange, propidium iodide, DiI, Perchlorate, DAPI, and yoyo1
Central canal of the spinal cord	Rabbit [5, 6]	Hematoxylin, Acridine orange, propidium iodide, DiI, Perchlorate, DAPI, and yoyo1
Subarachnoid space	Rat [3] and pig [7] spinal cords; rat brain [4]	Fluorescent nanoparticles, DAPI, and Phalloidin
Venous sinus	Rat cerebrum [8]	Chromium hematoxylin and DAPI
Surroundings of the brain	Rat cerebrum [9], pineal body [9], and spinal cord [4, 9]; rat [4, 9] and rabbit [10] cerebellums	Alcian blue, DAPI, trypan blue, Phalloidin, and DAPI
Surroundings of the peripheral nerve	Epineurium, perineurium, or endoneurium in rat sciatic nerve [4, 11]	Fluorescent nanoparticles and DAPI

Technical notes for dyes: DAPI, for nuclei; Phalloidin, for nuclei and F-actin; Acridine orange, for DNA particles; Propidium iodide, for nucleus and F-actin; DiI, for membrane phospholipid; Perchlorate, for microparticles inside the nerve primo vessel; Fluorescent nanoparticles, cobalt-ferrite embedded in silica shells with rhodamine B as a contrast agent during MRI.

system and discusses the technical concerns encountered in staining the primo vascular structures and its potential functional roles in acupuncture.

2. Discovery of the Primo Vascular Structures Alongside Central and Peripheral Nervous System

Although the primo vascular structures have been found in various areas of the body, such as the blood vessels, lymphatic vessels, and enteric organs, its identification in the area of the peripheral and central nervous system using various staining methods was only recent (Table 1). In the rat brain and spinal cord, the injection of fluorescent nanoparticles into the lateral ventricle stained the primo vessels floating in the cerebrospinal fluid of the 4th ventricle, as well as those lying alongside the blood vessels in the subarachnoid space in the dorsal surface of the spinal cord [4]. Similarly, the primo nodes and primo vessels on the arachnoid mater and primo node in the 4th ventricle of the rat brain were stained with trypan blue [5]. In the rabbit nervous system, primo vessels were observed in the mesencephalic aqueduct and 4th ventricle of the brain as well as in the central canal of the spinal cord by confocal laser scanning microscopy and electron microscopy [6]. Their structures contained DNA particles, other microparticles, and rod-shaped nuclei encircled by helix-shaped actins. In addition, primo vessels were observed in the 3rd and 4th ventricles and the central canal of the rabbits using hematoxylin staining, and the rod-shaped nuclei structure of the primo vessels was visualized by nucleus-specific staining dyes, such as $4'$,$6'$-diamidino-2-phenylindole, propidium iodide, and yoyo-1 [7]. Interestingly, the primo vessel was also observed for the first time in the subarachnoid space of the thoracic spinal nerve area in a pig [11]. Overall, these studies suggest the existence of the primo vascular structures in the brain and spinal cord, particularly in the ventricles, central canal, and arachnoid spaces (Table 1). On the other hand, the primo vessels were observed in the peripheral nervous system of rats using trypan blue staining [5] or fluorescent nanoparticles [12], mostly in the epineurium, perineurium, and endoneurium of the sciatic nerve.

3. Technical Considerations in Staining Methods

A range of staining dyes or fluorescent nanoparticles have been used to identify the structure of the primo vascular system in the nervous system and its surroundings (Table 1). On the other hand, the mechanism of staining with these dyes is based frequently on nonspecific binding because most dyes use the electrostatic interactions between the charges of the dyes and the charges of tissues. For example, hematoxylin, alcian blue and trypan blue used to stain the primo vascular structures forms salt linkages with the acidic or basic groups of various organic molecules in intracellular or extracelluar structures.

Hematoxylin is one of the most common dyes used for nuclear staining in histology. The application of hematoxylin to the 4th ventricle of frozen brain revealed the primo vessel that appeared like pale blue-stained thread along the midline of the fourth ventricle [6]. The primo vessel contained many fragmented DNA particles and rod-shaped nuclei (10~20 μm in size) with irregular distribution; the DNA particles or nuclei were stained dark blue. Thus, the primo vessel appeared as a thin thread with tiny blue dots under high power magnification. Even though the use of hematoxylin revealed the structure of the primo vessel, it should be noted that its value is not limited to the nuclear staining because it can be used to detect intracellular substances (e.g., chromosomes, keratohyalin), extracellular substances (e.g., elastin), ground substances (e.g., cement lines in bone), minerals (e.g., calcium, copper, etc.), and the central nervous system (e.g., myelin, neuroglia fibers, etc.) [13].

S. Lee and C. Lee [14] reported that alcian blue could visualize primo vessels and nodes above the pia mater of the brain without staining surrounding blood vessels. Because

alcian blue is a water soluble copper phthalocyanine that easily binds to acidic groups, such as acid mucosubstances and acetic mucins normally found in blood vessel walls [13], a careful use of alcian blue is recommended, especially in central nervous system with microvascular networks. Trypan blue is used to selectively stain dead cells or tissues because the chromophore is negatively charged and does not penetrate the cell membrane unless the membrane is damaged. If the dye enters live cells, it is exocytosed actively. Accordingly, live cells or tissues with intact cell membrane are not stained by trypan blue. Therefore, staining of the primo structures with this dye [3] might be due to long-term exposure of the dye because its increased negative charge under basic conditions can bind to the fibril in the cytosol after membrane penetration or inclusion of dead/dying cells in primo vessels. DiI (Molecular probes, OR, USA) is a fluorescent lipophilic carbocyanine dye bound to the membrane phospholipids that is used typically as a retrograde membrane tracer by neuroscience researchers. Therefore, DiI can bind to any cellular components containing phospholipids. Another technique to stain the primo structure is to use fluorescent nanoparticles composed of cobalt-ferrite embedded in silica shells with rhodamine B on a nanometer scale [4]. On the other hand, the mechanism by which nanoparticles stain specifically the primo vascular structures is unclear. Therefore, the development of staining methods specific to the primo vascular structures is needed to reveal the system as a novel structure supporting the acupuncture mechanism.

4. Potential Functions of the Primo Vascular Structures in Central and Peripheral Nervous System

The gross anatomical and histological findings of the primo vascular structures in various areas of the body, including the nervous system, support the anecdotal observations reported by Bonghan Kim, who proposed the primo structures, initially called Bonghan system, as a theory explaining the "meridians" [3]. In ancient oriental medicine, the meridians were believed to be a channel that allows invisible vital energy in live bodies, so-called "Qi," to flow through [2]. Therefore, he attempted to correlate the primo vascular system to the meridians. Although there is no direct evidence of a relationship between the primo structures and the theory of meridians, or any other functional system, the physiological roles of the primo vascular structures in the nervous system and its surroundings should be examined. For example, Kim reported that the primo vascular structures located in various body parts including the nervous system might supply nutrients to the nervous tissues to be maintained under healthy conditions or be regenerated after damage [3, 15]. This idea is in some way supported by a recent finding that F-actin of the primo vessels in the rat sciatic nerve might allow the structure to contract and to flow the fluid within the primo vessels [5]. On the other hand, the most attractive hypothesis would be that the primo vascular system might play a key role in acupuncture treatment because the primo vascular structures are believed to be the physical presence of acupuncture meridians [3, 7]. Therefore, this section discusses the primo vascular system in terms of its electrophysiological properties and potential relevance with the acupuncture points and meridian.

The primo nodes, which are found on the surfaces of the internal organs of rats, contain some cells, including macrophages, mast cells, and eosinophils [8]. When measured using whole-cell patch clamp recordings, the cells found in the slices of primo nodes showed large variability in the cell populations, which was characterized by a lower resting membrane potential ($-50 \sim -10$ mV), higher input resistance (200~1600 MΩ), and lower capacitance (5~20 pF) compared to the neurons in the hypothalamic paraventricular nucleus [9, 10]. In addition, no active components in the cell membrane properties were observed in the preparation of primo nodes [9, 10], suggesting that the cells found in the live slices of primo nodes are not excitable electrophysiologically [10]. When cells in the primo nodes are classified based on the current-voltage relations and the kinetics of the activation and inactivation of currents generated by the voltage pulses (600 ms) in voltage-clamp mode, one type of cell was found to be sensitive to relatively high concentrations of tetraethylammonium (IC_{50} = ~4.3 mM) [10], indicating that unidentified K^+ channels may be expressed in these cells. Although no electrophysiological study has attempted to analyze the cells found in the primo nodes of the surroundings of the central or peripheral nervous system, studies using whole-cell patch clamp recordings suggest that the primo nodes do not support the neural mechanism for acupuncture because skin stimulation with fine acupuncture needles might not generate any electrical signals in the primo nodes [2].

The meridian is considered a key concept in oriental medicine including acupuncture, even though its anatomical structures have not been identified. Soh's group proposed that the primo vascular system corresponds to the acupuncture meridian system and examined the correlations between the primo vascular system and acupuncture meridian system. In their previous reports, after injecting a fluorescent dye into the acupoint ST36, the fluorescent network of the primo vascular structures appeared on the layer of the superficial fascia around the stomach meridian from the knee to the tibia [12]. Thin thread-like structures were also observed in hypodermal layer of a rat after staining with trypan blue [16]. Unfortunately, there was no evidence of the role of primo vascular structures in the effect of acupuncture. Recently, Wang et al. (2012) [17] examined the effects of stimulation of the primo vessels on gastric motility as well as the roles of the primo vessels in mediating the effects of acupuncture on gastric motility [18, 19]. In their results, direct electrical stimulation of the primo vascular structures on the stomach did not affect the gastric motility, and the inhibitory or stimulatory effects induced by acupuncture at CV12 or ST36 were unchanged after the primo vascular structures had been cut. They suggested that the primo vascular structures are not involved in the acupuncture modulation of gastric motility. The possibility that the primo vascular system might utilize other biological processes to achieve the therapeutic effects of acupuncture on gastric disorders cannot be excluded because Wang et al.'s study used only one measurement of gastric

motility [17] and the primo vascular system was implicated in a range of biological processes, such as the immune responses, hormone, and regeneration [20]. Therefore, the functional roles of the primo vascular system in the effects of acupuncture on gastric motility are unclear.

Although Soh's group has reported that the primo vascular system mediates the transmission of acupuncture signals as an acupuncture meridian, many studies have shown that the afferent signals of acupuncture are conveyed via the peripheral nerve rather than the "Qi," meridian or other routes. The effects of acupuncture are blocked by a pretreatment with local anesthetic drugs around the acupoints [21, 22]. The responses elicited by stimulating the acupoints are blocked when the nerve lying under the acupoint is cut [23, 24], and direct stimulation of the nerves innervating acupoints also has a similar effect to that of acupuncture [24, 25]. Apart from lack of attempt to block selectively either nerves or primo vessels, it might be spoken up that further studies on the functional relationship between the primo vascular system and meridian are required for the suggestion that the primo vascular system, including primo vessel and nodes, corresponds to acupuncture meridian system and thus mediate the acupuncture effects. Moreover, slow flow rate (0.3 mm/sec) through the primo vessel [26], which in turn may take more than 400 sec to travels through a 12 cm long primo vessel in internal organs, should be reconciled with the fact that the time taken to initiate the response after stimulating the acupoints is immediate or occurs in several minutes [27, 28].

5. Conclusion

The primo vascular system has been proposed as the anatomical structure that mediates the effects of acupuncture. Nevertheless, the lack of specific staining methods that can distinguish the structures from other tissues has thwarted the easy and reproducible detection of the entire connections in the body, building an obstacle for a reliable and functional analysis of the system. Thus, an immunohistochemical staining based on molecular markers specific to the primo vascular structures needs to be developed in the future, giving support to them for the normal anatomical structures, not like pathological products. In addition, the finding that the cells in the primo nodes have only passive membrane properties, suggests that the primo vascular system might be unsatisfactory for mediating the rapid effects of acupuncture. Therefore, functional studies, such as cutting the primo vascular system selectively [22], might help understand the roles of the system in acupuncture. Moreover, identifying the molecular contents in the primo vascular structures as well as their functional release to needling in acupuncture will put the primo vascular system in the position of the real anatomical structure of acupuncture.

Acknowledgment

This work was supported by the National Research Foundation of Korea (NRF) Grant funded by the Korea Government (MEST) (no. 20120009400).

References

[1] "NIH Consensus Conference Acupuncture," *The Journal of the American Medical Association*, vol. 280, no. 17, pp. 1518–1524, 1998.

[2] J. C. Longhurst, "Defining meridians: a modern basis of understanding," *Journal of Acupuncture and Meridian Studies*, vol. 3, no. 2, pp. 67–74, 2010.

[3] K. S. Soh, "Bonghan circulatory system as an extension of acupuncture meridians," *Journal of Acupuncture and Meridian Studies*, vol. 2, no. 2, pp. 93–106, 2009.

[4] J. Lim, J. H. Jung, S. Lee et al., "Estimating the density of fluorescent nanoparticles in the primo vessels in the fourth ventricle and the spinal cord of a rat," *Journal of Biomedical Optics*, vol. 16, no. 11, Article ID 116010, 2011.

[5] B. C. Lee, K. H. Eom, and K. S. Soh, "Primo-vessels and Primo-nodes in Rat Brain, Spine and Sciatic Nerve," *Journal of Acupuncture and Meridian Studies*, vol. 3, no. 2, pp. 111–115, 2010.

[6] B. C. Lee, K. W. Kim, and K. S. Soh, "Characteristic features of a nerve primo-vessel suspended in rabbit brain ventricle and central canal," *Journal of Acupuncture and Meridian Studies*, vol. 3, no. 2, pp. 75–80, 2010.

[7] B. C. Lee, S. Kim, and K. S. Soh, "Novel anatomic structures in the brain and spinal cord of rabbit that may belong to the Bonghan system of potential acupuncture meridians," *Journal of Acupuncture and Meridian Studies*, vol. 1, no. 1, pp. 29–35, 2008.

[8] B. C. Lee, J. S. Yoo, V. Ogay et al., "Electron microscopic study of novel threadlike structures on the surfaces of mammalian organs," *Microscopy Research and Technique*, vol. 70, no. 1, pp. 34–43, 2007.

[9] T. H. Han, C. J. Lim, J. H. Choi, S. Y. Lee, and P. D. Ryu, "Viability assessment of primo-node slices from organ surface primo-vascular tissues in rats," *Journal of Acupuncture and Meridian Studies*, vol. 3, no. 4, pp. 241–248, 2010.

[10] J. H. Choi, C. J. Lim, T. H. Han, S. K. Lee, S. Y. Lee, and P. D. Ryu, "TEA-sensitive currents contribute to membrane potential of organ surface primo-node cells in rats," *The Journal of membrane biology*, vol. 239, no. 3, pp. 167–175, 2011.

[11] S. H. Moon, R. Cha, M. Lee, S. Kim, and K. S. Soh, "Primo vascular system in the subarachnoid space of the spinal cord of a pig," *Journal of Acupuncture and Meridian Studies*, vol. 5, no. 5, pp. 226–233, 2012.

[12] Z. F. Jia, B. C. Lee, K. H. Eom et al., "Fluorescent nanoparticles for observing primo vascular system along sciatic nerve," *Journal of Acupuncture and Meridian Studies*, vol. 3, no. 3, pp. 150–155, 2010.

[13] C. F. A. Culing, R. T. Allison, and W. T. Barr, *Cellular Pathology Technique*, Butterworths, 4th edition, 1985.

[14] H. S. Lee and B. C. Lee, "Visualization of the network of primo vessels and primo nodes above the pia mater of the brain and spine of rats by using Alcian blue," *Journal of Acupuncture and Meridian Studies*, vol. 5, no. 5, pp. 218–225, 2012.

[15] B. H. Kim, "Sanal theory," *Journal of Jo Sun Medicine*, vol. 108, pp. 39–62, 1965.

[16] B. C. Lee and K. S. Soh, "Visualization of acupuncture meridians in the hypodermis of rat using trypan blue," *Journal of Acupuncture and Meridian Studies*, vol. 3, no. 1, pp. 49–52, 2010.

[17] X. Wang, H. Shi, H. Shang et al., "Are primo vessels (PVs) on the surface of gastrointestine involved in regulation of gastric motility induced by stimulating acupoints ST36 or CV12?" *Evidence-Based Complementary and Alternative Medicine*, vol. 2012, pp. 1–8, 2012.

[18] B. H. Kim, "On the reality of acupuncture meridians," *Journal of Jo Sun Medicine*, vol. 9, pp. 5–13, 1962.

[19] B. H. Kim, "On the acupuncture meridian system," *Journal of Jo Sun Medicine*, vol. 90, pp. 6–35, 1963.

[20] M. Stefanov, "Critical review and comments on B.H. Kim's work on the primo vascular system," *Journal of Acupuncture and Meridian Studies*, vol. 5, no. 5, pp. 241–247, 2012.

[21] J. W. Dundee and G. Ghaly, "Local anesthesia blocks the antiemetic action of P6 acupuncture," *Clinical Pharmacology and Therapeutics*, vol. 50, no. 1, pp. 78–80, 1991.

[22] S. M. Wang, Z. N. Kain, and P. White, "Acupuncture analgesia: I. The scientific basis," *Anesthesia and Analgesia*, vol. 106, no. 2, pp. 602–610, 2008.

[23] E. Noguchi and H. Hayashi, "Increases in gastric acidity in response to electroacupuncture stimulation of the hindlimb of anesthetized rats," *Japanese Journal of Physiology*, vol. 46, no. 1, pp. 53–58, 1996.

[24] H. Y. Kim, S. T. Koo, J. H. Kim, K. An, K. Chung, and J. M. Chung, "Electroacupuncture analgesia in rat ankle sprain pain model: neural mechanisms," *Neurological Research*, vol. 32, no. 1, pp. S10–S17, 2010.

[25] P. Li, K. F. Pitsillides, S. V. Rendig, H. L. Pan, and J. C. Longhurst, "Reversal of reflex-induced myocardial ischemia by median nerve stimulation: a feline model of electroacupuncture," *Circulation*, vol. 97, no. 12, pp. 1186–1194, 1998.

[26] B. Sung, M. S. Kim, B. C. Lee et al., "Measurement of flow speed in the channels of novel threadlike structures on the surfaces of mammalian organs," *Naturwissenschaften*, vol. 95, no. 2, pp. 117–124, 2008.

[27] W. Zhou, S. C. Tjen-A-Looi, and J. C. Longhurst, "Brain stem mechanisms underlying acupuncture modality-related modulation of cardiovascular responses in rats," *Journal of Applied Physiology*, vol. 99, no. 3, pp. 851–860, 2005.

[28] M. Tatewaki, M. Harris, K. Uemura et al., "Dual effects of acupuncture on gastric motility in conscious rats," *American Journal of Physiology*, vol. 285, no. 4, pp. R862–R872, 2003.